

LIGHTNING, AND ITS
RELATION TO PRECIPITATION

by

DAVID E. PROCTOR

Ematek, Council for Scientific and Industrial Research
Pretoria, 0001, South Africa

Ematek report No. EMAP/C/92048

Report to the Water Research Commission on the Project
"Lightning Research - A study using Radio,
Radar, and Aircraft "

Director:	Dr. D. H. Swart
Programme Manager:	Dr. D. vd S. Roos,
Project Leader:	Dr. D. E. Proctor.

WRC Report No. 279/1/93
ISBN 1 874858 71 3

EXECUTIVE SUMMARY

LIGHTNING , AND ITS RELATION TO PRECIPITATION

by

DAVID E. PROCTOR

Ematek, Council for Scientific and Industrial Research
Pretoria, 0001, South Africa

Ematek report No. EMAP/C/92048/A

Supplementary to Ematek Report No. EMAP/C/92048 which is the
full report to the Water Research Commission on the Project
"Lightning Research - A study using Radio,
Radar, and Aircraft "

Director:	Dr. D. H. Swart
Programme Manager:	Dr. D. vd S. Roos,
Project Leader:	Dr. D. E. Proctor.

1.0 BACKGROUND AND MOTIVATION

In 1967 the Director of the National Institute for Telecommunications Research ordered an investigation to discover whether it would be possible to map points that lightning struck, by locating sources of radio disturbances caused by the lightning flashes themselves. This scheme proved to be feasible, and moreover it became evident that such a system could be used to construct three-dimensional maps of the paths taken by lightning even when the lightning had been hidden by cloud and rain. By measuring the differences in the times at which these radio disturbances arrived at four separate places, it was possible to produce time-resolved, three-dimensional maps of the paths followed by lightning flashes. We used five stations because the redundant data provided by an extra station could be used to verify each of the measurements. At first, a system of cameras that recorded radio signals displayed by 14 cathode ray tubes was used to record the progress of each flash for times that lasted a mere 200 milliseconds. These recordings were initiated by a trigger which did not always operate at the start of the lightning flash. In 1978, we acquired a laser-optical recorder specially designed and built for this project by Plessey Limited, Caswell, UK. This permitted recordings to be made continuously for sixteen minutes, and

greatly enhanced our capabilities. We designed and constructed a weather radar in order to compare lightning paths with the precipitation patterns of their host thunderstorms. It became evident that lightning paths were influenced by the presence of precipitation.

It was also clear that by somehow probing thunderclouds we would greatly enhance the observations we made. The means for probing thunderclouds existed at Nelspruit in the form of a Lear Jet aircraft which carried the appropriate instrumentation.

In 1986 this project was transferred to a Division of a reconstructed CSIR. This Division became known eventually as Ematek. Its stated aim was to derive financial profit from researches and other activities in the fields of Natural Science. Any project that did not derive external funds was placed under threat of closure. My appeal to the Water Research Commission was answered in a manner that permitted the project to continue. The objectives of the project were set out as follows:-

2.0 OBJECTIVES OF THE PROJECT

a). To map lightning in relation to three-dimensional precipitation patterns of the host storms, and in particular, to plot the starting points of flashes on radar maps of the storms, in order to see how lightning is related to precipitation.

b). To make some observations in real time, while storms are in progress, with a view to observing where lightning flashes begin, and then to direct an aircraft to these regions in an attempt to discover what characteristics are peculiar to the relatively small regions where lightning flashes begin.

c). To analyze some special data that have been recorded already. This will be done to investigate those processes which precede and accompany dart leaders. (Dart leaders are precursors of strokes that are not first strokes).

d) To analyze recordings of the relatively rare positive flashes to ground.

e). To study radar reflections from lightning using radar.

Thus the emphasis was placed on the relationships between lightning and precipitation, while devoting some effort to studies of lightning *per se*.

3.0 SUMMARY OF MAJOR RESULTS AND CONCLUSIONS

Objective (a) will be treated in two parts. The first is concerned with the regions where lightning flashes began. The second concerns the paths followed by lightning.

3.1 REGIONS WHERE LIGHTNING FLASHES BEGAN

We define the origin of a lightning flash to be the region

where the flash began. We located the origins of 773 flashes that occurred during 13 thunderstorms, by measuring the differences between the times at which radio pulses emitted by the lightning arrived at five widely spaced receiver stations stationed on the ground. We found that the distribution of origin heights was bimodal, with peaks at 5.3 and 9.2 km above sea-level. Flashes in the lower group were more numerous in ten storms. There was evidence to suggest that this condition depended on the phase of the storm. The properties and behaviour of flashes in the higher group were markedly different from those in the lower group. However both discharged negative electricity, as shown by electric field changes recorded by many whose paths were also known. Flash origins tended to cluster in regions that were a few kilometers or less in horizontal diameter. The origins of 658 flashes were mapped onto radar precipitation patterns of their host thunderstorms. We eventually arranged for our maps to show contours that marked the positions of surfaces at which the radar reflectivity just exceeded a value 100 mm^6 per cubic metre. The value 100 is equal to 20dBZ on the logarithmic scale, and therefore we designated these surfaces as S20. We found that 66% of the flashes began immeasurably close to the surfaces S20; 27% began inside these surfaces, and 7% began outside the surfaces S20. Similar results were found for the high flashes, but a greater percentage of the 195 ground-flashes began inside the surfaces S20; their scores being 54%, 36% and 9% for "ats", "ins" and "outs". We measured the distance between each origin and its nearest S20 surface. The distribution of these distances showed a marked peak near zero. We expect lightning to begin in regions where

the electric field is highest. It is easy to show that, in the case of a uniformly charged volume, the electric field is most intense at the surface, and we inferred that surfaces S20 enclosed regions that were charged. There was evidence that the charges had resided on smaller drops that co-existed with larger drops. This evidence, provided by calculations that showed that small droplets provided most of the capacitance (i.e. the facility to store charge), was supported by measurements reported by Christian et al [1980].

3.2 LIGHTNING PATHS

We mapped paths taken by 105 flashes. This did not include a group of 26 whose paths had been reported previously. We found that most flashes (79%) travelled down the radar reflectivity gradients; i.e. they extended from relatively wet regions into drier regions often extending beyond the surfaces S20. (Defined in the previous Section.) Sixty-one percent of the flashes that we studied were endowed with branches or segments that tracked the surfaces S20. We inferred that these surfaces were electrified, or that they were adjacent to charged regions. Of 186 branches mapped, 44 % terminated outside the volumes enclosed by the surfaces S20. 27% ended at the surfaces S20 and 29% terminated inside these surfaces. Storms usually exhibited a maximum horizontal area at a level near 3km. Although lightning extended beyond the surfaces S20 at the higher levels, it seldom extended more than 1 or 2 km beyond limits that could be defined by projecting, vertically, the outline at the level where the

area had been greatest. There was a tendency for lower portions of the flashes to occur inside S20, often well inside. At mid-levels the flashes occurred near S20, and at higher levels the flashes emerged and extended beyond the surfaces S20. There was a great variety in behaviour patterns, so that very few rules could be discerned that governed paths taken by lightning. Each flash followed a path that was mostly unique, except that in many flashes there were short segments of a few km where they followed paths that had been active during previous flashes.

3.3 OBSERVATIONS IN REAL TIME

We built the instrumentation required for these operations and acquired equipment needed for radio communication with the aircraft. It had been agreed that Messrs. Cloud Quest of Nelspruit would fly experiments in co-operation with us, at suitable times if the plane became available. There were five conditions that had to be satisfied before operations took place. The condition that failed most often was lack of suitable storms, followed by the condition that the plane and its crew should not be occupied with duties that had been given a higher priority. Six flights were undertaken, but there were no successful operations.

3.4 RADIO NOISE ASSOCIATED WITH SUBSEQUENT STROKES OF LIGHTNING

Many lightning flashes to ground consist of a series of similar events during which the flash strikes ground. These component events are called *strokes*. Subsequent strokes are strokes that are not the first to occur during the course of a flash. The radio noise that is emitted during these events is not easy to process, and it is only with some difficulty that its sources can be located. This work was devoted to locating some of these sources, and using the information so obtained to interpret high-speed recordings of electric field-change that had been recorded specially for this purpose. The exercise provided information regarding the behaviour of these events, their speeds of progression and it also showed that the ionized plasmas they produced shielded later radiation.

3.5 POSITIVE FLASHES TO GROUND

Most ground-flashes bring negative charge to ground. A minority carry excess positive charge. We had hoped to study examples of this kind of flash. Suspected candidates were noted by viewing electric field-changes of all the flashes whose radio noise emissions had also been recorded. Their noise recordings were processed in order to see whether they had in fact been positive flashes to ground. After expending a considerable amount of effort, we found that we had no recording of a positive flash to ground. These flashes are known to occur sometime after the main part of the storm has

passed. We had always terminated recording sessions when storms had passed, because of the high cost of film.

3.6 LIGHTNING FLASHES WITH HIGH ORIGINS

This was not mentioned specifically as one of the objectives perceived at the outset. This part of the work was undertaken in consequence of having found that there were two modal heights at which flashes began, and that flashes in the higher group behaved differently from the others. Twenty-one of these flashes were studied in detail. We obtained information regarding their directions and the speeds at which they extended, the line-densities of the charges they carried and the currents that flowed along them. Two flashes were of particular interest. One followed an almost circular path to end near its origin. This showed that lightning flashes are guided by the electric field at the tip, which in turn depends upon the instantaneous distribution of excess charge. The second remarkable flash changed its polarity when it penetrated a region which must have been charged positively, but charged with a density that had been insufficient to initiate the discharge.

3.7 RADAR OBSERVATIONS OF LIGHTNING

The literature contained reports to the effect that radar reflections from lightning persist, and that they are rejuvenated by subsequent events in a manner that permits

them to indicate the later history of a flash of lightning. These sentiments had been substantiated by earlier observations of our own. These characteristics distinguished radar observations from the kind we had been making by means of radio waves. The radio emissions occur when the air is being ionized; i.e. when the channels first come into being. They do not recur when current flows along a pre-existing channel, except where it extends the channel, or when the channel has been dormant for a time that exceeds 80 milliseconds (in which case its ionization has decayed, and the re-ionization radiates radio noise). Radio emissions occur during the incipient stages of a channel.

We built a suitable transmitter, and were disappointed with its output power, which had been misrepresented in the manufacturer's data. To make good the loss of performance, we increased the antenna gain, an action that restricted its coverage. We had illuminated a sector of sky that was almost sufficient for our purposes. The existing receiver network was used to locate the reflectors, as well as providing data for a radio picture of each flash. We were able to compare radio pictures with the radar reflections.

These comparisons showed that parts of the radar pictures had been obstructed by intervening lightning channels. We had a problem similar to one which occurs with weather radars that operate at short wavelengths: by varying degrees they fail to see rain through rain. Lightning flashes that consisted of a few long filamentary streamers, as is the case with many of the high flashes, would present few problems. On the other

hand, many of the lower flashes resemble a jungle of intertwined filaments so that the whole is an effectively opaque object. These radar pictures explained why the radio noise from lightning is so variable in amplitude. The reason was obstruction and attenuation, and its salvation was due to the very high intensities of the sources. This study showed that provided radar was used intelligently, which presupposes the provision of radio pictures of the flashes being studied, it could be a useful method for observing lightning.

4.0 ASSESSMENT

Most objectives were achieved. In some cases, they were exceeded. The principal shortcoming was the lack of joint operations with the aircraft.

Joint operations with the instrumented aircraft would have augmented this project very much. It was a great pity that this part of the work did not come about. Nevertheless, the experiments supplied new and interesting information which we venture to say is valuable, and most is unique. After 24 years' operation, we still have no serious competitor in the business of getting good pictures of lightning.

The failure to analyze positive flashes to ground was not due to a lack of taking records. Between February 1979 and February 1991, we took records successfully on 50 days, and we attempted to take records on a further 45 days, often

declining to start recording because storms had not been suitably placed.

These experiments showed clearly that lightning was affected by precipitation. We were unable to demonstrate the converse viz. how precipitation is affected by lightning. There have been reports of gushes of rain that followed lightning. We saw none. We noted regions of detectable precipitation that grew in size after being pervaded by lightning. There were regions that contained precipitation that was mapped by the radar, and these regions had been devoid of lightning, and yet they grew more rapidly in size than their counterparts that had been active electrically.

5.0 FUTURE RESEARCH

Joint operations with the aircraft must yield excellent results. The vicinity of Lanseria is not their place. It's too far from base. Here, the air lanes are too busy, and the radio network is plagued by interference from other services. Maybe we have a case for using a drone. Especially if it is controlled from the Lear Jet.

There is a need for recording one or two storms during which we compare the locations of sources of HF radiation with those of the VHF sources.

There is potential benefit to be gained by analyzing more

data obtained with the metric radar. There is also a need to improve the technique for displaying the radar echoes so that they make a sensible picture. This is a computing problem.

As of November 1992, we have two principal, unsolved mysteries in this field. (1) How do droplets become drops? The question is valid even in stratiform clouds. (2) How do thunderstorms electrify?

In an attempt to answer Question (1), I would post a student on a mountain, in misty conditions, and get him to observe droplets, when it rains and when it doesn't. I would attempt to answer (2) by probing regions adjacent to those where lightning begins.

6.0 TECHNOLOGY TRANSFER

I should very much like to publish these results in a journal such as *Journal of Geophysical Research*.

IBM compatible flexible discs on which all the lightning data have been listed have been given to WRC for archiving.

7.0 BIBLIOGRAPHICAL REFERENCE

Christian, H., C. R. Holmes, J. W. Bullock, W. Gaskell, A. J. Illingworth and J. Latham, Airborne and ground-based studies of thunderstorms in the vicinity of Langmuir Laboratory, *Quart. J. R. Meteorol. Soc.*, 106, 159-174, 1980.

ACKNOWLEDGEMENTS

The research in this report emanated from a project funded by the Water Research Commission and entitled:

"Lightning Research - A study using Radio, Radar, and Aircraft".

The Steering Committee responsible for this project, consisted of the following persons:

Dr. G. C. Green	Water Research Commission (Chairman)
Mr. H. Maaren,	Water Research Commission
Mr. F. P. Marais	Water Research Commission
Mr. R. T. Bruintjes	S. A. Weather Bureau
Dr. J. F. Eloff	Department of Agricultural Development
Mr C. G. Groenewald	S. A. Weather Bureau
Dr. J. A. Lindesay	University of Witwatersrand
Dr. G. Mather	Cloud Quest (Pty) Ltd.
Prof P. J. T. Roberts	Institute for Commercial Forestry Research
Dr. D vd S. Roos	CSIR
Dr. Alan Seed	Department of Water Affairs
Mr. D. Terblanche	S. A. Weather Bureau
Prof. J. M. de Jager	University of OFS
Prof J. van Heerden	University of Pretoria
Prog F. E. Steffens	UNISA

The author thanks the Water Research Commission for providing funds for this project. I gratefully acknowledge the efforts of the staff of the Water Research Commission.

My thanks are due also to the following:-

Ematek, CSIR., and in particular to Drs. Roos and Swart.

The SA Weather Bureau, who supplied Aerological Data, and to Mr. Deon Terblanche and Mr. H. G. Pienaar for a computer

programme for the analysis of the Aerological Data.

Mr. R Uytenbogaardt for his wisdom and for many hours of diligent and intelligent labour.

Project Leader	Dr. D. E. Proctor
Technician	Mr. R. Uytenbogaardt
Data Reader	Mrs. Annamaria Kelly

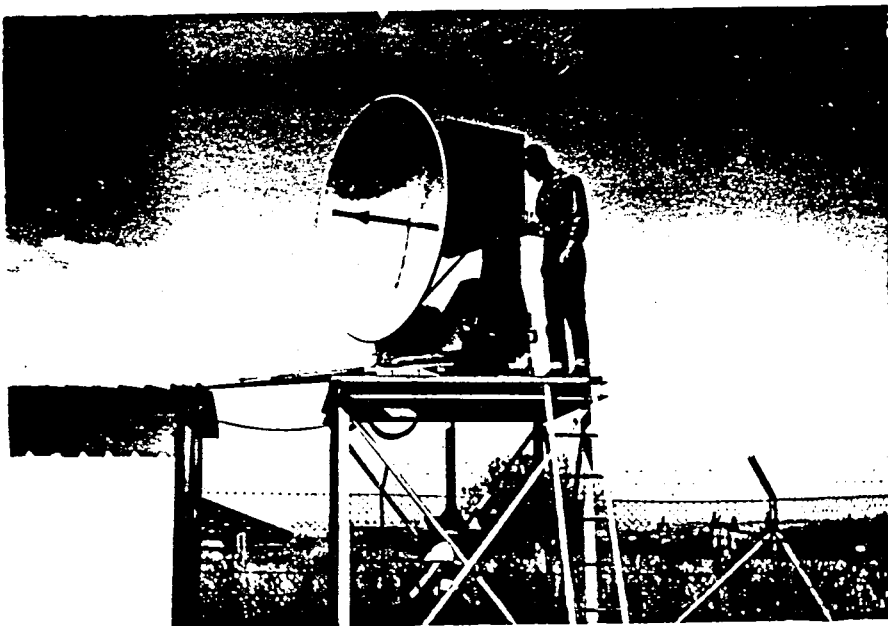
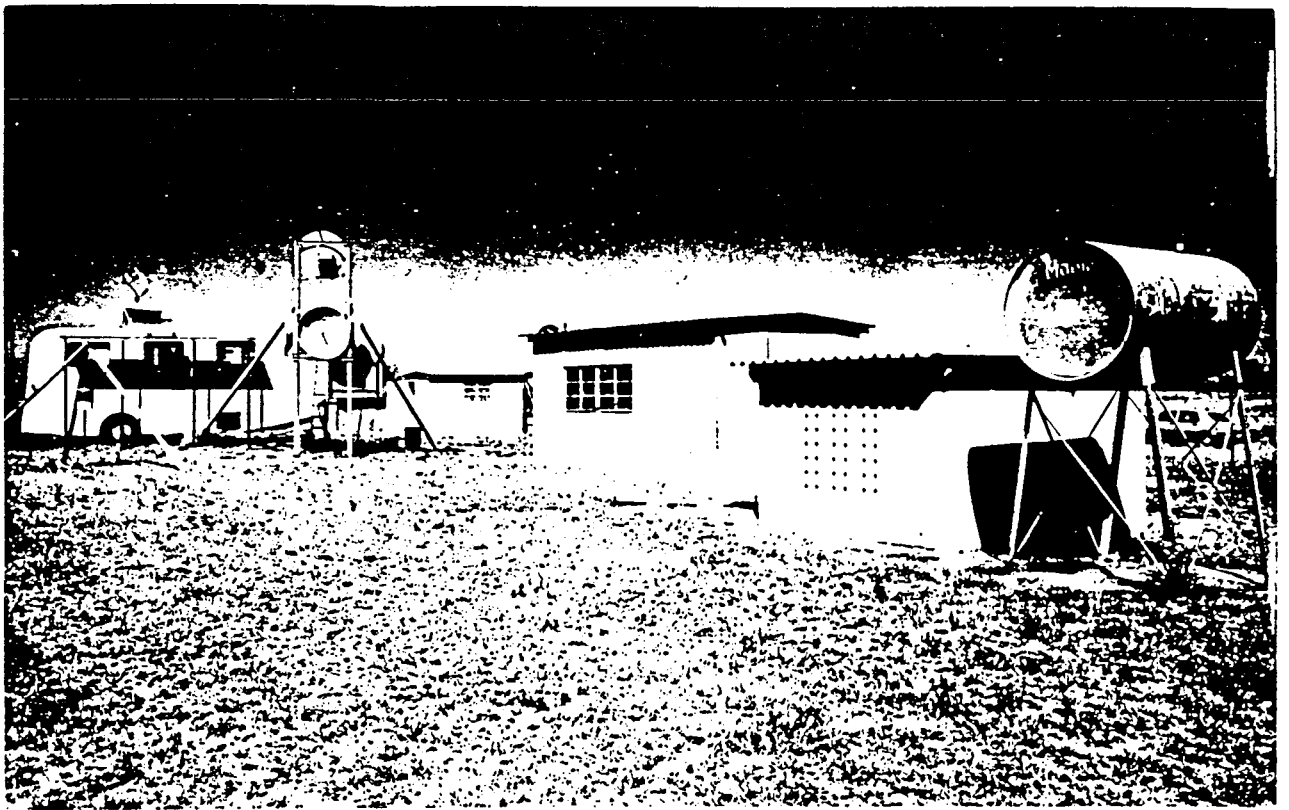
The technician and data reader were retrenched during April 1991. The Project Leader retired at the end of July 1992.

TABLE OF CONTENTS

	Page
1.0 INTRODUCTION	1
1.1 Aims	2
1.2 Some effects of electric fields on water drops	3
2.0 METHOD	6
2.1 Mapping VHF sources	6
2.2 Weather radar	7
2.3 Magnitudes of error	9
2.4 Metric radar	11
3.0 RELATIONSHIPS BETWEEN LIGHTNING AND PRECIPITATION Part 1 REGIONS WHERE LIGHTNING FLASHES BEGAN	11
3.1 Results	11
3.2 Discussion	18
3.3 Concluding remarks	20
4.0 RELATIONSHIPS BETWEEN LIGHTNING AND PRECIPITATION Part 2 LIGHTNING PATHS AND PRECIPITATION	21
4.1 Data handling	21
4.2 Results	22
4.3 Discussion	24
4.4 Concluding remarks	36
5.0 LIGHTNING FLASHES WITH HIGH ORIGINS	37
5.1 Introduction	37
5.2 Summary	42
6.0 REAL TIME OBSERVATIONS AND ATTEMPTS TO USE AN INSTRUMENTED AIRCRAFT	41
7.0 STUDY OF RADIATION AND ELECTRIC FIELD CHANGES PRODUCED BY PROCESSES THAT PRECEDE AND ACCOMPANY DART LEADERS	42
8.0 POSITIVE FLASHES TO GROUND	43
9.0 A STUDY OF RADAR REFLECTIONS FROM LIGHTNING	44
10.0 CONCLUSIONS	46
BIBLIOGRAPHICAL REFERNCES FOR THE MAIN SECTION	194

List of Appendices

		page
1	A short essay on lightning	48
2	Radio pictures of lightning	53
3	Reprint: Regions where lightning flashes began	58
4	The effects of electrical forces on drops of water	72
5	The distribution of charge in thunderstorms	84
6	A brief description of the storms	88
7	The numbers of drops per cubic metre contributing to radar reflectivity	92
8	Preprint: Lightning flashes with high origins	97
9	Report: Radio noise associated with subsequent strokes of lightning	130
10	The size of a sphere containing 3 Coulombs	160
11	Report: Radar studies of lightning	162



Top: Part of Nietgedacht Station
Centre: Protea Ridge Remote Station
Bottom: C-band radar

In 1968 the National Institute for Telecommunications Research (the oldest and most profitable lab in the CSIR) initiated an investigation in order to discover whether it was possible to map points that lightning struck, by locating sources of radio disturbances caused by the lightning flashes themselves. A scheme of this kind seemed feasible, and moreover it became evident that such a system could be used to observe lightning even when it was hidden by cloud and rain. By measuring the differences in the times at which these radio disturbances arrived at four separate places, it was possible to produce time-resolved, three-dimensional maps of the paths followed by lightning flashes. This evoked the idea that these maps should be superimposed on maps of the relevant thunderstorms in order to gain a better understanding of lightning. We therefore acquired an X-band (3 cm wavelength) radar, and found that its inability to see rain that was hidden by intervening heavy rain was a nuisance. For this reason, I designed and constructed a C-band (5 cm wavelength) radar to replace it. Radio pictures of a few flashes were plotted onto radar maps of the thunderstorms, and these showed that lightning paths had been influenced by the precipitation. Moreover, there were reports in the literature (reviewed in Section 1.2 and Appendix 4) to the effect that precipitation was modified by electrical effects. It was commonly observed that drops that had fallen from thunderclouds were much larger than those that fell from stratiform clouds, and the difference was ascribed to the effects of electric fields in thunderclouds. The aims of this

project were modified with a view to observing these effects. We argued that the enhancement of rainfall, and indeed an understanding of how rain was generated was probably more profitable than an understanding of lightning. It was also clear that by somehow probing thunderclouds we would greatly enhance the observations we made using methods of remote sensing. The means for probing thunderclouds existed at Nelspruit in the form of a Lear Jet aircraft which carried the appropriate instrumentation. These plans were laid just before we were struck by disaster: State revenues from mining and commerce had fallen. Government expenditure was to be reduced greatly. The CSIR reacted by attempting to abandon any activity that did not generate financial reward. This lightning project was transferred from the ambit of a hitherto successful and profitable Institute, which was immediately closed down, and transferred to the control of a comparatively indigent Division whose aim was to derive profit from basic research in natural sciences. Accordingly, the Water Research Commission was approached, and the aims of this project were set out as follows:-

1.1

AIMS

a). To map lightning in relation to three-dimensional precipitation patterns of the host storms, and in particular, to plot the starting points of flashes on radar maps of the storms, in order to see how lightning is related to precipitation.

b). To make some observations in real time, while storms are

in progress, with a view to observing where lightning flashes begin, and then to direct an aircraft to these regions in an attempt to discover what characteristics are peculiar to the relatively small regions where lightning flashes begin.

c). To analyze some special data that have been recorded already. This will be done to investigate those processes which precede and accompany dart leaders. (Dart leaders are precursors of strokes that are not first strokes).

d) To analyze recordings of the relatively rare positive flashes to ground.

e). To study radar reflections from lightning using radar.

Thus the emphasis was placed on the relationships between lightning and precipitation, while devoting some effort to studies of lightning per se.

1.2 SOME EFFECTS OF ELECTRIC FIELDS ON WATER DROPS

The effects of electric fields on drop coalescence

Lord Rayleigh [1879] showed that uncharged water drops do not coalesce when they collide in a region where there is no electric field, whereas collisions that occur in the presence of an electric field usually result in coalescence. Coalescence is one of the known mechanisms by which droplets that are too small to fall, grow to become raindrops. As

reported by Sartor [1969], Lord Rayleigh's experiments were repeated in 1969 by workers at NCAR, who developed special apparatus that caused drops of a constant size to collide in precisely the same position many times in succession. This permitted them to photograph not only the colliding drops, but also to photograph successfully the integrated total light from many very minute electrical discharges that occurred between the drops at the instants just preceding their collisions. Two of their pictures are reproduced here as Figures 1.1 and 1.2.

Lord Rayleigh's discovery evokes the question: Where do electric fields occur in thunderstorms? The answer, that electric fields are highest near concentrations of charge, leads to enquiries concerning the distribution of charges in thunderstorms. This subject is reviewed in Appendix 5. Information about the locations of strong electric fields can be obtained by locating the origins of lightning flashes, and by plotting their positions on maps of the thunderstorm. This has been one of the main thrusts of this research project, and Section 3 and Appendix 3 describe these efforts. Lightning paths are guided by distributions of charge of the polarity opposite to that which initiated the lightning. We mapped these paths, and this is the subject of Section 4.

Strong electric fields also cause large drops to "break-up"; i.e. to disrupt. The behaviour of water drops as they fall through regions where high electric fields are present is relevant to this work, as it has a bearing on heights at which lightning flashes began. It also concerns charging of

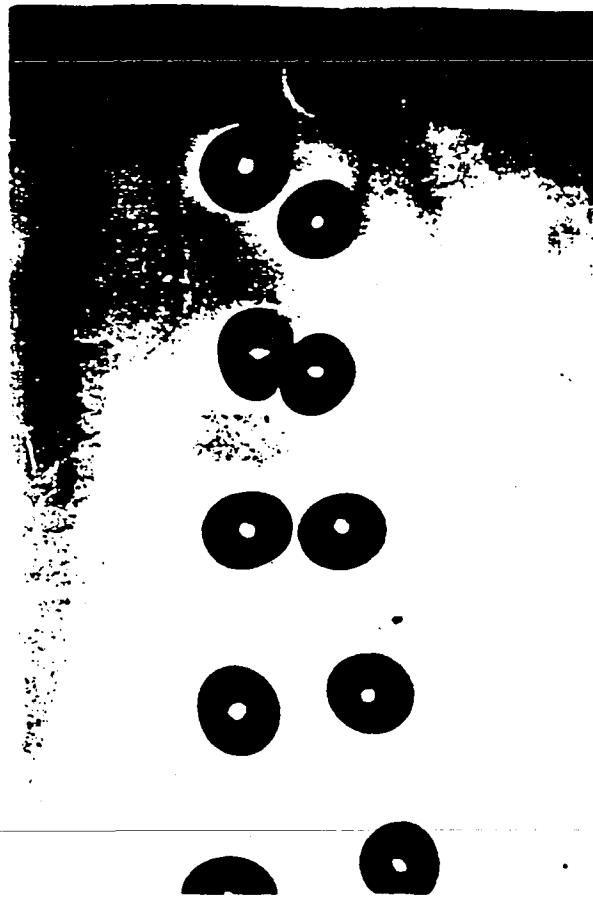
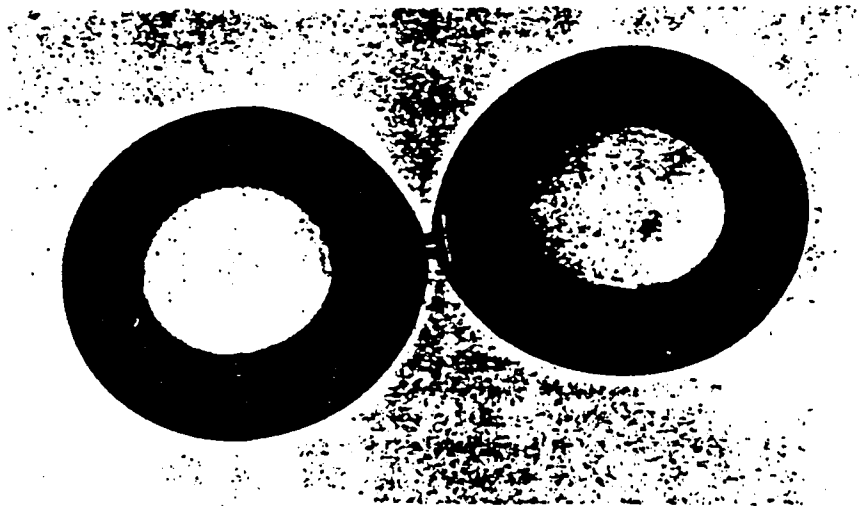


Figure 1.1 Uncharged water drops colliding in zero E-field. Photograph published by Sartor [1969].



STRONG-FIELD COALESCENCE. Here two uncharged drops, of 7.8×10^{-4} -cm radius, collide in a uniform field of 3.85 kV/cm parallel to their line of centers. The photograph was taken 15 microsec after the start of charge transfer, when charge has stopped flowing but water continues to flow into the neck.

Figure 1.2 Water drops colliding in a high Electric field, which causes them to coalesce. Published by Sartor [1969].

thunderstorms. It is reviewed in Appendix 4.

Some of the terminology used in the study of lightning has been set out as a short essay in Appendix 1.

2. METHOD

2.1 Mapping VHF Sources

Lightning flashes were mapped using the hyperbolic system described by *Proctor et al* (1988) and by *Proctor* (1983,1981,1971). Sources of radio signals emitted by the lightning were located by measuring the differences between times at which the signals were received at widely spaced receivers sited at ground level. An image of each flash emerged after locating and mapping positions of a large number of sources of radio signals emitted by the flash. Examples have been published by *Proctor* [1981,1983] and by *Proctor et al* [1988]. Positions were described in terms of a system of Cartesian coordinates whose X and Y axes were almost parallel to the earth's surface, and were oriented respectively 60 degrees and 330 degrees with respect to True North. The coordinate Z was very nearly vertical. The origin of this coordinate system was placed at the 'home' station. Physical characteristics of the recorder limited recordings to a maximum of sixteen minutes' duration, and considerations of flashing rate and economy sometimes caused us to terminate the recordings early. Storms drifted into and out of the coverage volume at various stages of their development, and therefore storms were not observed over their full lifetimes,

nor at the same phases. The auxiliary recordings concerned an interval approximately 20 minutes. Auxiliary records, which were recordings of radio signals emitted by the lightning together with recordings of electric field change (EFC), could be consulted in order to determine which flashes struck ground, as explained by Proctor [1983]. When paths followed by the flashes were known, these recordings of EFC could be used to determine magnitude and polarity of the excess charge redistributed by the flash. The recorded waveforms of radio noise showed when each flash had begun, when it had ended, and whether it had emitted pulses at high rates or at low rates. *Proctor et al [1988]* reported that this rate indicated whether the flash had begun at a high or a low altitude. The noise waveforms also bore evidence of a strike to ground, if this had occurred.

A discussion of this method for observing lightning, its benefits and limitations has been set out in Appendix 2.

2.2 *Weather radar*

We mapped paths of lightning flashes onto radar precipitation patterns of their host storms in order to discover how the paths were affected by precipitation. A weather radar which operated at a wavelength of 5.48 cm was used to provide three-dimensional precipitation patterns of the storms that generated the lightning flashes which we describe here. The main characteristics of the radar have been listed in Table 1. Echoes that were received from targets whose ranges were less than 25 km, were corrected for the effects of range.

Video data were integrated, averaged and stored in "bins" that represented 250 m increments in range, and then stored on magnetic tape. The contents of each bin was an average of twenty samples taken over 10 msec. The tape recordings could be replayed repeatedly through a special computer which allowed a variety of sectional views of the storm to be displayed and photographed. Examples are shown in the paper by Proctor [1991]. The CAPPI's are plan views of thin, horizontal slices, at heights stated in km above ground. Reflectivity factors were displayed in increments of 10 dB; the lowest was 20 dBZ. The threshold was applied to the video signals in the computer circuitry when the tapes were replayed in order to display the data. The threshold level was a minimum of 19 dB above the receiver noise level.

TABLE 1. Characteristics of C-Band Radar Set

Operating frequency	5.48 GHz
Antenna Beamwidth	2 degrees (H and V)
Beamshape	Gaussian
Nodding rate	88 degrees per sec.
Azimuthal rotation	360 degrees in 5 minutes
Pulsewidth	1 microsecond
p.r.f.	1000 Hz
Peak power	0.32 MegaWatt
Display threshold	20 dBZ out to 25 km
Receiver noise level	8.5×10^{-14} Watt
Received average power	$4 \times 10^{-5} ZR^2$ Watt *
Z displayed in increments of	10 dB
Length of range-gate	250 m
Radar site coordinates	(0, 0, 0) km

* Z in $\text{mm}^3 \text{m}^{-3}$ and R in metres.

2.3. *Magnitudes of error.*

The magnitude of errors incurred when comparing a component of a lightning path or channel with the precipitation pattern differs from the size of the error incurred when comparing the origin of a flash with the precipitation pattern. We shall estimate these in turn. The principal errors in the comparisons reported here will have been due to changes in the thunderstorms that occurred in the intervals T between the instants when we recorded the radar returns and the instants when the lightning flashed. Almost all these intervals were less than 2.5 minutes. The intervals T were distributed almost uniformly, and their average magnitude was approximately 75 seconds. Except for one storm that moved at 16 m/s, storms we report in this series of papers moved at speeds that ranged 0 to 7 m/s. The weighted average speed was 3.5 m/s. In 75 s a storm moving at 3.5 m/s would travel 263 m, and this distance would be an optimistic estimate of the error due to storm motion during the intervals T ; optimistic because even stationary storms displayed significant changes between successive scans. The accuracy with which the radar could locate the position of a particular feature decreased with range because of the finite beamwidth. At 6km range, the 2 degree beam illuminated a region 200 m across, but convolution with the receiver beam reduced the half-power diameter of the observation area to 140 m. Range bins were 250 m long. At this range, the radar could locate a target correct to 143 m. (The root of the sum of the squares of 125m and 70m). Errors in timing the VHF signals from lightning were large enough to cause rms errors of 25 meters in the X

and Y coordinates of each source. These were the coordinates that were parallel to the ground. There was no vertical baseline. As explained by Proctor [1971], we could determine the heights of the sources by making use of those hyperbolic surfaces that curved over the 'home' station. The divergence of these surfaces (also called lane-expansion) caused errors in the height coordinate, Z, to vary with position. Their rms magnitudes varied from 140 m to 250 m at the heights at which most of the lightning flashes that we describe here occurred. We may estimate an average error in the relative positions of an element of a precipitation pattern and one element of the lightning path (i.e. the position of one radio source of lightning noise) by adding the squares of error components (25 m in X and in Y, 140 m in Z, 143 m for the radar, and 263 m for storm drift; approximately 100 m error in mapping). We arrive at an estimate of 347 m. The magnitude of the error had to be estimated for each part of every flash. Some flashes were mapped on patterns that had been derived from successive radar scans in order to reduce these errors.

Errors in determining flash origins have to account for the fact that successively active sources were neither colocated nor immediately adjacent; instead they occurred in an erratic spatial sequence and so exhibited a scatter that contained a component not unlike the scatter of endpoints of steps in random flight. The extent of this scatter was larger than that due to errors of measurement. In due course, sources occupied adjacent positions, but the accuracy with which we could locate an origin had to be determined by taking statistics of the scatter of successive sources that had been

active initially in many flashes. These determinations showed that centroids of the first six sources could be determined with rms errors that were 20 to 80 metres in X or Y and 160 to 240 metres in the height coordinate. Figure 11 of Proctor [1981] maps positions of sources of successive pulses. Adding squares of error components (50 m in X and in Y, 200m in Z, 143 m for the radar, and 263 m for storm drift; approximately 100 m error in mapping) we arrive at an estimate of 380 metres for the expected error in the positions of origins that were mapped on precipitation patterns.

2.4 Metric Radar

A description of the metric radar used to observe lightning, is given in Appendix A11.

3. RELATIONSHIPS BETWEEN LIGHTNING AND PRECIPITATION

Part 1 REGIONS WHERE LIGHTNING FLASHES BEGAN

3.1. Results

Appendix 3 is a reprint of a paper that describes this work. The essential points and main results are listed as follows:-

1. An origin is defined to be a localized region where a lightning flash began. It is taken to collocate with the centroid of sources mapped by timing the leading edges of the first six to ten VHF radio pulses emitted by each flash. This centroid was found to lie right at the starting points of channels delineated by radio pictures.

TABLE 2. Median Heights of the Origins of Lightning Flashes and Corresponding Temperatures of Environmental Air.

Date of Storm	Lower group			Upper group			
	Height km msl	Temp deg. C	No.	Height km msl	Temp deg C	No.	Percent in upper
14 Feb 79	5.7	-5.5	42	8.9	-27	39	48
2 Mar 79	4.7 ave	NA	3	6.7 ave	NA	3	—
7 Mar 79	4.8	-2.0	26	—	—	0	0
27 Mar 79	4.9	-2.5	23	9.2	-32.5	13	36
8 Apr 79	5.4	-8.5*	26	—	—	0	0
24 Feb 84	5.2	-3.0	9	—	—	0	0
24 Oct 84	5.2	-4.0	33	8.2	-26.0	11	25
10 Dec 84	4.4*	+1.0*	22	7.5*	-21.1*	10	31
21 Feb 85	5.1	-2.1	69	9.1	-30.0	119	63
26 Mar 85	5.2	-3.0	8	8.4	-25.0	2	20
16 Nov 87	5.4	-4.1	36	9.4	-33.0*	15	29
23 Dec 87	5.7*	-2.1	33	9.7*	-27.5	107	76
23 Mar 89	5.5	-4.2	101	9.0	-31.0	23	19

* Extreme values (except 2-3-79)

No. is the number of flashes

Temperatures correspond to the median heights. They are not weighted means.

NA indicates that data are not available.

2. Heights at which 773 lightning flashes began (in thirteen storms) were distributed as shown by Figure 3.1a. Zero height of the histograms in Figure 3.1 was 1430 metres above mean sea level. The distribution resembles two overlapping Gaussian distributions with modal values 5.3 km and 9.2 km above mean sea level (amsl).

3. Flashes that began in the lower regions outnumbered those in the higher group by 431 to 342. In some storms the higher group were the more numerous. There was some evidence

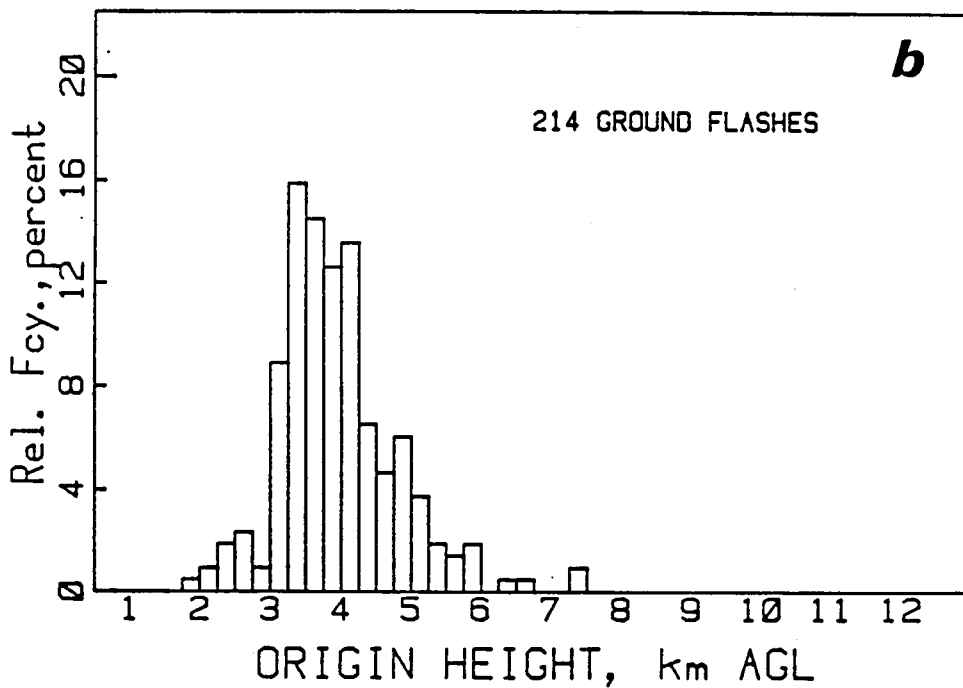
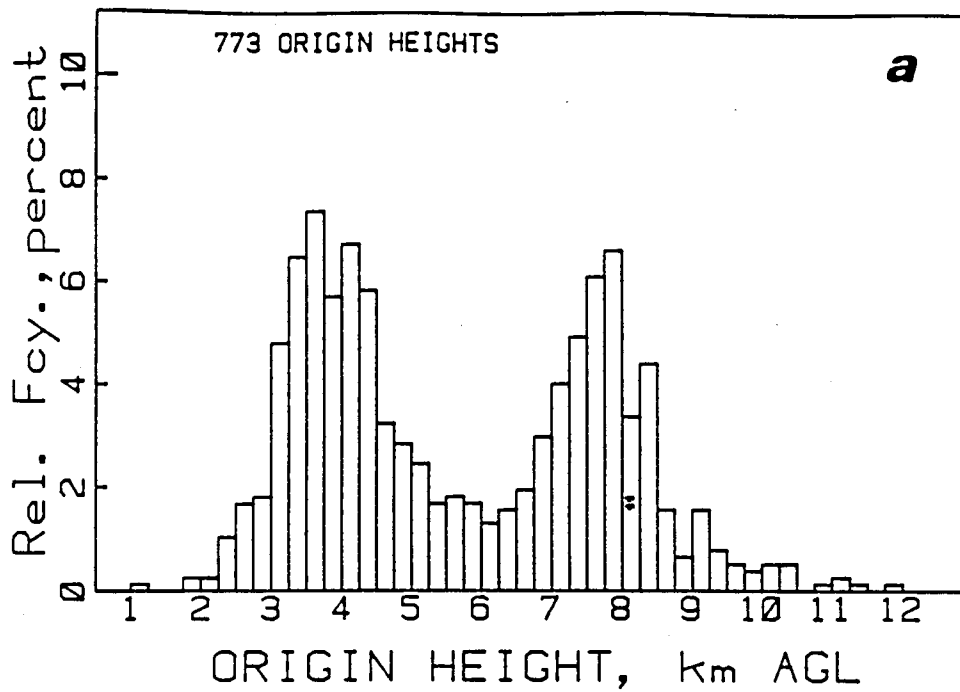


Figure 3.1 (a) Distribution of heights above ground level (at 1430 m above sea level) of the origins of 773 flashes of all kinds that occurred in 13 storms. (b) Distribution of origin heights of 214 flashes to ground.

to suggest that the ratio depended on the phase of the storm.

4. Flashes whose origins exceeded 7.4 km amsl exhibited properties that were distinctly different from those of flashes that began at heights below this level.

5. The measured distribution of heights of the origins of 214 ground-flashes is shown in Figure 3.1b. Nearly all belonged to the lower group.

6. Table 2 lists median heights of the origins and the corresponding temperatures of environmental air for each of the thirteen storms. Environmental temperatures at the median heights ranged from -8.5 degrees C to +1 C for the lower group and from -21 C to -33 C for the upper group.

7. Electric field-changes recorded by 165 flashes whose paths were known, and whose polarities could therefore be determined, were all negative flashes except for one flash. This result included 17 flashes whose origin-heights exceeded 7.4 km amsl. We inferred that the majority of 773 flashes were negative flashes, and that origin-height did not affect the polarity of a flash.

8. The origins of 658 flashes were mapped onto radar precipitation patterns of their host storms. We counted the numbers of origins that lay within the contours for 20 dBZ, as well as those that occurred outside of these contours. It became apparent that the majority lay very close to these contours. Table 3 lists the three categories for each of the

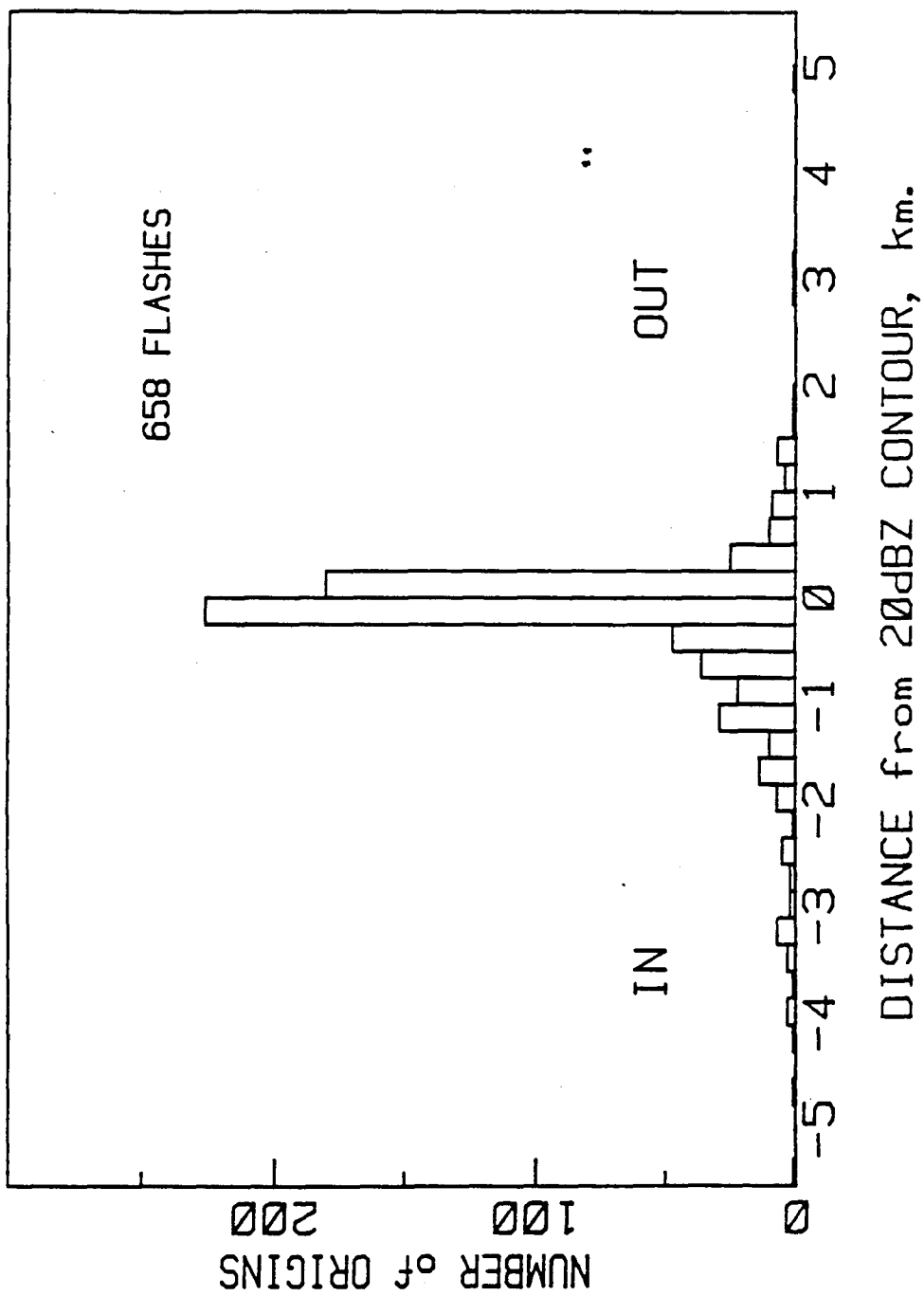
TABLE 3. Origins of Flashes with respect to the 20 dBZ Contours

Date of storm	Numbers of flashes whose origins were:-			Total
	At the 20 dBZ contour	Within contour: Z > 20 dBZ	Outside contour: Z < 20 dBZ	
14 Feb 79	26	28	1	55
2 Mar 79	4	2	0	6
7 Mar 79	21	5	0	26
27 Mar 79	25	10	0	35
8 Apr 79	18	7	1	26
24 Feb 84	6	3	0	9
24 Oct 84	33	2	3	38
10 Dec 84	17	15	0	32
21 Feb 85	71	52	7	130
26 Mar 85	8	1	1	10
16 Nov 87	29	14	7	50
23 Dec 87	97	31	6	134
23 Mar 89	80	5	22	107
Totals	435	175	48	658
Percent	66	27	7	100

TABLE 4. Origins of Ground Flashes with respect to the 20 dBZ Contours

Date of Storm	Numbers of Ground Flashes whose Origins were:			Total
	At the 20 dBZ Contour	Within contour: Z > 20 dBZ	Outside Contour: Z < 20 dBZ	
14 Feb 79	0	5	0	5
2 Mar 79	3	1	0	4
7 Mar 79	0	1	0	1
27 Mar 79	5	7	0	12
8 Apr 79	5	2	0	7
24 Feb 84	2	0	0	2
24 Oct 84	25	0	0	25
10 Dec 84	1	6	0	7
21 Feb 85	3	18	1	22
26 Mar 85	6	1	1	8
16 Nov 87	14	11	5	30
23 Dec 87	12	16	0	28
23 Mar 89	30	3	11	44
Totals	106	71	18	195
Percent	54	36	9	100

Figure 3.2 Distribution of distances of 658 origins from their nearest 20 dBZ contours.



thirteen storms. 66% of 658 origins occurred at the contours. 27% occurred within, and 7 % lay outside the contours.

9. Table 4 lists the three categories for 195 flashes to ground. The repective percentages were 54%, 36%, and 9% for the "ats", "ins", and "outs. Evidently, any tendency to originate in wetter regions was greater for ground-flashes.

10. For 276 flashes whose heights exceeded 7.4 km amsl, the scores were 73% : 19% : 8% for "ats, "ins", and "outs".

11. Because so many flashes began near the contours for 20 dBZ, the mapping process was repeated by a second person, who also measured the distance between each origin and its nearest contour for 20 dBZ. Figure 3.2 shows a distribution of distances between flash-origins and their nearest 20 dBZ contours. The assymetry of the distribution, and a study of the reflectivity gradients permitted us to estimate that the contour for 21 dBZ was the critical contour.

12. Maps were drawn which showed where the origins occurred. These maps showed that origins tended to cluster in relatively small regions, so that only small areas of the 20dBZ surfaces served to initiate flashes. These areas measured a few km in diameter or less. Densities ranged from 1.25 to 25 per cubic kilometre. Nearest neighbour distances ranged 190 metres to 510 metres. The NND's would have been enlarged by errors of measurement.

13. The origins were plotted onto various maps of

precipitation patterns of their host thunderstorms. These maps also showed storm directions and wind-speeds. No other consistent tendency or characteristic could be found that would relate storm morphology or wind direction and the origins of lightning flashes.

3.2 Discussion

Bimodal distributions of the heights of lightning channels have been reported by several investigators including Weber [1980], MacGorman et al [1981]. These reports lend credibility to the distributions of origin heights reported here.

We expect lightning to begin where the electric field is high. It is easy to show that the E-field is highest at the periphery of a uniformly charged volume. We found that most flashes began at the 20 dBZ contours, and these would have encompassed most of the heavy precipitation. It may be tempting to infer that excess charge resided on the precipitation and, moreover, inasmuch as high radar reflectivity is an indicator of large particles, to reason also that excess charge in those thunderstorms was carried by the larger particles. We found also that a significant number of flashes, which amounted to 27%, began inside the 20 dBZ contours. In cases where the density of excess charge had been concentrated centrally rather than having been distributed either uniformly or at the edges of the precipitation, we should expect to find that the high-field region occurred inside the precipitation. This fact, together

with the observation that those origins that occurred within the 20 dBZ contours did cluster around precipitation cores, again might be taken to indicate that the excess charge was carried by the larger particles. Calculations reproduced in Appendix 7 show that the smaller particles account for most of the capacitance because their numbers are so much greater than the numbers of larger particles. See the calculations listed in Table A7.2 in Appendix 7. We infer that charge was carried by small particles that coexisted with the larger. This notion is supported by results of previous investigations. Christian et al [1980] reported that negative charge was carried by the smaller particles. Gaskell et al [1978] reported that much of the charge on precipitation was carried by particles around 1 mm in size or smaller. Dye et al [1986] reported that in-cloud electric fields did not exceed 100 V/m until 5 mm graupel, ice-particle concentrations of 10 per litre, and reflectivities of 35 dBZ were present already. Dye et al [1988] reported that supercooled water, graupel, and ice particles were present together in charged regions of thunderclouds. Latham and Dye [1989] concluded that most of the charge in thunderstorms is carried on particles greater than about 0.2 mm in size.

A more detailed discussion appears in Appendix 3. Appendix 4 concerns the effects of electric fields on water drops, and gives an indication of the expected polarities of charged particles at various heights. A review of literature concerning the distribution of charge in thunderstorms is given in Appendix 5.

3.3 *Concluding remarks*

This study employed a relatively large body of data (several hundred flashes that occurred during 13 storms) to show that the distribution of origin-heights was bimodal, with peaks 5.3 km and 9.2 km above msl. We found that origins clustered in localized active regions that exhibited a propensity to occur at or near portions of surfaces where radar reflectivities were 20 dBZ.

It is evident that we need to probe thunderclouds, rather than relying solely on techniques of remote sensing. These are some questions we might ask: Are regions enclosed by 20 dBZ surfaces almost uniformly charged, or does the charge accumulate near these surfaces? Are there any special microphysical properties of the charged regions adjacent to the centers of electrical activity? Why should some storms produce a majority of high flashes? Why should some thunderstorms that we recorded, have produced very little lightning, even though their echo-tops reached great heights?

The surprising polarity of high flashes suggests that it would be profitable to make a special study of these flashes. That study is reported in Section 5.

4 RELATIONSHIPS BETWEEN LIGHTNING AND PRECIPITATION
Part 2 LIGHTNING PATHS AND PRECIPITATION

4.1 *Data handling*

We have compared the paths taken by 135 lightning flashes that occurred during 11 thunderstorms with the appropriate precipitation patterns. (109 flashes are the subject of this report, and 26 were considered by Proctor 1983). Because both the lightning channels and the precipitation patterns were shaped in a highly irregular manner, and because both were three-dimensional objects, a procedure was adopted in which plan views were produced of thin slices taken through the precipitation at constant heights. These CAPPI's were drawn at intervals of 1 km , for example at heights 1.0, 1.5, 2.5, 3.5 km,..... above ground level (AGL) and on these were plotted the lightning that had been active in layers 1 km thick. For example, lightning that occurred between levels of 2 and 3 km AGL was mapped onto the CAPPI centred at 2.5 km. The CAPPI for 0.5 km was not used because of the effects of ground reflections. Points of strike, and lightning branches below a height of 1 km were mapped usually onto the CAPPI taken at 1 km height. Before this could be done, it was necessary to determine which hemispherical radar scan was appropriate for each flash. To this end, graphs of radar Azimuth vs time were prepared, and plan views of each flash were consulted in order to ascertain what range of Azimuths were occupied by the flash. As explained earlier, this was

necessary because the precipitation patterns changed with time. A note was made of the time that had elapsed between the instant when the lightning flashed and the time when its environment was viewed by the radar. A few vertical sections were made also. These involved a fairly laborious graphical procedure, which has since been obviated by computer methods.

4.2 Results

One surprising observation, which recurred frequently, was the tendency for later flashes to follow segments of channels that had been active during previous flashes. This despite the fact that channels decay in 80 to 100 milliseconds. (As noted by Malan [1963] and confirmed many times by our radio pictures). Later flashes sometimes extended paths taken by previous flashes, although it was more common for later flashes to share a part of the previous channel. Evidently, lightning does strike the same place again.

In the following text it is convenient to use the terms V20 and S20 to denote the volumes enclosed by the surfaces S20, which are surfaces where the effective radar reflectivity was 20 dBZ.

Flashes, or branches of flashes could be sorted into the following categories:-

1. Flashes that were wholly inside the volumes V20.
2. Flashes or branches that began at one edge of V20,

threaded V20, and either terminated at another edge or emerged there to extend beyond S20.

3. Those that began at or near S20 and extended into regions outside V20.

4. Those that tracked S20; i.e. they coincided with S20, for some distance. Usually, this distance did not extend over the entire length of the lightning branch.

5. Those that ran parallel to S20.

Examples of flashes in each of these classes appear in Figures 4.1 through 4.8 . We noted which flashes produced first streamers that extended "uphill" into regions of higher radar reflectivity, as well as those that extended "downhill" with the reflectivity gradient. We counted flashes whose branches terminated in, at, and outside S20. Summaries of these results are listed in Table 5. We also noted where lightning occurred in each storm, and where it did not. Table 6 lists regions where flashes occurred in relation to either the storm direction, or if the storm had been stationary, the regions were described in terms of the directions of the mid-level winds. The storm for 7 March 1979 was an exception because the mid-level winds were light and variable, and the storm remained stationary while increasing in area. Most of the activity occurred in the SE portion.

TABLE 5. Directions and Termini of Flashes

Date of Storm	Numbers of flashes that extended:-			Numbers of termini:-		
	up reflectivity-gradients	down	partway along S20	Outside the surfaces	At S20	Within
2 Mar 79	0	4 + 1E	5	5	0	0
7 Mar 79	9	19	16	20	11	8
27 Mar 79	12	23	24	19	20	20
8 Apr 79	2	24	0	0	0	0
24 Feb 84	3 (2b)	7 + 1E	6	7	4	4
24 Oct 84	0	9	10	10	10	6
21 Feb 85	0	4	3	4	1	3
26 Mar 85	2	6	8	5	3	2
16 Nov 87	0	11	11	11	2	11
Totals	28	107 + 2E	83	81	51	54

E denotes flash that travelled along edge, ergo neither up nor down gradient.
 (2b) indicates that 2 flashes travelled in both directions.

There was a tendency for the lower portions of the flashes to occur inside the contours, often well inside. At mid-levels the lightning occurred near S20, and at higher levels channels emerged from V20 and extended into lighter precipitation. Heights of these "mid-levels" varied considerably.

4.3 Discussion

A short description of the storms that produced this lightning is given in Appendix 6.

TABLE 6. Positions of Lightning wrt Storm Motion or Mid-level Winds

Date of Storm	Storm Motion or air-flow towards	Height of lightning	Numbers of flashes or branches at or near:-					
			Leading Edge	Centre	Trailing Edge	Both Flanks	Right Flank	Left Flank
2.03.79	SE	High	0	1	0	1	2	2
		Low	0	2	0	0	2	1
27.03.79	E	High	0	2	4	0	3	6
		Low	2	9	9	0	3	3
24.02.84	NE	High	1	0	0	0	0	0
		Low	1	0	2	0	4	4
24.10.84	NE	High	0	1	2	0	0	1
		Low	0	0	10	0	0	0
		Pt. of Str	1	0	8	0	0	0
21.02.85	Stalled*	All	1	2	1	0	1	0
26.03.85	NE	High	3	1	0	0	2	1
		Low	1	1	0	0	1	2
		Pt. of Str	2	1	1	0	0	0
16.11.87	Stalled*	High	1	0	2	0	1	1
		Low	1	5	5	0	0	2
Total		High	5	5	8	1	8	11
Total		Low	5	19	26	0	11	12
Grand Total		H + L	10	24	34	1	19	23

* Airflow to NE: High 6-8 km AGL: Low 3-4 km AGL:
Pt. of Str. = Points of Strike.

The totals in Table 5 show that most first streamers and leaders (107/135 = 79%) extended down the radar reflectivity gradients. Most began at contours for 20dBZ, and some entered the precipitation before progressing down the gradient. Most were endowed with branches or segments that tracked S20. These numbered 83/135 flashes or 61%. A minority of branches (54/186 = 29%) ended within the precipitation,

Figure 4.1 Portion of a flash that occurred almost wholly within the precipitation as defined by V20. (Only a small high section emerged). Here the plan view of a branch whose sources lay between the 2 km and 3km levels is shown with the contour for 20 dBZ at 2.5 km AGL.

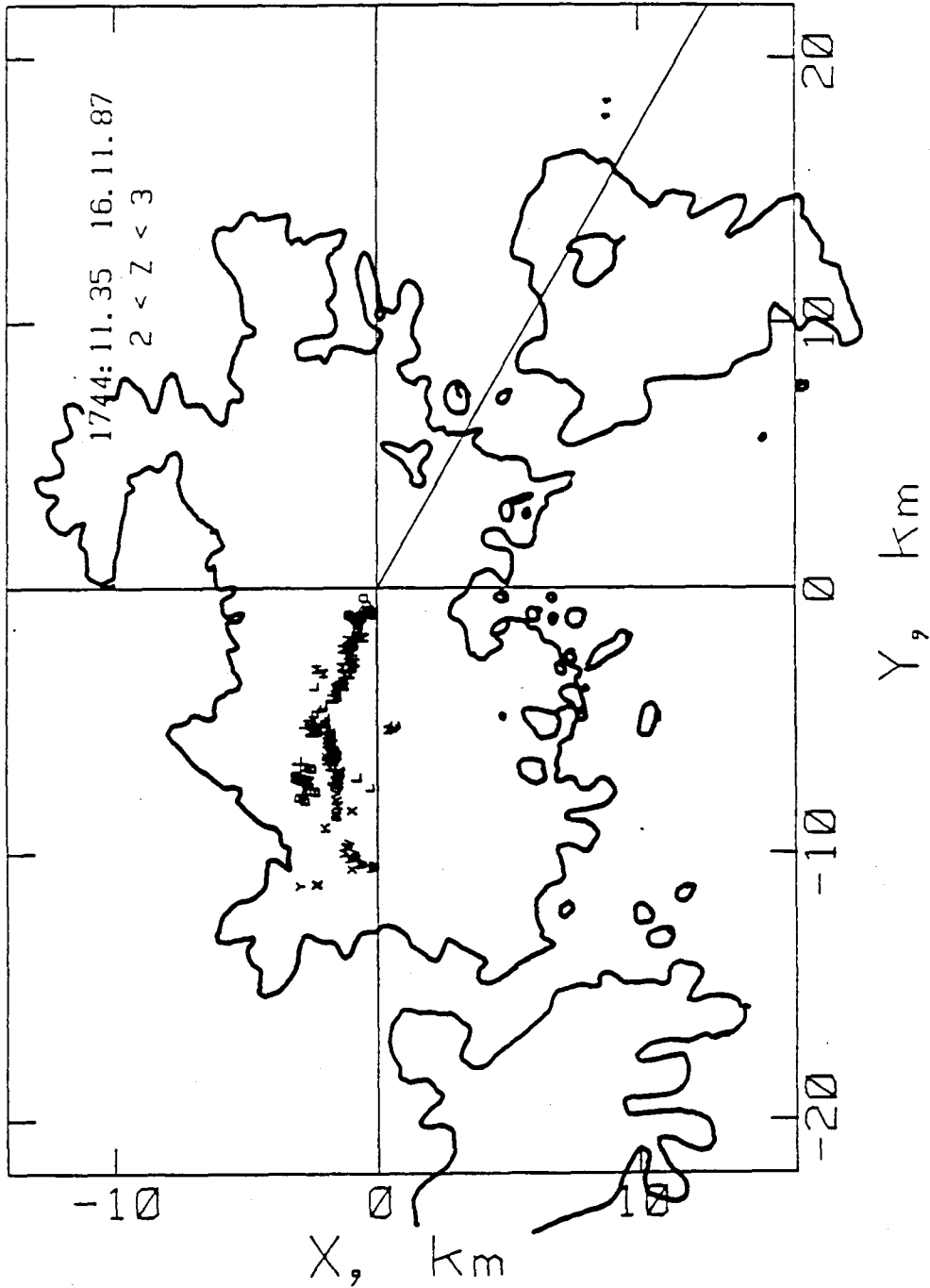


Figure 4.2 An example of a flash that began (at points A) at the 20 dBZ contour, and then threaded the precipitation so that one branch terminated at another part of the contour. (Points K) See also Figure 4.3.

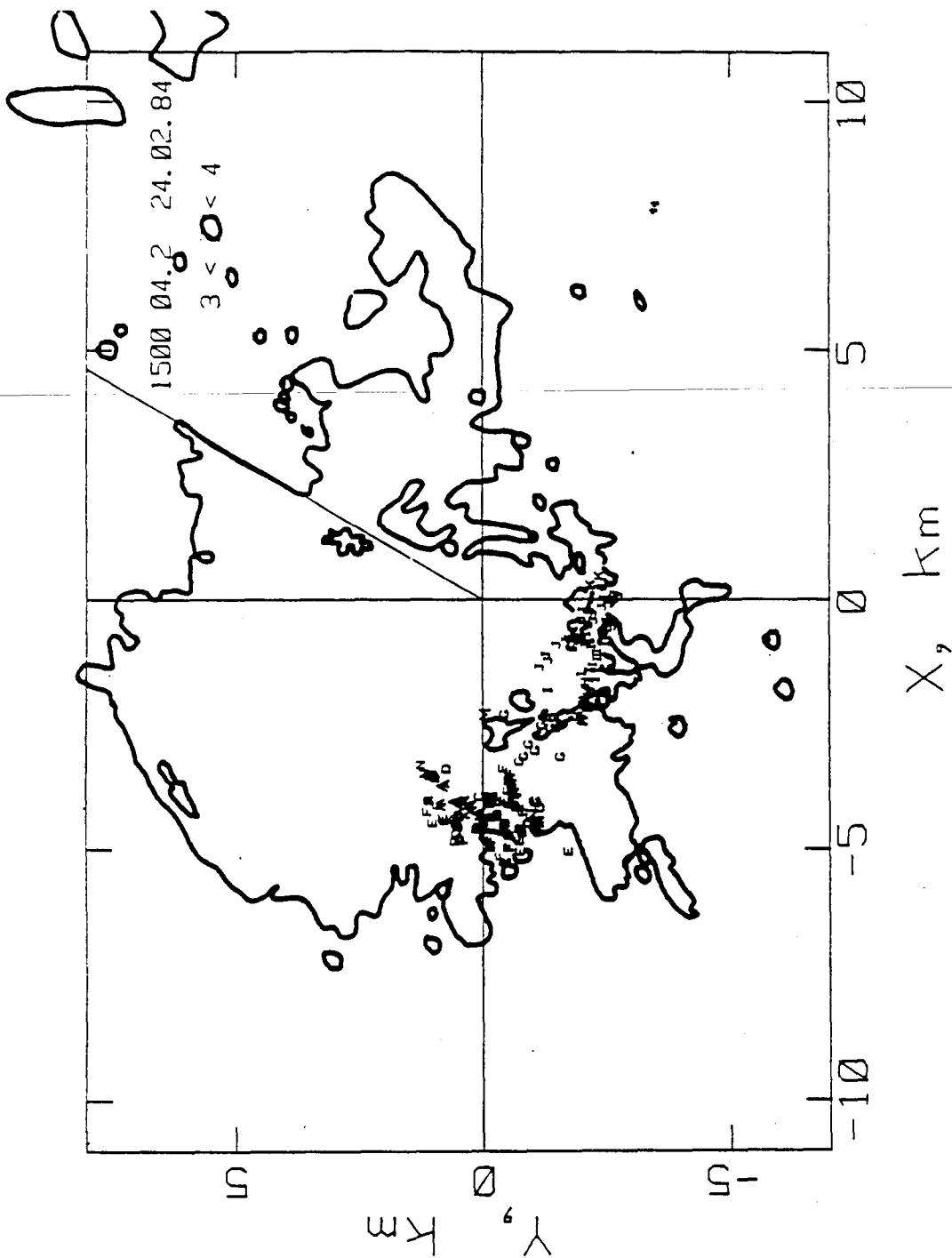


Figure 4.3 This flash began at A, on the 20dBZ contour. Branches that ended at G and K terminated at other parts of the 20 dBZ contour.

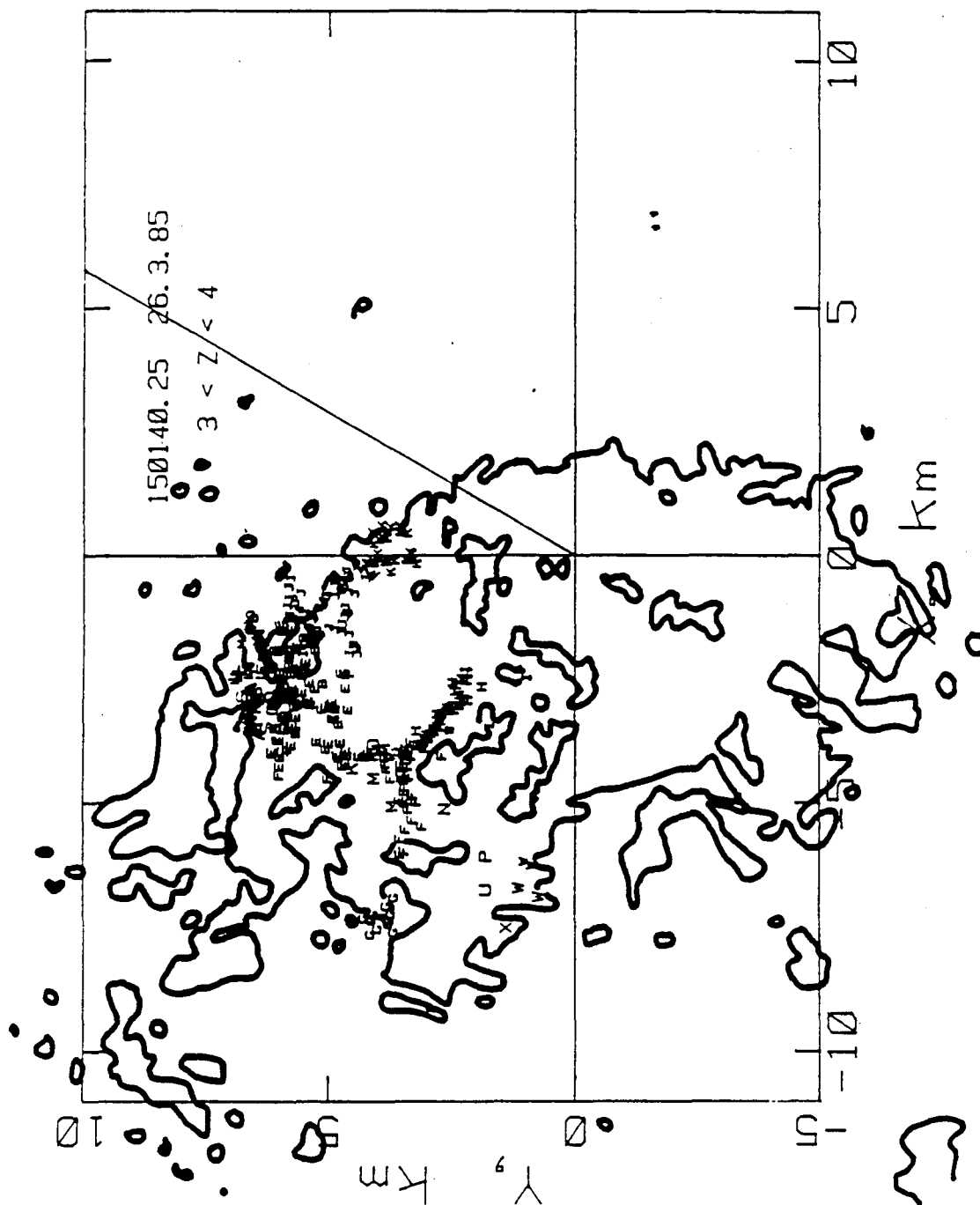


Figure 4.4 This flash began at A, on the contour for 20 dBZ, and extended to point 4, which was well outside V20. Notice the tendency to track the contour near the start.

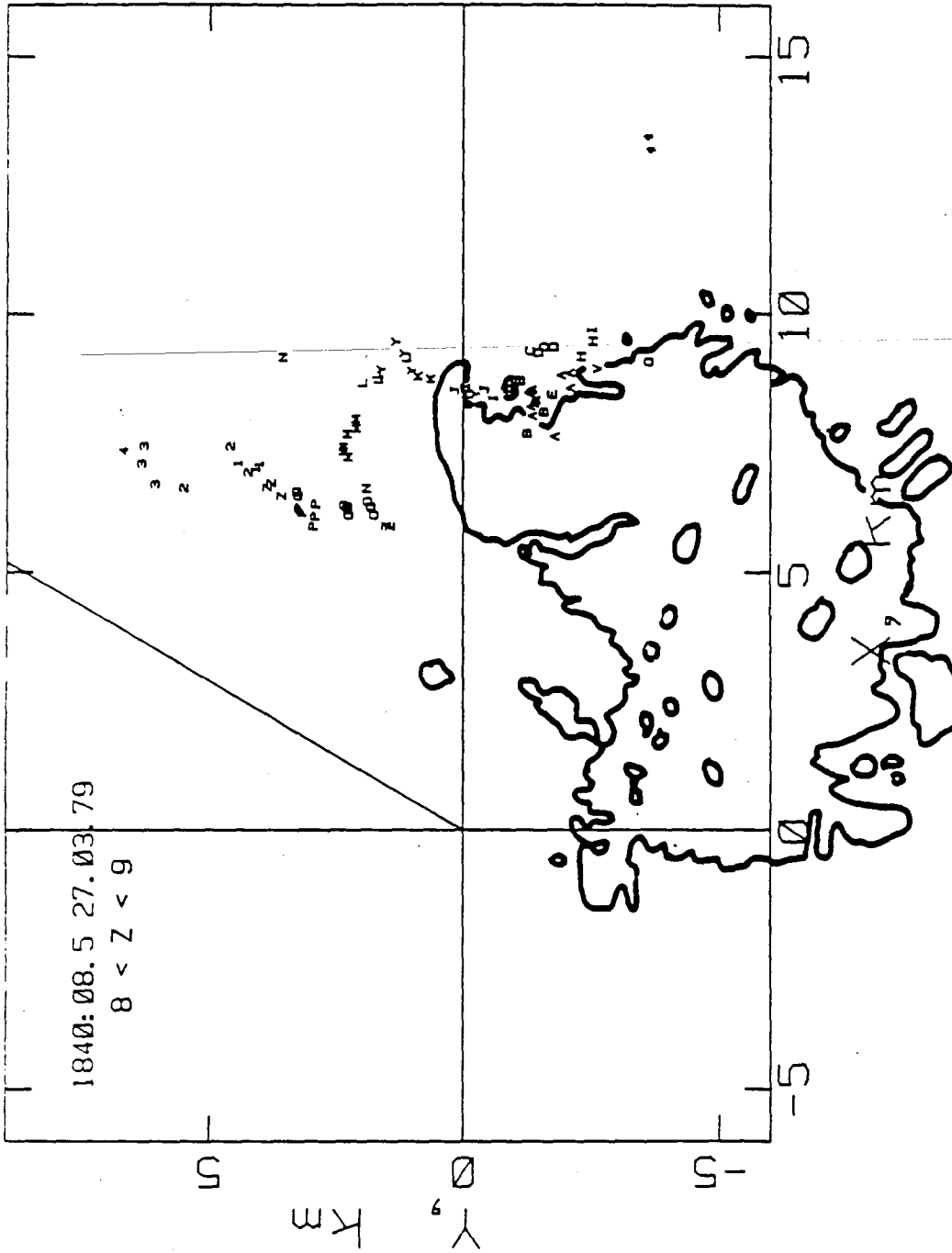


Figure 4.5 A vertical section through a storm, and through the main vertical part of this flash, a branch of which extended out and over the storm. The alphabetical symbol A marks a point near the origin of the flash, which was located 1 km behind the plane. The symbols Dot, Plus, Zero, Dash (., +, 0, -) indicate regions where radar reflectivity exceeded 20, 30, 40, and 50 dBZ respectively. The symbol h indicates enclosed regions where $Z < 20$ dBZ.

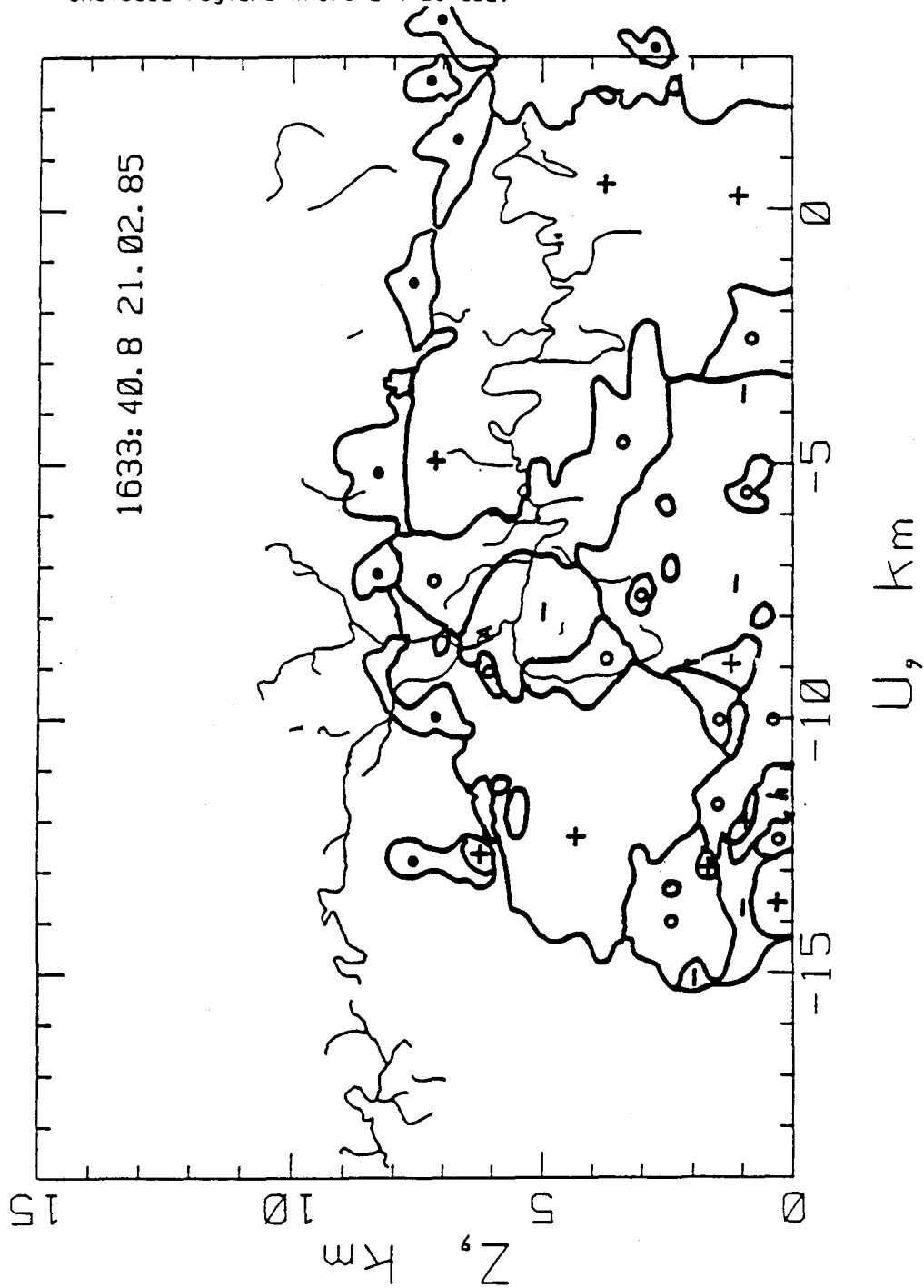


Figure 4.6 Plan view of Ground-Flash 150 in the height interval $3 < Z < 4$ km compared with the 20 dBZ contour at 3.5 km AGL. Alphabetical symbols indicate time increments of 10 milliseconds. The inset shows three views of the same flash. It is evident that the path of this flash had been guided by the precipitation. See also Figure 4.7, where symbols E plot this flash.

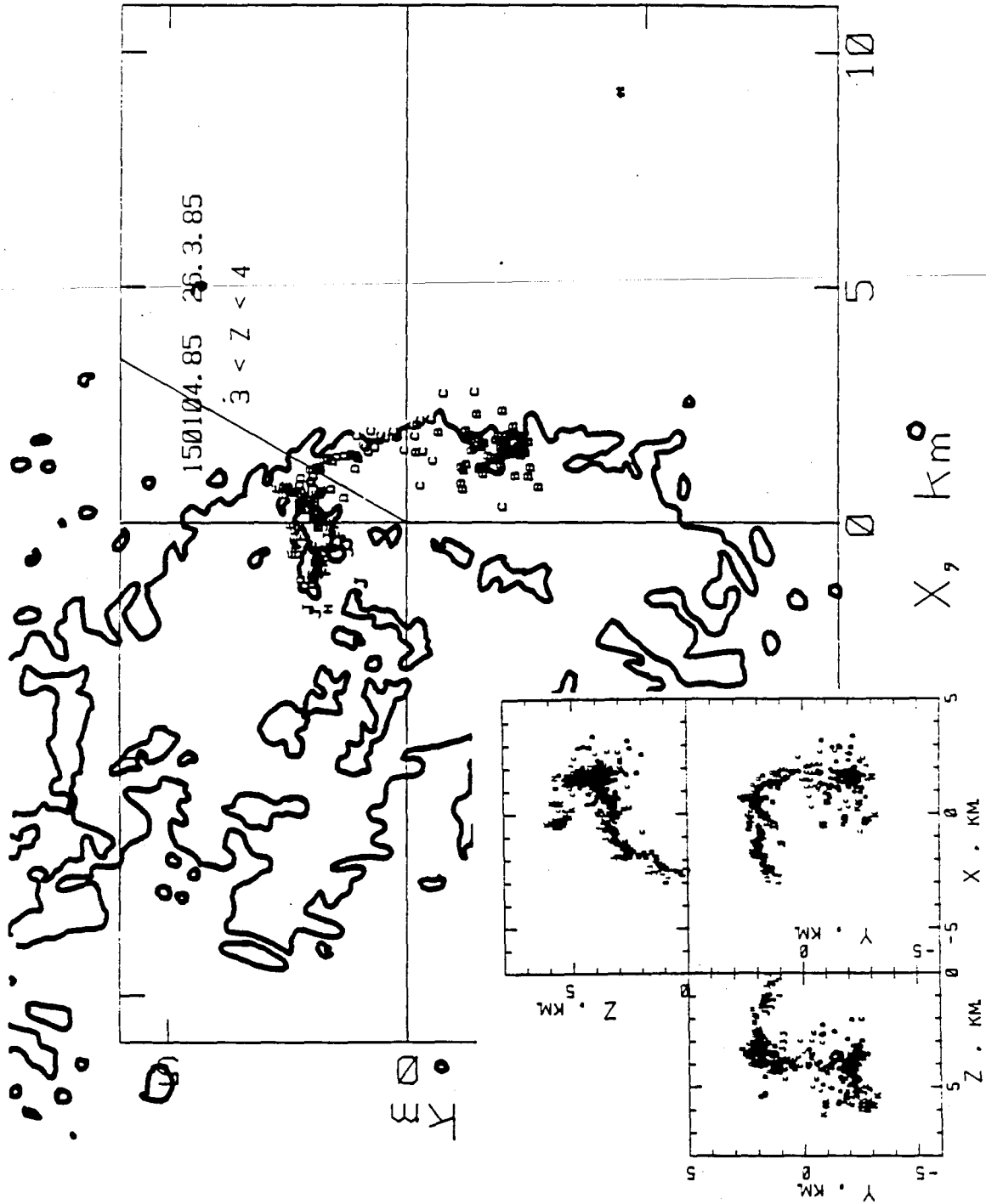


Figure 4.7 Plan view of the 20 dbZ contours at 3.5 km AGL showing portions of seven flashes at heights between 3 and 4 km. Alphabetical symbols denote the sequence of whole flashes. Flash 150 has the symbol E. The diagonal line is the North marker. Notice how much of the lightning occurs near the contours.

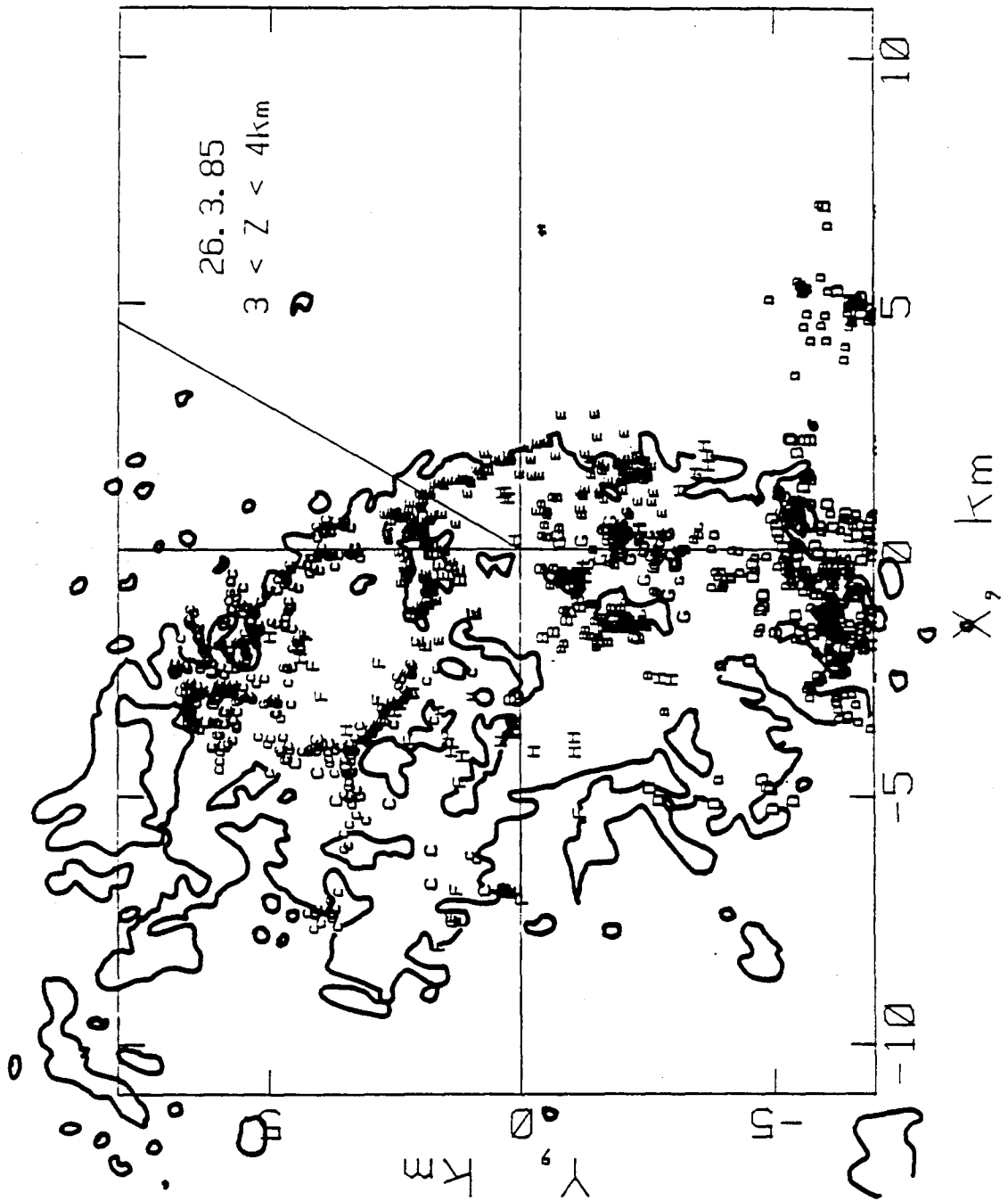
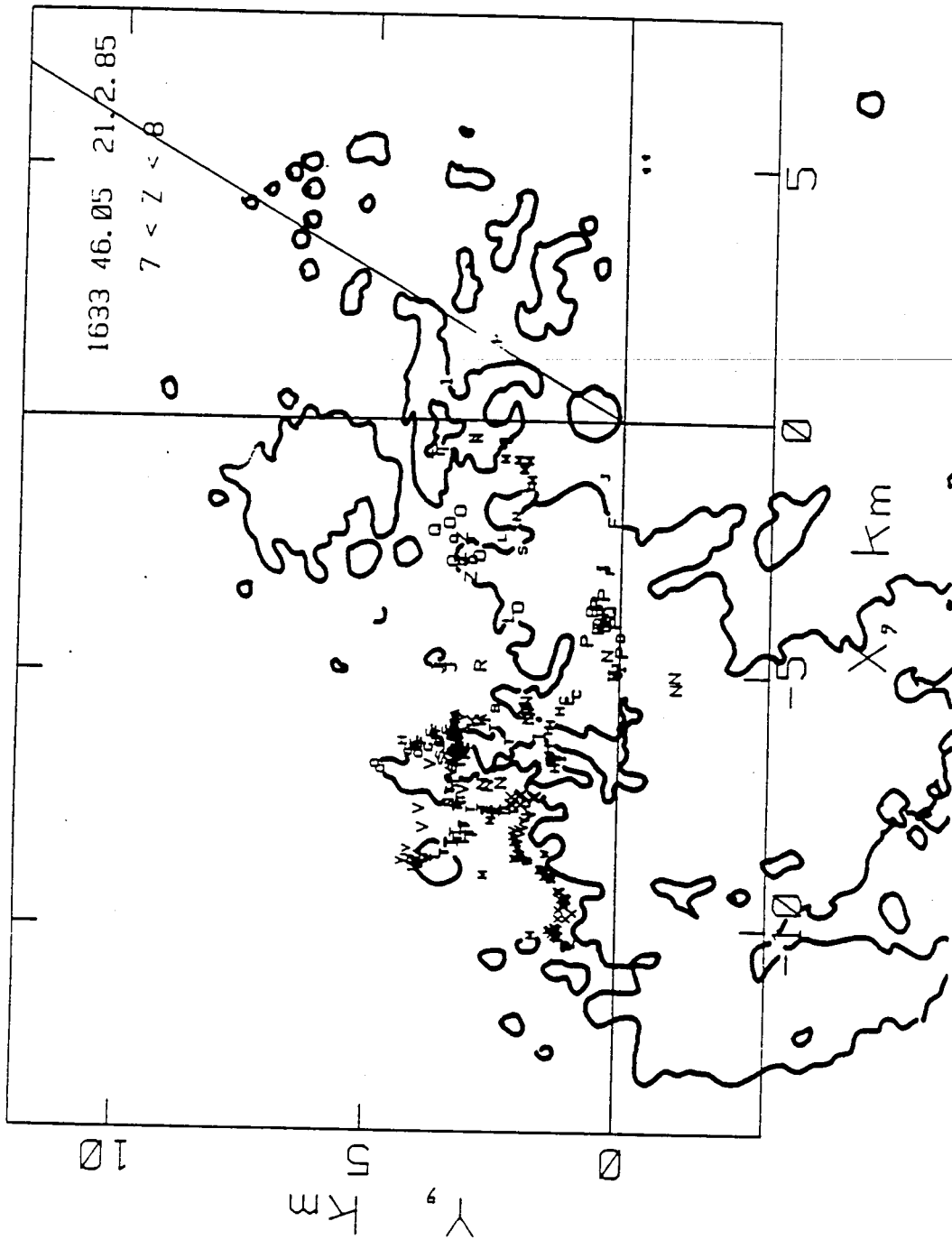


Figure 4.8 Plan view of portion of Flash 173 that lay between 7 and 8 km AGL shown with the contour for 20dBZ at 7.5 km. Notice how the branch TUVWXYZ ran parallel to the contour.



and most ended at S20 or outside. Table 6 shows that most channels occurred in the central region of the storms or near the trailing edges of the storms, and that there was an almost equal probability occurrence on either flank. This result must be qualified by the statement that these were small storms.

One of the more striking features of this exercise has been the degree of variability and inconsistency exhibited by the subject. One storm will behave in a certain way which appears to be reasonable and definite, and so creates an impression that the investigator has discovered a rule that governs the behaviour of thunderstorms. The next storm of that kind to be studied then breaks the newly found "rule" and does not behave in that way at all. One is given the impression that we have not observed the important factors which govern the behaviour of storms. Observations of known microphysical parameters may prove to be relevant, but it may be true to say that the really important quantities, principles and phenomena have not been discovered yet.

One characteristic has appeared more regularly than the others: This has been the tendency for lightning to occur near the surface for 20 dBZ. One example is shown by Figure 4.6 which shows a part of Flash 150. There were many cases in which the lightning image coincided with the contour, but this did not always happen. Some flashes marched right across the precipitation and ended at the other side of the storm as shown in Figures 4.2 and 4.3 Yet others extended into regions that did not reflect nearly strongly enough to cross our

detection thresholds. Examples are shown by Figures 4.4 and 4.5. Despite the varied behaviour, frequently it became evident that the surface that we called S20 had played a role. The question then arose as to whether this had been due to some intrinsic property, or whether S20 had merely served to envelop the functional region. Table A7.1 in Appendix 7 was produced to assuage a curiosity. Its calculation is subject to the assumptions that drop-sizes had been distributed according to the Marshall-Palmer law, and that no ice had been present. The outcome is not sensitive to changes in the drop-size distribution, provided that they reflect reality. The assumption concerning the absence of ice probably is not valid. Table A7.1 shows that the smaller drops provided most of the capacitance (which is proportional to drop radius) and that the smaller drops would store most charge if square-law mechanisms, such as one described by Dawson [1969] were in operation. Dawson's work is reviewed in Appendix 4.

If we pursue the notion that S20 enclosed the charge that caused an electric field high enough to initiate lightning, then the idea of a screening layer, put forward by Vonnegut [1963], and discussed by Brown et al [1971] comes to mind. This supposes that the thundercloud becomes charged in a diffuse manner so that the density of this internal charge is not sufficient to produce electrical breakdown, and yet is sufficient to attract charge of an opposite polarity and to cause it to migrate to the thundercloud, whereupon it eventually becomes attached to particles in the thundercloud. These particles are relatively immobile, so that the

attracted charge does not diffuse. Instead, it accumulates and so produces E-fields that are large enough to initiate lightning. This line of reasoning is not entirely convincing. The shielding layer must eventually shield-off and minimize the attractive force of the internal charge. What is interesting is the observation that lightning begins in particular regions which act repeatedly to initiate lightning, and furthermore, other regions, also on S20, become charged oppositely so that they serve to guide the lightning, which also happens more than once. (The idea that flashes are guided by local E-fields at streamer-tips is supported by observations that are to be described in Section 5 which relates to some properties of flashes with high origins.) Evidently, charge of either sign can accumulate in shielding layers, and evidently, we have to do not only with charge separation in thunderclouds, but also charge storage and intensification of charge in localized regions. The charge that was separated initially need not be intense. It merely has to occupy a large volume. There must be enough, say 3 to 5 Coulombs. It need not itself be sufficiently dense to be discharged by the lightning. It may just camp there and continue to attract external charge. These speculations highlight a need to probe thunderstorms.

4.4 *Concluding remarks*

Lightning followed a variety of paths, but frequently tracked, began and ended on surfaces for 20 dBZ. Sixty-one percent of the flashes had segments or branches that tracked S20. Most lightning extended down the reflectivity gradients; 22% did

not. Most lightning channels in the lower regions were located in the central regions of the storm or near the rear of these small storms.

5. LIGHTNING FLASHES WITH HIGH ORIGINS

5.1 *Introduction*

In Section 3 and in Appendix 3 we explained that we had found that flashes that began in the higher regions were also flashes that discharged excess negative charge. This result prompted a special study of 21 of these flashes. The report, as submitted to Journal of Geophysical Research for publication, appears here as Appendix 8. Only a few main points are set out in the next section.

5.2 *Summary*

1. These flashes have origins at heights greater than 7.4 km above msl. They have distinctive properties in that their steps are longer than the steps of the low flashes. Their radio sources (associated with step length) are greater, and they emit pulses very much less frequently. They carry more charge and current than the lower flashes.

2. Flash 87, shown in plan in Figure 5.1 began at (8.79, -4.7, 6.8) km. The Z -coordinate is stated with respect to ground level. The flash then followed an almost circular path and eventually reached points M and P within 1.5 km of the origin, instead of flashing across directly. Alphabetical symbols denote the time-scale. It is reasonable to suppose that the path had been determined by the instantaneous E-field

at the streamer tip, which in turn, had been determined by the distributed charge. Evidently, at time A, the E-field was directed more strongly towards the region B, and only when it had reached region K, was the E-field such as to direct the path to region M. Figure 5.2 shows the almost horizontal path mapped onto the precipitation pattern shown by the CAPPI for 7.5 km AGL. Again, the propensity to track the contours for 20 dBZ is evident.

:

3. Flash 123 began as a negative discharge. When it had reached a particular region, its polarity reversed and the flash continued as a positive flash, as shown by the electric field-change meter. The behaviour of this flash substantiates the assertion in the discussion of the previous section, where we stated that positive charge usually does not accumulate with sufficient density to initiate a flash in the active part of a thundercloud. Maps of this flash appear in Appendix 8 as Figure 10, 11 and 12.

4. In view of the published conjectures concerning the orientation of cloud flashes, (see for example Brook and Ogawa [1977] and Smith [1957]) some statistics are given regarding the numbers of horizontal branches (54/92) and vertical branches, and the directions in which the discharges took place.

5. This study confirmed that these flashes were negative flashes; i.e. they carried an excess of negative charge. An exception was noted under item 3, and even that flash began as a negative flash.

Figure 5.1 Plan view of pulse-sources active above an altitude of 6.5 km AGL during flash 87. Symbols change for every 20 milliseconds.

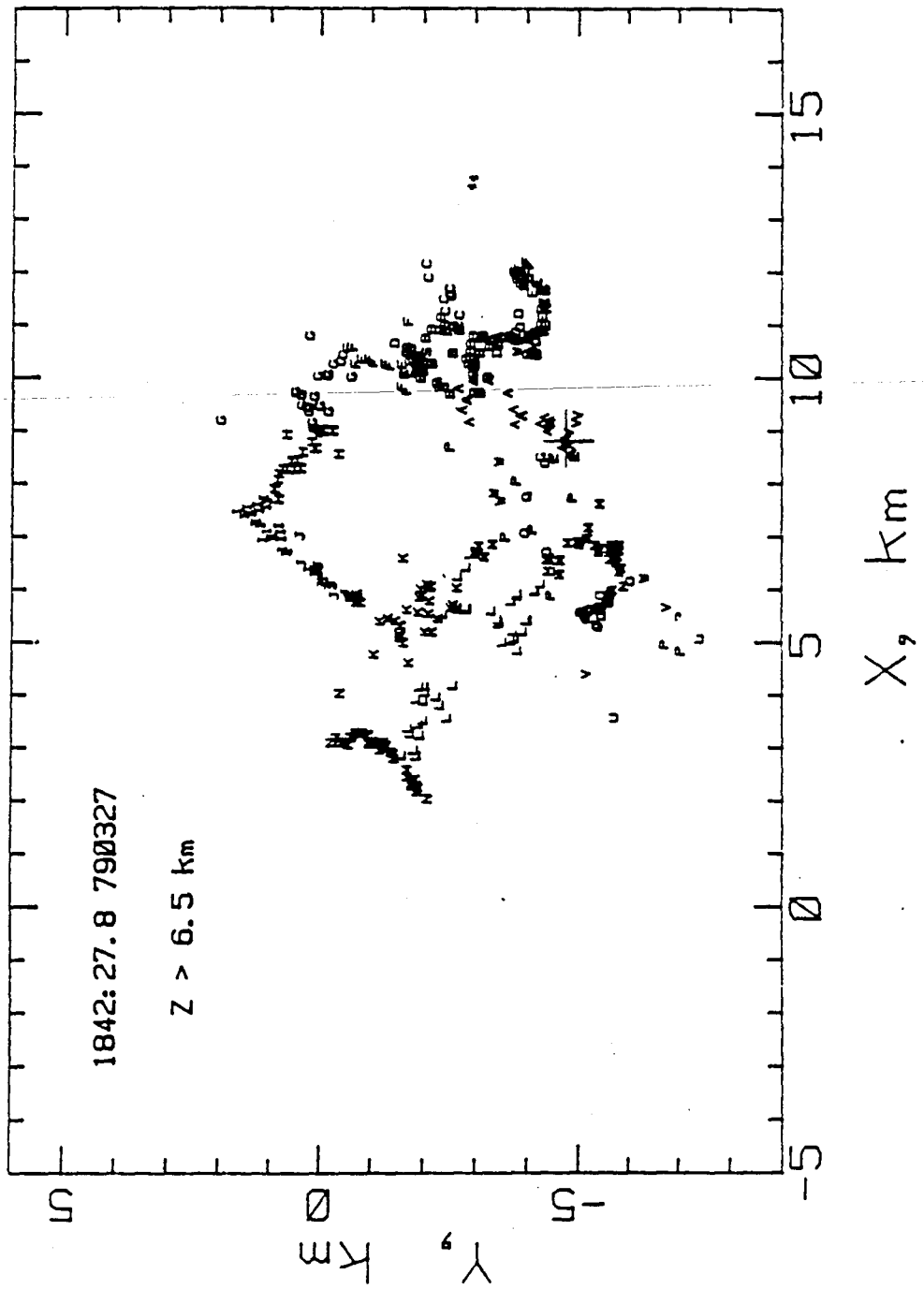
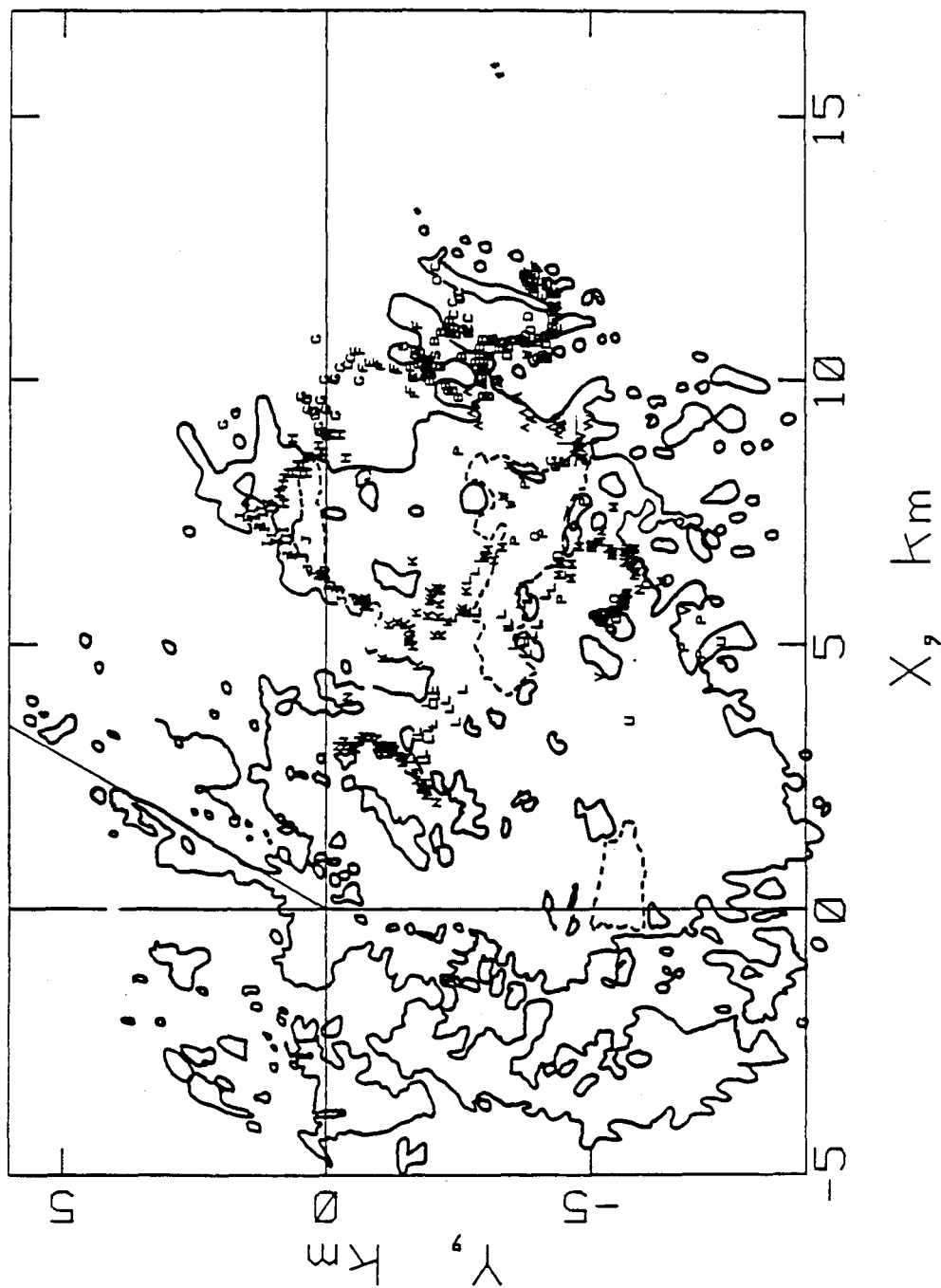


Figure 5.2 Sources of pulses active at heights above 6.5 km AGL during flash 87, and Radar Reflectivity contours for 20 dBZ and 50 dBZ (dashed) at a height of 7.5 km.



6. REAL-TIME OBSERVATIONS, AND ATTEMPTS TO USE AN
INSTRUMENTED AIRCRAFT

This is mentioned as item (b) in the work-plan set out at the beginning of this report. The need to probe these thunderstorms has been emphasized in previous sections of this report. We have found that many flashes begin at special places on the 20 dBZ surfaces. Moreover, flashes tend to track these surfaces. By probing the thundercloud, we could ascertain what constituents are present in each of the regions. Moreover, by probing we should be able to discover how the charges are distributed.

The aircraft was based at Nelspruit. Five conditions had to be satisfied, for joint operations to take place. The most important were:- (1) There had to be an approaching storm. (2). The aircraft had to be free of other responsibilities. Its work in the Eastern Transvaal had precedence. It so happened that on most occasions, stormy conditions at Nietgedacht coincided with similar conditions in the Eastern Transvaal. In spite of many attempts, no successful joint operations came about.

7.0 THE STUDY OF RADIATION AND ELECTRIC FIELD CHANGES
PRODUCED BY PROCESSES THAT PRECEDE AND ACCOMPANY DART
LEADERS.

This is mentioned in part (c) of the work-plan. A detailed account of the work is contained in a paper in Appendix 9. entitled "Radio Noise associated with Subsequent Strokes of Lightning".

Lightning emits radio disturbances of two kinds which differ in waveform. One kind is the pulsed emission. These pulses are typically one microsecond or less in duration, and are radiated by steps that occur in first streamers and stepped leaders. The second kind consists of relatively long trains of band-limited noise. This means that the details of the waveform depend on the apparatus to some degree. These waveforms often begin and end gradually, and it is then difficult to select features that can be recognized on waveforms received at separate stations. It seems that the gradual increase in amplitude occurs when the wave exits a channel having a decreasing degree of ionization. Another reason why common features are difficult to find on the waveforms received at different stations concerns the speed of the wave that causes the lightning to generate this noise. Another factor is the shape of the channel. Waves emerging from different parts superimpose in a different way in each direction. Both kinds of noise (pulses and trains) are caused by ionization of air. Currents that flow along channels that had been ionized by a previous event cause electric

field-changes that we can record and measure, but they do not cause the channel to radiate radio noise, except where the flow of current causes the channel to extend, which it does by ionizing the air. The paper demonstrates that shielding also occurs and so attenuates radiation from channels that had been ionized previously. The results also demonstrate some important limitations of radio methods for studying lightning, as well as providing new information regarding dart leaders and subsequent return strokes.

8. POSITIVE FLASHES TO GROUND

The recordings taken by us over the years since 1969 were searched in an attempt to find a recording made by a positive flash to ground. This was done by inspecting all the recorded electric field-changes, noting the possible candidates, and then reading the noise recordings. We have no record of a positive flash to ground. One reason is that positive flashes strike ground well after the storm has passed. The duration of our records was limited to 16 minutes, which was the time taken to use 1000 feet of film. We were loath to use more than one per storm in view of the high cost of film. However, one positive cloud-flash has been analyzed (it was reported by Proctor 1981) and also a cloud-flash that began as a negative flash and which changed polarity. This flash has been described in an earlier section of this report.

9. A STUDY OF RADAR REFLECTIONS FROM LIGHTNING

The benefits of using metric radar to study lightning appeared to be considerable. Radar could be used to supplement radio pictures, and to supply information that was not readily available from the radio pictures. Hewitt [1957] had shown that radar echoes from lightning persisted for many tens of milliseconds after their first inception. By contrast, radio noise accompanies ionization and therefore is emitted only during the incipient stages of lightning channels. Moreover, subsequent flows of current along existing channels cause no radiation at VHF except where they cause the channel to extend or to re-ionize, but these currents do cause increases in echo-intensity, and therefore the use of radar would detect them, and show which portions of the flash had been involved. Thus radar could supply information about lightning after the channels had formed. We therefore arranged to record radar returns from flashes while recording also their radio emissions, so that we could compare the radar pictures with radio pictures. These efforts are described at some length in Appendix 11. The main points can be summarized as follows:

There were several problems. First, the use of normal techniques to scan a volume of sky with a narrow-beam was not appropriate, because the chance that the lightning would occur in beam was too low, and the recorded history of a particular lightning flash would become punctuated, limited

and convoluted with the sequence of the antenna scan. I resorted to floodlighting a large sector of the sky with a powerful radar transmitter, and then locating the echoes in the same way as the sources of radio noise were located. One result was that some scenes were limited by the extent of the transmitter beam. Although wide, it had not been made wide enough. The restrictions in beamwidth had become necessary due to a lack of transmitter power. Second, the returns were affected, and their spatial extents had been limited by mutual interference of the reflected waves at the target because we had used single frequency (monochromatic) coherent transmissions. This difficulty could have been avoided by sweeping the transmitter frequency. The idea did not occur until I had attempted to explain why the echoes were so lacking in extent.

The pictures that we analysed and compared with the radio pictures showed that there were severe problems caused by the obstruction of the radar waves by other components of the lightning flashes that had been situated in places where they obscured the view. The problem is very similar to one which arises from the use of short wavelengths for weather radar. It is widely known that radars which operate at wavelengths much shorter than 7 cm are unable, in varying degrees, to see rain through rain. In this case we were unable to see lightning through lightning. Some flashes consisted of only one or two filaments. These were "open" structures, and the chance that one part of the flash would obscure another part of it was low. On the other hand, many flashes occupied considerable volumes, despite the fact that

their channels were also filamentary. Their branches were so long, so many in number, so profusely tangled and so intricately entwined, that they populated large volumes with networks of strongly ionized, overdense channels, with the result that the nearer, or exterior members very effectively shielded returns from the interior and more distant channels. These results explained why lightning echoes behaved in the way that has been described by previous investigators, such as Hewitt [1957] and Mazur [1986]. Incidentally, these results also explained why the radio emissions from lightning seem to vary so widely in amplitude. The reason is that they are often attenuated by intervening channels.

The comparisons that we made also showed that any lightning channel may reflect radar signals, and not just the "junction streamers" as some had reported previously. We recorded reflections from stepped leader channels, from return-stroke channels, and from cloud-flashes.

This work showed that, if radar is used intelligently, with prior knowledge of the streamer configuration and its relation to the radar having been supplied by other means, such as radio, then the radar echoes can provide useful information regarding lightning.

10. CONCLUSIONS

We determined the regions where several hundred lightning flashes began during thirteen storms, and found that most began at selected places on the surfaces where radar

reflectivities were 20 dBZ. Heights at which these flashes began were distributed about two modal heights which were 5.3 and 9.2 km above sea level. We expect lightning to begin where electric fields are highest, and we concluded that flash-origins were adjacent to regions where charge had accumulated, and that charged regions lay within the surfaces where radar reflectivities measured $100 \text{ mm}^6 \text{ m}^{-3}$. Paths taken by some 100 lightning flashes were compared with radar precipitation patterns. Sixty-one percent of these flashes were endowed with segments that tracked surfaces where radar reflectivities were 20 dBZ. 78% of the flashes extended down the reflectivity-gradients so that they progressed from relatively wetter to relatively drier regions.

Flashes that began at higher levels were found to have properties that differed from the lower flashes, and these properties were investigated. We also studied radio noise emitted from dart leaders and from return strokes, and found that many of these emissions had been shielded.

A specially-constructed metric radar was used to observe radar reflections from lightning channels, and to compare the positions of the echoes with radio pictures of the same flashes. It became evident that remote portions of these flashes had been obscured from view by the intervening lightning. The limitations and benefits of radar as a means for observing lightning were noted.

A SHORT ESSAY ON LIGHTNING

Lightning flashes are usually bounded in extent by the sizes of their host thunderstorms. Many are hidden by intervening cloud. When they emerge, their filamentary nature becomes obvious. The remainder appear as diffuse, two-dimensional flashes of light, and are misnamed sheetlightning. Approximately, one in every six flashes strikes ground. These ground-flashes evoke the most interest, because they cause damage, pain and death, and because they are more amenable for study than cloud-flashes. The electrical nature of lightning was demonstrated by Benjamin Franklin in 1749. Lightning differs in many respects from even the very longest laboratory sparks.

Ground-flashes begin with a precursor, called a *leader*. Usually, this leader progresses from cloud to ground. Most leaders carry an excess negative charge, which the leader distributes along its path. The line-density of this charge is approximately 1 Coulomb per kilometre. When it approaches within 100 or 200 meters of ground, or else when it strikes ground, the leader initiates a *return stroke*. This is a brilliant wavefront of luminosity that travels up the path or channel forged by the leader. The return stroke conducts the distributed charge to ground. Its brilliance diminishes with distance travelled up the channel. It is analogous to a reflected wave on a lossy transmission line whose end has been short-circuited.

During the course of a lightning flash, the sequence of events comprising the leader and return stroke, may repeat 0 to 30 times. The average is 4, but it is very variable, and in some seasons, few repeat. Intervals between successive strokes range 15 milliseconds to 160 milliseconds, with a modal value near 50 milliseconds. Separate strokes of a flash are shown in Figure A1.1.

Leaders of first strokes extend as successions of steps that form almost head-to-tail. Their lengths range 50 metres to 300 metres. Steps reach maximum brilliance in times less than 500 nanoseconds. During this time, the air temperature rises approximately 30 000 degrees Kelvin. (It is a truly remarkable natural explosion). The step may last one microsecond. Its luminosity decays in hundreds of nanoseconds. Darkness follows for some 50 microseconds until the next step forms. The path pulses with a faint luminosity, in the wake of each step. An early photograph of a stepped leader is shown in Figure A1.2.

Nearly all subsequent strokes follow paths taken by leaders of first strokes. Leaders of subsequent strokes differ from stepped leaders, which occur when new paths form. The leader of a subsequent stroke is termed a *dart leader*. As shown by Figure A1.3, it appears as a localized wavefront of luminosity that runs smoothly down the channel. Its speed is almost ten times the speed of stepped leaders. The speed of a return stroke is approximately one-third of the speed of light. A dart leader may travel at one hundredth of the speed

of light. A stepped leader progresses at an overall speed almost one-thousandth of the speed of light. These quantities exhibit considerable dispersion. Leaders carry currents of the order of 300 Amperes. Return stroke currents range 7 kiloAmperes to 300 kA, and the median is approximately 30 kA. Stepped leaders, and their counterparts that occur in cloud-flashes are often termed *streamers* because they are extending filaments of ionized gas. It is interesting perhaps to note that filamentary emissions from the sun bear the same name, although they are emissions of ionized gas that extend into vacuum at speeds more characteristic of dart-leaders.

Most of our knowledge of lightning was discovered in South Africa by Schonland and Malan and their colleagues in the years 1926 to 1956. Very little accurate information concerning cloud-flashes was available before they were studied by means of radio-pictures. This will be the subject of another section of this report.

Useful references of a general nature include the following:

Malan, D. J., *Physics of Lightning*, 176pp, The English Universities Press Ltd, London 1963.

Uman, M. A., *The Lightning Discharge*, 377pp, Academic Press Inc., 1987.

Golde, R. H., *Lightning Vol. 1: Physics of Lightning*, 496 pp, Academic Press, New York, 1977.

Bibliographical References used in Figure Legends:

Schonland, B. F. J., D. J. Malan, and H. Collens, Progressive lightning 2, *Proc. Roy. Soc. London, A*, 877, 595-625, 1935.

Schonland, B. F. J., The Lightning Discharge, in *Handbuch der Physik*, Edited by S. Flugge/Marburg, Vol 22, 576-628, Springer-Verlag, Berlin, 1956.

Figure A1.1 Photograph of a flash to ground taken by means of a Boys' Camera. The camera has two lenses mounted 180 degrees apart on a circular disc that rotates about an axis normal to the stationary film. Thus it produces a circular timebase in which any lateral motion of the flash can be unscrambled from the time-scale. Taken from Schonland et al [1935].



Figure A1.2 Photograph of a Stepped Leader and the following Return Stroke. Time elapses Right to Left. Taken by Malan in the open veld in a region now the suburb of Linden. Published by Schonland et al [1935].

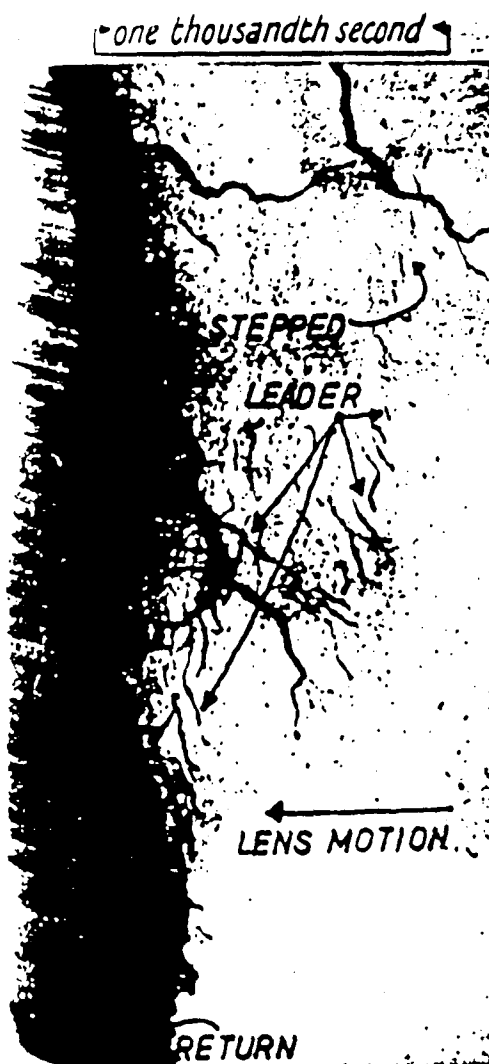




Figure A1.3 Boys Camera photograph of a Dart Leader (right) followed by a Return Stroke. Schonland [1956].

Appendix 2

RADIO PICTURES OF LIGHTNING

This is a short essay that describes the usefulness, efficacy and limitations of using radio pictures to study lightning.

In 1965 most of our knowledge of lightning had been gained from photographs of the portions of lightning flashes that emerged from cloud. This had been supplemented by measurements, taken at ground level, of electric field-changes (EFC's) caused by the lightning flashes. The interpretation of the EFC's was subject to many assumptions, some of which proved to have been false. Wilson [1920], p. 89 suggested that EFC's should be measured simultaneously at several stations in order to find what quantities of charge were involved. Krehbiel et al [1979] used eight stations to obtain some excellent results, but even these measurements were made subject to the assumption that the problem has only eight degrees of freedom, and therefore have their limitations. For example, there is a centroid of a region that supplies charge to the flash. We shall call it P1. The flash acts to take charge Q from P1 and to distribute it along the path. The centroid of the distributed charge is P2. There are seven unknowns: three spatial coordinates for P1, three for P2, and another is the quantity Q. The point P2 is often taken erroneously to be the endpoint of the discharge, whereas P2 may not even lie on the path.

Oetzel and Pierce [1969] published a suggestion that radio noise emitted by lightning could be used to track its progress. They suggested that a system of short baselines should be used. By this time, we had already obtained our first results using a long baseline system, which Dr. F. J. Hewitt had suggested might be useful to find points of strike. The three-dimensional, time resolved pictures that we obtained of the lightning flashes yielded accuracies 25m x 25m x 140m to 200m in the three spatial coordinates of each component point and these measurements were supplemented by measurements of EFC and by radar images of the precipitation patterns of the storms that hosted the flashes.

A2.2 *Results obtained using this method included:*

1. Contrary to the opinion of Malan [1965], cloud flashes were initiated by stepped leaders.
2. Cloud flashes produced subsequent strokes, in a manner similar to those observed in flashes to ground.
3. Flashes that began above a level near 7 km amsl had properties that differed markedly from lower flashes.
4. After the main channels had formed, lightning flashes proceeded to extend short rapid streamers from points close to the origin, in directions opposite to the initial extension. These streamers resembled the "roots" of the flashes, but did not cause large EFC's.

5. The main channels of many flashes numbered more than one, and in particular, flashes often followed multiple paths to ground.

6. Currents and charges that flowed in cloud-flashes could be measured by using recorded EFC's, because the lightning paths were known.

7. Statistics regarding lengths and directions of streamers were obtained. Better estimates of discharge-rates were deduced.

8. Accurate statistics of step-length, step-orientation and step-lifetimes were obtained.

9. Radio noise from lightning was associated closely with the ionization of air. It became evident that charge-separations which accompany the breakdown of the gas are the cause of the radio emissions.

10. As described in the main report, we were able to locate accurately both the starting points of flashes, and the paths which the flashes subsequently followed, and to map these on weather radar pictures of the storms.

A 2.3 *Limitations of this method include:*

1. The short, rapid streamers, mentioned in item 4 above, could not be mapped completely because radio noise emitted by

some portions of these streamers "overprinted" the noise emitted by other parts of the same streamers. Many of the waveforms of the noise radiated by these events were not amenable to accurate timing. This was in contradistinction to the pulsed emission from other processes. Figure A2.1 shows examples of the waveforms of radio noise.

2. Any radio noise emitted by current flows along streamers that had been ionized by a recent event, was screened by the ionized gas, and in consequence could not be received. This meant that return strokes and dart leaders (precursors of later strokes that follow previously-established paths) could not be observed except where they extended the older channels.

3. The process of measuring the time-delays, computing the source-positions, and mapping their positions was slow and tedious.

A 2.4 *Bibliographical References*

Krehbiel, P. R., M. Brook, and R. A. McCrory, An analysis of the charge structure of lightning discharges to ground, *Jour. Geophys. Res.*, 84, C5, 2432-2456, 1979.

Malan, D. J., The theory of lightning, in *Problems of Atmospheric and Space Electricity*, edited by S. C. Coroniti, p 324- 331, Elsevier Publishing Co., Amsterdam, 1965.

Oetzel, G. N., and E. T. Pierce, VHF technique for locating lightning, *Radio Science*, 4, 3, 199-202, 1969

Wilson, C. T. R., Investigations on lightning discharges and on the electric field of thunderstorms, *Phil. Trans. Roy. Soc. London A*, 221, 73-115, 1920.

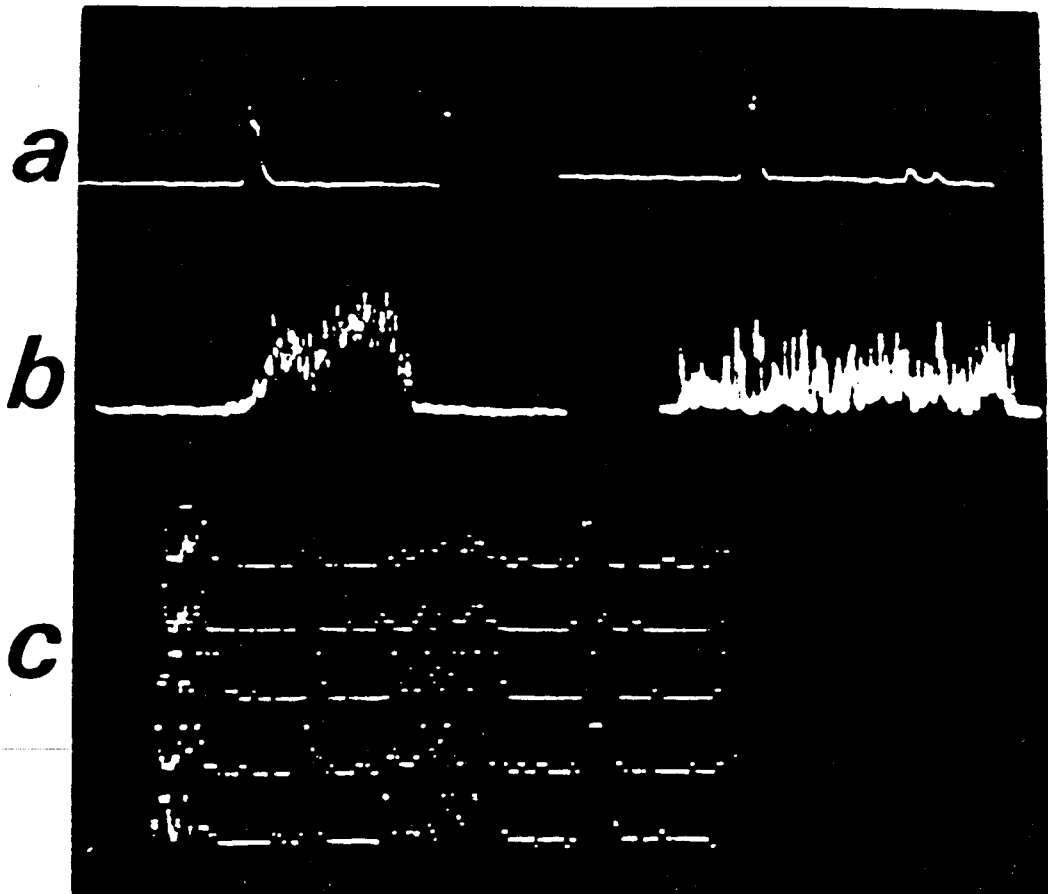


Figure A2.1 Waveforms of radio noise emitted by lightning.
 (a) Pulses approximately one microsecond wide.
 (b) Q-noise 30 μ s and 45 μ s in duration.
 (c) Pulses received at five widely spaced stations displayed after most of the relative delays had been removed. Trace length approximately 25 μ s. This noise was stored and manipulated by a device whose amplitude resolution was three bits.

Appendix 3

REGIONS WHERE LIGHTNING FLASHES BEGAN

The following is a reprint of a paper that has been published by the American Geophysical Union.

Regions Where Lightning Flashes Began

DAVID E. PROCTOR

*Division of Earth, Marine, and Atmospheric Science and Technology, Council for Scientific and Industrial Research
Honeydew, South Africa*

Regions where 773 flashes began during 13 thunderstorms were located by calculating centroids of the sources of the first six or 10 VHF pulses that were emitted by each flash. Sources were located by measuring differences in the times at which their pulses arrived at five widely spaced receivers stationed on the ground. We found that the distribution of origin heights was bimodal with peaks at 5.3 and 9.2 km above mean sea level (amsl). Standard errors in the coordinates of flash origins were estimated to be 20–80 m in X and Y and 160–240 m in the height coordinate Z . There were 431 flashes in the lower group and 342 in the higher. Flashes in the lower group were more numerous in 10 storms; in three storms, high flashes were in the majority. There was evidence to suggest that this condition depended partly on the phase of the host thunderstorm. Recorded E field changes produced by 165 flashes whose paths we had mapped convinced us that the vast majority of the 773 flashes, including the 342 high flashes, had also been negative. Flash origins tended to cluster in regions that were a few kilometers or less in horizontal diameter. Densities of flash origins in these regions ranged from 1.25 to 25 km⁻³. The origins of 658 flashes were mapped onto radar precipitation patterns of their host storms. We found that 66% of the flashes began within one picture element, approximately 270 m, of the contours for 20 dBZ; 27% began inside these contours, and most of these began at edges of high-reflectivity cores. The remaining 7% began outside the 20-dBZ contours. Similar results (73%: 19%: 8%) were obtained for 276 high flashes that began at heights above 7.4 km amsl, but 195 ground flashes scored 54%: 36%: 9% and showed a greater tendency to begin inside the 20-dBZ contours. The distribution of distances between origins and their nearest 20-dBZ contours showed a marked peak near zero. We concluded that charge-density in thunderclouds was affected by the presence of heavy precipitation and that 20-dBZ surfaces enclosed regions that carried excess negative charge.

1. INTRODUCTION

The quest to discover how thunderstorms become electrified has evoked an interest in finding where lightning begins. At what heights do lightning flashes start? In which part of the thunderstorm are they created? Are we able to specify their origins in the scant terms of thunderstorm morphology? Several good attempts to locate the positions of lightning flashes and to map them onto radar precipitation patterns of their host thunderstorms have been undertaken. These have been reported by *Christian et al.* [1980], *Holmes et al.* [1980], *Krehbiel* [1986, 1981], *Krehbiel et al.* [1979, 1984], *Lhermitte and Krehbiel* [1979], *Lhermitte and Williams* [1985], *MacGorman and Taylor* [1979], *MacGorman et al.* [1983], *Mazur and Rust* [1983], *Mazur et al.* [1986], *Proctor* [1983], *Ray et al.* [1987], *Taylor* [1983], and *Taylor et al.* [1984]. Some aspects of these have been reviewed *inter alia* in a paper by *Williams* [1985]. Most of these authors have supplied information regarding one or two thunderstorms and have been concerned with the location of lightning flashes or portions of lightning flashes. This paper presents information concerning the origins of 773 lightning flashes that were observed during 13 thunderstorms which occurred over an area, 1430 m above mean sea level (amsl), north of Johannesburg. The sample included 214 flashes that struck ground.

2. METHOD

2.1. Mapping VHF Sources

Lightning flashes were mapped using the hyperbolic system described by *Proctor et al.* [1988] and by *Proctor* [1983, 1981, 1971]. Sources of radio signals emitted by the lightning were located by measuring the differences between times at which the signals were received at widely spaced receivers sited at ground level. An image of each flash emerged after locating and mapping positions of a large number of sources of radio signals emitted by the flash. Examples have been published by *Proctor* [1981, 1983] and by *Proctor et al.* [1988]. We had already mapped the paths followed by 165 flashes, but this number was deemed to be too small for the purposes of this investigation. Therefore we supplemented it by locating sources of the first six or 10 pulses that had been emitted by another 608 flashes. We calculated the centroid of each set of six to 10 sources for all 773 flashes. Our experience has shown that we may regard this centroid as being the "origin" or "starting point" of the respective flash. Positions were described in terms of a system of Cartesian coordinates whose X and Y axes were almost parallel to the Earth's surface and were oriented 60° and 330°, respectively, with respect to true north. The coordinate Z was very nearly vertical. The origin of this coordinate system was placed at the "home" station. Physical characteristics of the recorder limited recordings to a maximum of 16 min duration, and considerations of flashing rate and economy sometimes caused us to terminate the recordings early. Storms drifted into and out of the coverage volume at various stages of their development, and therefore storms were not observed over their full lifetimes nor at the same phases. The auxiliary recordings concerned an interval approximately 20 min. Auxiliary records, which were record-

Copyright 1991 by the American Geophysical Union.

Paper number 90JD02120.
0148-0227/91/90JD-02120\$05.00

TABLE 1. Characteristics of C Band Radar Set

Characteristic	Value
Operating frequency	5.48 GHz
Antenna beam width	2°, H and V
Beam shape	Gaussian
Nodding rate	88° s ⁻¹
Azimuthal rotation	360° in 5 min
Pulse width	1 μs
Pulse repetition frequency	1000 Hz
Peak power	0.32 MW
Display threshold	20 dBZ out to 25 km
Receiver noise level	8.5 × 10 ⁻¹⁴ W
Received average power	4 × 10 ⁻⁵ ZR ⁻² W*
Z displayed in increments	10 dB
Length of range gate	250 m
Radar site coordinates	(0, 0, 0) km

*Z is in mm⁶ m⁻³, and R is in meters.

ings of radio signals emitted by the lightning together with recordings of electric field change (EFC), could be consulted in order to determine which flashes struck ground [Proctor, 1983]. When paths, followed by the flashes, were known, these recordings of EFC could be used to determine magnitude and polarity of the excess charge redistributed by the flash. The recorded waveforms of radio noise showed when each flash had begun, when it had ended, and whether it had emitted pulses at high rates or at low rates. Proctor *et al.* [1988] reported that this rate indicated whether the flash had begun at a high or a low altitude. The noise waveforms also bore evidence of a strike to ground, if this had occurred.

2.2. Weather Radar

We mapped 658 origins onto radar precipitation patterns of their host storms in order to discover which regions of the storms had produced lightning. A weather radar which operated at a wavelength of 5.48 cm was used to provide three-dimensional precipitation patterns of the storms that generated the lightning flashes which we describe here. The main characteristics of the radar have been listed in Table 1. Echoes that were received from targets whose ranges were less than 25 km were corrected for the effects of range. Video data were integrated, averaged, and stored in "bins"

that represented 250-m increments in range and then stored on magnetic tape. The contents of each bin was an average of 20 samples taken over 10 ms. The tape recordings could be replayed repeatedly through a special computer which allowed a variety of sectional views of the storm to be displayed and photographed. Examples are shown in Figures 6, 7, and 8. The range-height indicators (RHIs) show sections that are almost vertical, some slant having been due to the slow, continuous azimuthal rotation. The constant altitude plan position indicators (CAPPIs) are plan views of thin, horizontal slices, at heights stated in kilometers above ground. Reflectivity factors were displayed in increments of 10 dB; the lowest was 20 dBZ. (In the work reported by Proctor [1983], the threshold was 25 dBZ.) The threshold was applied to the video signals in the computer circuitry when the tapes were replayed in order to display the data. The threshold level was a minimum of 19 dB above the receiver noise level.

2.3. Magnitudes of Error

The principal errors in the comparisons reported here will have been due to changes in the thunderstorms that occurred in the intervals between the instants when we recorded the radar returns and the instants when the lightning flashed. Almost all of these intervals were less than 2.5 min. The intervals were distributed almost uniformly, and their average magnitude was approximately 75 s. Except for one storm that moved at 16 m/s, storms that we report here moved at speeds that ranged from 0 to 7 m/s. The weighted average speed was 3.5 m/s. In 75 s a storm moving at 3.5 m/s would travel 263 m, and this distance would be an optimistic estimate of the error due to storm motion during the intervals. Even stationary storms displayed significant changes between successive scans.

The accuracy with which the radar could locate the position of a particular feature decreased with range because of the finite beam width. At 6-km range the 2° beam illuminated a region 200 m across, but convolution with the receiver beam reduced the half-power diameter of the observation area to 140 m. Range bins were 250 m long. At this range the radar could locate a target correct to 143 m (the root of the sum of the squares of 125 and 70 m). Errors in

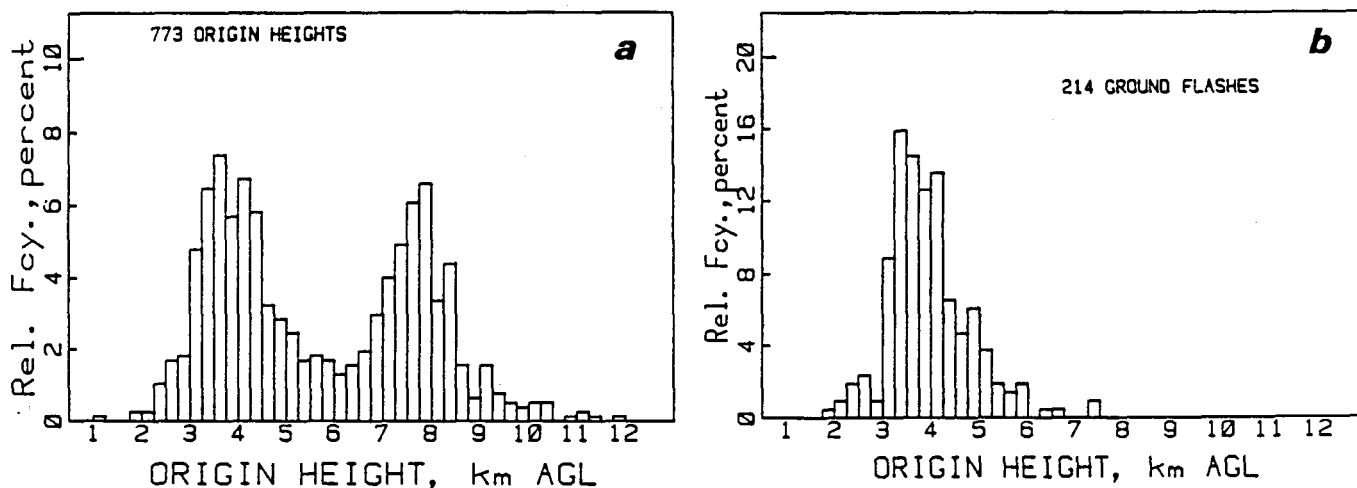


Fig. 1. Distribution of (a) heights above ground level (at 1.43 km amsl) of the origins of 773 flashes, cloud to ground (CG) and intracloud (IC), that occurred in 13 storms; and (b) origin heights of 214 flashes to ground.

TABLE 2. Median Heights of the Origins of Lightning Flashes and Corresponding Temperatures of Environmental Air

Date of Storm	Lower Group			Upper Group			Percent in Upper
	Height, km amsl	Temperature, °C	Number of Flashes	Height, km amsl	Temperature, °C	Number of flashes	
Feb. 14, 1979	5.7	-5.5	42	8.9	-27	39	48
March 2, 1979	4.7*	NA	3	6.7*	NA	3	...
March 7, 1979	4.8	-2.0	26	0	0
March 27, 1979	4.9	-2.5	23	9.2	-32.5	13	36
April 8, 1979	5.4	-8.5†	26	0	0
Feb. 24, 1984	5.2	-3.0	9	0	0
Oct. 24, 1984	5.2	-4.0	33	8.2	-26.0	11	25
Dec. 10, 1984	4.4†	+1.0†	22	7.5†	-21.1†	10	31
Feb. 21, 1985	5.1	-2.1	69	9.1	-30.0	119	63
March 26, 1985	5.2	-3.0	8	8.4	-25.0	2	20
Nov. 16, 1987	5.4	-4.1	36	9.4	-33.0†	15	29
Dec. 23, 1987	5.7†	-2.1	33	9.7†	-27.5	107	76
March 23, 1989	5.5	-4.2	101	9.0	-31.0	23	19

Temperatures correspond to the median heights. They are not weighted means. NA indicates that data are not available.

*Average.

†Extreme values (except February 2, 1979).

timing the VHF signals from lightning were large enough to cause rms errors of 25 m in the X and Y coordinates of each source. These were the coordinates that were parallel to the ground. There was no vertical baseline. As explained by Proctor [1971], we could determine the heights of the sources by making use of those hyperbolic surfaces that curved over the home station. The divergence of these surfaces (also called lane expansion) caused errors in the height coordinate Z to vary with position. Their rms magnitudes varied from 140 to 250 m at the heights at which lightning flashes began. Errors in determining flash origins differed slightly from these values, because successively active sources were neither collocated nor immediately adjacent; instead, they occurred in an erratic spatial sequence and so exhibited a scatter that contained a component not unlike the scatter of the endpoints of steps in random flight. The extent of this scatter was larger than that due to errors of measurement. In due course, sources occupied adjacent positions, but the accuracy with which we could locate an origin had to be determined by taking statistics of the scatter of successive sources that had been active initially in many flashes. These determinations showed that centroids of the first six sources could be determined with rms errors that were 20–80 m in X or Y and 160–240 m in the height coordinate. Figure 11 of Proctor [1981] maps the positions of sources of successive pulses. Adding the squares of error components (50 m in X and in Y , 200 m in Z , 143 m for the radar, and 263 m for storm drift; approximately 100-m error in mapping), we arrive at an estimate of 380 m for the expected error in the positions of origins that were mapped on precipitation patterns.

3. RESULTS

3.1. Heights at Which Flashes Began

Figure 1a is a histogram of heights at which 773 flashes began. The distribution is clearly bimodal with modal values 5.3 and 9.2 km amsl. Pressures and average environmental temperatures for the 13 stormy days were 540 and 317 mbar and -3.3° and -27.7°C , respectively, at these two modal heights. (Aerological data were supplied by the South African Weather Bureau, which took soundings 30 km NE of the

home station at approximately 1200 UT every day.) The distribution appears to consist of two normal distributions. The tails of the two overlapping distributions intersect near 6 km above ground level (agl) which is 7.43 km above msl. We classified flash origins according to whether they were above or below this level. Table 2 lists the median heights for each storm and the corresponding temperatures of the environmental air. Table 2 shows that the median heights ranged from 4.4 to 5.7 km for the lower groups and from 7.5 to 9.7 km for the upper groups and the environmental temperatures at median heights ranged from $+1^\circ$ to -8.5°C and -21.1 to -33°C , respectively. (Data for March 2, 1979, are ignored here because the sample was too small.) In any one storm the range of environmental air temperatures at the measured origin heights was relatively large. For example, the 10 percentile values for February 21, 1985, a storm during which we recorded many flashes, were $+4.5^\circ\text{C}$ (4 km amsl) and -8°C (5.9 km) for the lower group and -20°C (8.2 km) and -32°C (9.8 km) for the higher group. The greatest range in temperatures corresponding to the 10 percentile heights was 18.5° for the lower group. There was one of 15° , and the remainder ranged over 5° or 10° . We emphasize that the temperatures were inferred; the heights were measured accurately.

Flashes that originated below 7.43 km amsl outnumbered those that originated above 7.43 km by 431 to 342. Both the percentages of high flashes and the distributions of origin heights varied from one storm to another. Figure 2a shows a distribution in which the lower group outnumbered the flashes with high origins. This was the more usual condition. Figure 2b shows the distribution of origin heights of flashes that were recorded during a storm we observed on February 21, 1985, when members of the upper group were the more numerous. Table 2 shows that only three storms out of the total of 13 produced large percentages of flashes that began at the higher levels. These percentages were 76, 63, and 48. In the 10 remaining storms the percentages of high flashes ranged from 0 to 36%. Two reviewers suggested that these conditions might depend on the phase of the storm, rather than being attributes of special storms. Precipitation had reached ground in all the storms we studied. Therefore the active cells had passed the cumulus stage [Browning, 1986].

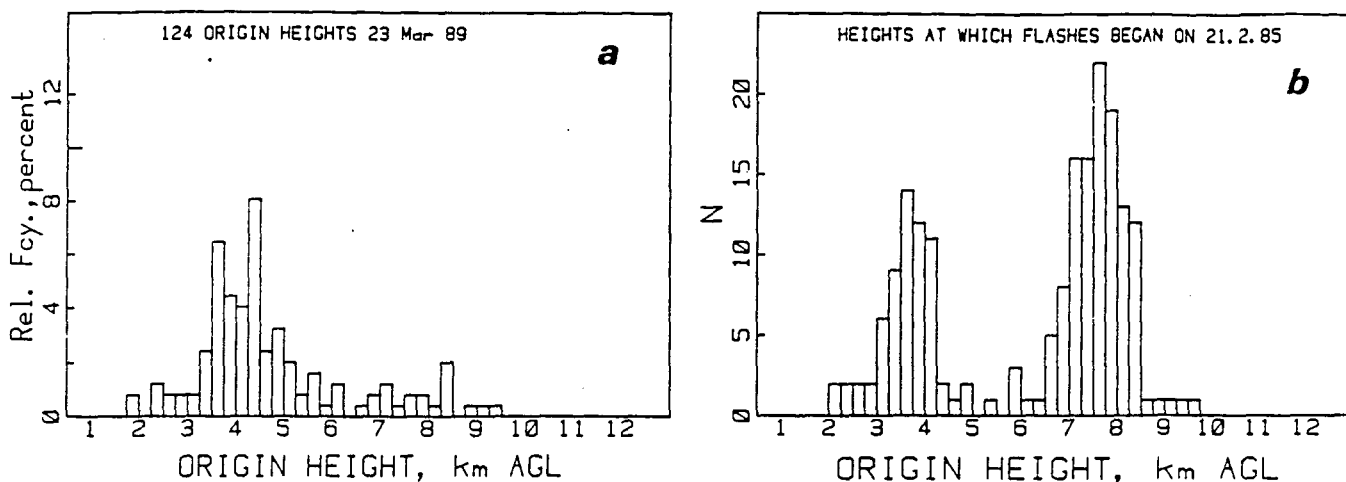


Fig. 2. Distribution of (a) origin heights of flashes recorded on March 23, 1989, during a storm that produced more flashes with low origins (typical of 75% of the storms); and (b) 188 origin heights when higher origins were more numerous (February 21, 1985).

We measured flashing rates in order to see whether activities were increasing or not. The numbers of flashes per minute were plotted for each storm. Of six storms where the numbers of high flashes permitted comparisons to be made, there were five in which the rates of high flashes peaked a few minutes before the flashing rates of low flashes reached their maxima and one in which the two rates peaked simultaneously. There were intervals of several minutes when rates were increasing, were roughly constant, or were decreasing. During five intervals when overall flashing rates increased, the percentage of flashes with high origins were 0, 54, 34, 71, and 77%. During five intervals when flashing rates were roughly constant, the percentages of high flashes were 48, 33, 36, 36, and 19%. During five periods when the overall flashing rates decreased, the percentages of high flashes were 0, 15, 55, 0, and 83%. These figures indicate that the percentage of high flashes changed during the lifetimes of the storms and that they usually decreased when the storm aged, but storm phase was evidently not the only factor that influenced the numbers of high flashes. Figure 1b shows how origin heights of 214 flashes to ground were distributed. It is clear that the vast majority (perhaps all) belong to the lower group, although the tail extended to 8.9 km amsl. The median value was also 5.3 km amsl, although the modal value was approximately 4.9 km amsl.

3.2. Regions Where Flashes Began

Figures 3, 4, and 5 show flash origins mapped in elevation and in plan. It is evident from these maps that on some days the lightning originated from relatively small regions, rather than originating anywhere in thunderstorms, and that there were definite centers of activity in these storms. Some active regions were as small as 2 km \times 0.1 km \times 0.8 km. Origin densities in 13 centers ranged from 1.25 to 25 km⁻³, and nearest neighbor distances between flash origins ranged from 510 to 190 m, which will have been enlarged by errors of measurement. This tendency for origins to cluster was evident in the plots for nine storms. Maps of three more storms contained too few origins for any clustering to be noticeable. In yet another storm the flash origins appeared to have been scattered. This may have been due to the wind. On this day (March 27, 1979) the environmental midlevel

winds blew relatively strongly, 15–27 m/s, whereas environmental wind speeds at midlevels ranged from 1 to 7 m/s on the 12 other stormy days. The scatter in any particular group varied from one interval of time to another, but the scatter did not increase overall with the passage of time. The Z/X view in Figure 5 clearly shows the two layers in which flashes began.

Figures 6, 7, and 8 show RHIs and CAPPis onto which origin positions, determined in the manner described above, were mapped. These are examples of a great many that were prepared. Most of the maps showed that there was a tendency for flashes to begin at or near the contours for 20 dBZ. There were 658 origins for which we could reproduce appropriate radar records. We counted origins in three categories: (1) those within one range-bin of the contour or within a tangential distance of the contour that was less than the distance between adjacent radial traces at that range (traces occurred approximately every 0.8° on RHI, but some were separated by 2.5° on CAPPis); these conditions were termed "at the contour"; (2) those that fell inside the contours; and (3) those that were mapped outside the 20-dBZ contours. There were 435 origins that occurred at the 20-dBZ contours. Of these, 157 higher origins were located at the upper contours, on the tops of the storms, as shown in Figures 6 and 7; 192 occurred at the sides of the turrets. The precipitation patterns were endowed with many holes, voids, or tunnels, and 86 flashes began there at the 20-dBZ contours. Examples are shown in Figure 8. There were 175 flashes that began in the heavier precipitation, where $Z > 20$ dBZ, but even in those cases, we found that there was a tendency for flashes to begin at the edges of precipitation cores and to begin in regions where reflectivity gradients were high. Examples of this behavior are shown in Figure 7. There were 48 that began outside the 20-dBZ contours. Table 3 lists the number of cases for each of 13 storms and also gives the relative frequencies for all 658 flashes. Sixty-six percent were located at the 20-dBZ contours; 27% were located in regions enclosed by the 20-dBZ contours; and 7% were located outside the contours for 20 dBZ. The above mentioned statistics concerned flash origins of all heights. For 276 flashes whose heights exceeded 7.4 km amsl, the scores were 73%: 19%: 8% for "ats," "ins," and "outs."

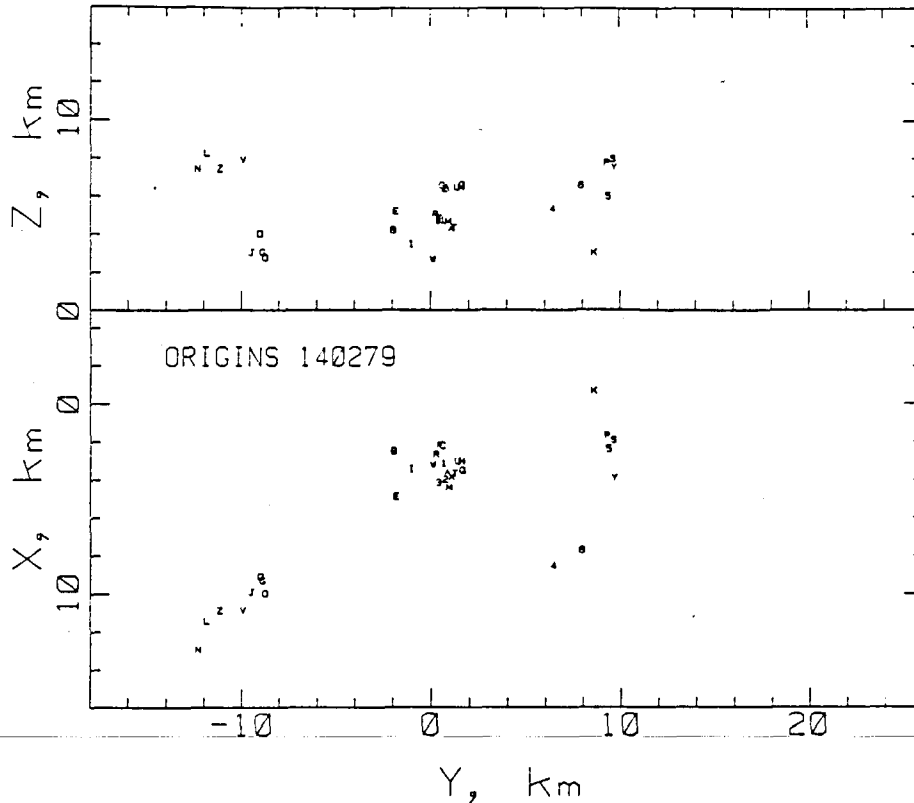


Fig. 3. Plan and elevation views of the origins of 32 out of 35 flashes that occurred during a 7-min interval on February 14, 1979. Symbols A-Z and then 1-6 label flash sequence.

respectively. The exercise was repeated for 195 ground flashes, and Table 4 shows that these scored 54, 36, and 9% in the three categories. Evidently, ground flashes exhibited a greater tendency than cloud flashes to begin in heavier precipitation. The aforementioned results prompted us to measure the distances that separated origins from the contours for 20 dBZ. Figure 9 shows how 658 distances were distributed. These were the shortest distances to the contours measured on either RHI or CAPPI displays. Where the origins were more than 500 m from a hole, the distance to the outer contour was measured, and the hole was ignored. The tendency for flashes to begin near some boundary where Z was approximately $100 \text{ mm}^6 \text{ m}^{-3}$ is shown clearly by the distribution.

Sketches shown in Figure 10 have been prepared in an attempt to collect and to summarize the information yielded by the many plots such as Figures 6, 7, and 8. For the sake of simplicity, Figure 10 shows CAPPIs at only one or two heights for each storm. The actual heights were chosen after inspecting the distribution of origin heights of the particular group to be displayed. We did not show the origins of flashes that had occurred when the 20-dBZ contours had changed so that they had become greatly different from the outlines shown in Figure 10. Origins were sorted into "low" and "high" categories, and their positions were transferred onto the sketches so that they maintained approximately the same positions with respect to the outlines and other features of the precipitation patterns onto which they had first been plotted accurately. This practice permitted us to show the origins together, having accounted for the movements of the storms to some degree. The sketches show the environmental airflows at 500 mbar and at the higher level where

necessary, but the hodographs have not been shown because we believe that the winds in the regions surrounding some of the storms had been modified. The tendency for flashes to begin at 20-dBZ contours has been masked partly, in some sketches, because the third dimension is lacking. The tendency is nevertheless obvious. Figures 4 and 5 may be compared with the appropriate sketches in Figure 10. Figure 5 compares with the sketches for 1636. Sketches for February 21, 1985, show how the storm shrunk while stalled.

Table 5 has been prepared in order to compare the numbers of flashes mapped, shown as the numerator, with the numbers of flashes that registered on the auxiliary records while the main recordings were made, shown as the denominator. Durations of the main recordings are shown in column 3. Flashes that registered on the auxiliary records included some too distant to have been mapped. The numbers of flashes were counted for each minute. Table 5 indicates the minimum and maximum numbers of flashes per minute recorded during each storm and indicates whether rates increased or decreased with time and in which minute these rates were maximum. Maximum turning points in the flashing rates are labelled P. Table 5 also lists the type of storm.

3.3. Polarities of the Flashes

The EFCs recorded by 165 flashes whose paths were known as functions of time enabled us to deduce the polarities of those flashes unambiguously. All but one of the flashes that we have analyzed carried an excess of negative charge from their respective origins. This one was the positive cloud flash 1653, described by Proctor [1981]. In

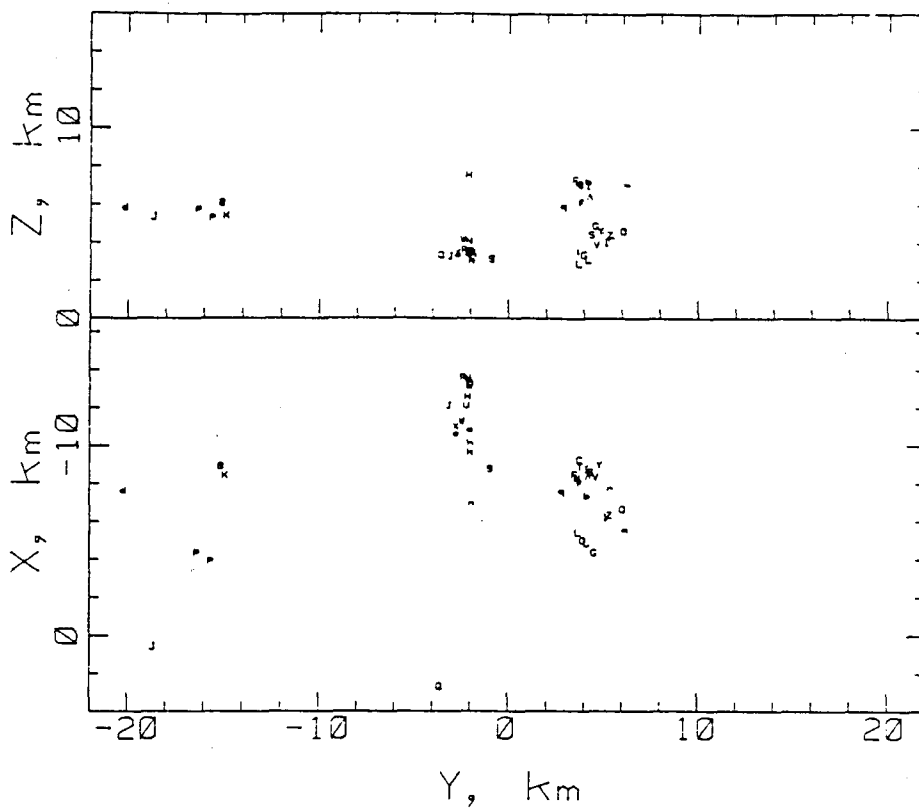


Fig. 4. Plan and elevation views of the origins of 44 out of a total of 46 flashes that occurred during an interval of 7 min of a storm on October 24, 1984. Symbols A-Z and then a-r label individual flashes sequentially. Flashes on extreme left occurred in an adjacent storm. See also Figure 10.

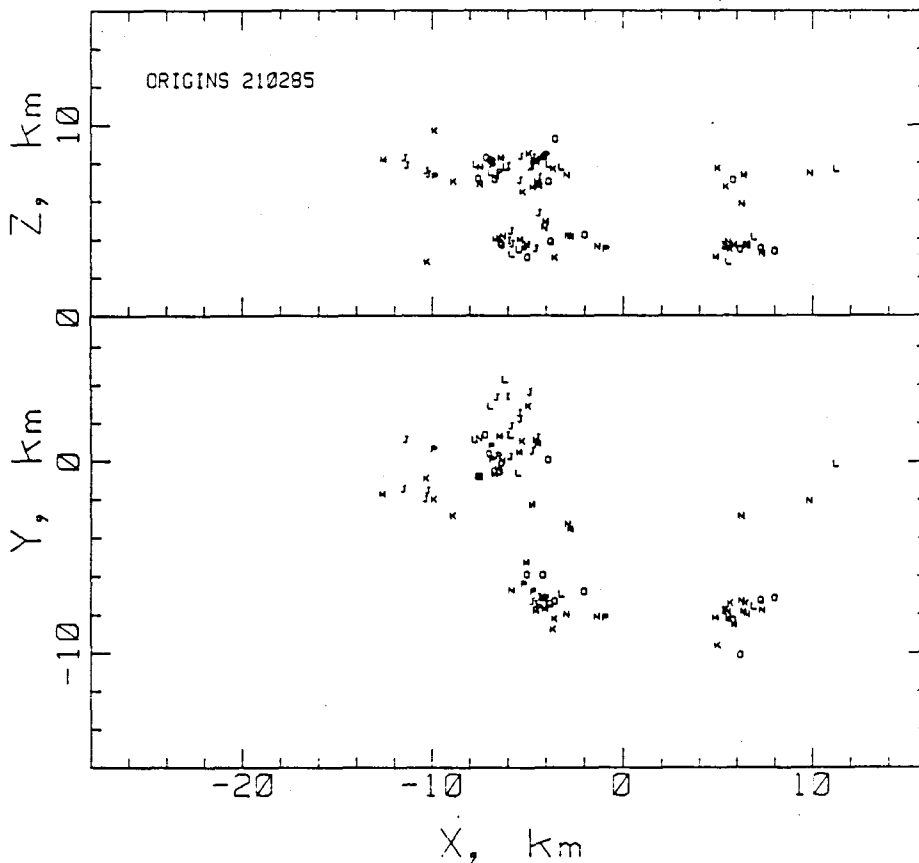


Fig. 5. Plan and elevation views of the origins of 95 flashes out of a total of 122 that occurred during an interval of 7.3 min on February 21, 1985. There were 10 main centers of activity. Symbols I-Q change at the start of each minute after 1638 LT.

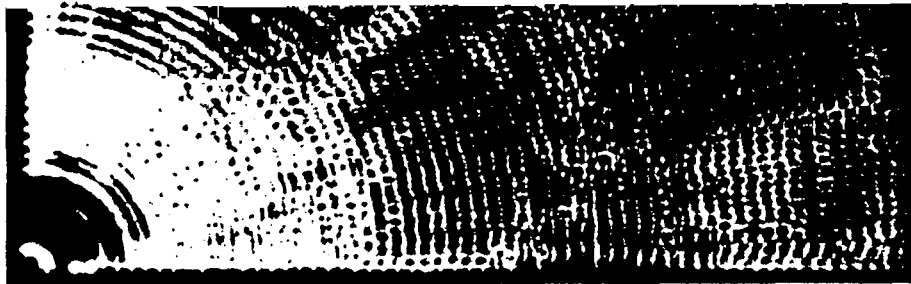


Fig. 6. Radar RHI (vertical section) showing precipitation patterns recorded on February 21, 1985, at 1633:46 LT. Azimuth: 213°. Five flash origins are mapped near the echo top above a core. Four symbols, solid circle, plus, open circle, and minus, denote Z values that exceeded thresholds of 20, 30, 40, and 50 dBZ, respectively. Range rings appear every 5 km. Maximum range in this presentation is 15 km, but smaller-scale maps were also printed in order to display the storm edge.



Fig. 7. Flash origins that were located at either side of a precipitation core. Another occurred at the echo top, recorded at 1640:05 LT on February 21, 1985. Azimuth: 117°. See caption for Figure 6.

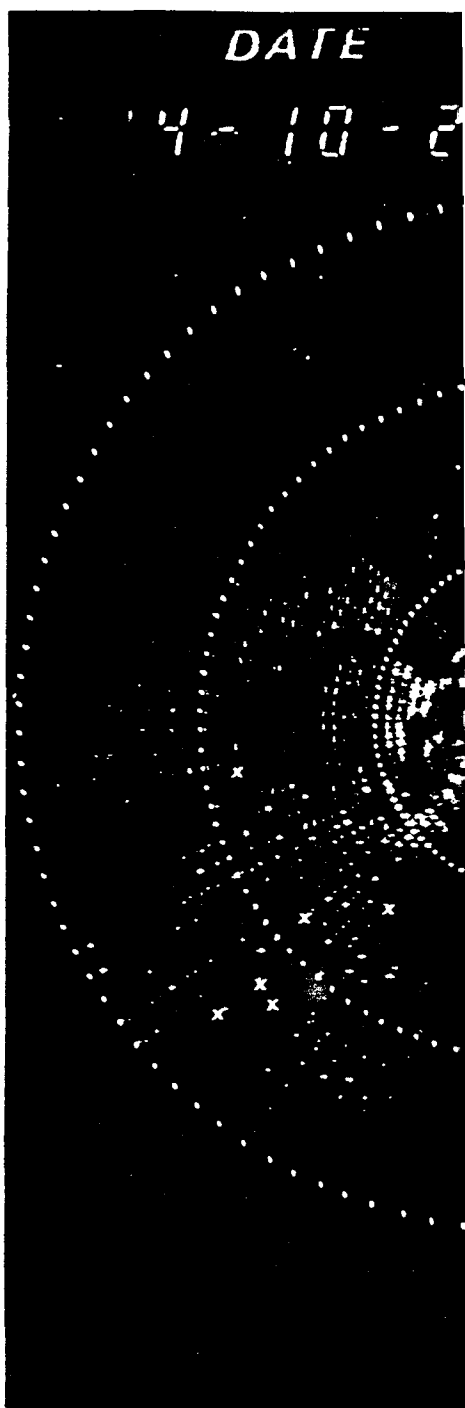


Fig. 8. Radar CAPPI showing a plan view of precipitation pattern recorded during 5 min after 16 here. Distance rings every 5 km from a point abo

particular, we analyzed radio pictures and EFCs of 1 flashes whose origin heights exceeded 7.4 km and four they all began as negative flashes. We infer that the m of the 342 high flashes reported here were also ne flashes.

4. DISCUSSION

4.1. *Origin Heights*

Bimodal distributions of channel heights were repo Weber [1980], MacGorman *et al.* [1981], Taylor *et al.* [



15 3.50

Fig. 8. Radar CAPPI showing a plan view of a 250-m-thick horizontal slice (at a height of 3.5 km agl) of the precipitation pattern recorded during 5 min after 1653:45 LT on October 24, 1984. Eight flash origins have been mapped here. Distance rings every 5 km from a point above the radar.

particular, we analyzed radio pictures and EFCs of 17 high flashes whose origin heights exceeded 7.4 km and found that they all began as negative flashes. We infer that the majority of the 342 high flashes reported here were also negative flashes.

4. DISCUSSION

4.1. Origin Heights

Bimodal distributions of channel heights were reported by Weber [1980], MacGorman *et al.* [1981], Taylor *et al.* [1984],

Mazur *et al.* [1984, 1986], and Ray *et al.* [1987]. Mazur *et al.* [1986] reported that a bimodal distribution was observed in only one cell and then only during its initial development. Ray *et al.* [1987] observed a bimodal distribution in the heights of the sources of VHF pulses radiated by lightning in a multicell storm, whereas in the supercell storm the two groups were not separated sufficiently in height to have been resolved. Photographs described by Mackerras [1968] showed that cloud flashes near Brisbane, Australia, occurred at two height ranges that were 1–8 km and 4–12 km amsl. These reports that lightning channels were observed in two

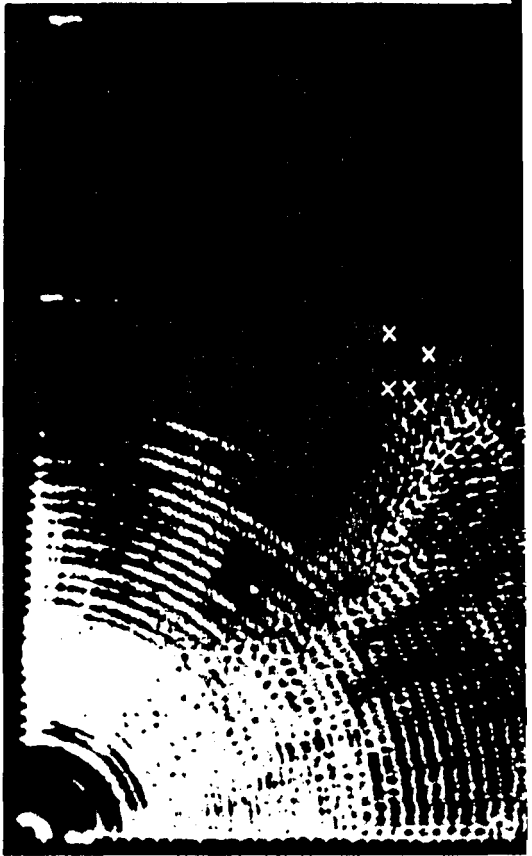


Fig. 6. Radar RHI (vertical section) showing February 21, 1985, at 1633:46 LT. Azimuth: 213°. the echo top above a core. Four symbols, solid circles denote Z values that exceeded thresholds of 20, Range rings appear every 5 km. Maximum range smaller-scale maps were also printed in order to di

TABLE 3. Origins of Flashes With Respect to the 20-dBZ Contours

	Number of Flashes			Total
	At Contour	Within Contour, Z > 20 dBZ	Outside Contour, Z < 20 dBZ	
Feb. 14, 1979	26	28	1	55
March 2, 1979	4	2	0	6
March 7, 1979	21	5	0	26
March 27, 1979	25	10	0	35
April 8, 1979	18	7	1	26
Feb. 24, 1984	6	3	0	9
Oct. 24, 1984	33	2	3	38
Dec. 10, 1984	17	15	0	32
Feb. 21, 1985	71	52	7	130
March 26, 1985	8	1	1	10
Nov. 16, 1987	29	14	7	50
Dec. 23, 1987	97	31	6	134
March 23, 1989	80	5	22	107
Total	435	175	48	658
Percent	66	27	7	100

layers lend credibility to the distribution shown by Figure 1a.

Standard deviations of lower and higher modes shown in Figure 1a are approximately 625 and 560 m. These dispersions would have been increased from 480 and 392 m, respectively, by errors of measurement. This shows that the dispersion shown by Figures 1a and 1b is mostly real and that it is not due primarily to errors of measurement.

Previous measurements of channel and origin heights have been listed in Table 6, and Table 7 lists the heights of charged regions in thunderclouds that were probed by earlier investigators. The upper portion of Table 6 lists measurements that were made by observing changes in electric field due to lightning and therefore relates to the positions of the charges that supplied the flashes. The lower portion of Table 6 concerns direct observations of lightning. Nearly all the

TABLE 4. Origins of Ground Flashes With Respect to the 20-dBZ Contours

	Number of Ground Flashes			Total
	At Contour	Within Contour, Z > 20 dBZ	Outside Contour, Z < 20 dBZ	
Feb. 14, 1979	0	5	0	5
March 2, 1979	3	1	0	4
March 7, 1979	0	1	0	1
March 27, 1979	5	7	0	12
April 8, 1979	5	2	0	7
Feb. 24, 1984	2	0	0	2
Oct. 24, 1984	25	0	0	25
Dec. 10, 1984	1	6	0	7
Feb. 21, 1985	3	18	1	22
March 26, 1985	6	1	1	8
Nov. 16, 1987	14	11	5	30
Dec. 23, 1987	12	16	0	28
March 23, 1989	30	3	11	44
Total	106	71	18	195
Percent	54	36	9	100

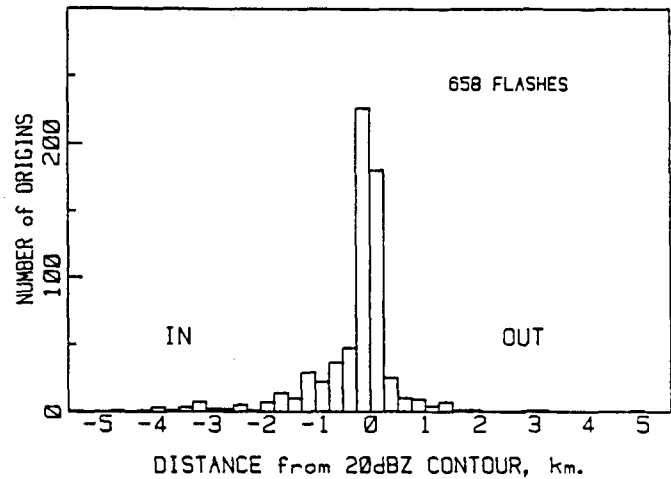


Fig. 9. Distribution of the distances of 658 origins from their nearest 20-dBZ contours. See text.

heights listed on the left-hand side of Table 6 are greater than the modal height, 5.3 km, that we report here, and all the heights in the higher group listed on the right-hand side of Table 6 are greater than our value of 9.2 km. First, consider the lower group of flashes. The middle 10 heights of 20 listed in Table 7 range from 5.5 to 7 km. The mean of all 20 is 6.3 km. These are heights of charge centers. The upper portion of Table 6 also refers to charge centers. The mean of nine heights is 7.4 km. The lower portion of Table 6 refers to lightning channels. There, the mean of 12 heights is 6.8 km. The two means differ by 600 m, which may be expected. The lower mean height (6.8 km) is higher than the mean of the heights in Table 7 (6.3 km), and all three are higher than the modal height (5.3 km) of our 431 flash origins. We cannot explain this discrepancy.

Second, consider origins and flashes that belong to the upper mode. Most of the heights of lightning channels listed in Table 6 ranged from 11 to 12 km. These are 1.8–2.8 km higher than the modal height (9.2 km) obtained for 342 flash origins. Maybe some of the flashes were not horizontal. Both of our model heights are lower than most listed in Tables 6 and 7. We have no explanation to offer for this. Table 7 makes no mention of centers of charge at heights near the height of the upper mode, even though most of the probes were lifted sufficiently high. Probes that crossed cloud boundaries and precipitation boundaries, and operated by Winn *et al.* [1974, 1978, 1981], registered high *E* fields there, and we infer that the remaining high probes happened to miss the upper concentrations of excess negative charge.

4.2. Relationship to Precipitation Patterns

We expect lightning flashes to begin in regions where the electric field is high. It is easy to show that the *E* field is highest at the periphery of a uniformly charged volume. We found that most flashes began at the 20-dBZ contours, and these would have encompassed most of the heavy precipitation. It may be tempting to infer that excess charge resided on the precipitation and, moreover, inasmuch as high radar reflectivity is an indicator of large particles, to reason also that excess charge in those thunderstorms was carried by the larger particles. We also found that a significant number of flashes, which amounted to 27%, began inside the 20-dBZ

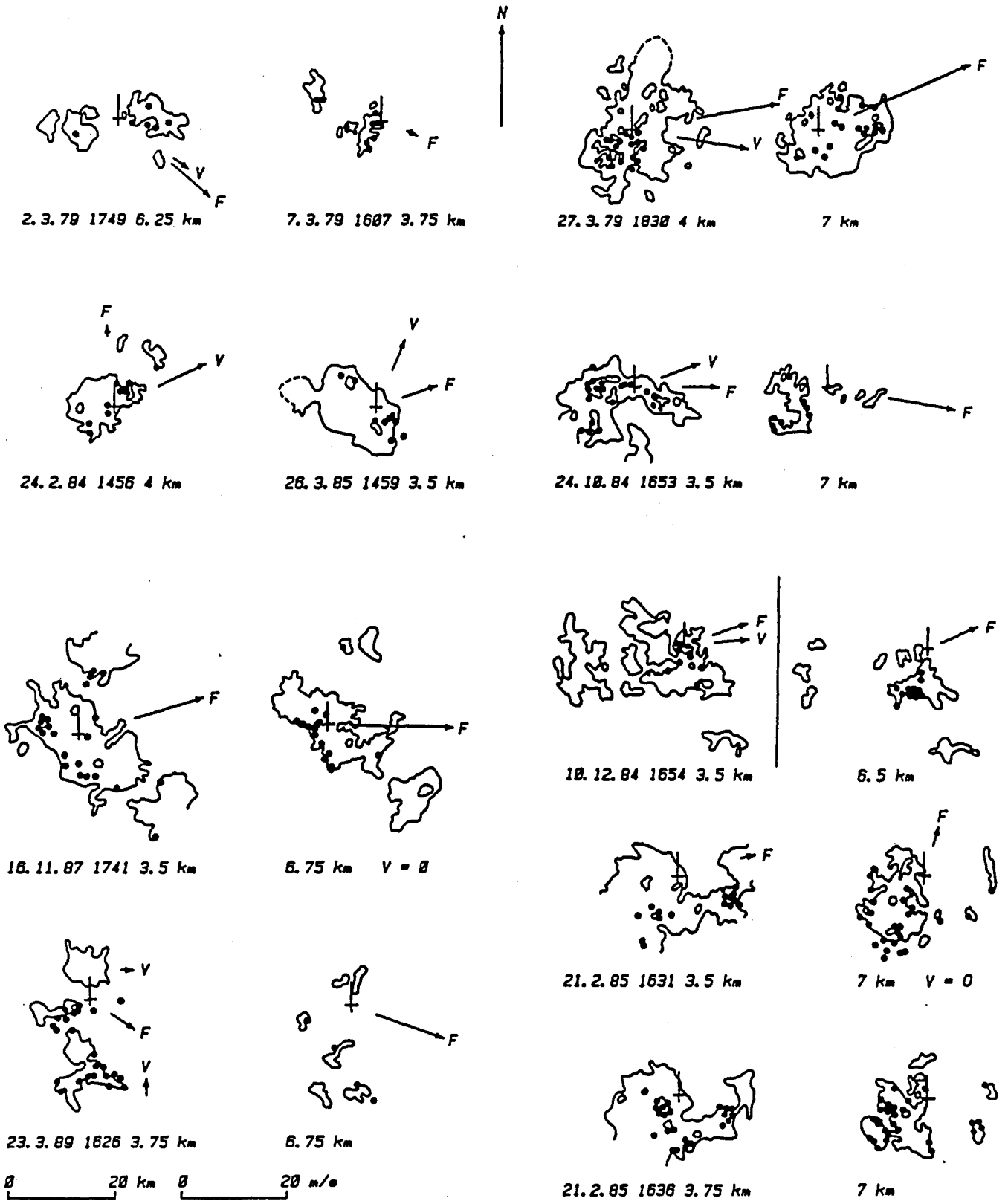


Fig. 10. Tracings of the 20-dBZ outlines of CAPPIs at the stated dates, times, and heights. Origins of lightning flashes have been mapped with dots. V indicates the speed and direction of each storm. Vectors F indicate environmental airflows (their directions are opposite to the wind directions). N indicates true north. The storm of March 7, 1979, did not translate during the observation period but spread in all directions. Crosses mark the position of the home station. See text.

TABLE 5. Numbers of Flashes Recorded and Mapped, Flashing Rates, and Storm Type

Date	Number of Flashes Plotted/Number Recorded on Auxiliary	Main Record Duration, min	Storm Type	Flash Rates, min ⁻¹		Time of Maximum or Peak,* min
				Minimum	Maximum	
Feb. 14, 1979	48/88	15.3	MC	4	10 dec	0 M
March 2, 1979	6/32	17	MC	3	4 id	8 P
March 7, 1979	26/32	16	U	1	16 dec	1 M
March 27, 1979	35/203	16	SS	10	15 almost steady	
April 8, 1979	26/26	9.1	MC	1	8 dec	1 M
Feb. 24, 1984	9/10†	9	MC	14	29 inc	13 M
Oct. 24, 1984	38/46	7.5	MC	5	10 id	3 P
Dec. 10, 1984	32/45	16	MC	1	5 id	13 P
Feb. 21, 1985	130/246	15.8	SQL	10	21 id	11 P
March 26, 1985	10/264	15.4	SQL	11	26 id	9 P
Nov. 16, 1987	50/71	14.3	SQL	2	9 dec	2 M
Dec. 23, 1987	134/185	13.2	SQL	6	23 id	8 P
March 23, 1989	107/225	14.9	MC	8	18 dec	4 M

MC, multicell; U, single cell; SS, steady state; and SQL, squall line; dec, decreasing; inc, increasing; and id, increase followed by decrease; M, a maximum; P, peak (turning point).

*Time in minutes from the start of the auxiliary record.

†Near.

contours. In cases where the density of excess charge had been concentrated centrally rather than having been distributed either uniformly or at the edges of the precipitation, we should expect to find that the high-field region occurred inside the precipitation. This fact, together with the observation that those origins that occurred within the 20-dBZ contours did cluster around the precipitation cores, again might be taken to indicate that the excess charge was carried

by the larger particles. There are two caveats: The first has been demonstrated in laboratory experiments by Williams *et al.* [1985]. According to their findings, our results show merely that there was a discontinuity in charge density at the contours for 20 dBZ. Our results do not show which carried more charge, the heavier precipitation and larger particles or the regions where radar reflectivities were lower. We therefore invoke results published by Gardiner *et al.* [1985], Dye

TABLE 6. Heights and Temperatures at Flash Origins and Channels Measured by Remote Sensing

Investigator	Place	Lower Group		Higher Group		Comment
		Height, km amsl	Temperature, °C	Height, km amsl	Temperature, °C	
Krehbiel <i>et al.</i> [1979]	New Mexico	6.3-7.8	-9 to -17	four CG flashes
Krehbiel <i>et al.</i> [1984]	Florida	6.8	-15	15 IC flashes
Krehbiel [1981]	Florida	5.2-9.3	-10 to -25	26 CG flashes
Jacobson and Krider [1976]	Florida	6-9.5	-10 to -34	70 CG flashes
Krider [1989]	Florida	8 modal	multi-E field
		8	43 CG flashes
						multi-E field
Holmes <i>et al.</i> [1980]	Langmuir, New Mexico	8 modal	-20	radar observations of 156 channels
MacGorman <i>et al.</i> [1981]	Florida	6.5	-17	11	-47	acoustic
	Arizona	6.3	-5	8	-25	sources
	Colorado	6.0	-7	
MacGorman <i>et al.</i> [1983]	Colorado	6.1				acoustic VHF
	Colorado	7.0				sources
Mazur <i>et al.</i> [1984]	Wallops Island, Virginia	6-8	...	11-15	...	radar observations of many channels
Ray <i>et al.</i> [1987]	Oklahoma	5.5	-10	11	-40	VHF multicell
		8.4	-30	11		VHF supercell
Rustan [1979]	Florida	7.1-9.8	VHF sources, six flashes
Taylor <i>et al.</i> [1984]	Oklahoma	6	...	12	...	VHF sources
Weber [1980]	New Mexico	6.5	...	9.5	...	acoustic
This study	Transvaal	5.3	-3	9.2	-28	431 low + 337 high origins

TABLE 7. Heights and Temperatures of Negatively Charged Regions Measured by Probing

Investigators	Place	Height, km amsl	Temperature, °C
<i>Simpson and Scrase</i> [1937]	United Kingdom	5	...
<i>Moore et al.</i> [1958]	Mount Withington, New Mexico	4.1	+7
<i>Winn et al.</i> [1974]	Langmuir	5.9 and 6	...
<i>Winn et al.</i> [1978]	Langmuir	6.4–8.1	–8 to –20
<i>Christian et al.</i> [1980]	Langmuir	5.9	–7
<i>Winn et al.</i> [1981]	Langmuir	4.8–5.8	–2 to –5
<i>Marshall and Winn</i> [1982]	Langmuir	7.5	–15
<i>Weber et al.</i> [1982]	Langmuir	5.5–8	–5 to –20
<i>Weber et al.</i> [1983]	Langmuir	6.6	–12
<i>Byrne et al.</i> [1983]	Florida	4.3–6.5	0 to –8
<i>Dye et al.</i> [1986]	SE Montana	7	–20
<i>Dye et al.</i> [1988]	Langmuir	7	–20
<i>Breed and Dye</i> [1989]	Langmuir	5.5–7.3	–3 to –15

et al. [1986, 1988], and *Breed and Dye* [1989], who all probed thunderclouds and found that high E fields were associated with localized regions of high-radar reflectivity, and we then infer that 20-dBZ surfaces enveloped negatively charged regions. Below we argue that higher flashes began at screening layers, in which case the 20-dBZ surfaces will also have enclosed regions of diffuse positive charge. Second, the charge might have been carried by small particles that coexisted with the larger. *Christian et al.* [1980] reported that negative charge was carried by the smaller particles. *Gaskell et al.* [1978] reported that much of the charge on precipitation was carried by particles around 1 mm in size or smaller. *Dye et al.* [1986] reported that in-cloud electric fields did not exceed 100 V m^{-1} until 5-mm graupel, ice particle concentrations of 10 L^{-1} , and reflectivities of 35 dBZ were present already. *Dye et al.* [1988] reported that supercooled water, graupel, and ice particles were present together in charged regions.

Many of the 20-dBZ contours were situated inside the main body of the storm. There were 85 flashes which began at the edges of weakly echoing regions or holes in the precipitation. The frequency with which the origins collocated with the holes, sometimes with the only holes in the radar picture, was convincing evidence that these holes were not without importance. Some of these holes were large enough to have been indraft regions. We counted 58 "large" holes with extents of 1 km or more and 27 that were "small," 250–1000 m in "diameter." Some of these measurements will have been affected by the radar resolution. At 6-km range the volume of confusion of the radar return was $140 \text{ m} \times 140 \text{ m} \times 250 \text{ m}$, as discussed above. At first we wondered whether the holes had been caused by the flashes that originated there. (Such a possibility has been proposed by *Vonnegut and Moore* [1965], who suggested that holes in the precipitation patterns were due to ice nucleation caused by thunder. The example that they displayed grew to a considerable size, almost $2 \text{ km} \times 1 \text{ km}$.) Then we found that about half of the number of small holes had existed before the respective flashes occurred. It seems that even these small holes were large enough to have caused a significant discontinuity in the distribution of charge and so to have produced a region where the E field became high enough to initiate a flash. There were more holes in some storms than in others. They were most numerous in the precipitation patterns for two of the four most electrically active storms.

This suggests that the holes had been caused by lightning and leaves us with the thought that we might have mapped the origins of later flashes there because lightning flashes tend to begin in a few favored places. If the holes had been caused by earlier flashes, then it follows that the flashes begin there for a reason that is not associated with the discontinuity in precipitation. The overall statistics obtained from this exercise contradict this idea. The critic may argue that holes that were a mere 250 m across were hardly large enough to warrant our attention and that we should have counted flashes that began on the edges of small holes as having begun inside the precipitation. We would point out that changing totals in Table 3 by 27 does not significantly alter the outcome. The respective percentages would then be 62%:31%:7%. We do not know how the small holes come into being nor whether they are the cause or the effect of lightning. It would appear that they are a cause.

Screening layers could have formed at the outer boundaries of the precipitation patterns. The existence of screening layers probably explains why all 17 of our sample of high cloud flashes (for which we had radio pictures) were of negative polarity. Almost 73% of 342 high flashes began at the 20-dBZ contours. It is reasonable to surmise that some of these flashes were initiated at screening layers, where charge had accumulated. This would explain why the flashes did not originate in a diffuse and central region containing positive charge. It does not readily explain why flashes began at holes. Screening layers have been discussed by *Vonnegut* [1963] and *Brown et al.* [1971] and also by *Winn et al.* [1978].

The statistics of the distribution shown by Figure 9 are badly affected by the extreme values. The mean, -276 m , and the standard deviation, 2.95 km , are not physically significant because there was more than one influence at work, and there are three regimes. The width of the main peak is less than we should have expected from our estimates of error. The distribution indicates that there were 226 origins placed just inside the contours and only 180 just outside of them. Although these results have been contaminated by errors of measurement, this asymmetry does suggest that the effective boundary occurred where the reflectivity factor had been slightly greater than 20 dBZ (perhaps 1 dB greater).

Flashes that are the subject of this study were major events. The waveforms of both the EFCs and the radio noise that they caused could be recognized as being characteristic

of lightning flashes. The data relate to first strokes only. Results presented in this paper may contain a bias that is a consequence of our having favored making observations of smaller thunderstorms. Large thunderstorms such as those that occur during the early months of our summer seasons frequently extend beyond the limits of our coverage area. Most, maybe all, consist of many cells that are active simultaneously. Their flashing rates exceed one flash per second. Their VHF emissions are incessant, and their records are difficult to read. Characteristics of Transvaal thunderstorms have been reported by *Held and Carte* [1973] and by *Preston-Whyte and Tyson* [1988], who also describe the climate of the region. *Held and Carte* [1973] observed squall lines 400 km in length. They describe many storms that were 80 km in width, at the 27-dBZ level, and their Figure 26 shows one that extended more than 125 km.

4.3. Previous Reports Concerning Regions Where Lightning Began

MacGorman [1978] located thunder sources and found that one end of any lightning flash was usually near one cell of 45 dBZ, while the rest of it was downwind in a region where reflectivities lay between 35 and 45 dBZ. *Lhermitte and Krehbiel* [1979] employed the VHF fixes obtained by the lightning detection and ranging (LDAR) system of Lennon and found that lightning began just above the high-reflectivity core; lightning occurred also near the 50-dBZ core and on the side of updrafts. Results similar to those shown by Figure 6 were reported by *Krehbiel* [1981]. See *Krehbiel's* [1981] Figures 3.2.23, 3.2.35, 3.2.39, and 3.2.40. Thunder sources located by *Winn et al.* [1978] are depicted in their Figures 6 and 7 as having occurred just above the 20-dBZ contour. This result is similar to those reported by *Krehbiel* [1981] and by *Winn et al.* [1974] in their Figure 11. It is also similar to the result implied by Figure 6 of this paper. *Proctor* [1983] found that the 26 flashes of April 8, 1979, all started in two turrets. Table 3 shows that 18 began at the precipitation edges, a fact that came to light by consulting two orthogonal views of the appropriate precipitation patterns.

5. CONCLUDING REMARKS

This study employed a relatively large body of data (several hundred flashes that occurred during 13 storms) to show that the distribution of origin heights was bimodal, with peaks 5.3 and 9.2 km amsl. We found that origins clustered in localized active regions that exhibited a propensity to occur at or near portions of surfaces where radar reflectivities were 20 dBZ.

It is evident that we need to probe thunderclouds, rather than relying solely on techniques of remote sensing. These are some questions we might ask: Are regions enclosed by 20-dBZ surfaces almost uniformly charged, or does the charge accumulate near these surfaces? Are there any special microphysical properties of the charged regions adjacent to the centers of electrical activity? Why should some storms produce a majority of high flashes? Why should some thunderstorms that we recorded have produced very little lightning, even though their echo tops reached great heights?

Acknowledgments. I thank the CSIR for providing funds and facilities necessary for this research and also for granting permission

to publish this paper. I am indebted to the Water Research Commission for financial assistance. Special thanks are due to George Green for his interest and good offices. I am greatly indebted to Dick Uytendogaardt for his efforts and knowledgeable assistance. I am grateful to the SA Weather Bureau for supplying aerological data.

REFERENCES

- Breed, D. W., and J. E. Dye, The electrification of New Mexico thunderstorms, 2, Electric field growth during initial electrification, *J. Geophys. Res.*, 94(D12), 14,841–14,854, 1989.
- Brown, K. A., P. R. Krehbiel, C. B. Moore, and G. N. Sargent, Electrical screening layers around charged clouds, *J. Geophys. Res.*, 76(12), 2825–2835, 1971.
- Browning, K. A., Morphology and classification of middle-latitude thunderstorms, in *Thunderstorm Morphology and Dynamics*, edited by E. Kessler, pp. 133–152, University of Oklahoma Press, Norman, 1986.
- Byrne, G. J., A. A. Few, and M. E. Weber, Altitude, thickness, and charge concentration of charged regions of four thunderstorms during TRIP 1981 based upon in situ balloon electric field measurements, *Geophys. Res. Lett.*, 10(1), 39–42, 1983.
- Christian, H., C. R. Holmes, J. W. Bullock, W. Gaskell, A. J. Illingworth, and J. Latham, Airborne and ground-based studies of thunderstorms in the vicinity of Langmuir Laboratory, *Q. J. R. Meteorol. Soc.*, 106, 159–174, 1980.
- Dye, J. E., J. J. Jones, W. P. Winn, T. A. Cerni, B. Gardiner, D. Lamb, R. L. Pitter, J. Hallett, and C. P. R. Saunders, Early electrification and precipitation development in a small, isolated Montana cumulonimbus, *J. Geophys. Res.*, 91(D1), 1231–1247, 1986.
- Dye, J. E., J. J. Jones, A. J. Weinheimer, and W. P. Winn, Observations within two regions of charge during initial thunderstorm electrification, *Q. J. R. Meteorol. Soc.*, 114, 1271–1290, 1988.
- Gardiner, B., D. Lamb, R. L. Pitter, and J. Hallett, Measurements of initial potential gradient and particle charges in a Montana summer thunderstorm, *J. Geophys. Res.*, 90(D4), 6079–6086, 1985.
- Gaskell, W., A. J. Illingworth, J. Latham, and C. B. Moore, Airborne studies of electric field and the charge and size of precipitation elements in thunderstorms, *Q. J. R. Meteorol. Soc.*, 104, 447–460, 1978.
- Held, G., and E. A. Carte, Thunderstorms in 1971/72, *CSIR Res. Rep. 322*, Council for Sci. and Ind. Res. Pretoria, 1973.
- Holmes, C. R., E. W. Szymanski, S. J. Szymanski, and C. B. Moore, Radar and acoustic study of lightning, *J. Geophys. Res.*, 85(C12), 7517–7532, 1980.
- Jacobson, E. A., and E. P. Krider, Electrostatic field changes produced by Florida lightning, *J. Atmos. Sci.*, 33(1), 103–117, 1976.
- Krehbiel, P. R., An analysis of the electrical field-change produced by lightning, vols. 1 and 2, Ph.D. thesis, N. M. Inst. of Min. and Technol., Socorro, 1981.
- Krehbiel, P. R., The electrical structure of thunderstorms, in *The Earth's Electrical Environment*, pp. 90–113, National Academy Press, Washington, D. C., 1986.
- Krehbiel, P. R., M. Brook, and R. A. McCrory, An analysis of the charge structure of lightning discharges to ground, *J. Geophys. Res.*, 84(C5), 2432–2456, 1979.
- Krehbiel, P. R., R. Tennis, M. Brook, E. W. Holmes, and R. Comes, A comparative study of the initial sequence of lightning in a small Florida thunderstorm, paper presented at the Seventh International Conference on Atmospheric Electricity, Am. Meteorol. Soc., Albany, N. Y., June 3–8, 1984.
- Krider, E. P., Electric field changes and cloud electrical structure, *J. Geophys. Res.*, 94(D11), 13,145–13,149, 1989.
- Lhermitte, R., and P. R. Krehbiel, Doppler radar and radio observations of thunderstorms, *IEEE Trans. Geosci. Electron.*, GE-17(4), 162–171, 1979.
- Lhermitte, R., and E. R. Williams, Thunderstorm electrification: A case study, *J. Geophys. Res.*, 90(D4), 6071–6078, 1985.
- MacGorman, D. R., Lightning location in a storm with strong wind shear, Ph.D. thesis, Rice Univ., Houston, Tex., 1978.
- MacGorman, D. R., and W. L. Taylor, Lightning location relative to storm structure in an Oklahoma thunderstorm, paper presented at

- Eleventh Conference on Severe Local Storms, Am. Meteorol. Soc., Kansas City, Mo., Oct. 2-5, 1979.
- MacGorman, D. R., A. A. Few, and T. L. Teer, Layered lightning activity, *J. Geophys. Res.*, 86(C10), 9900-9910, 1981.
- MacGorman, D. R., W. L. Taylor, and A. A. Few, Lightning location from acoustic and VHF techniques relative to storm structure from 10-cm radar, in *Proceedings in Atmospheric Electricity*, edited by L. H. Ruhnke and J. Latham, pp. 377-380, A. Deepak, Hampton, Va., 1983.
- Mackerras, D., A comparison of discharge processes in cloud and ground lightning flashes, *J. Geophys. Res.*, 73, 1175-1183, 1968.
- Marshall, T. C., and W. P. Winn, Measurements of charged precipitation in a New Mexico thunderstorm: Lower positive charge centers, *J. Geophys. Res.*, 87(C9), 7141-7157, 1982.
- Mazur, V., and W. D. Rust, Lightning propagation and flash density in squall lines as determined with radar, *J. Geophys. Res.*, 88(C2), 1495-1502, 1983.
- Mazur, V., J. C. Gerlach, and W. D. Rust, Lightning flash density versus altitude and storm structure from observations with UHF- and S-band radars, *Geophys. Res. Lett.*, 11(1), 61-64, 1984.
- Mazur, V., W. D. Rust, and J. C. Gerlach, Evolution of lightning flash density and reflectivity structure in a multicell thunderstorm, *J. Geophys. Res.*, 91(D8), 8690-8700, 1986.
- Moore, C. B., B. Vonnegut, and A. T. Botka, Results of an experiment to determine initial precedence of organized electrification and precipitation in thunderstorms, in *Recent Advances in Atmospheric Electricity*, edited by L. G. Smith, pp. 333-360, Pergamon, New York, 1958.
- Preston-Whyte, R. A., and P. D. Tyson, *The Atmosphere and Weather of Southern Africa*, 375 pp., Oxford University Press, New York, 1988.
- Proctor, D. E., A hyperbolic system for obtaining VHF radio pictures of lightning, *J. Geophys. Res.*, 76(6), 1478-1489, 1971.
- Proctor, D. E., VHF radio pictures of cloud flashes, *J. Geophys. Res.*, 86(C5), 4041-4071, 1981.
- Proctor, D. E., Lightning and precipitation in a small multicellular thunderstorm, *J. Geophys. Res.*, 88(C9), 5421-5440, 1983.
- Proctor, D. E., R. Uytendogaardt, and B. M. Meredith, VHF radio pictures of lightning flashes to ground, *J. Geophys. Res.*, 93(D10), 12,683-12,727, 1988.
- Ray, P. S., D. R. MacGorman, W. D. Rust, W. L. Taylor, and L. W. Rasmussen, Lightning location relative to storm structure in a supercell storm and a multicell storm, *J. Geophys. Res.*, 92(D5), 5713-5724, 1987.
- Rustan, P. L., Properties of lightning derived from time series analysis of VHF radiation data, Ph.D. thesis, Univ. of Fla., Gainesville, 1979.
- Simpson, G. C., and F. J. Scrase, The distribution of electricity in thunderclouds, *Proc. R. Soc. London, Ser. A*, 161, 309-352, 1937.
- Taylor, W. L., Lightning location and progression using VHF space-time mapping technique, in *Proceedings in Atmospheric Electricity*, edited by L. H. Ruhnke and J. Latham, pp. 381-384, A. Deepak, Hampton, Va., 1983.
- Taylor, W. L., E. A. Brandes, W. D. Rust, and D. R. MacGorman, Lightning activity and severe storm structure, *Geophys. Res. Lett.*, 11(5), 545-548, 1984.
- Vonnegut, B., Some facts and speculations concerning the origin and role of thunderstorm electricity, *Meteorol. Monogr.*, 5, 224-241, 1963.
- Vonnegut, B., and C. B. Moore, Nucleation of ice formation in supercooled clouds as the result of lightning, *J. Appl. Meteorol.*, 4(5), 640-642, 1965.
- Weber, M. E., Thundercloud electric field soundings with instrumented free balloons, Ph.D. dissertation, Rice Univ., Houston, Tex., 1980.
- Weber, M. E., H. J. Christian, A. A. Few, and M. F. Stewart, A thundercloud electric field sounding: Charge distribution and lightning, *J. Geophys. Res.*, 87(C9), 7158-7169, 1982.
- Weber, M. E., M. F. Stewart, and A. A. Few, Corona point measurements in a thundercloud at Langmuir Laboratory, *J. Geophys. Res.*, 88(C6), 3907-3910, 1983.
- Williams, E. R., Large-scale charge separation in thunderclouds, *J. Geophys. Res.*, 90(D4), 6013-6025, 1985.
- Williams, E. R., C. M. Cooke, and K. A. Wright, Electrical discharge propagation in and around space charge clouds, *J. Geophys. Res.*, 90(D4), 6059-6070, 1985.
- Winn, W. P., G. W. Schwede, and C. B. Moore, Measurements of electric fields in thunderclouds, *J. Geophys. Res.*, 79(12), 1761-1767, 1974.
- Winn, W. P., C. B. Moore, C. R. Holmes, and L. G. Byerley III, Thunderstorm on July 16, 1975, over Langmuir Laboratory: A case study, *J. Geophys. Res.*, 83(C6), 3079-3092, 1978.
- Winn, W. P., C. B. Moore, and C. R. Holmes, Electric field structure in an active part of a small, isolated thundercloud, *J. Geophys. Res.*, 86(C2), 1187-1193, 1981.

D. E. Proctor, EMATEK, CSIR, P.O. Box 1327, Honeydew 2040, Republic of South Africa.

(Received February 21, 1990;
revised September 21, 1990;
accepted September 24, 1990.)

Appendix 4

THE EFFECTS OF ELECTRICAL FORCES ON DROPS OF WATER

A 4.1 *Introduction*

Several attempts to measure electric fields in thunderstorms have returned magnitudes well below those required to initiate sparking under laboratory conditions. Although these endeavours may have met with bad luck, and in all probability regions of high field are limited in extent and transient in nature, and therefore are difficult to locate, some writers have argued that lightning may be initiated — because waterdrops distort in a manner that causes their shapes to be conducive to the formation of streamers even when the electric field strength is relatively low. Figure A4.1 shows water drops distorted by electric fields and photographed by Macky [1931].

A 4.2 *Review*

Calculations published by Lord Rayleigh [1882] on the stability of electrically charged water drops were based on the assumption that the drop is spherical in shape and that the field acts radially to disrupt the drop mechanically, and that these forces are restrained by surface tension. The critical charge, which is now known as the Rayleigh charge, is

$$Q = (16 \pi a^3 / T)^{0.5} \quad \text{esu}$$

where a is the drop radius, the surface tension $T = 75$

dynes/cm (which is a mild function of temperature and is 77 at -8 C , 71 at 80 C). In Coulombs:-

$$Q = 8.08 \times 10^{-11} D^{1.5} \text{ Coulombs}$$

where D is the diameter in cm. [One factor $4 = n + 2$, where n is the mode of the distortion or Legendre order, usually 2].

Macky [1931] published results of experiments in which he allowed water drops to fall between plates that established electric fields that were either vertical or horizontal. He attempted also to allow enough fall for drops to acquire some speed, but this was less than the terminal speed in air. He also conducted the experiments at various pressures, to simulate those aloft, and he also introduced cloud droplets into the environment of the experiment. His results were remarkable. The drops elongated at both ends under the influence of the electric forces. The anode of the drop produced long filament. See Figure A4.1. Either corona or sparking occurred near a field-strength given by $E*(a)^{0.5} = 3840$, (the radius, a, in cm and E in V/cm).

The critical field for the discharge was found to be independent of pressure right down to the value that caused the plates to arc across in the absence of the drop. He found that the presence of cloud droplets had no influence. The inference was that the drops distorted so that they would initiate sparking at a field strength much lower than would be required in uniform fields, and this was achieved by virtue of the reduced radius of curvature on the drops, which

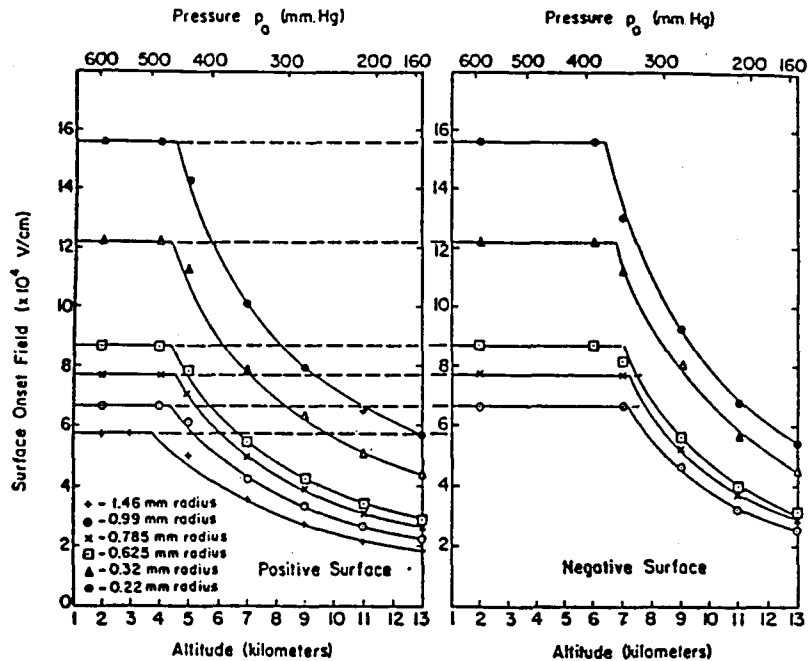


Figure A4.2 Electric fields at the onset of corona measured by Dawson [1969]. Below 4.5 km, mechanical instability occurs first. Above 7 km negative corona is favoured, and positive corona occurs first when $4.5 < Z < 7$ km.

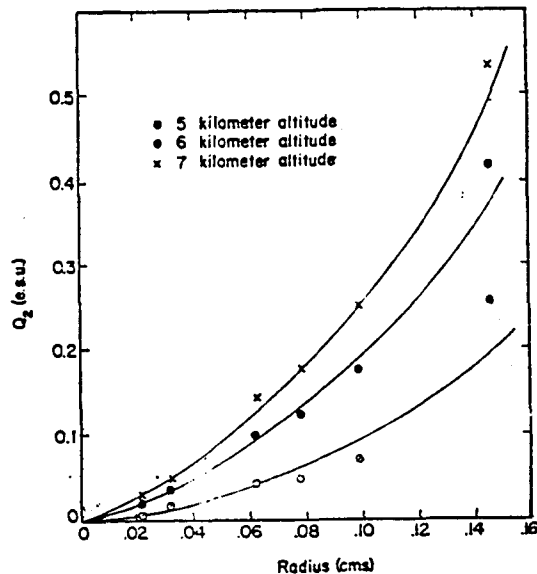


Fig. 5. The maximum final charge Q_2 attainable by a drop as a result of exposure to an electric field, as a function of drop radius.

Figure A4.3 The maximum charge attainable by a drop as a result of exposure to an electric field, calculated by Dawson [1969].



Figure A4.1 Water drops distorted by electric fields. The magnitude of the electric field was 8300 Volts/cm. The filament was drawn out from the anode of the drop, and produced sparking. Magnification was 2.3. Taken from Macky [1931].

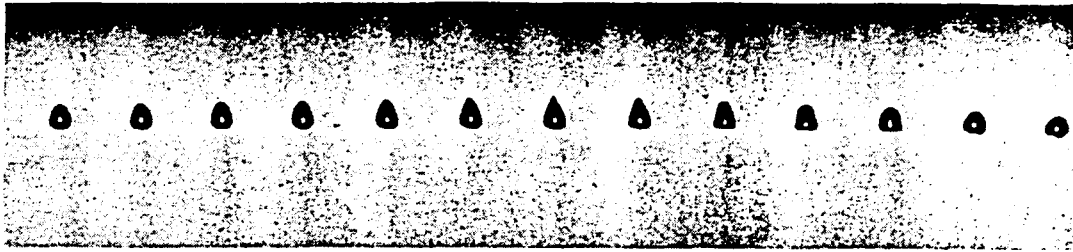


Fig. 1. Typical instability of a medium-sized uncharged water drop of radius 2.0 mm in a slowly increasing vertical field. In all figures, time increases from left to right, and successive frames are 2.5 msec apart. A drop oscillation ends with the formation on the upper surface of a point that then suddenly collapses.

Figure A4.4 Oscillations during the first instability, taken from Richards and Dawson [1971].

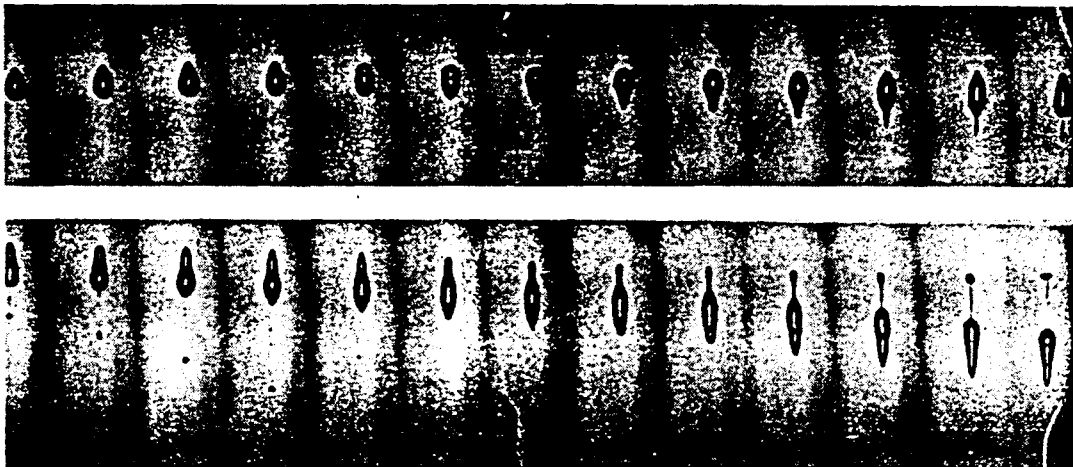


Fig. 6. The instability of a water drop of radius 2.1 mm carrying approximately half its equilibrium charge in a field of 85 kv cm^{-1} . The drop is practically levitated, reducing the aerodynamic flattening of the drop base.

Figure A4.5 The higher instability of a charged drop, shown by Richards and Dawson [1971].

caused the field to intensify at both ends of the drop.

Sir Geoffrey Taylor [1964] showed that the drop is unstable when its length equals or exceeds 1.9 times its equatorial diameter, and that the quantity $(r/T)^{0.5} E = 1.635$, where E is in V/cm, which is 7% higher than Macky's constant. Taylor was also first to notice that Macky's drops had entered the strong field too suddenly, but it was George Dawson that made the major advances in this line of work. He found that the scale of Macky's apparatus had been too small, the field had been applied too suddenly, and that conditions are altered greatly when the drop falls at terminal speed.

The following is a summary of the work published by Dawson [1969, 1970a, 1970b] and by Richards and Dawson [1971]: The stress on an electrified drop can be relieved either by corona, which partially discharges the drop, or else by causing the drop to eject charged mass. The former method dominates at lower pressures, and is pressure dependent. Both the onset of surface disruption (the mechanical effect due to electrical forces) and the onset of corona are proportional to the square root of the radius, so that the radius does not determine which will occur first. The pressure also influences whether positive, or both negative and positive corona, or just negative corona will occur. Negative corona was observed at much lower pressures. Dawson [1969] specifies two transitions which he states in terms of heights of the NACA standard atmosphere instead of pressure. Below an upper limit of 4.5 km amsl, drops that have been stressed sufficiently by electrical forces will become mechanically

unstable first (though corona may follow), whereas at heights above 4.5 km they will go directly into corona. There exists a transition region between 4.5 km and 7 km. In this region, a drop subjected to, say, an increasing field-strength will emit positive corona first. It is assumed that the drop, whether charged or not, has polarised, and the positive corona will occur at the surface where the positive charge has collected. The drop emits positive ions, and the drop becomes negative. In the transition region, drops encountering high electric fields of either polarity will become charged negatively. The larger the drop, the larger the charge, and the lower will be the field required to produce the charging. Above 7km, negative corona is favoured, but Dawson says little of it, except to say that the negative surface emits mostly negative droplets. His measurements are shown in Figure A4.2. I reproduce also his calculated maximum charges in Figure A4.3. It has to be emphasized that the abovementioned apply when drops are stressed slowly. Further discussion of these results was supplied by Dawson [1970b].

Richards and Dawson [1971] describe the hydrodynamic instability of drops falling at their terminal velocities, in the presence of vertical electric fields. All drops of all sizes (in the range studied), charged or uncharged, in fields of either polarity, both pulsed and slowly varying, have always become unstable by the formation of a conical point at their upper surface. No mass-loss was ever observed at the top instability (unless the drop was overstressed as described below), but the drops oscillated in shape, forming a point at the top, which then collapsed to a rounder shape

and the drop then accelerated downward against the supporting airstream. This is called the first instability. Their Figure A4.4 illustrates this. Uncharged water drops exhibited their first instability at fields much higher than predicted by Taylor [1964] or by Macky [1931]. A second instability could be induced only at a still higher field. For a drop of 2mm radius, the two field-strengths were 10 kV/cm and 13 kV/cm. Unless overstressed, no mass-loss occurred. No corona was seen, but its occurrence was suspected (this does not conflict with the results of Dawson [1969], although pressure was 1 bar, as the corona followed the mechanical instability). Drops acquired charge which was estimated to be 5×10^{-10} Coulombs. Instability did not depend on drop radius.

As these fields were so high, Richards and Dawson [1971] restricted their study of charged drops to conditions that lowered the onset of instabilities and decreased terminal velocities. Drops were charged to their full Wilson limit:

$$Q = 3 r^2 E \quad \text{esu}$$

Here the undistorted drop radius is r and, E is the ambient electric field, in esu. Drops levitated in the applied E field, except if their radii exceeded 2.7 mm, in which case they became unstable first (at fields around 5.5 kV/cm). Thus the charged drops became unstable at lower fields. The drop became unstable at its top, followed by an instability at bottom centre, and they elongated and gave off droplets, sometimes from both ends. Figure A4.5 shows an example.

Upward branching spark channels were seen when the applied field was negative, so that the drop anode was on top. If the charged drops had been charged positively, their instabilities caused them to lose the positive charge in the range 10^{-9} to 4×10^{-9} , and always these drops then became charged negatively to a value approximately 5×10^{-10} Coulombs.

Drops are overstressed by suddenly applying a field greater than the stability limits, or when sudden mass-losses occur.

Dawson and Warrenden [1973] found that the application of vertical E fields produced exceedingly small increases in terminal velocities. Richards and Dawson [1971] state that the large instability onset fields, and the independence of radius, cause problems for theories of lightning initiation. The aerodynamics of falling drops have a surprisingly great influence on the discharge of stressed drops. An interim report by Bourdeau and Chauzy [1989] emphasizes that smooth ice particles can hold higher charges than drops of the same diameter, as they cannot distort. Griffiths and Latham [1974] showed that ice below -18 C does not go into corona, and so perhaps can charge even more highly.

A 4.3 *Discussion and more Calculations*

The abovementioned was studied in order to see there was any theory that could be found to explain why we measured a bimodal distribution of origin heights, and perhaps also to explain why these modal heights were 5.3 and 9.2 km amsl, and

whether there was any reason for making a division near 7.4 km. It is to be noted that only the lower modal height falls within the transition region as defined by Dawson. It was 0.8 km higher than the lower transition. The upper modal height was 2.2 km higher than his transition at 7 km. Higher drops subjected to strong E-fields produce negative corona, and become charged positively. This positive charge would induce negative screening layers, and the evidence we have is that flashes in the higher group began at screening layers. The results obtained by Dawson are therefore compatible with the results that we obtained. At heights near the upper modes temperatures were -21 to -33 C (Table 2, Section 3.1) and one guesses that most hydrometeors there were solid. Lightning flashes that began below 7.4 km were altogether more vigorous than flashes that began higher, and perhaps this has to do with the greater conductivity of water and its ability to deform. A streamer advancing at 2×10^5 m/s will traverse 100 m in 0.5 millisecc, and the resulting increase in E field at a particular group of raindrops surely results in overstressing, so that the behaviour described by Dawson for overstressed drops might apply. These drops are surely reduced to a nascent state by the arrival of an event that raises their temperature by 30 000 degrees Kelvin in a time that spans less than 500 nanosecs. By considering the many reported studies of electrical discharges in air, and how these descriptions change as the scale is increased, one cannot but think that the study of small coronas from drops in the laboratory has limited applicability to the discharge processes, and is more relevant to problems of thundercloud charging.

These studies do give us some estimates of particulate charge, which we can use to guess at the sizes of the volumes that had been charged sufficiently to cause lightning. We may use the values for Σnd^2 calculated in Appendix 7. to estimate the total charge per cubic metre that the maximum charge given by Dawson [1969] would yield. These charges are given here by Figure A4.3 and his curve for a height 5 km can be approximated sufficiently well by the expression

$$Q = 0.1 r^2 \text{ esu for the radius } r \text{ in mm}$$

Brook et al [1962] state that their most frequently measured value for the charge brought down by first strokes was 3 to 4 Coulombs. Our own values ranged 3 to 13 C overall. We take 3 C as a minimum value, and then calculate the volume required to collect this charge at the density given by Dawson's result and our tables in Appendix 7. The radius is then calculated and the E field at the surface of such a volume, uniformly charged. The result for 30 dBZ is a radius of 60 metres and an E-field of 7.4 MegaVolts per metre, which is above the breakdown field given by his curves. These calculations are set out in Appendix 10.

Bourdeau and Chauzy [1989] have pointed out that the measurements reported by Christian et al [1980] for actual thunderstorms show that many drops in the charged volumes have been charged to maximum Wilson charge. We may calculate these charges only by assuming a value for the electric field. However, if we assume a low value of charge for a core volume, of say 10 metres radius, and then suppose an "onion"

structure exists with skin thicknesses of 10 metres, where the E field is generated by the enclosed charge, only five layers, charged at the maximum charge yield enormously high E fields at the outside surface. It is therefore not difficult to account for electric fields that are high enough to generate lightning.

A 4.4 *Bibliographical References*

Bourdeau, C., and S. Chauzy, Maximum electric charge of a hydrometeor in the electric field of a thunderstorm, *Jour. Geophys. Res.*, 94, D11, 13121-13126, 1989.

Brook, M., N Kitagawa, and E. J. Workman, Quantitative study of strokes and continuing currents in lightning discharges to ground, *Jour. Geophys. Res.*, 67, 2, 649-659, 1962.

Dawson, G. A., Pressure dependence of water-drop corona onset and its atmospheric importance, *Jour. Geophys. Res.*, 74, 28, 6859-6868, 1969.

Dawson, G. A., The Rayleigh instability of water drops in the presence of external electric fields, *Jour. Geophys. Res.*, 75, 3, 701-705, 1970a.

Dawson, G. A., Electrical corona from water-drop surfaces, *Jour. Geophys. Res.*, 75, 12, 2153-2158, 1970b.

Dawson, G. A., and R. A. Warrender, The terminal velocity of raindrops under vertical electric stress, *Jour. Geophys. Res.*, 78, 18, 3619-3620, 1973.

Griffiths, R. F., and J. Latham, Electric corona from ice hydrometeors, *Q. J. R. Meteorol. Soc.*, 100, 163-180, 1974.

Macky, W. A., Some investigations on the deformation and breaking of water drops in strong electric fields, *Proc. Roy. Soc. London, A*, 133, 565-587, 1931.

Proctor, D. E., Regions where lightning flashes began, *Jour. Geophys. Res.*, 96, D3, 5099-5112, 1991.

Rayleigh, Lord, J. W. S., On the equilibrium of liquid conducting masses charged with electricity, *Phil. Mag.*, 14, 184-186, 1882.

Richards, C. N., and G. A. Dawson, The hydrodynamic instability of water drops falling at terminal velocity in vertical fields, *Jour. Geophys. Res.*, 76, 15, 3445-3455, 1971.

Taylor, Sir G., Disintegration of water drops in an electric field, *Proc. Roy. Soc. London, A*, 280, 383-397, 1964.

THE DISTRIBUTION OF CHARGE IN THUNDERCLOUDS

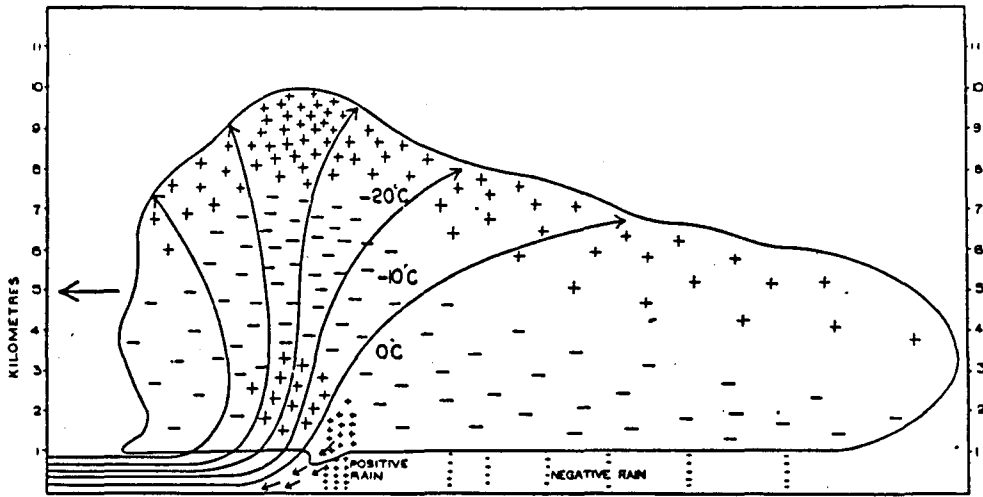
Charge distributions in thunderclouds were inferred by previous investigators from ground-based observations of electric field recorded during the advance of a storm, by observations of lightning, and some were deduced from balloon-borne measurements. The more widely known of these were due to Simpson and Scrase [1937] and Wilson [1920], the first of which is represented in Figure A5.1, and was obtained from balloon-borne instruments. Wilson's did not include the lower positive charge. Wilson [1920], p 102, deduced that the thickness of the negative region was 350 metres to 500 metres. Malan and Schonland [1951] reported their use of five methods to determine the extent of the region that supplied negative charge to lightning flashes, and claimed that it extended from a height 5.5 km amsl to 10.8 km amsl. Malan [1963] p 73 suggested that the width of the column might be 1 to 2 km. Ogawa and Brook [1969] showed that all five methods that had been employed by Malan and Schonland [1951] were open to question. Imjanitov and Schwarz [1969] show a typical distribution in Cu and Cu Congestus. This is reproduced here in Figure A5.2. Although they say that the distributions change markedly with time, they do not venture a distribution for Cumulo-Nimbus clouds. The incipient thunderclouds probed by Christian et al [1980] and Gaskell et al [1978] gave only one or two peaks in electric field and the inference was that there were only that number

of electrified regions of a particular polarity. Byrne et al [1983] probed four storms that had bipolar distributions, the lower negative region was 1 km thick and it formed between levels at 0 C and -10 C. Results of other investigators have been listed in Table 7 of Appendix 3 . Most of those results were obtained in the Magdalena Mountains, and those storms probably had been subjected to orographic influences. With the exception of the distribution modelled by Weber et al [1982], who used 7 spherical regions at one level to model the negative charge, the distributions were much simpler than those published by Imjanitov and Schwarz [1951]. A recent publication by Marshall and Rust [1991] describes results of 12 balloon soundings. Their distributions were more complex, as shown by part of their Figure 1, reproduced here as Figure A5.3, and the numbers of charged regions ranged from 4 to 10 including screening layers. Some of their results for Oklahoma and Alabama agree more closely with those of this report. Not counting the New Mexico results, six had high-field regions (that had resulted from negative charge) in the levels 4 to 6km, and two between 7 and 9 km. Their results showed how variable the heights of the high-field regions had been.

Bibliographical references

Byrne, G. J., A. A. Few, and M. E. Weber, Altitude, thickness and charge concentration of charged regions of four thunderstorms during TRIP 1981 based upon in situ balloon electric field measurements, *Geophys. Res. Ltrrs*, 10 1, 39-42, 1983.

Christian, H., C. R. Holmes, J. W. Bullock, W. Gaskell, A. J. Illingworth, and J. Latham, Airborne and ground-based studies of thunderstorms in the vicinity of Langmuir Laboratory, *Quart. J. R. Meteor. Soc.*, 106 , 159-174, 1980.



[Reproduced from London, *Proc. roy. Soc., A*, 161, 1937, p. 350.

Figure A5.1 The electrical structure of a thundercloud according to Simpson and Scrase [1937].

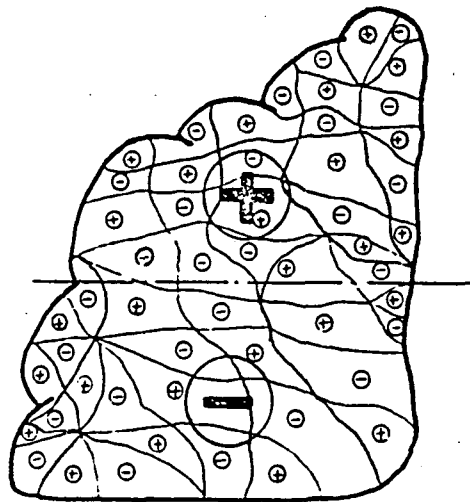


Figure A5.2 The electrical structure of Cu and Cu Cong clouds, after Imjanitov and Schwarz [1969].

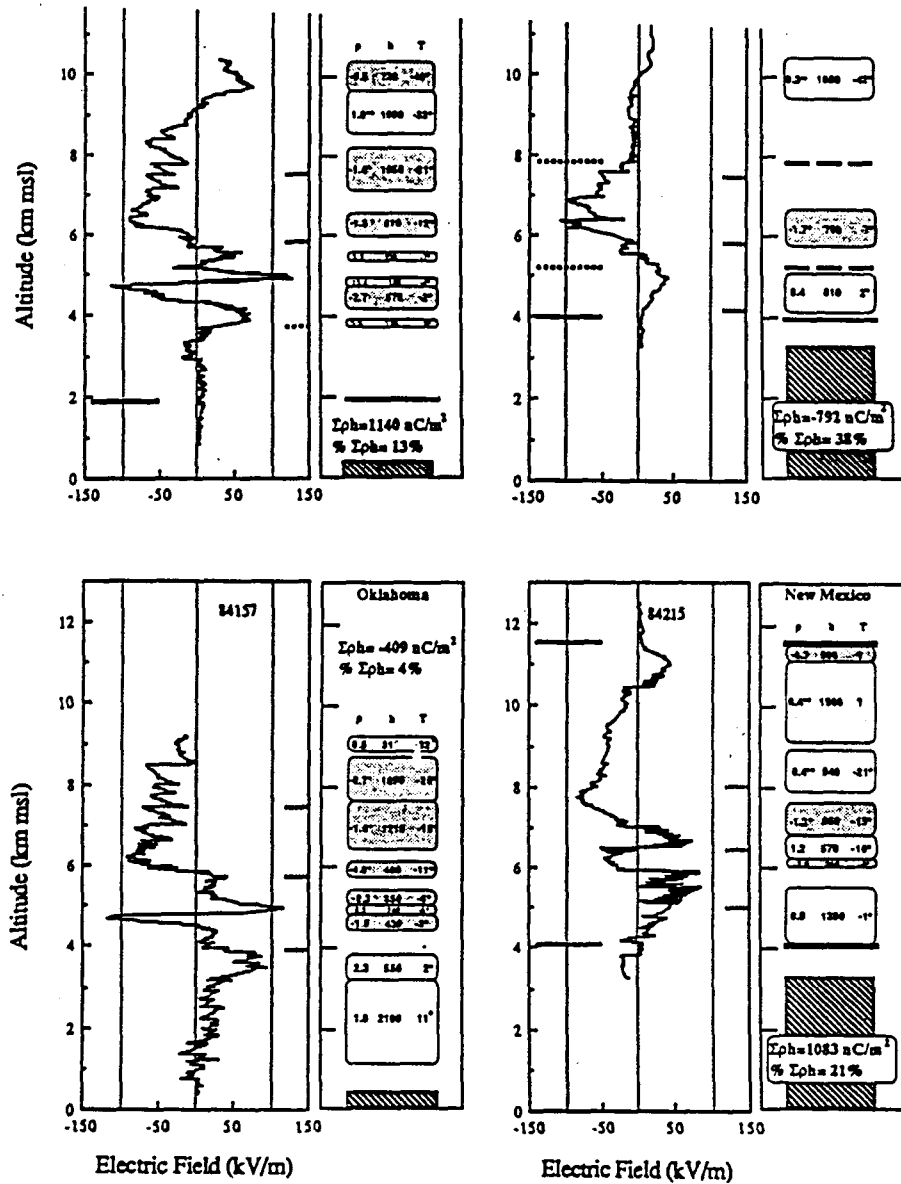


Fig. 1. Data and inferred charge regions for 12 storms. For each storm there are two boxes of information. The sounding data (electric field versus altitude) are displayed in the left-hand box. The right-hand box contains a vertical stack of smaller rounded rectangles which represent the charge regions inferred from the sounding: shaded rectangles represent negative charge regions and open rectangles represent positive charge regions. Each rectangle contains the inferred charge density, ρ , in nC/m^3 , the vertical thickness, h , of the region in meters, and the temperature, T , at the middle of the region in degrees Celsius. Note that the minimum thickness that can be represented in the figure is about 250 m; some of the charge regions are thinner than that. The solid black lines denote the top or bottom boundary of the cloud; the dashed lines mark the boundaries of 100% relative humidity with respect to ice. The top of the dark boxes beneath the charge regions represents the local ground level (3.2 km in New Mexico). Further details found in the text.

Figure A5.3 Some of the charge distributions measured by Marshall and Rust [1991].

Gaskell, W., A. J. Illingworth, J. Latham, and C. B. Moore, Airborne studies of electric fields and the charge and size of precipitation elements in thunderstorms, *Quart. J. R. Meteor. Soc.*, 104, 447-460, 1978.

Imjanitov, I. M., and Ja. M. Schwarz, Research into electricity in clouds, *WMO Bull.*, 18, 4, 221-229, 1969.

Ogawa, T., and M. Brook, Charge distribution in thunderstorm clouds, *Quart. J. R. Meteor. Soc.*, 95, 513-525, 1969.

Malan, D. J., Physics of Lightning, 176 pp, The English Universities Press Ltd., London, 1963.

Malan, D. J., and B. F. J. Schonland, The distribution of electricity in thunderclouds, *Proc. Roy. Soc., London*, A, 209, 158-177, 1951.

Marshall, T. C., and W. D. Rust, Electric field soundings through thunderstorms, *Jour. Geophys. Res.*, 96, D12, 22297-22306, 1991

Simpson, G., and F. G. Scrase, The distribution of electricity in thunderclouds, *Proc. Roy. Soc., London*, A 177, 309-352, 1937.

Weber, M. E., H. J. Christian, A. A. Few, and M. F. Stewart; A thundercloud electric field sounding: Charge distribution and lightning, *Jour. Geophys. Res.*, 87, C9, 7158-7169, 1982.

Wilson, C. T. R., Investigations on lightning discharges and on the electric field of thunderstorms, *Phil. Trans. Roy. Soc. London A*, 221, 73-115, 1920.

Appendix 6

A BRIEF DESCRIPTION OF THE STORMS

The limited extent of the five-station network caused us to select the smaller storms for study. Large thunderstorms frequently extend beyond the limits of the network. Most, maybe all the large storms consist of many cells that are active simultaneously. Their flashing rates exceed one flash per second. Their VHF emissions are incessant, and their records are difficult to read.

A set of graphs similar to one shown in Figure A6.1 were drawn for each storm that we studied. These compared the electrical activity, as represented by the flashing-rate with the height of the echo-tops, and with the horizontal area enclosed by the 20 dBZ contours at 4 km height. Usually, a peak in the flashing rate occurred within several minutes of a peak in the height or area. In one storm (7 February 1979) the area continued to increase, so that the area did not appear to be a useful parameter for thunderstorms. Peaks in the flashing rate preceded and trailed peaks in the heights of the echo-tops in equal number. The delays ranged -15 minutes to +10 minutes. Heights of echo-tops ranged 9.4 to 14 km amsl. Six were above 12 km amsl. The storms that we studied are listed in Table A6.1. Complete lightning paths were plotted for only nine of these storms.

Hodographs were plotted for each storm. Lightning activity did not appear to be related at all to the airflow directions or to wind-shear. There was often evidence to suggest that the thunderstorms had modified the airflows in their vicinity. Of nine storms, two deviated to the left of the environmental airflows at mid-levels, one deviated to the right, one moved with the airflow. In three cases the storms had stalled. In one of these cases, and on another day the winds were almost absent, and one storm moved in a way that was unrelated to the published environmental winds.

Mr Deon Terblanche kindly provided a Fortran Programme for calculating various indices from Aerological data. This was transcribed into Basic, and run for each of the storms.

Predicted cloud-top heights correlated roughly with peak flashing rates. No other parameter appeared to relate to the electrical activity.

TABLE A6.1
Storm Types and Flashing Rates

Date of Storm	Type	Flashing rate per minute	
		minimum	maximum
14 Feb 79	Multi-cell	4	10
2 Mar 79	Multi-cell	3	4
7 Mar 79	Single cell	1	16
27 Mar 79	Single-cell, Steady state	10	15
8 Apr 79	Multi-cell	1	8
24 Feb 84	Multi-cell	14	29
24 Oct 84	Multi-cell	5	10
10 Dec 84	Multi-cell	1	5
21 Feb 85	Squall-line	10	21
16 Nov 87	Squall-line	2	9
23 Dec 87	Squall-line	6	23
23 Mar 89	Multi-cell	8	18

Bibliographical References

Held, G., and A. E. Carte, Thunderstorms in 1971/72, CSIR Research Report 322, 77 pp, 1973.

Held, G., and H. J. C. van den Berg, A pre-frontal squall line on 14 November 1975, Arch. Met. Geoph. Biokl., Ser A, 26, 361-379, 1977.

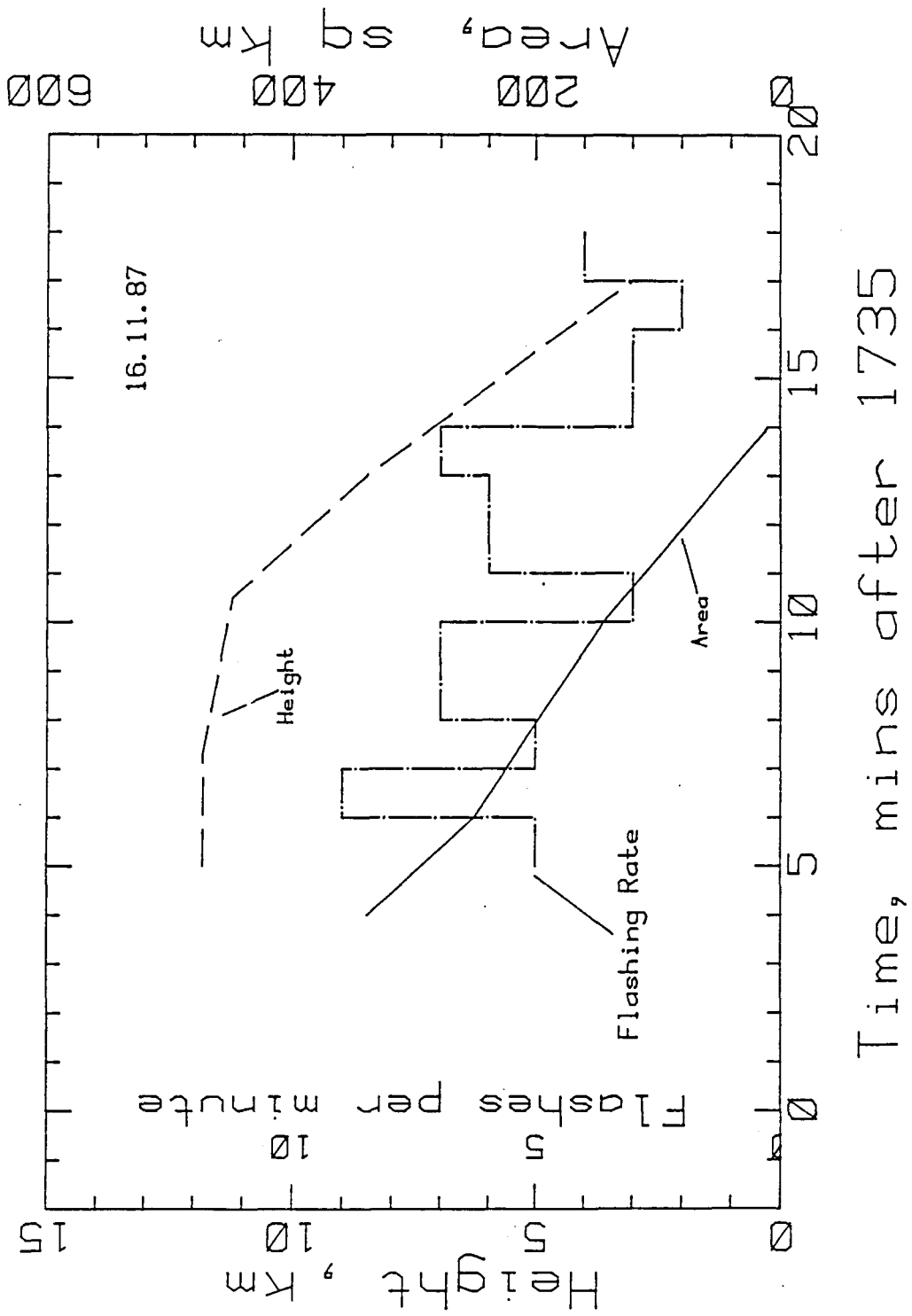


Figure A6.1 Horizontal Area, flashing rate, and height of echo-top for the storm of 11 November 1987.

Appendix 7

THE NUMBERS OF DROPS PER CUBIC METRE CONTRIBUTING TO RADAR
REFLECTIVITY

In this exercise, we assume that all the particles are in a liquid state, and that their sizes are distributed according to the Marshall-Palmer law, stated by Battan [1973] p 85 as:

$$N_D = N_0 \exp(-AD) \text{ per cc, per cm increment in } D$$

where $A = 4.1 R^{-0.21} \text{ per cm}$

and where $N_0 = 0.08 \text{ per cm}^{-4} \text{ per cc}$

and D is the drop diameter, and $N_D dD$ is the number of drops per unit volume in the diameter-interval D to $D + dD$. R is the rainfall rate in mm/hour. The formula for A is due to Gunn and Marshall [1958], and is for rain.

The radar reflectivity, $Z = \sum (N D^6)$ in units $\text{mm}^6 \text{ m}^{-3}$.

The Basic programme is listed below, as is the printout of a sample run for the case where $Z = 100$ (i.e. 20 dBZ), which is Table A7.2.

This calculation shows that for 20dBZ, the total number of drops is 1304 per cubic metre. Half the reflectivity is due to the largest 2.6 drops in every cubic metre and their diameters exceed 1.3 mm. Three-quarters of the value of Z is

due to reflections from the largest 11 drops in every cubic metre (amounting to 0.84% of the total), and their diameters exceed 1 mm. Moreover 1185 drops, (or 90 % of the total per unit volume) whose diameters were less than 0.5 mm did not contribute as much as 2 % of the total reflectivity. Some of these values are shown for other reflectivities in Table A7.1.

TABLE A7.1
Densities and Sizes of Drops Contributing to 50% and 75% of the Radar Reflectivity

Radar Reflectivity, Z in dBZ	Total No. of drops per m ³	Half Z due to		75% of Z due to	
		number n m ⁻³	above dia. mm	number n m ⁻³	above dia. mm
10	847	1	1	8	0.7
20	1304	2.6	1.3	11	1
30	1947	4	1.8	16	1.4
40	2845	4.5	2.6	20	2
50	4103	5.5	3.7	28	2.8

The abovementioned assumes Marshall-Palmer drop-size distribution and that contributions to Z by solid particles were negligible.

These calculations show that radar reflectivity is an indicator of large drops, and that the drops whose diameters are less than 0.75 mm (approximately) all together make a contribution that is negligibly small. These calculations will err from the true conditions that prevail in thunderclouds because they neglect the contributions made by ice, particularly graupel. Dye et al [1986] reported that 5mm

graupel was present in reflecting regions that also caused high electric fields. Data published by Battan [1973] shows that reflections from ice particles are a factor 4.6 down on reflections from water drops of equal size. Departures from the drop-size distribution used here will have caused the results of these calculations to represent conditions that differ slightly from those in the real thunderstorm, and neither of these two factors will vitiate the inferences that are to be drawn from these calculations.

The tabulated quantities ΣnD and ΣnD^2 are discussed in Section 3.2, in Appendix 4.3, Appendix 3.4.2, and in Appendix 10.

A 7.2 *Bibliographical References*

Battan, L. J., *Radar Observation of the Atmosphere*, 324 pp, University of Chicago Press, Chicago, 1973.

Dye, J. E., J. J. Jones, W. P. Winn, T. A. Cerni, B. Gardiner, D. Lamb, R. L. Pitter, J. Hallett, and C. P. R. Saunders, Early electrification and precipitation development in a small, isolated Montana cumulonimbus, *Jour. Geophys. Res.*, 91, D1, 1231-1247, 1986.

Gunn, K. L. S., and J. S. Marshall, The distribution with size of aggregate snowflakes, *Jour. Meteor.*, 6, 243-248, 1958.

TABLE A7.2

RUN
PROGRAM TO WORK Z FROM DROP-SIZE DISTRIBUTION, GIVEN RAINFALL RATE
zxdsd
INPUT RAINFALL RATE IN mm/hr :- ? 0.48

D mm	CUMULATIVE N per cubic m	Z mm ⁶ /m ³	SIGMA ND m /m ³	SIGMA N D ² m ² /m ³
9.999999E-02	495.86	0	4.958565E-02	4.958565E-06
.2	803.2	.02	.1110541	1.725225E-05
.3	993.6999	.159	.1682032	3.439697E-05
.4	1111.77	.643	.2154327	5.328881E-05
.5	1184.95	1.786	.2520251	7.158498E-05
.6	1230.32	3.903	.2792419	8.791507E-05
.7	1258.43	7.210001	.2989231	1.016919E-04
.8	1275.88	11.779	.3128645	1.12845E-04
.9	1286.66	17.519	.3225859	1.215943E-04
1	1293.35	24.214	.3292809	1.282893E-04
1.1	1297.5	31.565	.3338456	1.333104E-04
1.2	1300.08	39.246	.336932	1.370142E-04
1.3	1301.67	46.941	.3390045	1.397084E-04
1.4	1302.66	54.38101	.3403879	1.416452E-04
1.5	1303.27	61.357	.3413066	1.430232E-04
1.6	1303.65	67.72601	.341914	1.43995E-04
1.7	1303.89	73.40601	.342314	1.44675E-04
1.8	1304.03	78.36601	.3425785	1.451476E-04
1.9	1304.12	82.61901	.3427483	1.454739E-04
2	1304.18	86.204	.3428603	1.45698E-04
2.1	1304.21	89.18301	.3429333	1.458511E-04
2.2	1304.23	91.623	.3429806	1.459553E-04
2.3	1304.25	93.59801	.3430113	1.460259E-04
2.4	1304.26	95.179	.3430312	1.460735E-04
2.5	1304.26	96.43001	.343044	1.461056E-04
2.6	1304.26	97.412	.3430522	1.46127E-04
2.7	1304.27	98.17401	.3430575	1.461414E-04
2.8	1304.27	98.763	.343061	1.46151E-04
2.9	1304.27	99.21301	.3430632	1.461573E-04
3	1304.27	99.554	.3430646	1.461615E-04
3.1	1304.27	99.81201	.3430655	1.461643E-04
3.2	1304.27	100.006	.343066	1.461662E-04
3.3	1304.27	100.15	.3430664	1.461674E-04
3.4	1304.27	100.257	.3430666	1.461682E-04
3.5	1304.27	100.336	.3430668	1.461687E-04
3.6	1304.27	100.394	.3430669	1.461691E-04
3.7	1304.27	100.436	.3430669	1.461693E-04
3.8	1304.27	100.467	.3430669	1.461695E-04
3.9	1304.27	100.489	.343067	1.461696E-04
4	1304.27	100.505	.343067	1.461696E-04
4.1	1304.27	100.516	.343067	1.461697E-04
4.2	1304.27	100.525	.343067	1.461697E-04
4.3	1304.27	100.531	.343067	1.461697E-04
4.4	1304.27	100.535	.343067	1.461697E-04

RAINFALL RATE = .48 mm /hr. dBZ = 20.02355

OK

```

LIST
1 DIM N(90),D(90),Z(90)
3 PRINT"PROGRAM TO WORK Z FROM DROP-SIZE DISTRIBUTION, GIVEN RAINFALL RATE"
4 PRINT"zxdsd"
20 PRINT"INPUT RAINFALL RATE IN mm/hr :- ";
21 INPUT R
22 R1=-41*R^(-.21) ' per cm;part of the exponent
23 D2 = .01 'drop diameter increment in cm
35 N=0
36 D=0
37 Z=0
38 N8 = 0
39 N7 =0
40 PRINT "D mm ", "CUMULATIVE N", "Z .mm^6/m3", "SIGMA ND", "SIGMA N D^2 "
41 PRINT " ", " per cubic m", " ", " m-/m^3", " m^2/m^3"
50 FOR I =1 TO 90
52 D=D+D2 ' drop diameter in cm
53 D(I)= D * .01 ' in metres
54 D3= D*10 ' in mm
60 N9 = .08*(EXP(R1*D)) ' No of drops/cm^3 in 1cm increment as per MP dsd
62 N(I)= N9 * 1000000! * D2 ' per cubic metre per D2 increment
63 N=N+N(I) 'cumulative No. of drops
64 D3 = .01 *(INT (100* D3+.5))
65 N3= .01*(INT(100*N+.5))
69 Z6=N(I)*D(I)^6*1E+18 'increment in Z in units of mm^6/m^3
70 Z=Z+Z6
72 W2=4.343*(LOG(Z)) 'dBZ
75 Z9= .001*(INT(Z*1000+.5))
76 N8=D(I)*D(I)*N(I) + N8 ' sigma nd ^2
78 N7 = N7 + D(I)* N(I) ' sigma nd
90 IF N(I) <.0000004 THEN 120
95 PRINT D3,N3,Z9,N7 ,N8
96 NEXT I
120 PRINT "RAINFALL RATE = ";R;" mm /hr. dBZ = "; W2
130 PRINT
131 PRINT
132 PRINT
150 END
Ok

```

LIGHTNING FLASHES WITH HIGH ORIGINS

by

David E. Proctor

Ematek, CSIR, P. O. Box 1327, Honeydew 2040, South Africa.

ABSTRACT

We studied VHF radio pictures of 21 cloud flashes that began at altitudes above 7.4 km msl. Most were branched and followed complex paths. 54/92 branches were directed principally in horizontal directions; 14 branches were directed downward and 26 extended in directions that were mainly upward. First streamers progressed relatively slowly, at speeds near 10^4 m/s, but they appeared to carry more charge than charges carried by branches of flashes with low origins. Thirteen charge line densities, inferred from measurements of electric field change, ranged 0.7 to 8.7 C/km (median value 3.3 C/km), and the corresponding leader currents ranged 37 A to 630 A, with a median value of 130 A. All 21 flashes were negative. All emitted pulses slowly from relatively large pulse sources. Detailed maps of four flashes are shown. These provide some insight into the behavior of lightning flashes. One was typical of most. Another followed an almost circular path, and a third changed its polarity during the course of the flash.

1. Introduction

Our first trial recordings, taken in 1967, showed that there were two kinds of flashes: those that emitted radio pulses at rates above 10^5 per second, and flashes that emitted pulses at rates near 1 per millisecond. *Proctor et al* [1988] and *Proctor* [1991] reported that flashes which began in the lower regions of thunderclouds emitted pulses rapidly, but that flashes which began at heights greater than 7.4 km above msl, approximately, emitted radio pulses at the lower rates. Figure 1 of the paper by *Proctor* [1991] shows the distribution of heights at which 773 flashes began. The distribution is bimodal, with peaks near 5.3 km and 9.2 km above msl. Approximately 44 percent of that sample of 773 flashes belonged to the higher group. We have made a detailed study of 21 flashes of that kind, and this paper describes some of their properties.

2. Method.

Three-dimensional maps that are also time-resolved were plotted for each of the flashes described here. These maps were constructed by mapping sources of radio signals emitted by lightning. Sources were located by measuring differences in the times at which these radio signals were received at stations that were widely spaced and sited at ground level. The hyperbolic method is known well, and this application of it has been described previously by *Proctor* [1971]. Time resolution of 70 nanoseconds permitted sources to be located in space with rms errors 25 m, 25 m and 140 m to 250 m in the

three spatial coordinates. Recordings of electric field-changes (EFC's) due to the flashes were used in conjunction with the radio maps in order to calculate values of charge and current that had been carried by the flashes; details of the method were given by *Proctor et al* [1988]. The radio maps provided information regarding the temporal behavior of the flashes. In particular, they showed the overall shapes and extents of the flashes as well as the speeds and directions in which the streamers extended, and the locations of their origins ("starting points"). Currents that flowed in first streamers were calculated by taking the products of charge line-densities and the speeds at which the channels extended. First streamers are leader streamers in cloud flashes; they are the counterparts of stepped leaders in flashes to ground. Details of the coordinate system used here have been supplied by *Proctor* [1971,1981,1991].

3 Results.

3.1 *Origin heights*

Origin heights of 21 flashes ranged 7.7 km to 9.9 km above mean sea level (msl). The median value was 8.8 km above msl.

3.2 *Flash sizes and orientations*

In order to describe their sizes, we determined the sizes of imaginary boxes that would have enveloped the flashes. Their volumes ranged from 9 to 1260 km³. Horizontal extents ranged 0.5 to 15.5 km; half lay within limits 4.5 to 8.5 km.

Vertical extents ranged 0.5 to 12.5 km; half were 3.5 to 5.5 km thick. Histograms of horizontal and vertical extents are shown in Figure 1. Fifty-two out of 92 first streamer branches were mainly horizontal; 26 extended in directions that were mainly upward; 14 were mainly downward.

3.3 *Speeds at which streamers extended*

Thirty-two channels extended at speeds that ranged 1.3×10^4 m/s to 1.2×10^5 m/s. Their modal value was 6 to 7×10^4 m/s, and the median value was 6.4×10^4 m/s. The slower speeds were measured where streamers had extended intermittently. The distribution of streamer speeds is shown by Figure 2a. These data relate to first streamers.

3.4 *Polarities*

Radio maps and the EFC's recorded by 21 flashes of this kind, showed that all discharged excess negative charge. Flash 123 changed its polarity while in progress. This flash will be described in a later paragraph.

3.5 *Charge line-densities and currents*

Thirteen densities were measured. These ranged 0.7 to 8.7 Coulombs/km. the median value was 3.3 C/km. Currents in first streamers ranged 37 A to 630 A, and the median of 13 currents was 130 A. See Figure 2b.

Table 1 shows how these data compare with corresponding data

for cloud-flashes that pulsed rapidly (and which began at lower heights). Data relating to source sizes and nearest neighbor distances have been taken from *Proctor* [1981].

3.6 *Morphology*

These flashes varied in their appearances and behavior. One flash produced five short radial streamers; in another flash, pulse sources were distributed like raisins in a fruit cake, and this flash probably consisted of many radial branches that had been spaced too closely for them to be resolved with this system. Two flashes produced streamers that appeared to encircle their origins like woolballs. In one case, two flashes occurred in quick succession, one high and one low, so that we recorded a sudden change in pulse-rate. Only two flashes produced only one first streamer each. The remaining eighteen extended along multiple paths. Ten out of twenty flashes produced relatively long streamers. Long streamers tended to form successively in time. Only one pair formed simultaneously, and then only for some of the time. Short streamers often extended simultaneously. In two respects Flash 151 may be nearest to being typical: it produced long streamers that extended in opposite directions, and they formed in succession. Except for its orientation and number of branches, flash 165 resembled many other cloud flashes.

3.7 Selected examples

1. Flash 165, recorded at 1654:40.8 on 23 December 1987

Two elevation views of this flash are shown in Figure 3. The flash began 6.23 km AGL. Its first streamer extended 6.8 km in 92.4 msec (ie at 7.3×10^4 m/s), although for the first 10 msec its speed was approximately 3×10^5 m/s. This first streamer extended to points mapped as J in Figure 3. We located positions of the sources of 131 pulses emitted by the streamer, as well as one Q-source at time D and four points E that were components of another Q-streamer. The graph of Z versus time in Figure 4 shows that activity ceased for 20 msec after time J (92.4 msec). Seventeen Q-streamers were recorded in the interval between 115 msec and 180 msec. The last activity produced both pulses and Q-streamers between 249.4 and 250.6 msec. Figure 5 shows the relative positions of the pulsed emission and the Q-sources. The majority (123/131) of pulse-sources were located in the main channel, which lay above the origin; the vast majority of Q-sources emanated from streamers that occurred below the origin. Only two Q-sources were high. The auxiliary record showed that a gradual EFC whose final amplitude reached 720 V/m was caused by the first streamer, and that the Q-streamers caused no measurable EFC. Figure 6 compares the recorded EFC with a curve calculated by assuming that every pulse-source became charged at the expense of charge that had resided in the vicinity of the origin of the flash. Reasonably good agreement between the curves resulted when the center of the origin charge had been chosen to be 5.73 km AGL and the

line-density was 1.65 C/km. The charge was negative.

2. Flash 151 recorded at 1502:12.3 on 26.3.85

Sources of pulses have been mapped in Figures 7 and 8. Letter symbols denote time in increments of 20 milliseconds. The maps show how first streamers A-G and A-Q extended in opposite directions. Figure 9 compares the recorded EFC with the EFC calculated by supposing that the mapped channels became charged negatively at the expense of a supply at the origin. One reason for the discrepancies between the two curves was the effect of a simultaneous flash near (0,-13,3), which we mapped only in part.(Not shown).

3. Flash 123, recorded at 1633:46.5 on 21.2.85

Figure 10 shows a plan view of pulse sources whose heights were above 6.4 km agl, a restriction that was introduced for the sake of clarity. Figure 11 shows an elevation view of 898 pulse sources that were active during this flash. The flash began at origin A (-6.2, 3.16, 7.6) km, and carried an excess negative charge along the path A to G, mapped with letter symbols in Figure 12, and mapped with dots in Figures 10 and 11. The recorded EFC, drawn as a thin line in Figure 13, could not be reproduced, even approximately, unless we assumed that the flash intercepted a new origin at H at (-6.48, 3.8, 5.36) km, which supplied positive charge to the flash. If this assumption were not made, then the calculated curve of EFC continued to decrease after 190 millisc., instead of following the thick curve shown in Figure 13. One

reason for the remaining discrepancies between the two curves of EFC shown in Figure 13 was due to our not having allowed for the change in sign of charge deposited along the section A-G.

4. Flash 87, recorded at 1842:27.8 on 27. 3. 79

Most of this flash was contained in a horizontal slice approximately 1 km thick. Its plan view is shown in Figure 14. The flash began by discharging along three short radial branches, and then followed a long, roughly circular path that nearly closed upon itself. It poses the question: why did it not discharge along a more direct path from origin to terminus? Some of the answer was provided by comparing the path with the radar precipitation pattern. The CAPPI reproduced in Figure 15 is a plan view of a thin horizontal slice. The figure shows how the flash followed paths close to and parallel with the 20 dBZ contour. It also tracked contours of higher reflectivity, at times K, L, and M.

4. Discussion

4.1 *Classification by pulse rate*

Kitagawa and Brook [1960] reported that flashes emitted radio pulses at two rates. They claimed that they could distinguish cloud flashes from ground flashes by observing pulsed emissions from lightning at frequencies below 1 MHz. Our observations would agree with theirs if there were no cloud

flashes that began at the lower levels, a state of affairs that might have existed in the storms that they studied in New Mexico. It is not the case in Transvaal. Cloud flashes begin in both low and high regions of thunderclouds. Therefore there are cloud flashes that pulse rapidly, indeed they are the majority, as well as cloud flashes that pulse slowly. We are not able to distinguish cloud flashes from ground flashes by observing pulse-rates. However, we have not yet observed one ground flash that emitted pulses slowly. In that respect we agree with *Kitagawa and Brook* [1960].

Although we have been able to show that there was no important difference between first streamers in cloud flashes and ground-flash stepped leaders (except for their destinations), we have not been able to reconcile our observations of pulse rate with those reported by Schonland. *Schonland et al* [1938] claimed that there were two kinds of stepped leader. They named them alpha and beta types. Beta leaders extended relatively rapidly by taking long, bright steps; alpha leaders advanced slowly but more uniformly, by taking smaller, less luminous steps. Alpha leaders advanced at speeds near 10^5 m/s (which is near the lower limit of speeds at which the more rapid, high pulse frequency flashes extend). Beta leaders extended at speeds 8×10^5 m/s to 2.4×10^6 m/s. They mentioned no counterpart that extended with speeds at which low pf flashes extend. *Thomason and Krider* [1982] showed how scattering by particles prevented the pulses of light emitted by channels that extended inside thunderclouds coinciding with the radio pulses they radiated. This explains some difficulties experienced in this regard by

Schonland et al [1938]. *Beasley et al* [1983] showed that pulses of light from stepped leaders below cloud coincide with their radio pulses, and this is why we should have expected to find some measure of agreement between our pulse-rates and those reported by *Schonland et al* [1938] and by *Schonland* [1956]. We suppose that some of their measurements were limited by the lack of the third dimension. The matter warrants further attention.

4.2 *Polarity. The distribution of charges in clouds.*
Orientations and extents of streamers

All twenty-one flashes whose origins were high carried excess negative charge. *Proctor* [1991] reported that the majority began near contours for 20 dBZ. The model of charge-distribution proposed by *Wilson* [1920], page 98, indicated that at these heights thunderclouds were charged positively, and we concluded that these flashes originated at screening layers, described by *Vonnegut* [1963] and by *Brown et al* [1971]. Screening layers form when negative space-charge migrates to the thundercloud under the influence of the upper, diffuse positive charge, attaches to precipitation elements, and so becomes relatively immobile. The study reported by *Proctor* [1983] and several *in situ* measurements reviewed by *Williams et al* [1985] showed that the vertical extent of the lower, negatively charged region amounted to 1600 m at most. On the other hand, *Malan* [1956] concluded that there existed a vertical column of negative charge that reached heights of 9.8 km above msl, and that its

horizontal extent was 8 km. *Malan and Schonland* [1951] stated that it extended from 0 degree C to -40 degree C levels. It now appears that the lower region of excess negative charge has a vertical thickness less than 1.6 km and that the upper negatively charged regions are relatively small, and are distributed on the surface for 20dBZ, near the peripheries of the volumes occupied by precipitation.

Many attempts have been made to discover whether cloud flashes are mostly vertical or mostly horizontal, with a view to finding how charge is distributed in thunderclouds. These efforts have been reviewed by *Brook and Ogawa* [1977] and by *Uman* [1987]. The work described here indicates that most high flashes discharge horizontally (56% of this rather small sample were horizontal).

Preliminary comparisons with precipitation patterns of the host storms indicate that flashes never extended horizontally more than some 2 km beyond the 20 dBZ contour of the CAPPI that had the greatest extent in the direction of the lightning branch. It is therefore true to state that the extents of the flashes are determined by the sizes of the host thunderstorms. For reasons stated previously (*Proctor* 1991), we have elected to study small thunderstorms, and therefore flashes reported here would be similarly affected.

4.3 *Speeds at which first streamers extended*

Table 1 shows that high flashes extended more slowly than flashes that originated at the lower levels. We suppose that

the speed is influenced by the availability of charge at the origin, which may be determined by the particle density, and perhaps by the lower conductivity of ice. When we attempt to compare our measurements with those made by other workers, we have to take origin height and type of streamer into account. *Sourdillon* [1952] measured 5×10^4 m/s for the leader of his flash T35, which he designated as Type 1. *Isikawa* [1961] (page 123) measured 5×10^4 m/s for the "slow streamer initiating a cloud discharge" but did not state the origin height. *Takagi* [1961] (page 52) measured 1.3×10^4 m/s and indicated that the flash began in the upper regions of the cloud. *Brook and Ogawa* [1977] reported a speed of 8×10^3 m/s. Speeds reported by *Brantley et al* [1975] ranged 5.6×10^3 to 1.1×10^4 and they probably related to the retrogressive actions of flashes rather than to first streamers. *Krehbiel* [1981] (page 144) measured 3×10^4 for the first streamer of flash 46 that originated at an altitude near 12 km.

4.4 *Charges and currents*

We attempted to reconstruct the waveforms of EFC recorded by the flashes. The reconstructed waveforms were calculated by assuming that the pulse sources became charged at the expense of charge situated near the origin. Calculated EFC's agreed reasonably well with the recorded versions for a time that was roughly the first 75 % of the duration of the EFC for each flash. Except for very simple flashes, the calculated waveforms differed appreciably from the measured waveforms in the latter stages of the pulsed phase, presumably because the

last few streamers and branches were supplied from new origins. The EFC's took place during the time when the flashes emitted pulses. This phase corresponds to the phases which *Kitagawa and Brook* [1960] named the *Initial* and *Very Active (VA)* phases. While studying most flashes reported here we have purposely omitted paths taken by streamers that radiated the non-pulsed radiation, which we named *Q noise*, and which occur mostly during the final stages or *J-type phases* of the flashes. (Flash 165, presented as Example 1, is an exception in this regard). Q-streamer paths tend to clutter up the maps. Some Q-streamers can be associated with small step-changes in electric field which *Kitagawa and Kobayashi* [1958] named K-changes. Our inability to reconstruct exactly the EFC's recorded during the later phases of the pulsed emission meant that we were unable to calculate total quantities of charge that had been discharged by each flash. The best we could do was to calculate line-densities for portions of each flash. Seven of the twelve values we measured are larger than values we measured previously. These seven values range from 3.3 to 8.7 C/km. The remaining five range 0.7 to 2 C/km. *Proctor* [1981] measured values 0.9 to 2 C/km for high pf cloud flashes. *Uman* [1969] estimated 1 C/km using data reported by others. Most of our calculations were based on a surmise that the origin of charge was close to the starting point of the flash, and only when better agreement between calculated and measured waveforms resulted from taking the origin of charge lower, was this done. Moving the origin of charge down, resulted in lower values of charge and line density because the moment had been increased. *Mazur* [1989] believes that a

nonradiating, slow positive streamer begins at the flash origin, and penetrates the charged volume at a speed near 10^4 m/s. This streamer, which acts to drain the charged volume, is too slow to affect the calculations for high pf cloud flashes whose first streamers extend at speeds near 2×10^5 m/s, but this streamer will have increased the distance between flash origin and the effective center of the charged region in the case of those low pf flashes that extend slowly. An increase of this distance would result in lower values of calculated charge, charge line density, and current, and for this reason our measurements of current, charge and line-density are probably higher than their true values. The foregoing is further evidence of the existence of Mazur's positive streamers.

4.5 *Discussion of the selected examples of radio maps*

Example 1 illustrates behavior patterns observed in all lightning: pulsed emission accompanies the advance of leaders and first streamers, and Q noise is radiated by rapid streamers that accompany extensions on the opposite side of the origin of the flash. Streamers that produce pulsed emission also cause substantial changes in the Electric field at ground. Some Q-streamers are associated with K-changes. Except for those Q-streamers that accompany return-strokes of ground flashes (usually strokes of order 1 or 2), few Q-streamers produce large changes in electric field. In all the aforementioned respects, ground-flashes and cloud flashes are similar. These results supplement and confirm those reported by *Proctor et al* [1988]. Most Q-streamers occur

during intervals that *Kitagawa and Brook* [1960] termed *final* or *j-type* phases. Cloud flashes differ from first strokes to ground in that the Q-noise from cloud flashes, during their final stages, begins only after a delay of some milliseconds has elapsed following the cessation of growth or extension of the pulse-emitting streamer. A similar delay was noted also by *Sourdillon* [1952], during his photographic studies of cloud-flashes. Example 1 did not exhibit an *initial* stage; the extension of the first streamer began without preamble. Six pulse-sources that were located well below the extending streamer-tip were unusual. See Figure 4. Pulsed activity is usually confined to regions near the advancing tips of the streamers.

Most lightning channels carry excess negative charge. Nevertheless, isolated concentrations of positive charge have been probed by *Dye et al* [1988]. Flash 123 demonstrates that sometimes these positive concentrations are great enough to supply extensive flashes. It is also worth noting that the negative streamers began first, and that the positive supply was engaged only after it had been intercepted by the negative streamer. The pulsed emission from the advancing streamer was apparently unaltered by the change in polarity.

Flash 87 provides us with information regarding factors that guide discharges. It appears that the electric field at the tip determined the path. It is also evident that charges resided near some 20 dBZ surfaces and on surfaces where reflectivity gradients were steep. It also demonstrates that this flash acted to distribute negative charge along the

path, (or to neutralize positive charge that had been distributed along a region that was eventually threaded by the path), rather than discharging between two poles. Another example of this type of flash was described in detail by Proctor [1981]. In that example, the extent of the activity during each pulse was also taken into account.

All four examples shown here, and indeed the three dimensional pictures of most all the flashes we have mapped hitherto have demonstrated that the shapes of lightning paths have to be known when calculating charge from measured electric field changes. Streamers act to distribute charge along their paths, and consequently the shapes and extents of these paths are important.

5. Conclusions

We have displayed four further examples of cloud flashes with high origins. We have also provided information regarding origin heights, extents, orientations, first streamer speeds, polarities, charge line-densities and currents that were observed in 21 flashes of this kind.

Acknowledgements

I thank the CSIR for providing funds and facilities necessary for this research, and also for granting permission to publish this paper. I am indebted to the Water Research Commission for financial assistance. Special thanks are due to Dr. George Green for his interest and good offices. I am greatly indebted to Dick Uytendogaardt for his efforts and for his knowledgeable assistance.

Bibliographical References.

- Beasley, W. H., M. A. Uman, D. M. Jordan, and C. Ganesh, Simultaneous pulses of light and electric field from stepped leaders near ground level, *Jour. Geophys. Res.*, 88, C13, 8617-8619, 1983.
- Brantley, R. D., J. A. Tiller, and M. A. Uman, Lightning properties in Florida thunderstorms from video tape records, *Jour. Geophys. Res.*, 80, 24, 3402-3406, 1975.
- Brook, M., and T. Ogawa, *The Cloud discharge*, in *Lightning*, Vol 1, pp 191-230, edited by R. H. Golde, Academic Press, New York, 1977.
- Brown, K. A., P. R. Krehbiel, C. B. Moore, and G. N. Sargent, Electrical screening layers around charged clouds, *Jour. Geophys. Res.*, 76, 12, 2825-2835, 1971.
- Dye, J. E., J. J. Jones, A. J. Weinheimer and W. P. Winn, Observations within two regions of charge during initial thunderstorm electrification, *Q. J. R. Meteorol. Soc.*, 114, 1271-1290, 1988.
- Isikawa, H., Nature of lightning discharges as origins of atmospherics, *Proc. Res. Inst. of Atmosphericics*, Nagoya University, 8A, pp 1-273, 1961.
- Kitagawa, N., and M. Brook, A comparison of intracloud and cloud-to-ground lightning discharges, *Jour. Geophys. Res.*, 65, 4, 1189-1201, 1960.
- Kitagawa, N., and M. Kobayashi, Field-changes and variations of luminosity due to lightning flashes, in *Recent Advances in Atmospheric Electricity*, edited by L. G. Smith, pp 485-501, Pergamon Press, London, 1958.
- Krehbiel, P. R., An analysis of the electrical field-change produced by lightning, Vols 1 and 2, Ph.D. Thesis, UMIST, Report T-11, New Mexico Institute of Mining and Technology, Socorro NM 87801, 1981.
- Malan, D. J., Visible electrical discharges inside thunderclouds, *Geofisica pura e applicata - Milano*, 34, 221-223, 1956.
- Malan, D. J., and B. F. J. Schonland, The distribution of electricity in thunderclouds, *Proc. Roy. Soc.*, A 209, 158-177, 1951.
- Mazur, V., Triggered lightning strikes to aircraft and natural intracloud discharges, *Jour. Geophys. Res.*, 94, D3, 3311-3325, 1989.
- Proctor, D. E., A hyperbolic system for obtaining VHF radio pictures of lightning, *Jour. Geophys. Res.*, 76, 6, 1478-1489, 1971.
- Proctor, D. E., VHF radio pictures of cloud flashes, *Jour. Geophys. Res.*, 86, C5, 4041-4071, 1981.

Proctor, D. E., Lightning and precipitation in a small multicellular thunderstorm, *Jour. Geophys. Res.*, 88, C9, 5421-5440, 1983.

Proctor, D. E., Regions where lightning began, *Jour. Geophys. Res.*, 96, D3, 5099-5112, 1991.

Proctor, D. E., R. Uytendogaardt and B. M. Meredith, VHF radio pictures of lightning flashes to ground, *Jour. Geophys. Res.*, 93, D 10, 12 683-12 727, 1988.

Schonland, B. F. J., The lightning discharge, *Handbuch der Physik*, edited by S. Flugge/ Marburg, 22, pp 576-628, Springer-Verlag, Berlin, 1956.

Schonland, B. F. J., D. B. Hodges, and H. Collens, Progressive lightning 5, A comparison of photographic and electrical studies of the discharge process, *Proc. Roy. Soc. of London*, A 924, 166, 56-75, 1938.

Sourdillon, M., Etude a la chambre de Boys de l'eclair dans l'air et du coup de foudre a cime horizontale, *Ann. de Geophysique*, 8, 4, 349-379, 1952.

Takagi, M., The mechanism of discharges in a thundercloud, *Proc. Res. Inst. of Atmospheric*, Nagoya University, 8B, pp 1-106, 1961.

Thomason L. W., and E. P. Krider, The effects of clouds on the light produced by lightning, *Jour. Atmos. Sci.*, 39, 9, 2051-2065, 1982.

Uman, M. A., *Lightning*, 264 pp Mc Graw-Hill Book Co., New York, 1969.

Uman, M. A., *The Lightning Discharge*, 376 pp, Academic Press, New York, 1987.

Vonnegut, B., Some facts and speculations concerning the origin and role of thunderstorm electricity, *Meteor. Monogr.*, 5, 224-241, 1963.

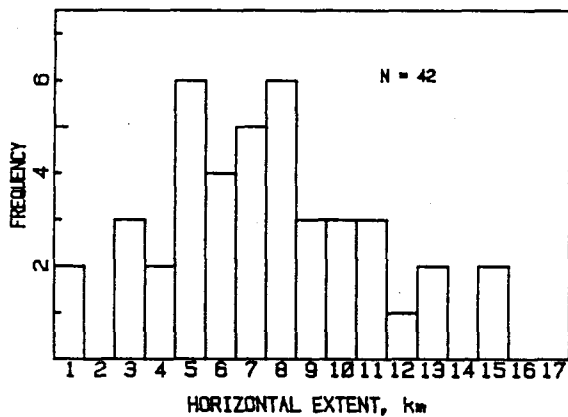
Williams, E. R., C. M. Cooke and K. A. Wright, Electrical discharge propagation in and around space charge clouds, *Jour. Geophys. Res.*, 90, D4, 6059-6070, 1985.

Wilson, C. T. R., Investigations on lightning discharges and on the electric field of thunderstorms, *Phil. Trans. Roy. Soc., London.*, A 221, 73-115, 1920.

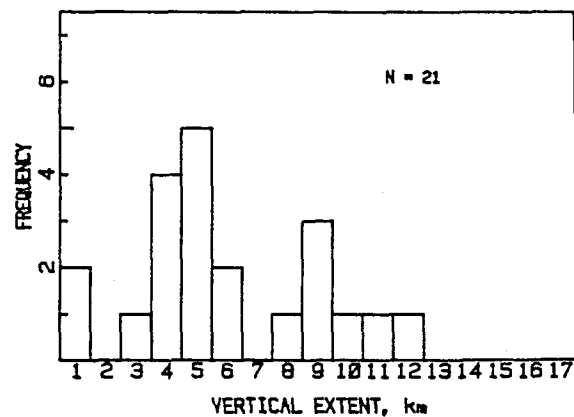
TABLE 1. Comparison of Flashes with Low and High Origins.

Attribute:-	Flashes with:		Units
	Low origins	High origins	
Origin height	2.4 to 7.4	7.4 to 14	km amsl
Pulse rates	2×10^5 to 2×10^6	2×10^3 to 4×10^4	s^{-1}
Typical source lengths	60	300	m
Pulse source NND's	30 to 60	30	m
Speeds of channel extension	6×10^4 to 5×10^5	1.3×10^4 to 1.2×10^5	m/s
Charge line-density	10^{-3}	7×10^{-2} to 8.7×10^{-3}	C/m

NND is Nearest Neighbor Distance
amsl = above mean sea level.

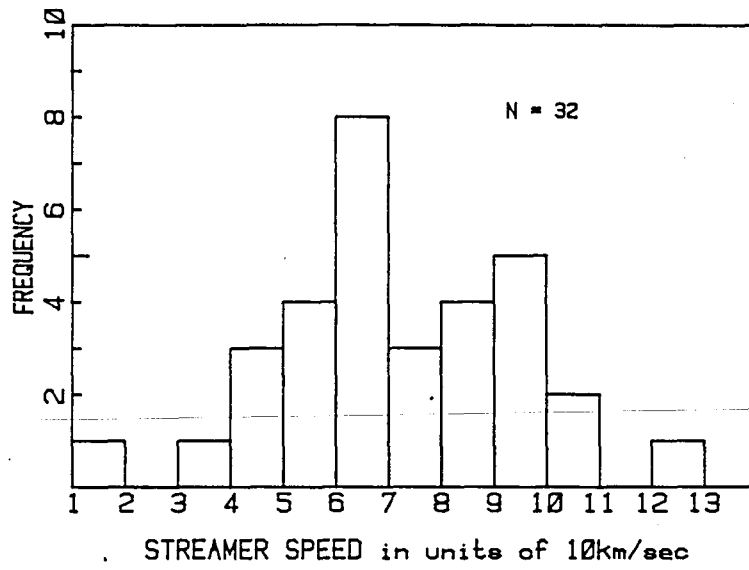


(a)

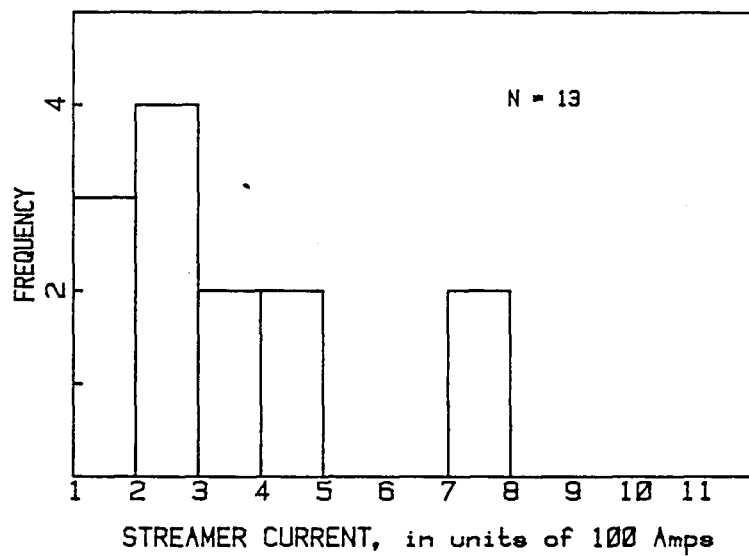


(b)

Figure 1 a). Distribution of 42 horizontal extents of cloud flashes with high origins. b). Histogram of their vertical extents. First streamers only.



(a)



(b)

Figure 2. a). Histogram of the speeds at which 32 first streamers extended. b). Histogram of 13 currents in first streamers.

Figure 4. Heights of sources active during flash 165 plotted to a base of time. Small letters denote pulse-sources; larger letters denote Q-sources.

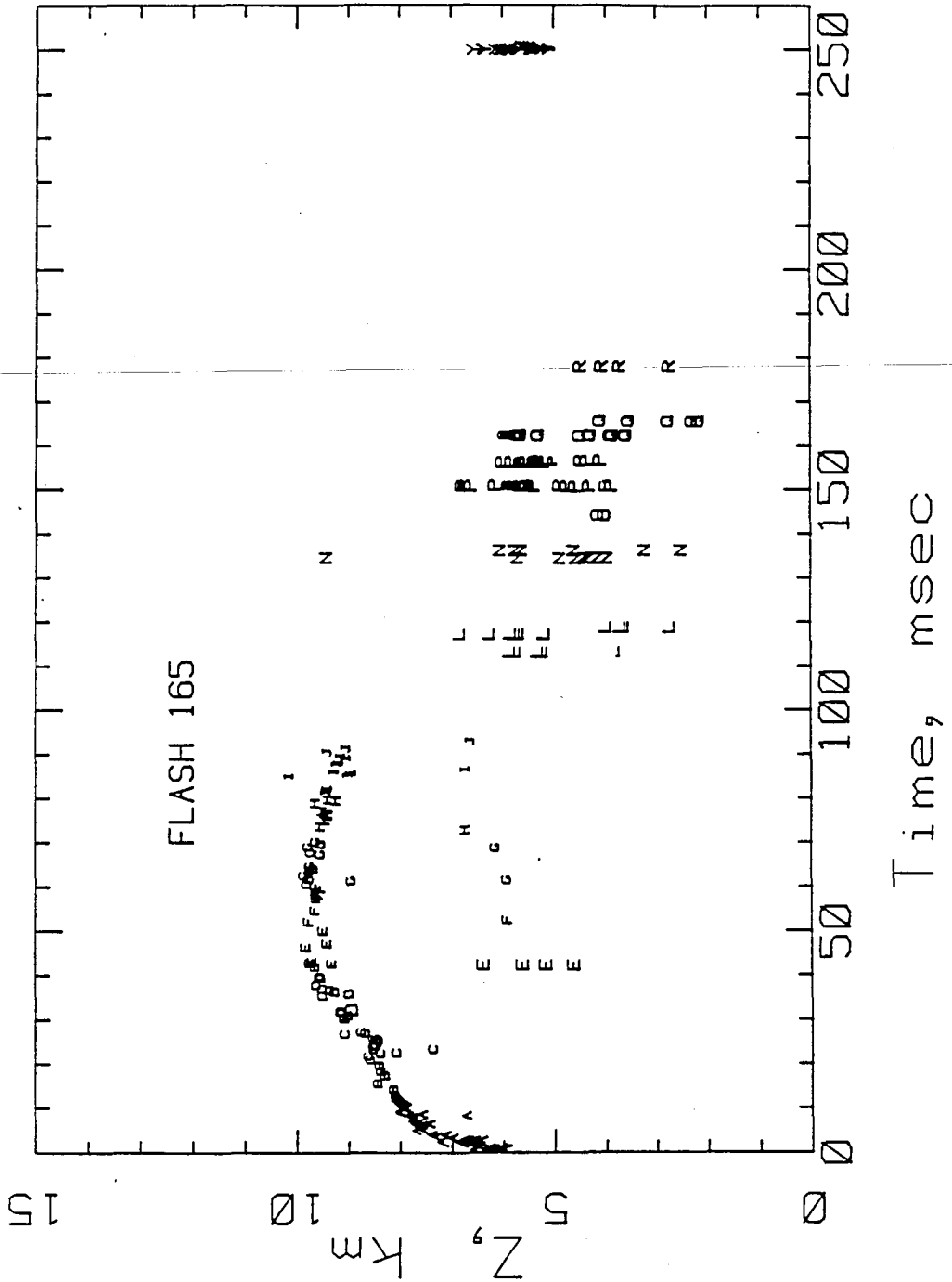


Figure 6. Electric field change generated by flash 165 as observed at ground, shown as continuous line. Dashed line is the calculated curve. See text. Polarity is such that a change from zero to a fair-weather field would cause an upward deflection.

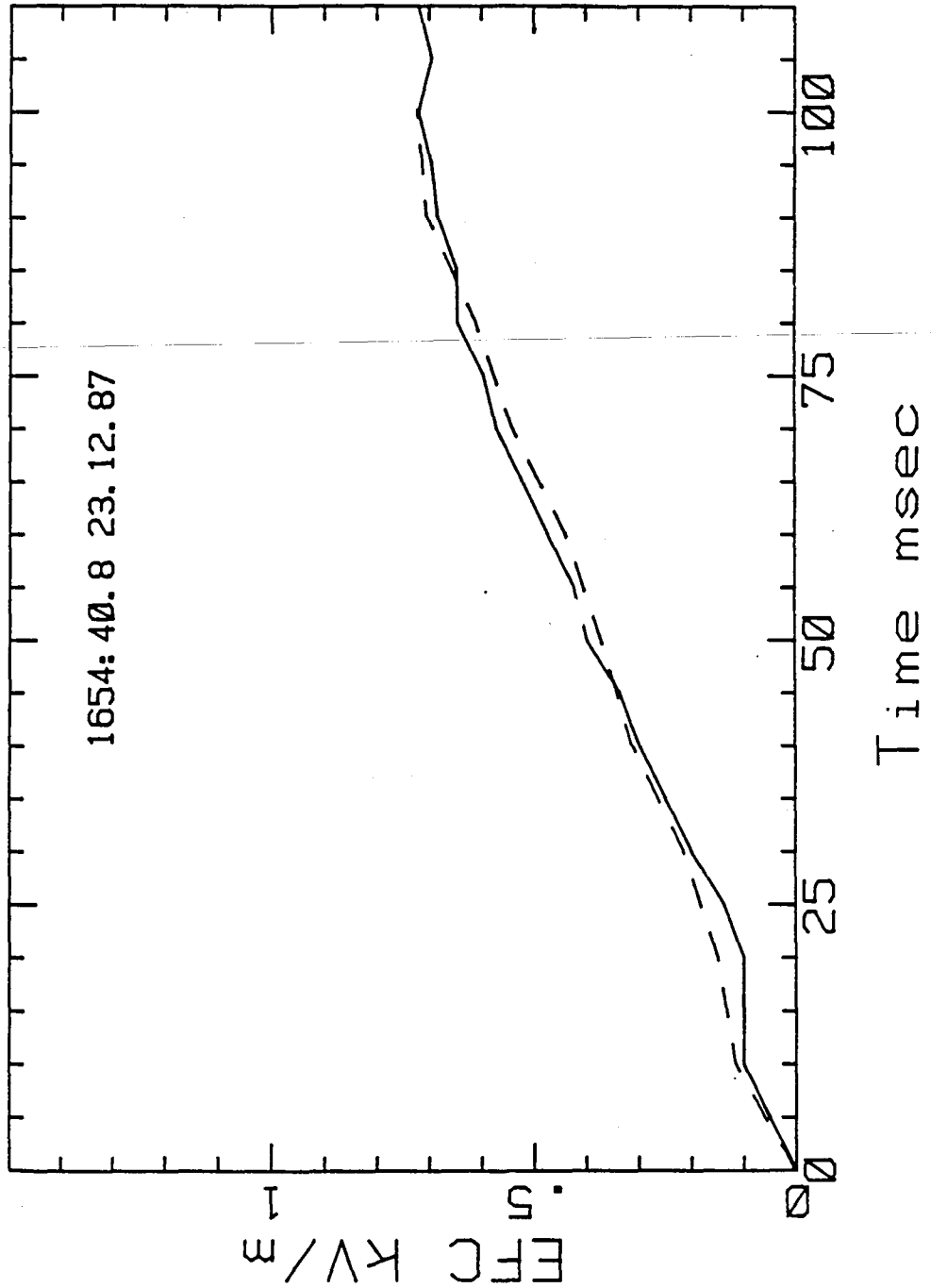


Figure 7. Plan view of pulse-sources that were active during Flash 151. Time scale is indicated by alphabetical symbols that change for every 20 milliseconds.

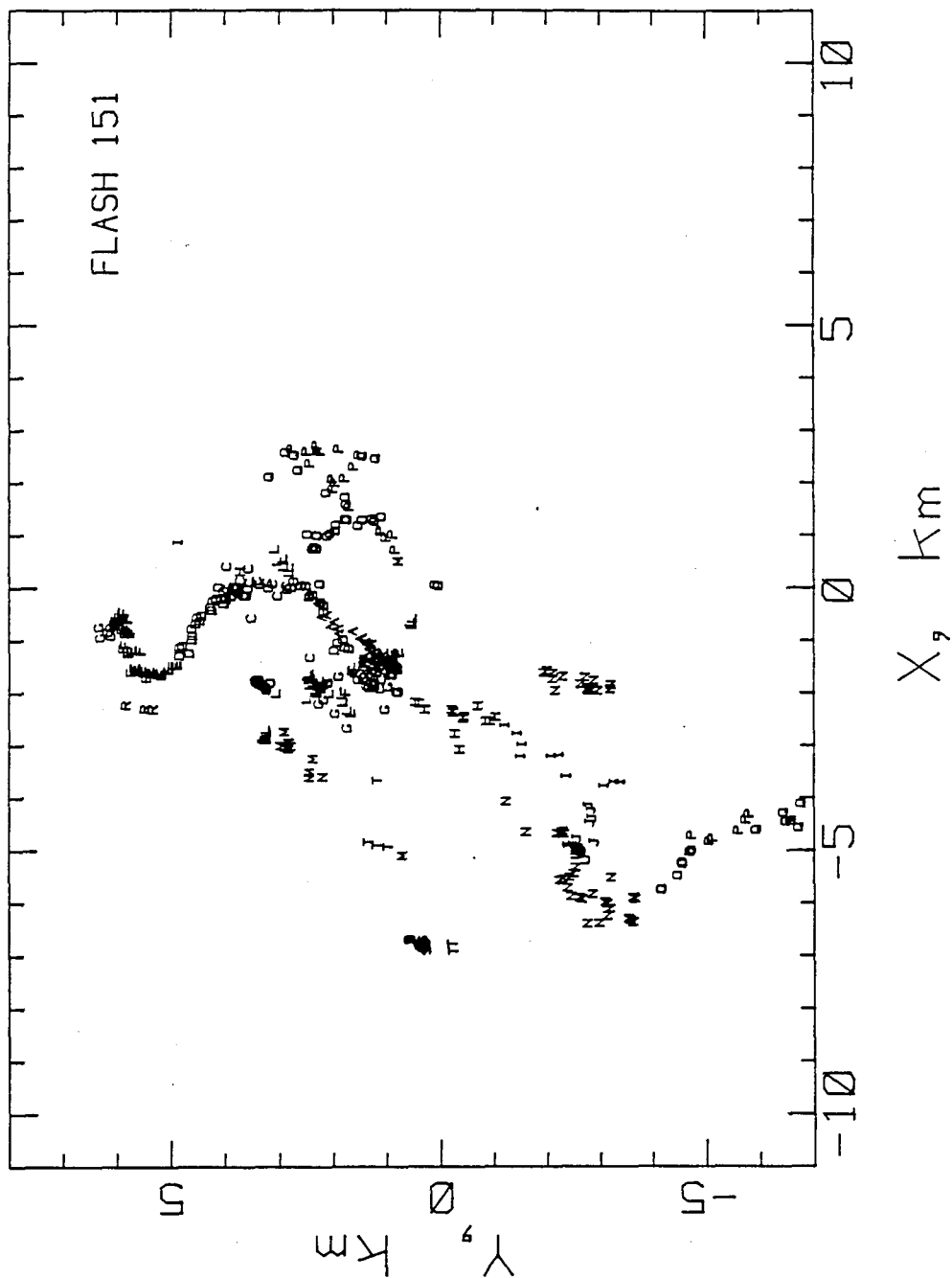


Figure 8. Elevation view of pulses active during flash 151.

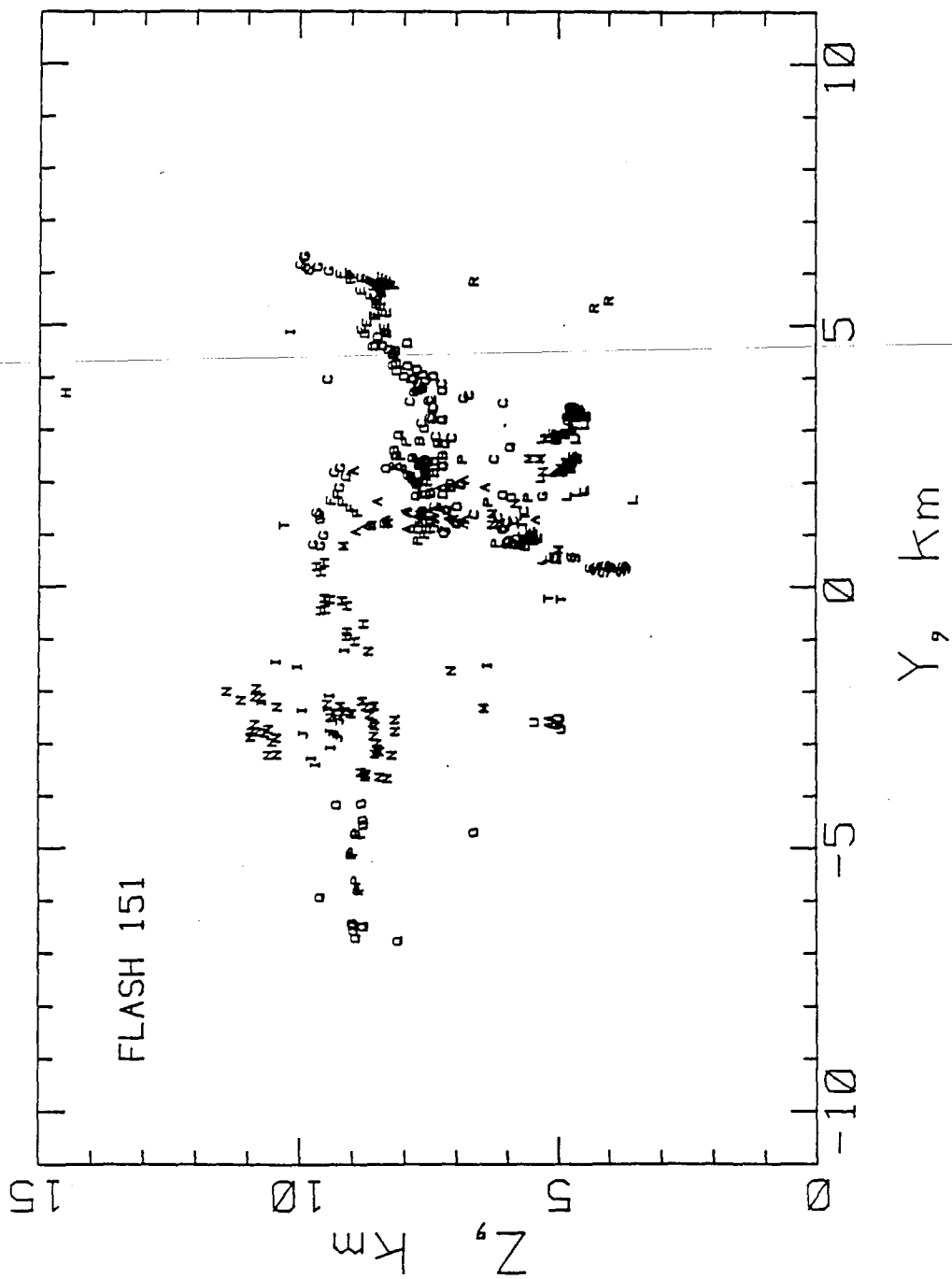


Figure 9. Comparison between the recorded EFC and the EFC calculated from the known path for the first 230 milliseconds of Flash 151.

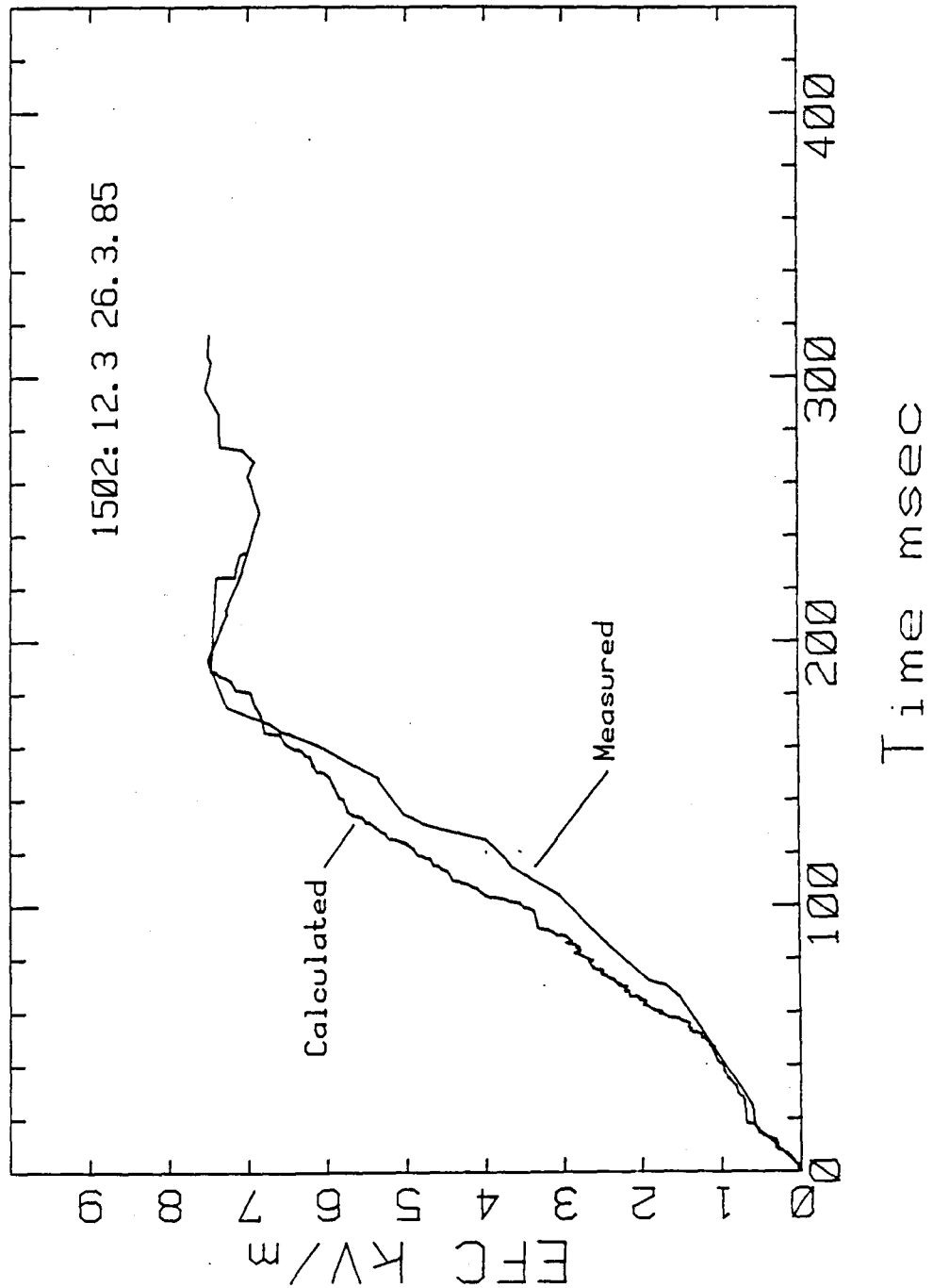


Figure 10. Plan view of pulse sources active above a height of 6.4 km agl during Flash 123. The negative streamer A to G has been mapped with dots. Letter symbols map the paths of the positive streamers. Letter symbols change for every 20 milliseconds.

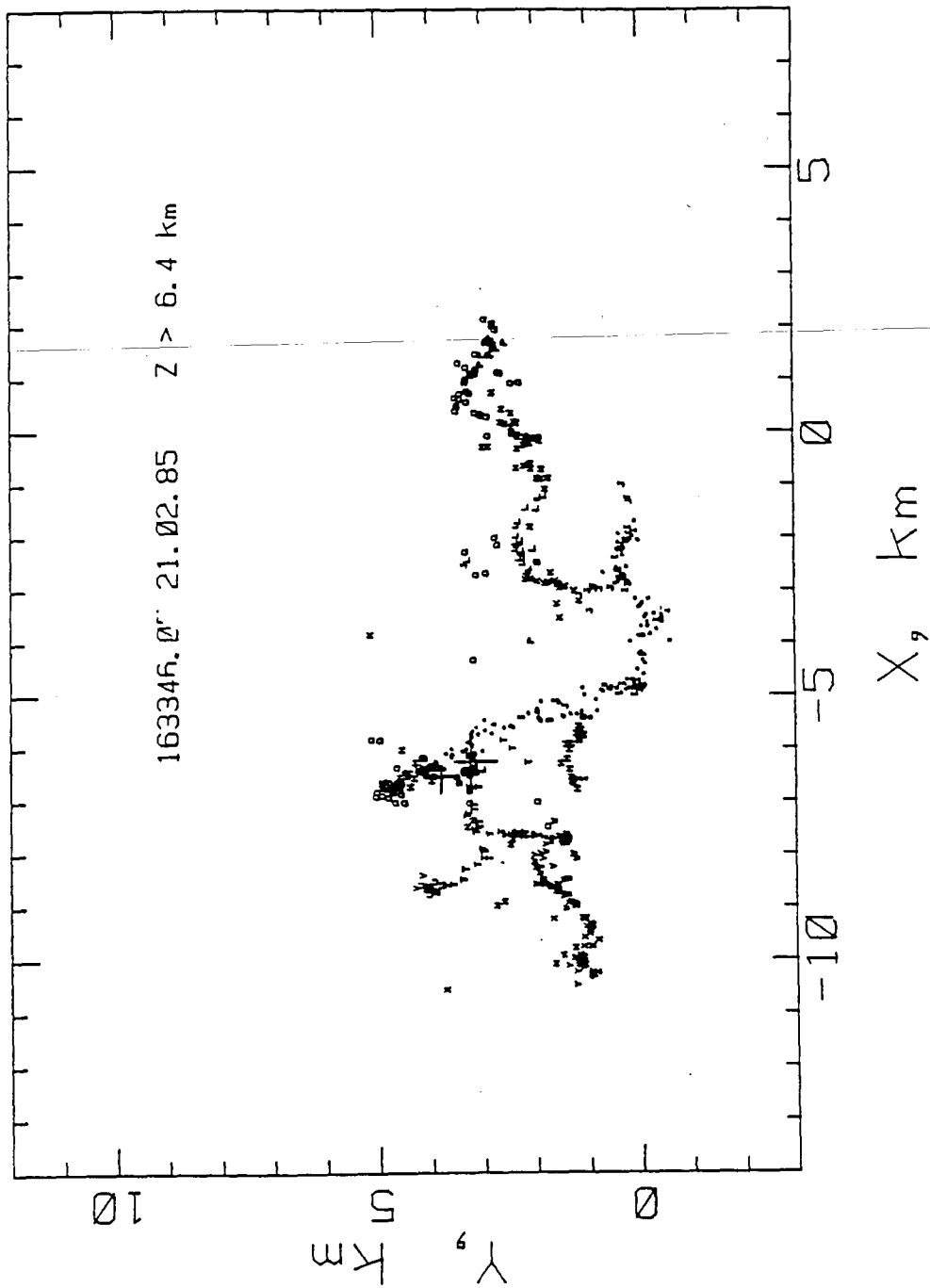


Figure 11. An elevation view of all 898 pulse sources active during Flash 123. The negative path A to G has been mapped with dots.

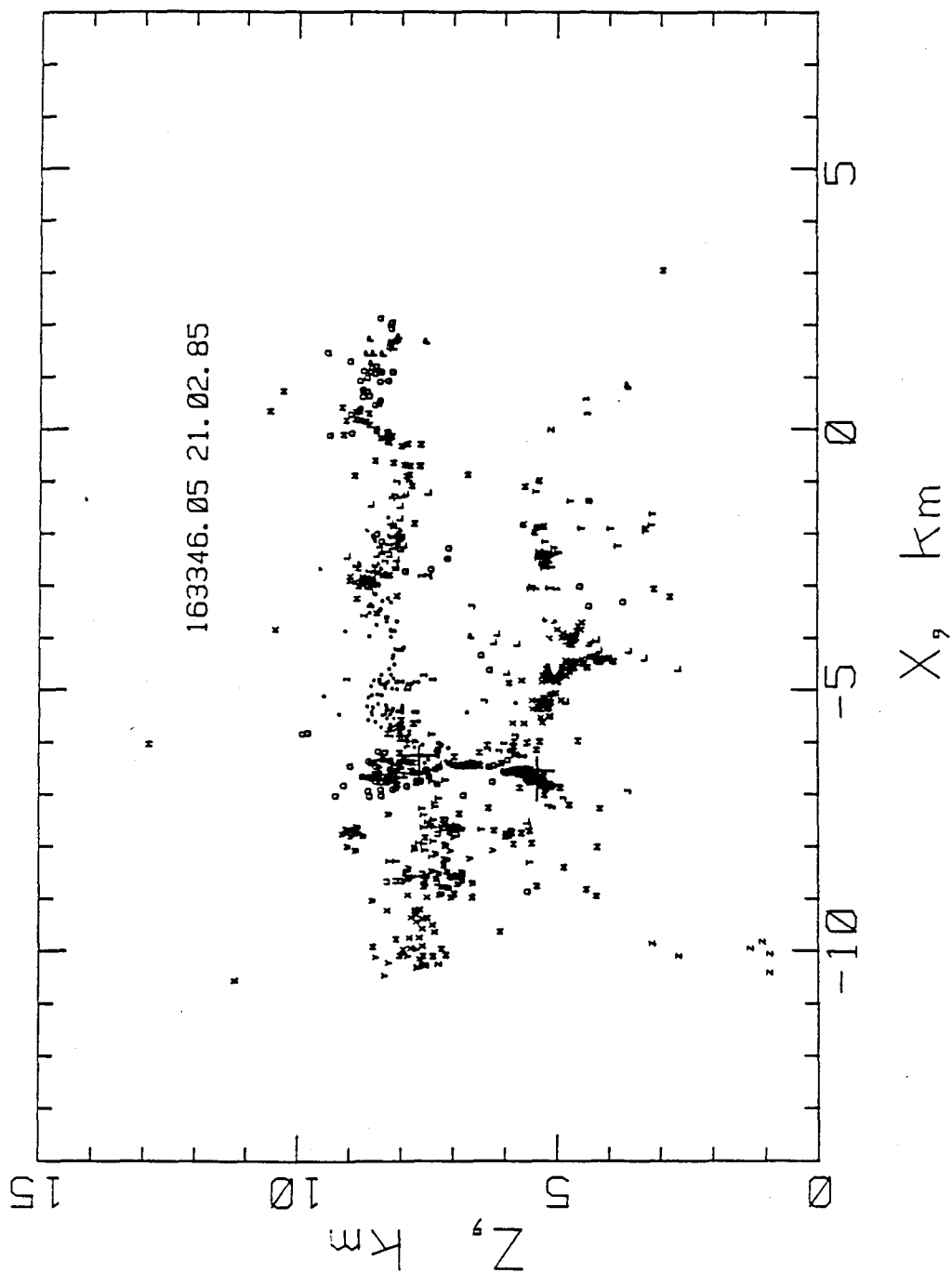


Figure 12. Plan view of pulse sources A to G active during the first 140 millisecc. of Flash 123. The polarity was negative during this time.

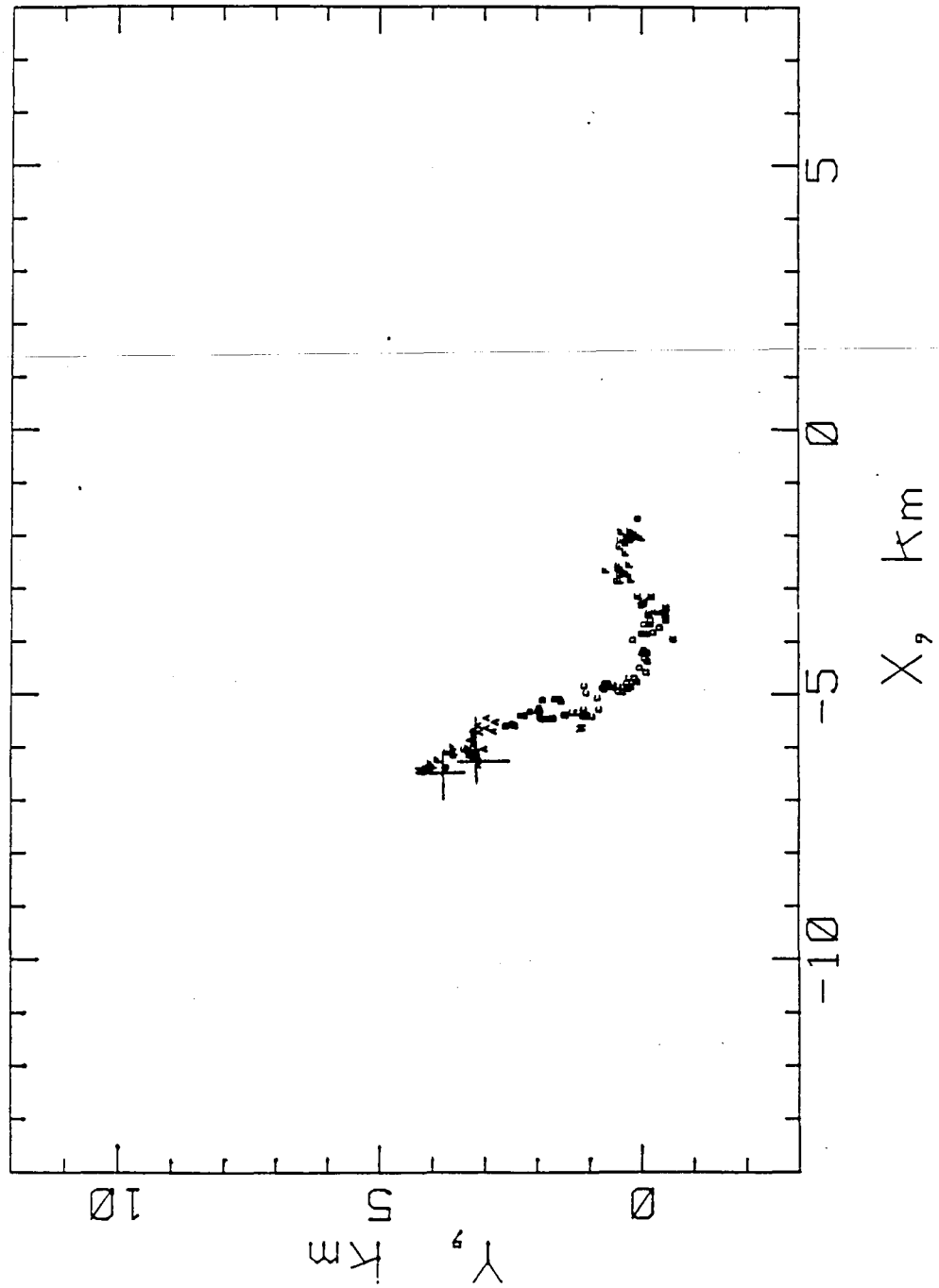


Figure 13. A comparison between the measured EFC, plotted as a thin line, and the EFC calculated from the known path of Flash 123. See text.

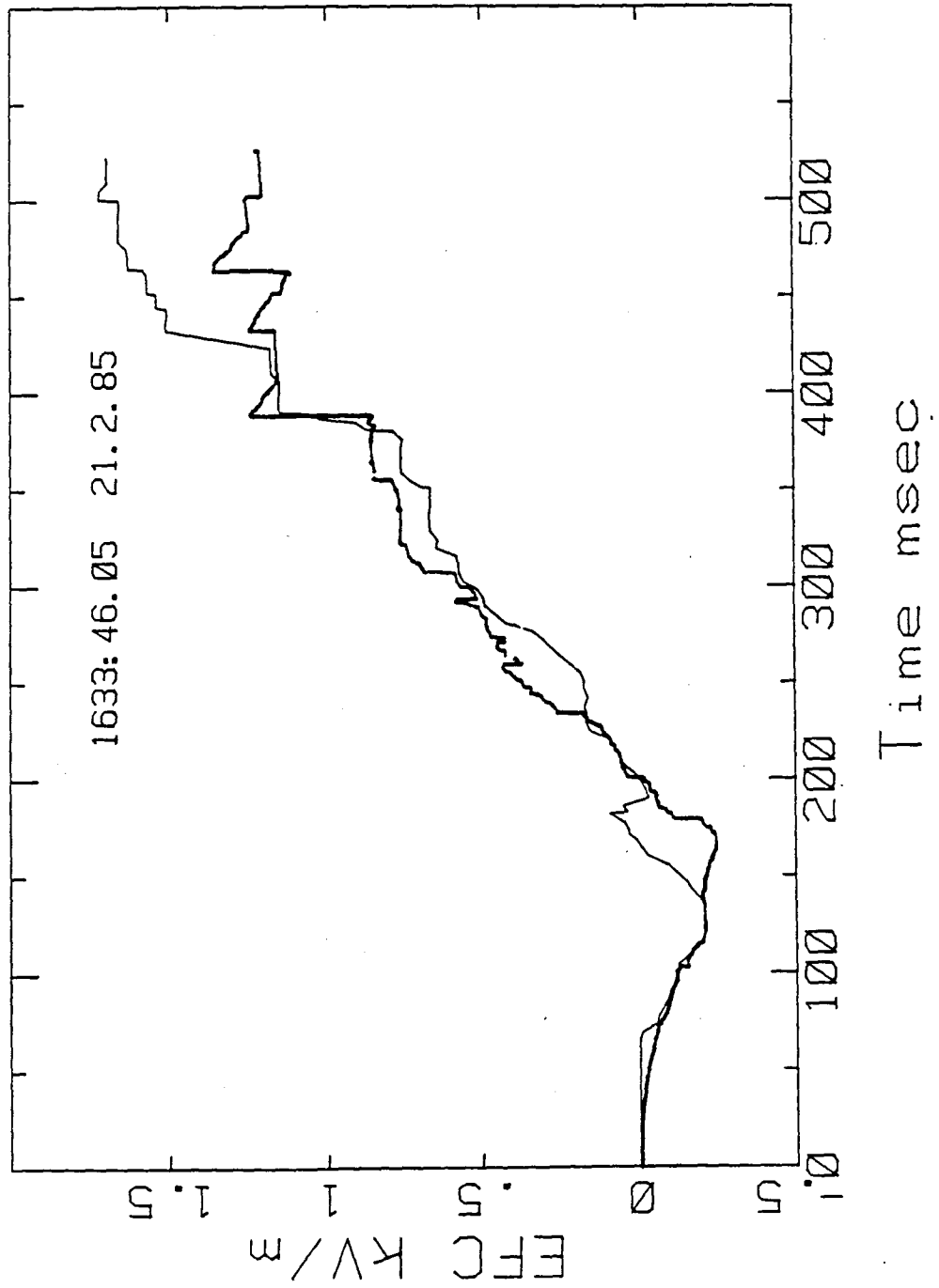


Figure 14. Plan view of pulse sources active above an altitude of 6.5 km agl during flash 87. Symbols change for every 20 millisecc.

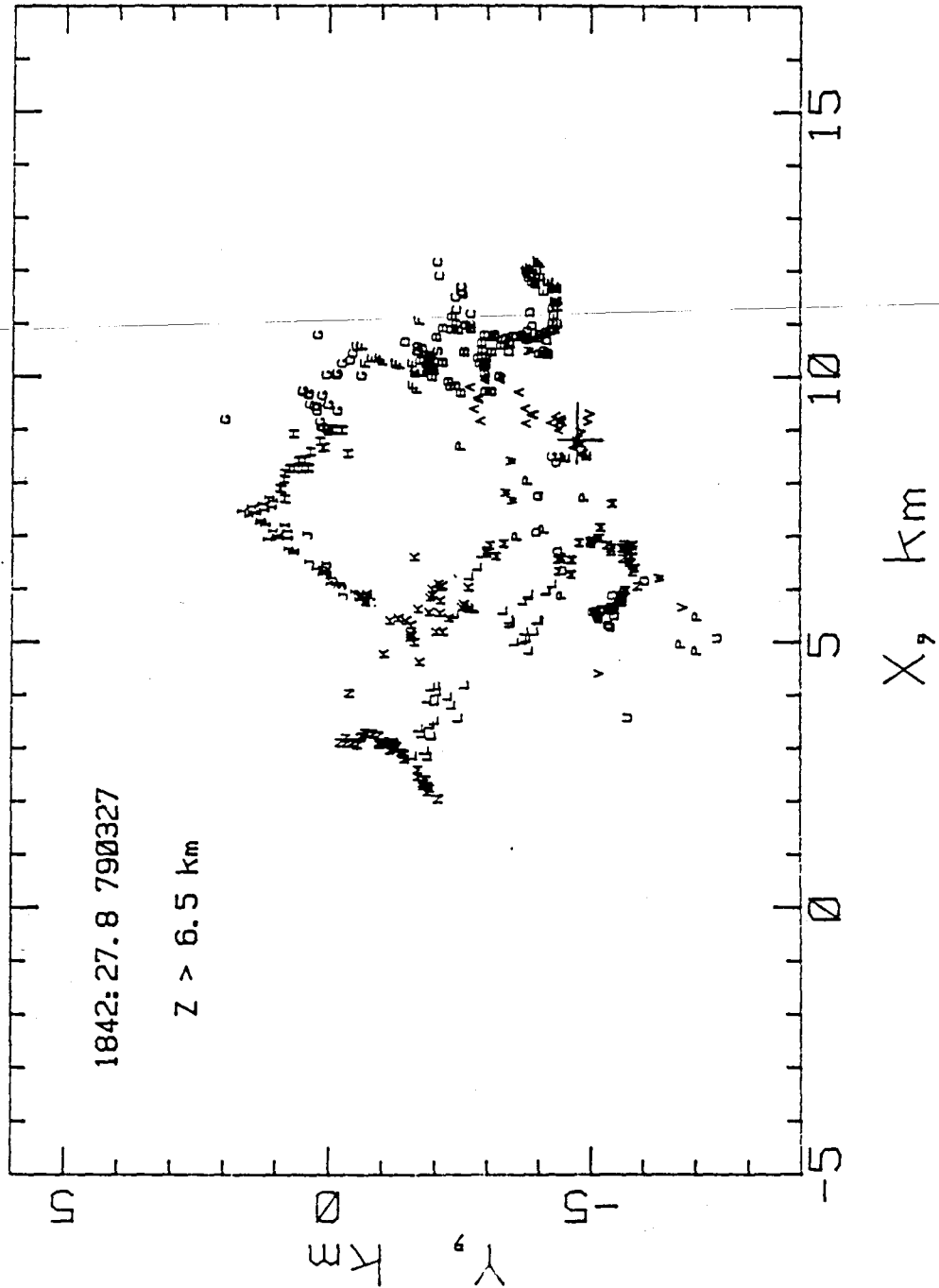
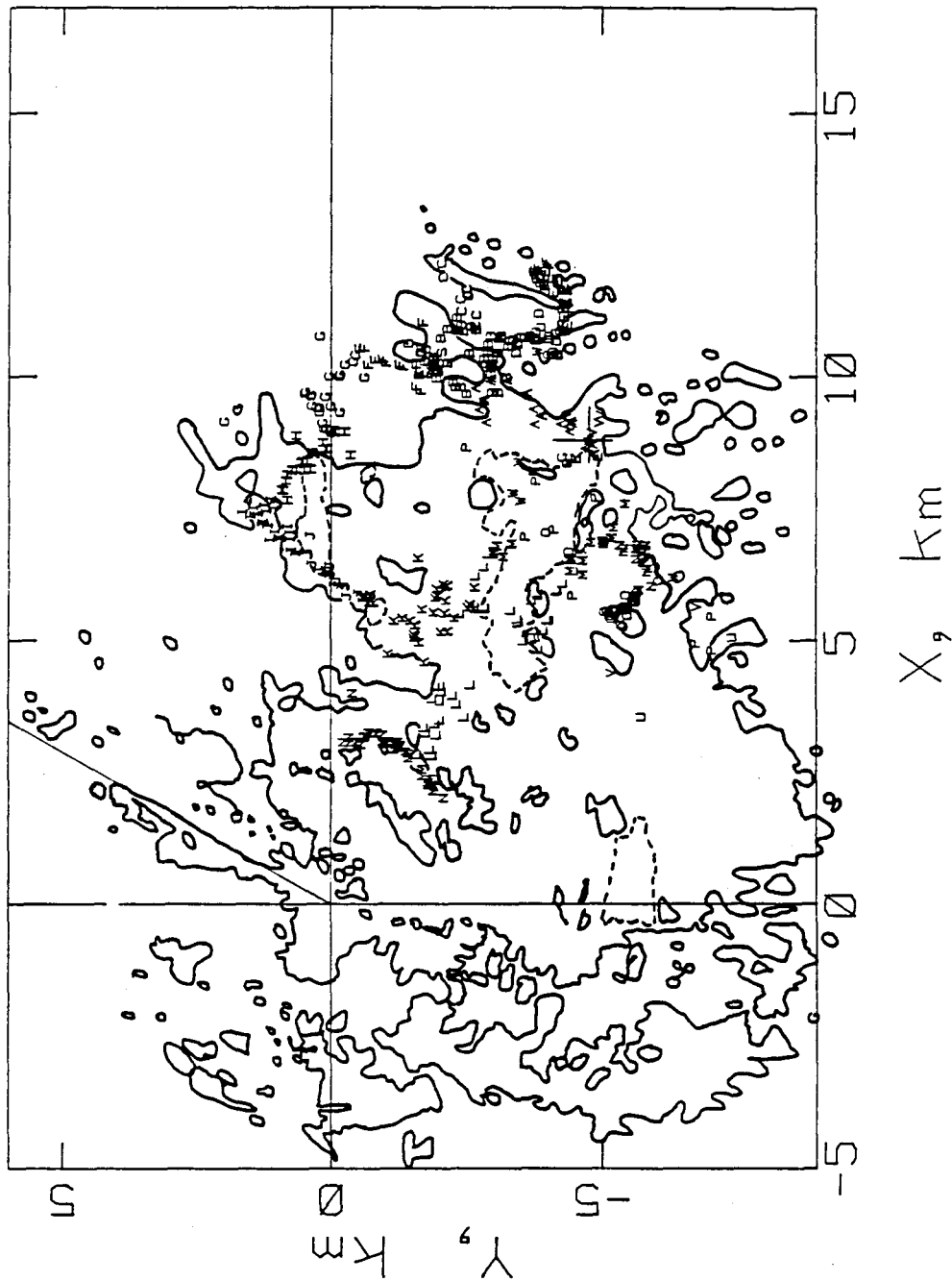


Figure 15. Sources of pulses active at heights above 6.5 km during flash 87, and Radar Reflectivity contours for 20 dBZ and 50 dBZ (dashed) at a height of 7.5 km.



Appendix 9

RADIO NOISE ASSOCIATED WITH SUBSEQUENT STROKES OF LIGHTNING.

by

David E. Proctor

Ematek, CSIR, P. O. Box 1327, Honeydew, South Africa.

ABSTRACT

We studied the waveforms of VHF radio noise emitted during dart leaders and subsequent strokes that occurred during two flashes. In particular, arrangements were made so that the times at which the various waveforms occurred could be related to the times at which the return stroke electric field-changes occurred, to an accuracy approximately 10 microseconds. We noticed a tendency for the noise to abate during the time of the return stroke, as reported by Brook and Kitagawa [1964], Takagi [1969] and by Le Vine and Krider [1977]. We located sources of the noise, and found that noise during first return strokes originated from gaps in the channel delineated by sources of VHF noise from the stepped leader. It also originated from sources adjacent to the lower parts of the channel and where the upper extremities of the channel had been extended by the return stroke at speeds 5.4×10^7 m/s and 9.4×10^7 m/s. Sources of noise emitted during low order subsequent return strokes originated from points adjacent to the lower channel but were removed a distance approximately 1 km from the channel, suggesting that sources closer to the channel had been screened. Sources also occurred at the top extremities of the channel and these

radiated during the later stages of the return strokes, so indicating that these occurred when the return stroke extended the channel. Sources active during dart leaders of low order subsequent strokes showed downward progressions at speeds 2.3×10^7 m/s and 2.8×10^7 m/s. One dart leader produced two of these which extended to ground in quick succession. This showed that there was a need for more photographic observations of dart leaders. We showed that the cessation of noise from dart leaders and return strokes, reported previously, could also be due to instrumental effects.

1. Introduction

It may have been E. C. Halliday who first saw that lightning flashes often consist of partial discharges or *strokes*. Schonland and Collens [1933] reported that each stroke consisted of two components: a *leader* which moved out along the path, and which was reflected by contact with the ground to become a brighter and faster *return stroke*. Malan [1963] stated that the leader-return stroke combination recurred at intervals that ranged 10 msec to 160 msec., and that the most probable intervals ranged 20 msec to 70 msec. In Florida USA, Brantley et al [1975] found that the most probable intervals were 50 to 80 msec. I found that the number of strokes per flash is highly variable. Malan [1963] stated that the most usual number was four. Carte and de Jager [1979] reported that 57% of flashes to ground carried only one stroke. Strokes are classified according to whether they are first strokes or subsequent strokes. Schonland et al [1934]

reported that first strokes were preceded by leaders, which they called *stepped leaders*, and that these differed in character from leaders that preceded subsequent strokes, and which Schonland and Collens [1933] likened to downward fireballs or darts. These leaders were termed *dart leaders* by Schonland et al [1935], and are one of the objects of our interest in this paper.

Brook and Kitagawa [1964] observed VHF and UHF radiation from lightning and reported that radiation from dart leaders often terminated 50 to 150 microseconds prior to the step-change in electric field due to the return stroke. They also reported that radiation from return strokes was often weak, absent, or delayed 60 to 100 microseconds. Similar observations were made by Takagi [1969]. Delays of this kind were reported also by Le Vine and Krider [1977]. This paper describes our own findings in this regard, and considers also the effects of various instrumental deficiencies that may have affected the results published by previous investigators.

2. Aim.

The aim of this study was to identify radio signals emitted by lightning during dart leaders and during subsequent return strokes and to locate the sources of these radio signals in order to obtain a better understanding of the processes that occur during dart leaders and subsequent return strokes.

3. Method.

3.1 *Waveform identification*

Prior to 1979, we recorded radio signals received from lightning at five receiver stations by photographing a display that was an assembly of 14 cathode ray tubes. We arranged for electric field changes (EFC's) to be displayed alongside the traces that were deflected by radio noise. Return-strokes produce characteristic step-changes in electric field, as described by Schonland et al [1938] and by Chapman [1939], and we used these EFC's to identify radio noise from return strokes by observing their coincidence (or near coincidence) with the radio noise due to these events. This process of identification was aided by the fact that these processes emit long trains of noise, which we call Q-noise, whose waveform is quite different from the pulsed waveform of signals radiated by stepped leaders and by first streamers of cloud-flashes. Observations of the temporal coincidence was made possible because the display introduced cross-timing errors, between the trace which carried noise received at the home station and the trace that displayed EFC's, that were less than 10 microseconds. The step-changes could be used also to identify waveforms of radio noise emitted by lightning during the progress of dart leaders, because dart leaders immediately precede return strokes. According to Schonland and Collens [1934], dart leaders take a time less than 1.7 msec. to travel from cloud base to ground. Therefore noise recorded during times that preceded the step-changes in E-field by times slightly more than 1.7

msec could be ascribed, at least tentatively, to dart leaders or to processes that accompanied them. In 1979 we installed a laser-optical recorder. Although this new recorder was vastly superior to the system used previously, it was not amenable to an extension that would have permitted it to record EFC's alongside the noise. An auxiliary photographic recorder, used for EFC's, introduced timing errors approximately 2 msec. Although the auxiliary recorder served many purposes, its cross-channel timing accuracy was inadequate for the study we describe here. A seven channel tape recorder was installed in 1986 to supply this deficiency, and it recorded both radio noise and EFC's. It enabled us to display the recorded events on a time scale that was intermediate between the 70 nanosec resolution of the Plessey laser-optical recorder and the 2 msec resolution of the auxiliary record. We measured the timing errors between the two channels whose outputs we used here, and we found them to be less than 15 microseconds. We measured the frequency responses of all tape recorder channels and found that the 3 dB bandwidths were 50 Hz to 100 kHz. These interchannel timing errors plus the risetimes of 3.5 microseconds were negligibly small. The limited low-frequency response of the tape recorder caused the recorded EFC's to be differentiated. The 100 kHz limit of the high-frequency response of the tape recorder attenuated the amplitudes of the pulsed noise and caused separate pulses, and even separate trains of Q-noise to merge on the replayed traces. The bandwidth of the EFC meter was 3 kHz, and therefore the tape recorder did not affect the risetimes of the EFC's.

3.2 *Source location*

Sources of radio noise were located by measuring differences between times at which the radio noise was received at widely spaced stations sited at ground level. Details regarding this application of the hyperbolic method have been given by Proctor [1971, 1983].

4. *Results*

Example 1: Flash 156 recorded at 1614:38.85 on 8 Feb 1986

This flash produced two strokes to ground. It began as a cloud flash, and ended as another cloud flash. We recorded radio noise, light, electric field change (EFC), and VHF radar reflections from it. Events in this flash are labelled according to a time scale that has been denoted by alphabetic symbols, some of which are shown on Figure 1, which is a reproduction of the auxiliary record. Figure 1 shows the radio noise from the first cloud flash (ABCDE) and its accompanying EFC, the stepped leader noise (FGHI), the dart leader noise (M), as well as the EFC's due to the two leaders. The top trace shows, as downward deflections, the light from the two strokes (J and N). Their accompanying EFC's are shown also. The leader EFC's were negative because the leaders occurred near the EFC meter. The noise trace also shows that the VHF radar triggered just before the first stroke to ground. We are interested primarily with the second stroke. Figure 2, taken from the tape recording of radio noise and EFC's associated with the first and second strokes,

shows the sequence of events displayed on an expanded base of time. A list of these events appears in Table 1. In spite of the distortion of the EFC waveforms caused by the inadequate low-frequency response of the tape machine, it is possible to see, in Figure 2, that the Q-noise trains, that we labelled M, accompanied the downward excursion in EFC, characteristic of near leaders, according to Malan [1963] (p. 49). The bandwidth of the tape recorder was not sufficient to show the individual components of the event M. Figure 3 shows how the heights of sources M changed with time. The events during interval M began with a short burst of Q-noise, 27 microseconds in duration, with sources 3.5 to 3.9 km above ground. Then followed a series of pulses (we located sources of 21) that grouped closely in space, within a volume that was found to be 218m x 229m x 613m, after correcting for measurement errors. We have often noticed that pulses from densely packed sources occur when flash-origins form, at the start of high flashes. Then followed two downward waves of Q noise that reached ground (or approached it). These streamers traveled 4.1 km and 3.6 km at 2.8×10^7 m/s and 2.3×10^7 m/s respectively. The second major wave was preceded by a short Q-streamer that extended downward 500 m at 1.5×10^7 m/s. The last Q-streamer M occurred above the rest ($Z = 5.2$) and was displaced laterally almost 2 km. Figure 4 shows views of the flash up to the time of the second cloud-flash, and Figure 5 shows the positions of the Q-sources MNO PQ. Notice that there were two paths to ground. Careful comparison shows that sources M were displaced laterally in X by 500 m to 700 m from both previous channels to ground.

Figure 6 shows how the heights of sources N behaved with time. Pulse sources, mapped with smaller letters, were active at 4.9 km agl. Some Q sources also began high up. Next, an upward wave traveled at 5.4×10^7 m/s. Then followed some pulsed activity near the top of the channel, and a Q-streamer extended 1 km at 9.4×10^7 m/s, followed by higher activity. All this activity preceded the step-change in electric field. Sources O were active as descending and ascending waves. Sources P and Q were high and their streamers extended upwards. Sources N and low sources O were displaced laterally from previous paths to ground. The auxiliary record shows that four pulses of light occurred in rapid succession during 4 msec near the time of the second stroke. The second was the most intense, and occurred approximately 2.8 msec after the first. This suggests that the first accompanied M and the second accompanied the step EFC. The final two probably accompanied events O and P, and behaved similarly to pulses of light which Malan and Collens [1937] named M-components.

Figure 2 a) and b) have been presented in order to show how noise from the second stroke differed from VHF noise emitted by the first return stroke. Contrary to the report by Le Vine and Krider [1977], the noise due to the return stroke was not delayed. It accompanied the step change in E field. In the case of the subsequent stroke, the noise tended to abate during the step change in E field.

Table 1. Events surrounding the second stroke of Flash 156.

Symbol	Event	Time, msec.	
		Start	End
L	Previous interstroke noise	218.97	223.74
M	Dart leader pulses and Q noise	228.064	228.517
N	Rapid waves of Q noise	230.259	230.746
	Step EFC of second stroke	230.71	230.96
O	Q-noise, typical of return strokes	231.617	231.821
P	Q-noise, high sources	232.010	232.695
Q	Q-noise prior to echo enhancement	234.407	234.611

Example 2. Flash 164 recorded at 1745:30.78 on 16 Nov 1987

The auxiliary record, Figure 7, shows that this flash produced two stepped leaders (A-D and E-J), both of which were close to the EFC meter. The second was followed by two or three weak partial strokes, as shown by very small step-changes, two of which were negative, and a third, subsequent stroke (U), which emitted at least two pulses of light. Figure 8 shows VHF noise and EFC's recorded by the tape recorder during two events which were the second (J) and third (U) strokes. The second stroke (J) was preceded by a stepped leader (E-J) and was the first stroke along the path (HIJ) shown in Figures 9 and 10. The third stroke (U) was a subsequent stroke.(i.e. it was preceded by a dart leader). Figure 8 b) shows that the VHF noise abated during the step-change in E field. Figure 8 a) shows that VHF noise accompanied the step change during a "first" stroke of that flash. Figure 8 b) also shows that at least two bursts of strong Q-noise occurred at the time of the dart leader, just prior to the step-change. We located sources of 418 pulses during the two stepped leaders. The elevation views, Figures

9 and 10, show the two paths (AD) and (EJ) to ground. The Q-noise radiated by the three major strokes (D, J and U) was uncommonly difficult to fix. There were three reasons for this. The noise exceeded the amplitudes of the frame trigger-pulses, which indicate the start of each frame in the recorder. This invalidated the timing function in cases where a strong noise-train occupied more than one frame. The Q-noise radiated by this dart leader and by these return strokes was endowed with very few gaps or features which could be timed accurately, and the Q-noise trains began by waxing slowly in amplitude, so that the places where they began could not be found accurately. Figures 9 and 10 show that low sources D and J occurred immediately alongside the leader channels. J was active in both channels. Low source U was displaced laterally, as were two sources D. Most of the sources U were located high above the paths to ground. These sources have been mapped separately in Figure 11.

5. Discussion

Both examples presented here showed that VHF noise abated during the step-change in E field caused by subsequent strokes. Exactly similar behavior was shown by Proctor [1976] in his Figures 8.17, 8.36 and 8.47. As stated in the introduction, similar results were reported by Brook and Kitagawa [1964] and by Le Vine and Krider [1977]. The immediate response of an Electrical Engineer on seeing waveforms such as those published by Brook and Kitagawa [1964] and by Le Vine and Krider [1977] is to suppose that

the cessation of noise was due to two instrumental effects. These are discussed in the appendix. We had ensured that neither would afflict the results that we obtained. We conclude that the failure of dart leaders and subsequent return strokes to radiate noise, particularly during the late stages of dart leaders and during the early phases of return strokes, particularly those of high order, is real, and moreover that it is due to shielding by dense plasmas. The reasons for reaching this conclusion are stated in the following paragraph.

1. Proctor [1981] reported that subsequent discharges along paths that had been ionized previously did not radiate VHF noise unless those channels had been dormant for approximately 80 msec or longer. 2. Proctor et al [1988] reported that first return strokes radiated from gaps in the leader channel, or from the edges or sides of the stepped leader channels. Examples of this are sources J in Figure 5 of that paper, sources D in Figure 8 of that paper, sources T in Figure 17 and sources O of Figure 21. These effects are features of the flashes described here. 3. Low sources active during early subsequent strokes locate at places some distance from the main channels. Examples are shown by sources G in Figure 8 of Proctor et al [1988] and by sources M and N of Example 1 and by a source U of Example 2. 4. High order return strokes radiate less noise than early strokes. This noise is delayed progressively after the step-change in E-field due to the return stroke. This has been reported by Brook and Kitagawa [1964] and by Proctor et al [1988] who also found that the sources of this noise were located at the

channel top. This explains the delays. 5. The tapered waveform of many Q-noise trains is consistent with the observations that these sources emerge from the extremities of conducting channels. The noise amplitude waxes as the degree of ionization decreases. This was discussed by Proctor [1981]. 6. Q-noise radiated by subsequent strokes is sometimes endowed with gaps. The speeds at which waves traverse these gaps averages a speed just less than the speed of light. An example of this was discussed by Proctor [1976] in Figures 8.15 and 8.16 and Table 21. These data suggest very strongly that the gaps are caused when streamers intersect previously ionized channels. 7 Stepped leaders and first streamers radiate strongly.

All these observations are consistent with the hypotheses that a) VHF and HF noise from lightning is caused by ionization of virgin, unionized air, and that b) the absence of noise from channels that carry dart leaders and subsequent return strokes is due to shielding by dense plasmas.

We should expect to have seen two dart leaders at time M in Example 1. The resolution of the auxiliary record was not adequate to show this. The pictures taken by Schonland and his colleagues were limited by lack of exposure and size. Recently reported video recordings have been taken with standard equipment, which lacks, by far, the time resolution necessary to record the optical manifestations of lightning. It cannot be very difficult to adapt modern techniques in order to record light from lightning flashes in a manner that will provide adequate temporal and spatial resolution as well

as adequate sensitivity.

Our tape recorder was installed in January 1986. However, since that time we have concentrated our data reading efforts on locating flash-origins and on mapping paths of cloud-flashes with high origins. Consequently, we have mapped very few flashes to ground since the tape recorder was installed. This work is continuing.

Conclusions

We have studied events that occurred during subsequent strokes in two flashes, and have noted their timing with respect to the return stroke EFC's. Reasons have been given for the absence of VHF noise at some times during these events.

Acknowledgements

I thank the CSIR for providing funds and facilities necessary for this research, and also for granting permission to publish this paper. I am indebted to the Water Research Commission for financial assistance. Special thanks are due to Dr. George Green for his interest and good offices. I am greatly indebted to Dick Uytenbogaardt for his efforts and for his knowledgeable assistance. Thanks are due to Mrs. Kelly for her mastery of the difficult task of reading the data.

Appendix.

The instrumental effects that affect the detection of radio signals from lightning include the effects of ground reflections, and capacitive or inductive coupling between cascaded stages of receivers and amplifiers.

A.1.1 Antenna response

The effects of antenna directivity in the horizontal plane are obvious, and need not be discussed here. The effects of ground reflections on the vertical directivity are more subtle, and are a possible cause of weak signals from sources in the lower parts of lightning channels. Appendix A 1.2 gives calculations of received signal field strength when the receiver antenna height is approximately 0.25 wavelength, and also when the receiver antenna is elevated approximately 3 wavelengths above ground. In the case of the low antenna, a source 10 km distant and 200 meters high will give rise to a field strength 20 dB below the field strength from the same source at the same distance but elevated 4000 meters above ground. In the case of the antenna elevated three wavelengths (3 meters above ground) the two received signals differ in field strength by a few dB. When a low antenna is employed, it is possible to set the receiver gain so that although strong signals are received from lightning, signals from sources near ground are not detected or displayed. This is particularly true when the receiver amplitude response is linear instead of being logarithmic.

A 1.2

VHF radio propagation above ground. Vertical polarization

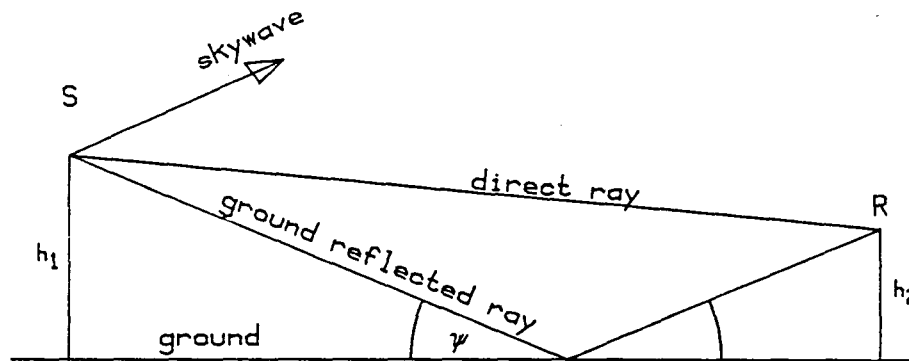


Figure A1 depicts both direct- and ground-reflected rays from a transmitter, labelled S to a receiver, labelled R. The transmitter antenna is elevated a height \$H_1\$ and the receiver antenna is elevated a height \$H_2\$ above ground whose conductivity and relative permittivity are known. The received electric field at R is the vector sum of the two components. Their magnitudes fall inversely as the distance; their phase difference depends also upon the difference in path lengths. For cases where the earth can be considered as being smooth and flat we derived the formula for excess path as:-

$$D = 4 H_1 H_2 / (R_1^2 + R_2^2)$$

Where \$R_1\$ and \$R_2\$ are the lengths of the direct and ground-reflected paths respectively.

On reflection, the magnitude and phase depend upon the reflection factor. According to Terman [1943] or Jordan [1950] this is given by: -

$$R_v = \frac{A \sin \Psi - \sqrt{A - \cos^2 \Psi}}{A \sin \Psi + \sqrt{A - \cos^2 \Psi}}$$

where $A = (\epsilon_r - j x)$, and $x = \frac{\sigma}{\omega \epsilon}$; $\epsilon = \epsilon_0 \epsilon_r$; $\epsilon_0 = \frac{1}{36 \pi 10^9}$; $\omega = 2 \pi f$ and f is the frequency in Hz.

Taking ground constants $\sigma = 5 \times 10^{-3}$ mhos and $\epsilon_r = 5$, we get $x = 0.253$ at $f = 355$ MHz. This yields the curves shown in Figures A2 and A3 for the magnitude and phase of the reflection factor. Simple calculations yield the curves shown in Figures A4 and A5 for stated values of H_1 and H_2 . The effects of antenna height can be seen in Figures 2 and 3 of the paper by Le Vine and Krider [1977]. In their Figure 2 there is no delay as claimed, and the signals merely increased in amplitude in the expected manner.

A.2 AC coupling

In the case of capacitive interstage coupling of video amplifiers, the direct voltage across the capacitor is altered by the advent of strong signals. This may have the effect of biasing the following stage to a point where it cuts-off so that subsequent signals are amplified only if they exceed the cut-off threshold. Weak signals are therefore removed from the displayed train of pulses, until such time as the quiescent condition restores sufficiently to cut the stage on once more. D.C. restoring diodes do not remedy this malady which arises with non-continuous, transient stimuli. Although this problem has been discussed here for the case of capacitive coupling, similar troubles arise when either inductive or transformer coupling is used. Tape recorders are particularly prone to these problems unless FM techniques are employed.

Bibliographical References

Brantley, R. D., J. A. Tiller and M. A. Uman, Lightning properties in Florida thunderstorms from video tape records, *Jour. Geophys. Res.*, 80, 24, 3402-3406, 1975.

Brook, M., and N. Kitagawa, Radiation from lightning discharges in the frequency range 400 to 1000 Mc/s, *Jour. Geophys. Res.*, 69, 12, 2431-2434, 1964.

Carte, A. E., and J. C. G. de Jager, Multiple-stroke flashes of lightning, *Jour. Atmos. and Terr. Phys.*, 41, 95-101, 1979.

Chapman, F. W., Atmospheric disturbances due to thundercloud discharges: Part 1, *Proc. Phys. Soc. London*, 51, 876-894, 1939.

Le Vine, D. M., and E. P. Krider, The temporal structure of HF and VHF radiations during Florida lightning return strokes, *Geophys. Res. Lettrs.*, 4, 1, 13-16, 1977.

Malan, D. J., *Physics of Lightning*, 176 pp, The English Universities Press, London, 1963.

Malan, D. J., and H. Collens, Progressive lightning 3--The fine structure of return lightning strokes, *Proc. Roy. Soc. London*, A 162, 175-203, 1937.

Proctor, D. E., A hyperbolic system for obtaining VHF radio pictures of lightning, *Jour. Geophys. Res.*, 76,6, 1478-1489, 1971.

Proctor, D. E., A radio study of lightning, Ph. D. Thesis, University of Witwatersrand, Johannesburg, 1976.

Proctor, D. E., VHF radio pictures of cloud flashes, *Jour. Geophys. Res.*, 86,C5, 4041-4071, 1981.

Proctor, D. E., Lightning and precipitation in a small multicellular thunderstorm, *Jour. Geophys. Res.*, 88,C9, 5421-5440, 1983.

Proctor, D. E., R. Uytendogaardt and B. M. Meredith, VHF radio pictures of lightning flashes to ground, *Jour. Geophys. Res.*, 93, D 10, 12 683-12 727, 1988.

Schonland, B. F. J., and H. Collens, Development of the lightning discharge, *Nature*, 132, 407-408, 1933.

Schonland, B. F. J., and H. Collens, Progressive lightning, *Proc. Roy. Soc.*, A 143, 654-674, 1934.

Schonland, B. F. J., D. J. Malan, and H. Collens, Progressive lightning 2, *Proc. Roy. Soc. London*, A 877, 152, 595-625, 1935.

Schonland, B. F. J., D. B. Hodges, and H. Collens, Progressive lightning 5. A comparison of photographic and electrical studies of the discharge process, *Proc. Roy. Soc. London*, A 924, 166, 56-75, 1938.

Takagi, M., VHF radiation from ground discharges, p 535-538, in *Planetary Electrodynamics*, edited by S. C. Coroniti and J. Hughes, Gordon and Breach Science Publishers, New York, 1969.

Terman, F. E., *Radio Engineers' Handbook*, 1019 pp McGraw-Hill Book Co., New York, 1943.

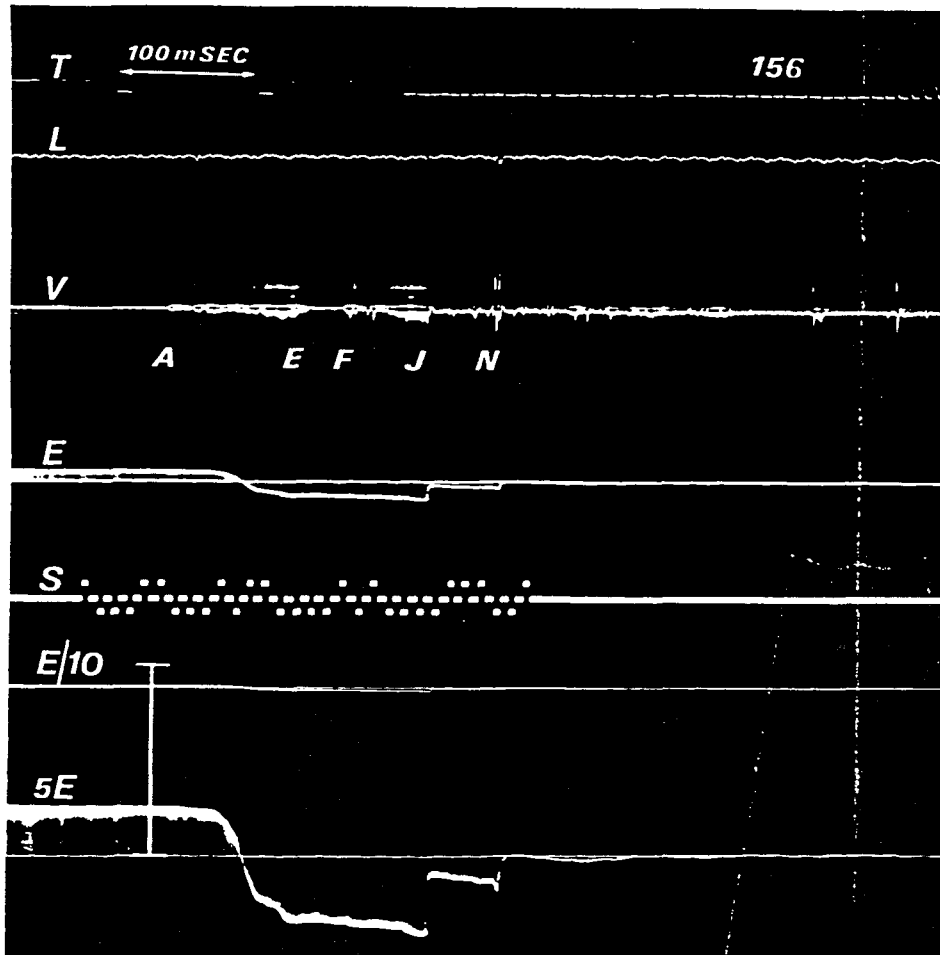
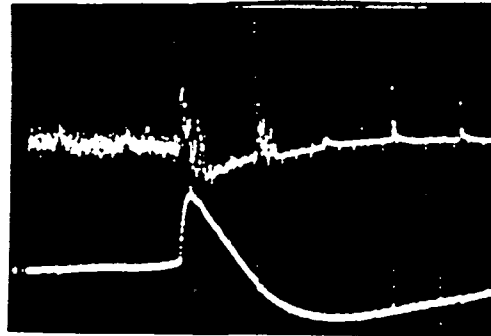
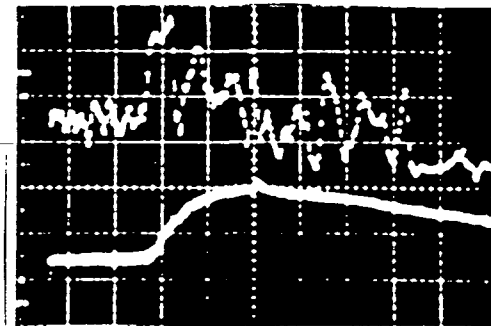


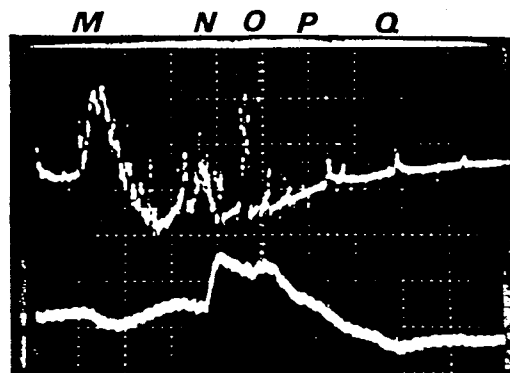
Figure 1. The auxiliary record of Flash 156. Time increases from left to right. Time pulses at intervals of 100 msec appear on the top trace. Trace L was deflected downward by light falling on a silicon diode mounted above an "all-sky" reflector. Trace V carried VHF noise received at the home station. Traces E, 5E and E/10 were deflected by the responses of the EFC meter. The bar indicates the size of a deflection for a change of 5 kV/m. A change from zero to a fair-weather field would deflect the trace upwards. Trace S displays a serial time-code supplied to all recorders used at the station.



a



b



c

Figure 2. The upper traces of each pair show VHF noise replayed by the tape-recorder (Bandwidth 50 Hz to 100 kHz). Lower traces are recorded responses of the EFC meter whose upper break point was 3 kHz. EFC's have been differentiated by the limited low-frequency response of the tape-recorder. Figures a and b concern the first return stroke of Flash 156, and Figure c was recorded near the time of the second return stroke. Time scales of a and c are 1 msec per large division; in b it is 100 microseconds per large division. Letter codes above Figure c are explained in Table 1. Event M accompanied the dart leader.

Figure 3. Heights of sources M in Flash 156 plotted to a base of time.

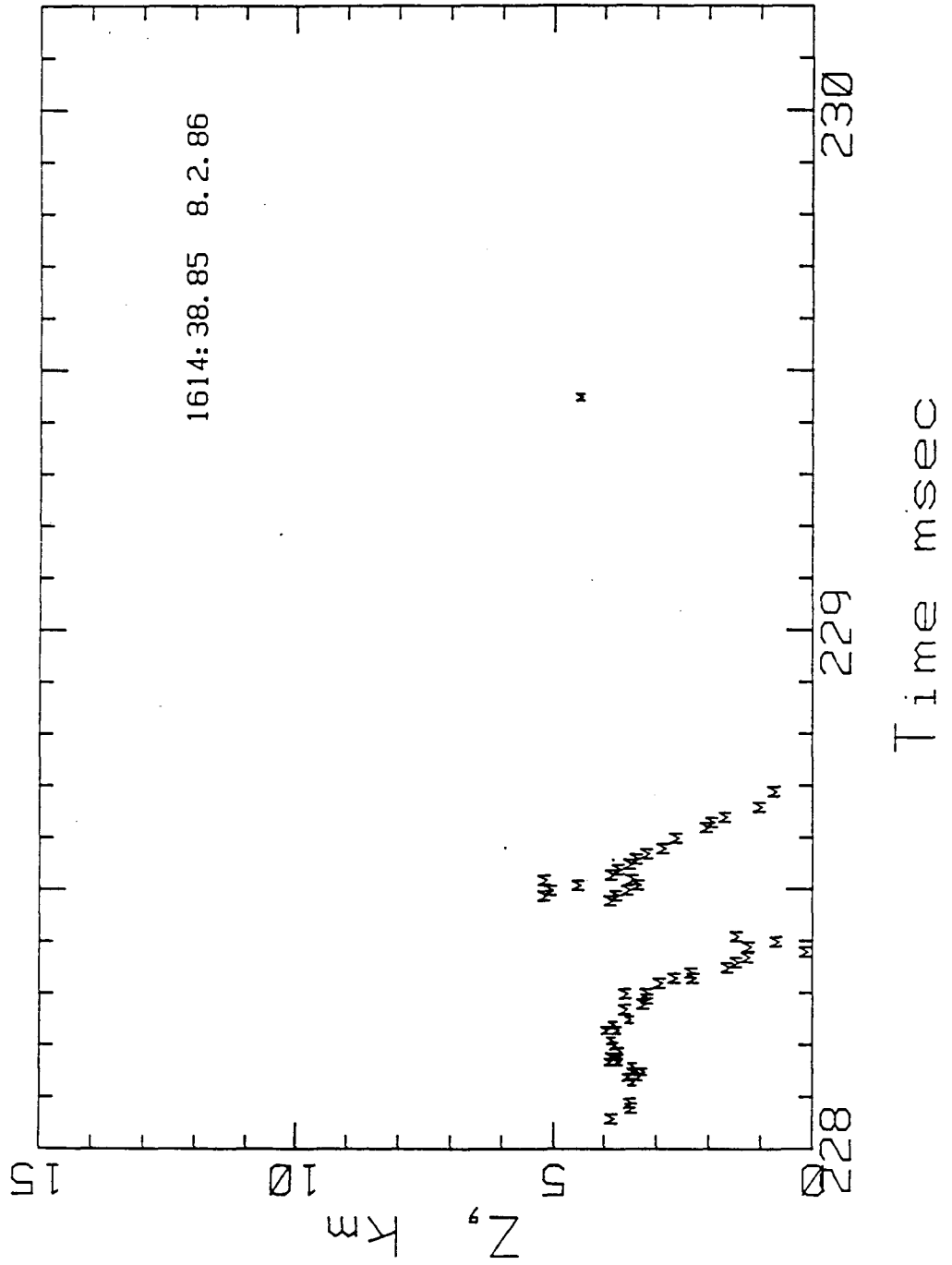


Figure 4. Elevation views of Flash 156. The second cloud-flash has not been plotted. Letter symbols relate to time and change at intervals roughly 20 msec. Sources of Q-noise are mapped with larger letters.

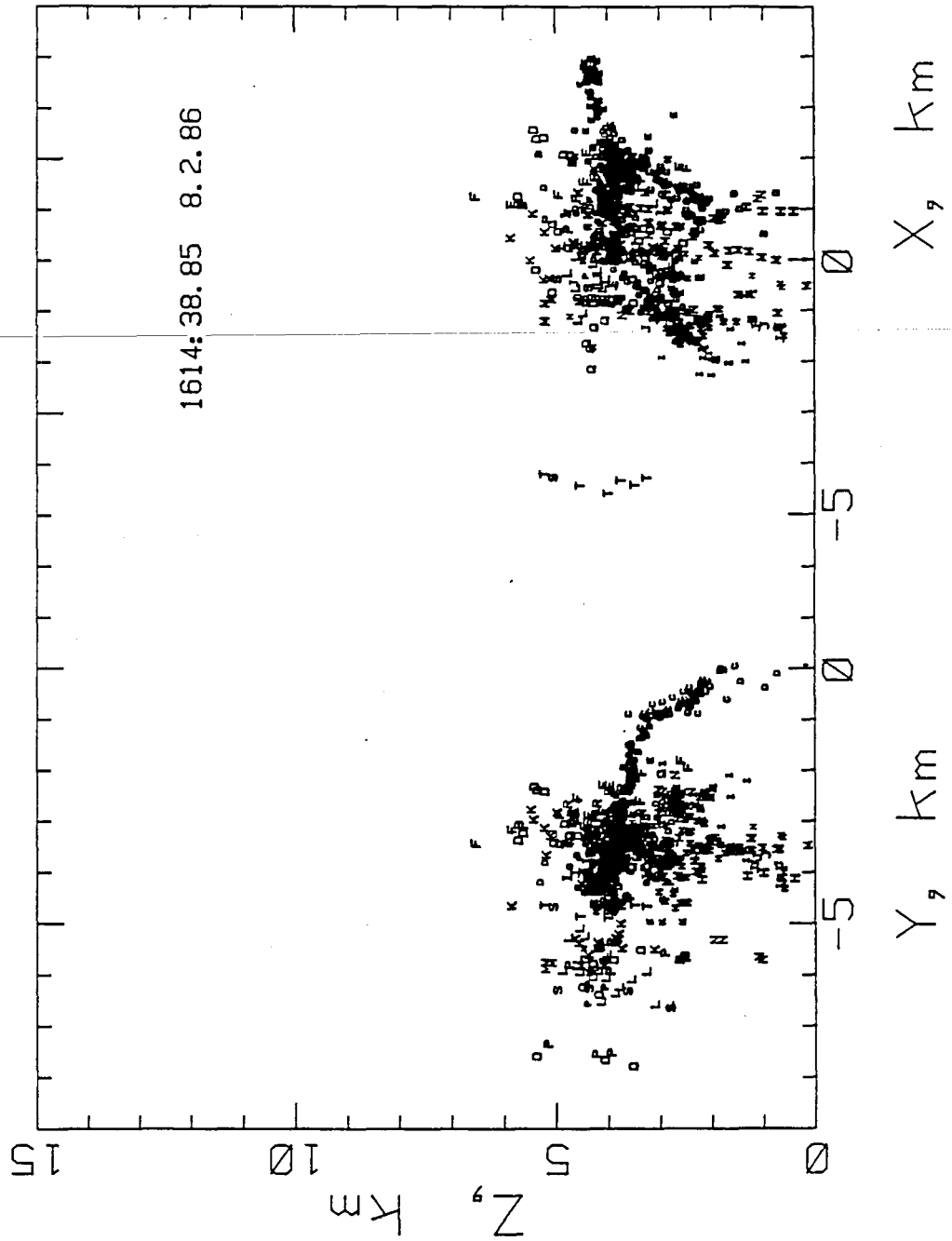


Figure 5. Elevation views of sources M,N,O, and P of Flash 156.

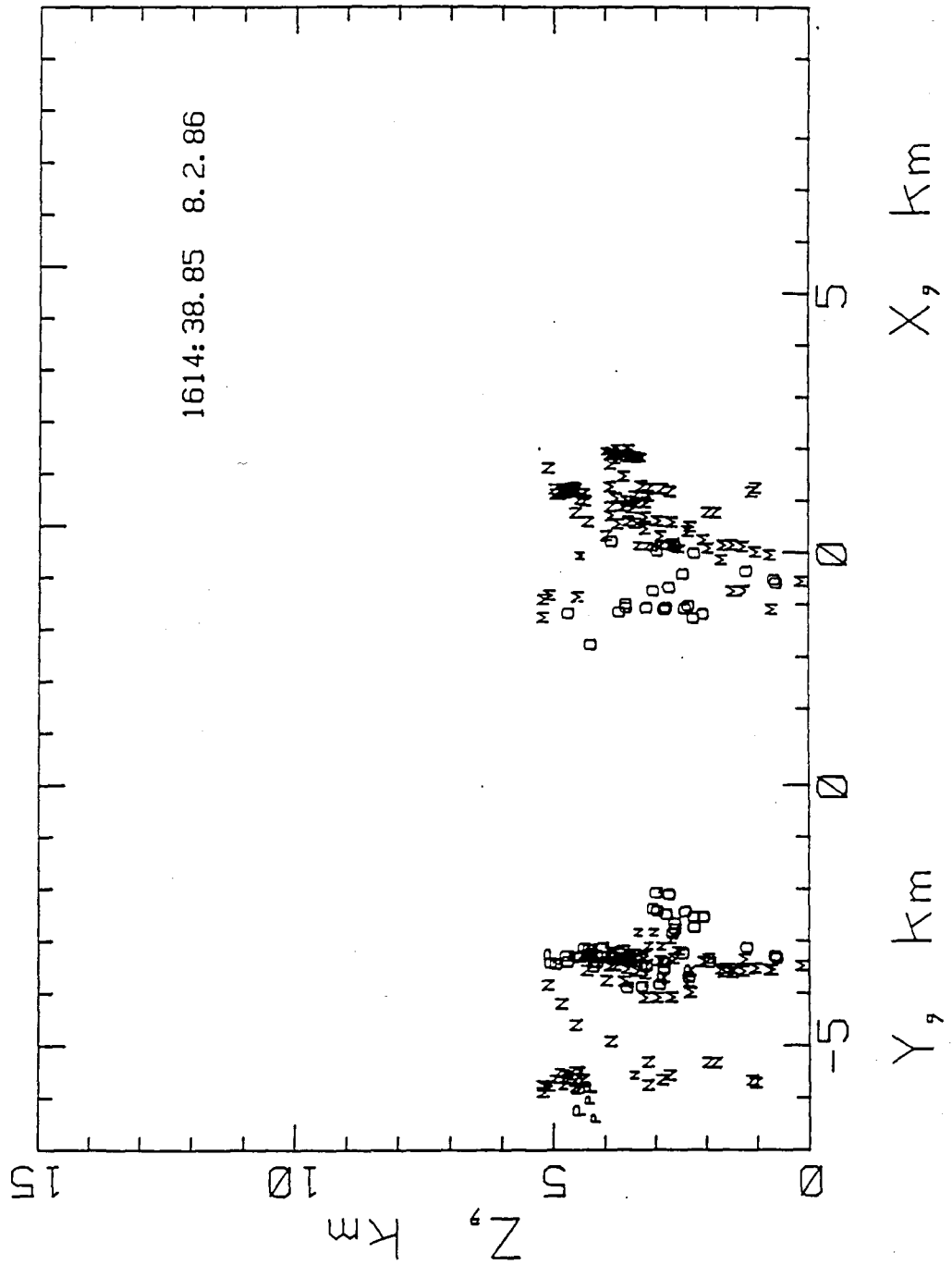
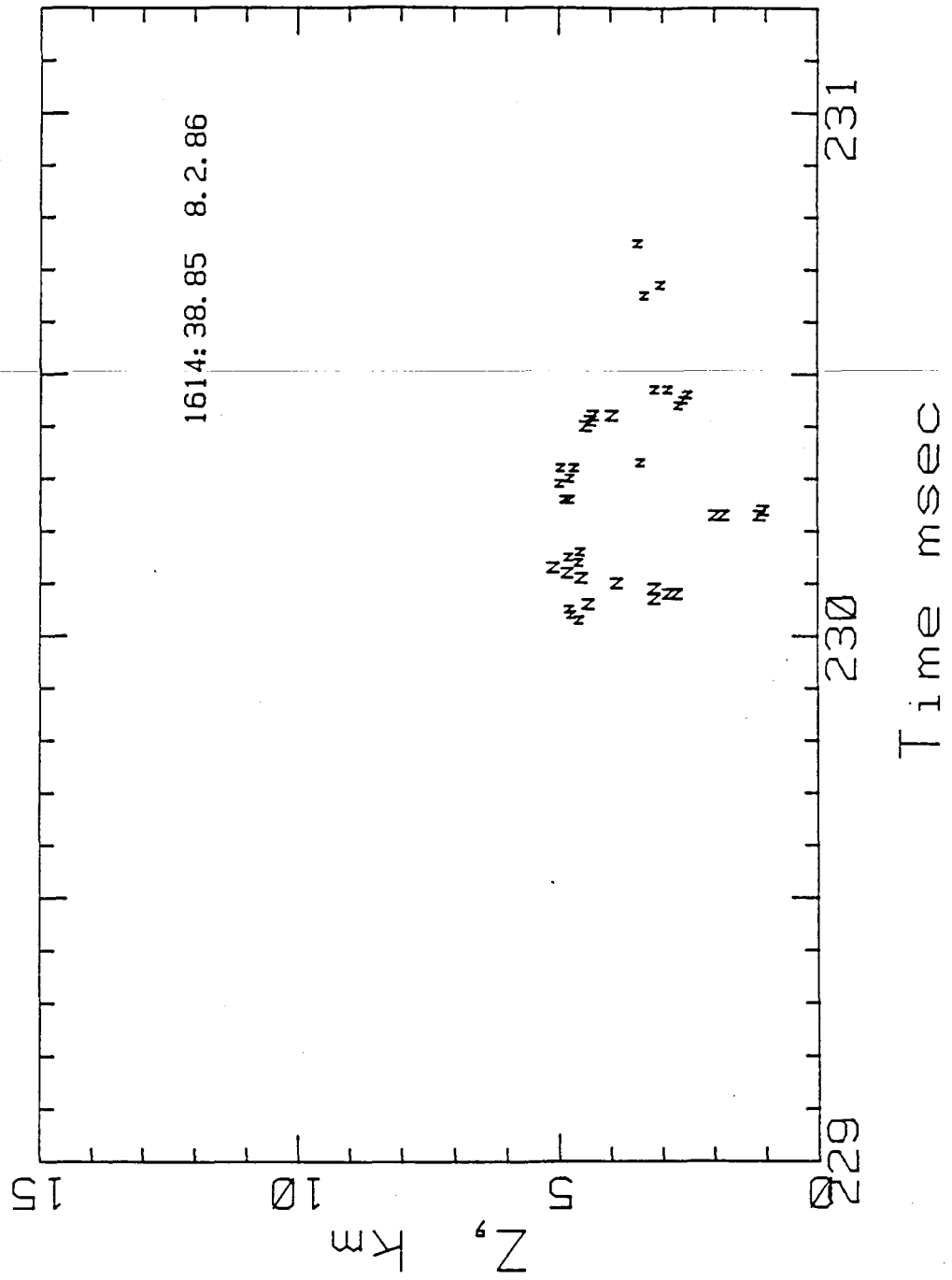


Figure 6. Heights of sources N in Flash 156 plotted to a base of time.



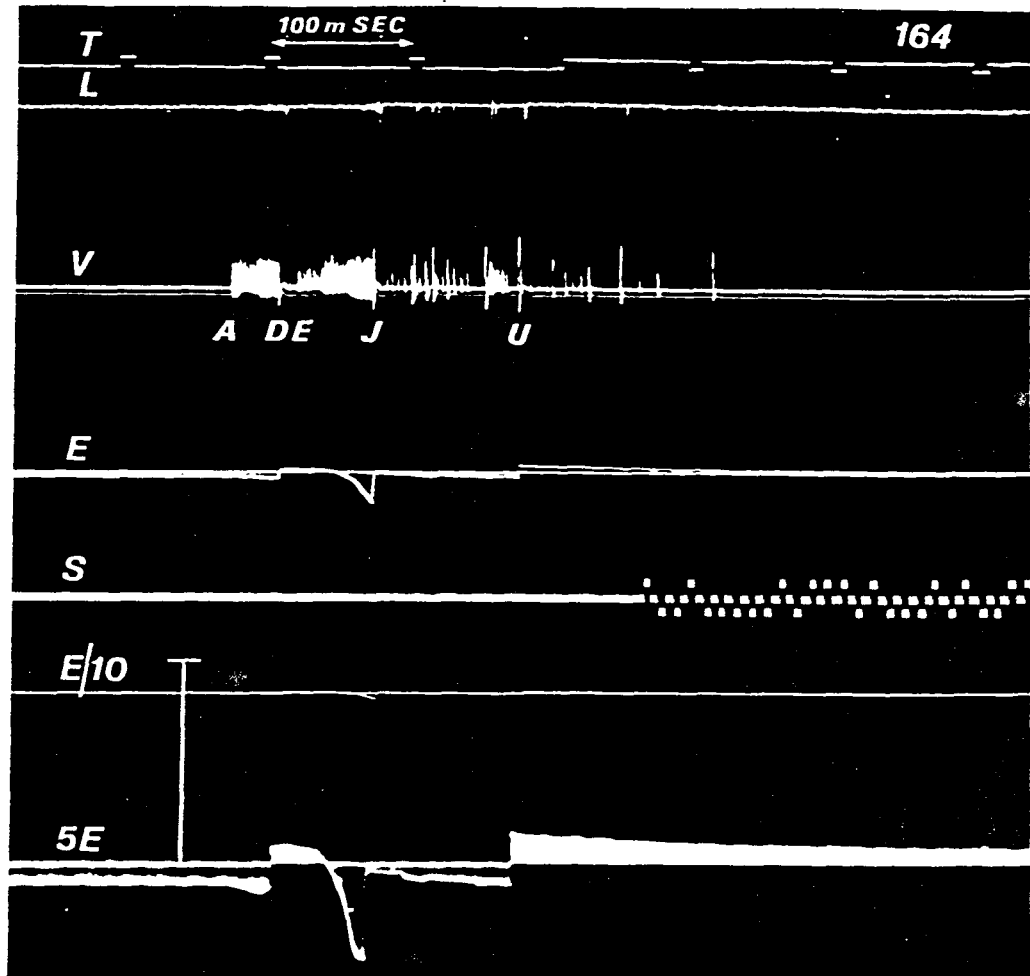
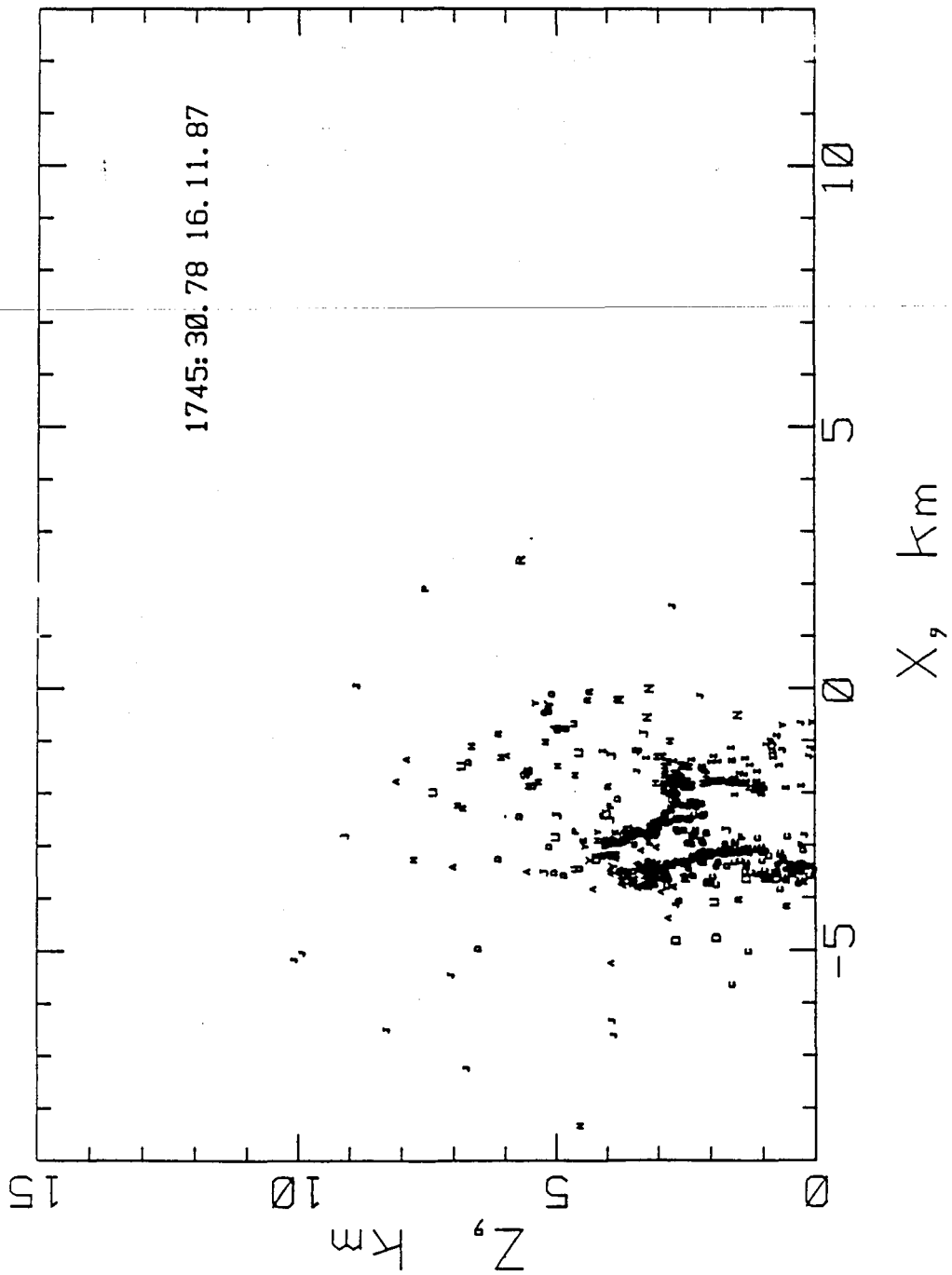


Figure 7. The auxiliary record of Flash 164. See legend for Figure 1.

Figure 9. Z/X elevation view of 532 sources active during Flash 164. Sources of Q-noise have been mapped with larger letters.



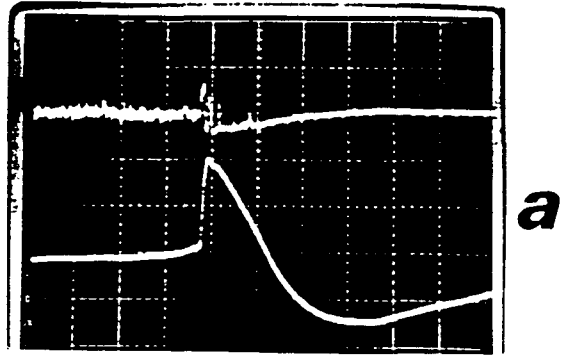


Figure 8. Tape recorder responses of VHF noise and EFC's recorded by stroke 2 (a "first stroke ") and, in b, stroke 3 of Flash 164. Time-scale 1 msec per large division. See legend for Figure 2. Notice absence of delay in a.

Figure 10. Z/Y elevation view of Flash 164.

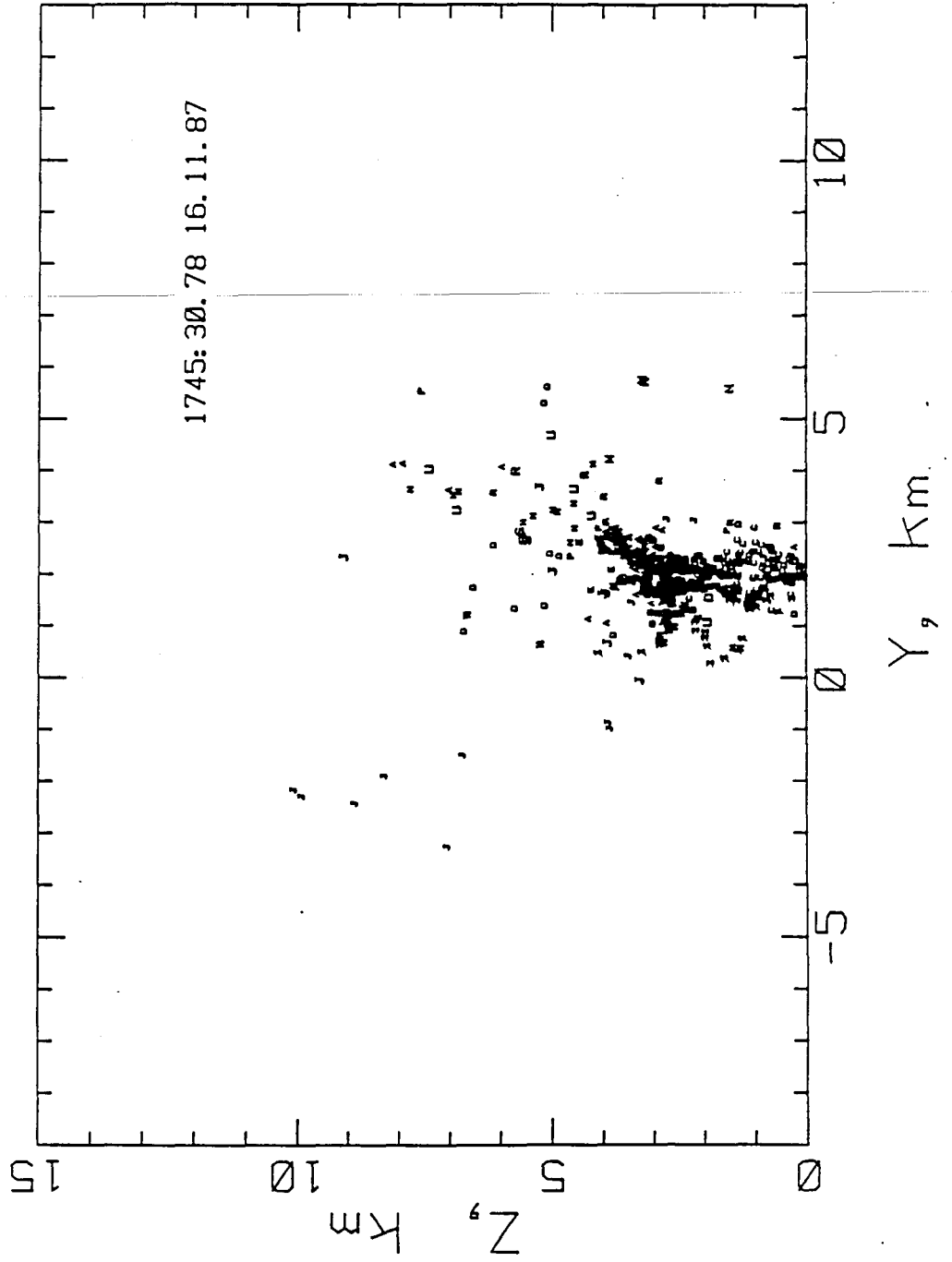
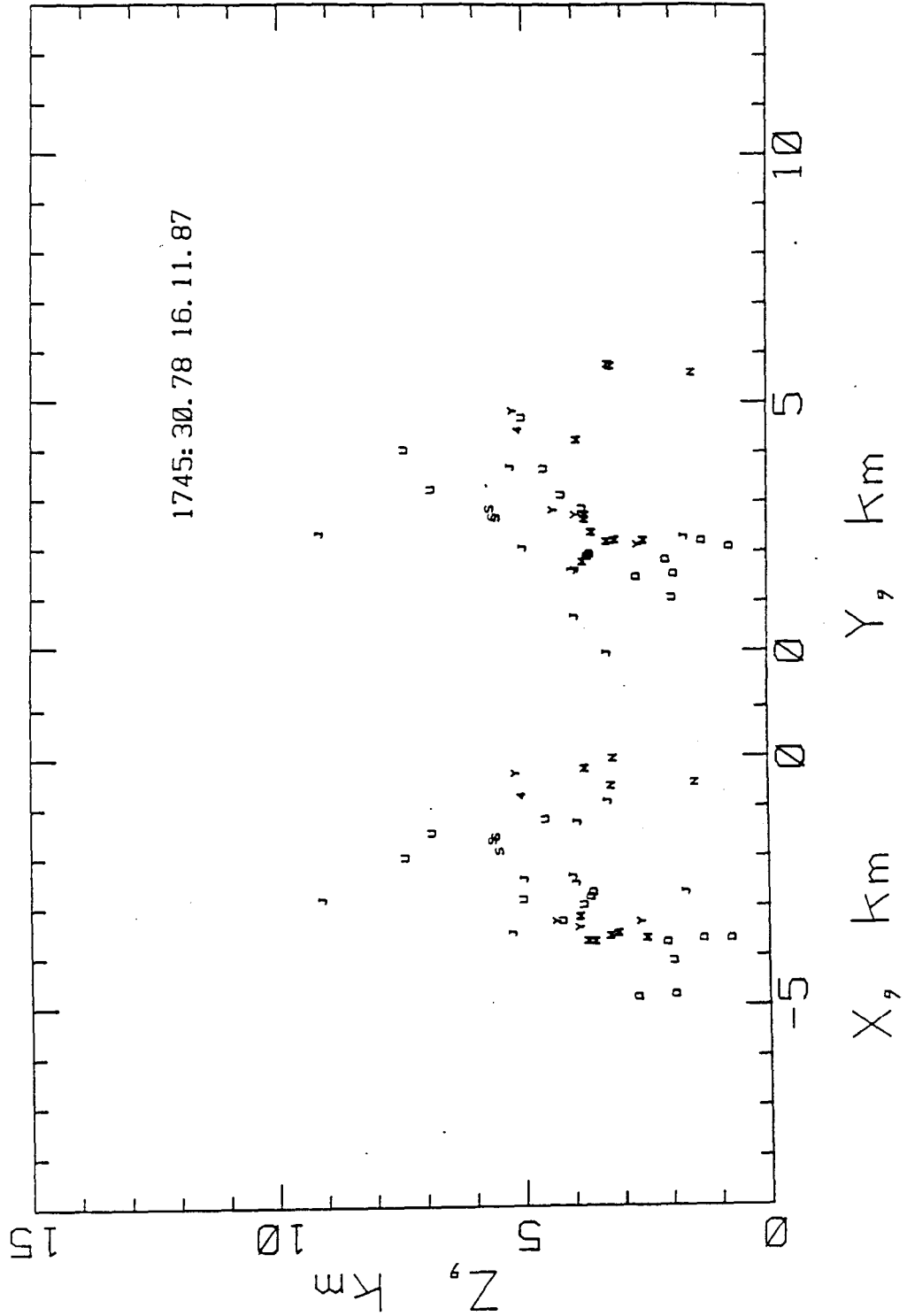


Figure 11. Elevation views showing only the Q- sources located for Flash 164.



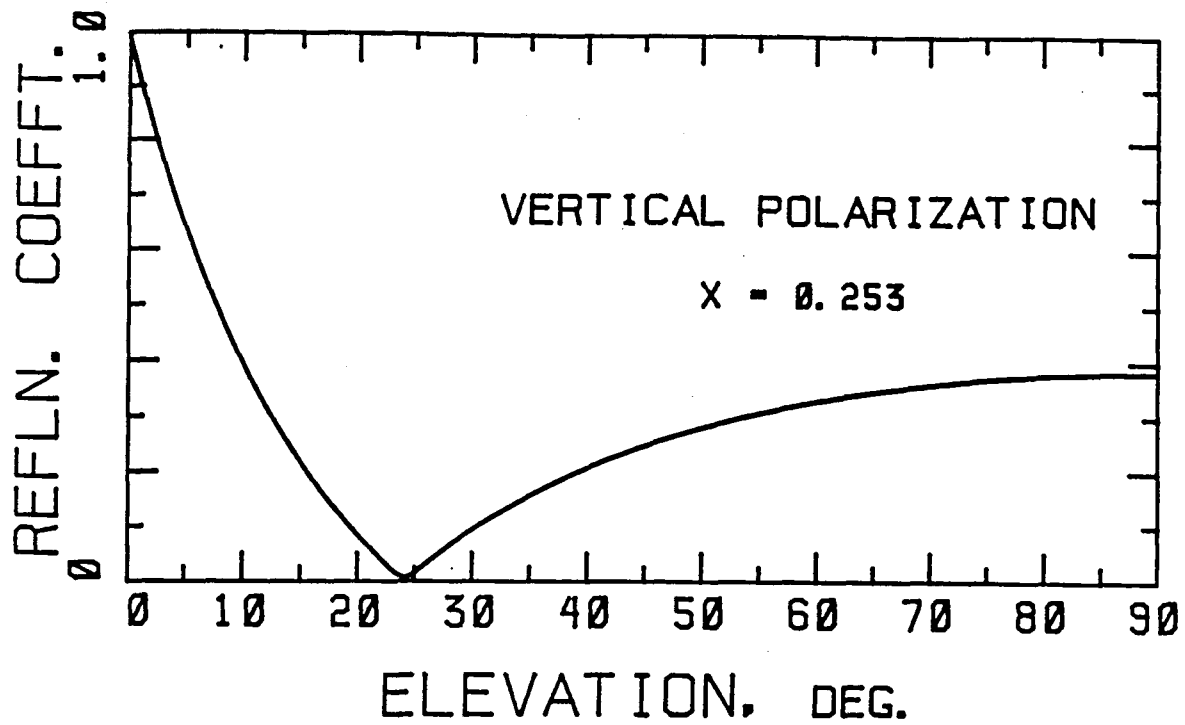


Figure A.2. Magnitude of the ground reflection coefficient.

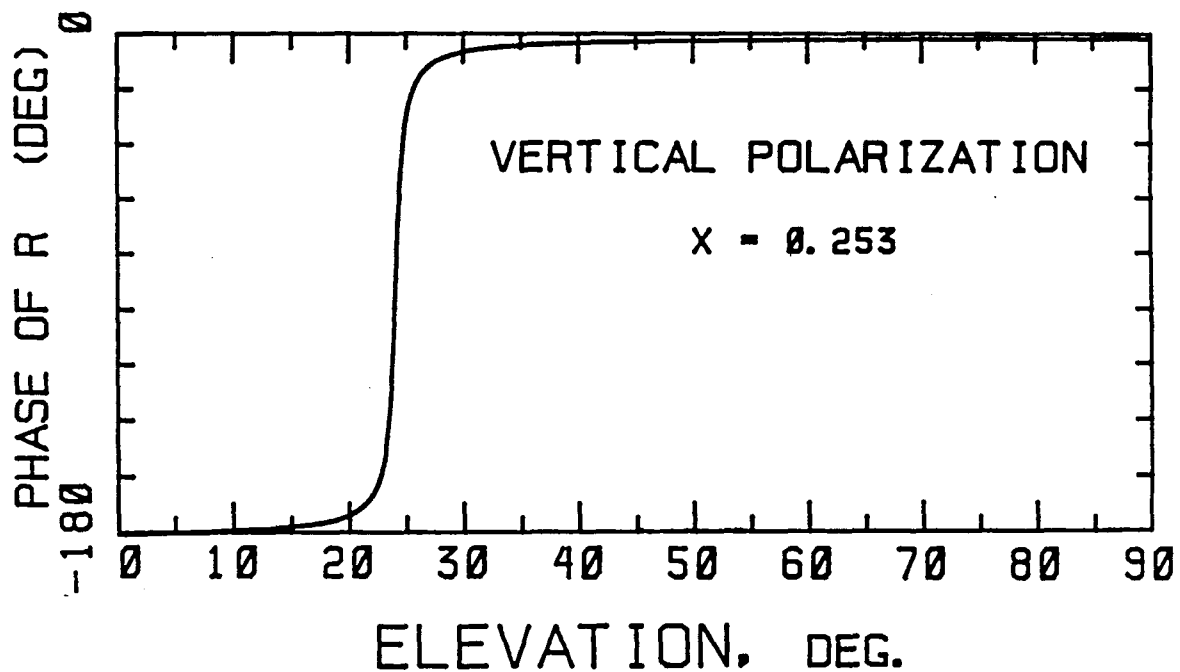


Figure A.3. Phase of the ground reflection coefficient.

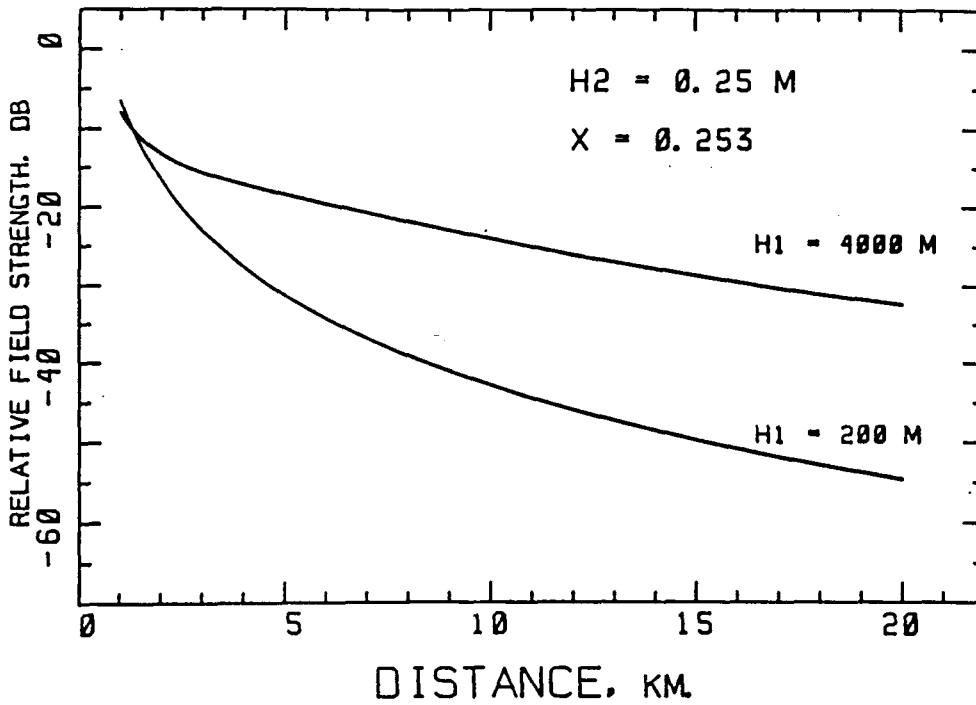


Figure A.4. Relative E-field strengths of signals received from a source at two heights, H_1 above ground. The height of the receiver antenna is one quarter wavelength.

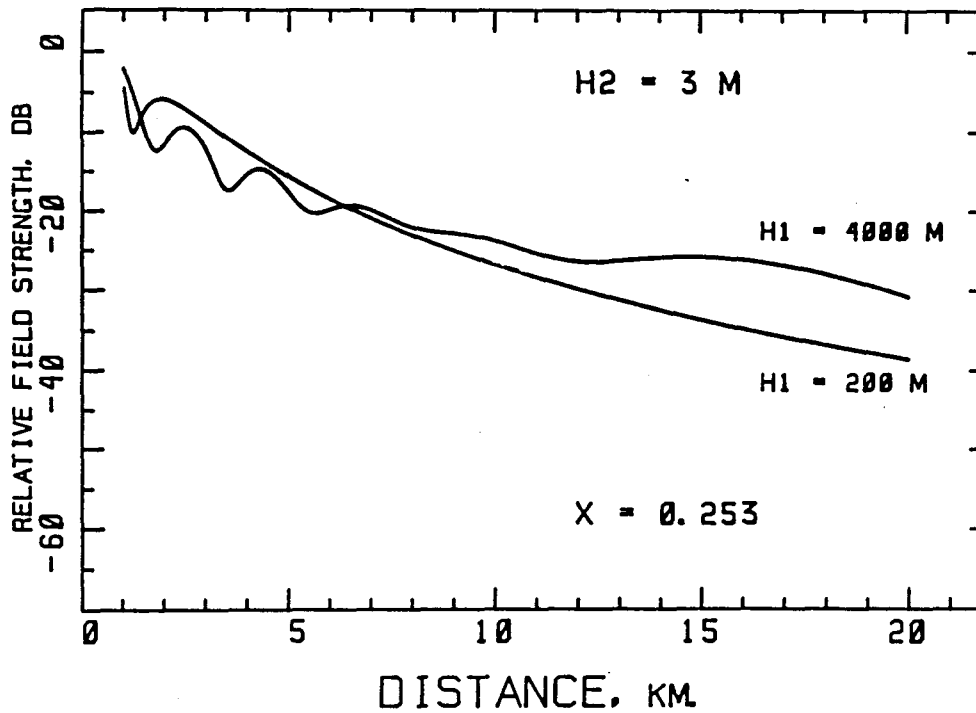


Figure A.5. As in Figure A.4 except that the height of the receiver antenna is 3 wavelengths above ground.

THE SIZE OF A SPHERE CONTAINING 3 COULOMBS

These calculations are based on the assumptions:

1. The charge is distributed uniformly.
2. The drop-size-distribution follows Marshall-Palmer.
3. Drops are charged as described by Dawson [1969].

Dawson's [1969] curve for charge in esu on a drop of radius r mm at a height 5 km can be approximated by:

$$Q = 0.1 r^2 \quad \text{esu}$$

Values for Σnd^2 for all drops in one cubic metre were calculated for various values of radar reflectivity using procedures outlined in Appendix 7. The totals were:

dBZ	Σnd^2 per m^3 mks
10	5.4 E-05
20	1.46E-04
30	3.92E-04
40	1.05E-03
50	2.82E-03

We use these totals, and the formula derived from Dawson's curve to calculate the total charge in one cubic metre. We then find the volume that would hold 3 Coulombs, its radius and the electric field at the surface of that volume. A Basic

programme and its output are listed below. The magnitude of the electric field is then compared with the onset fields published by Dawson[1969]. This comparison shows that a reflectivity of 30 dBZ or higher would produce breakdown.

```

LIST
1 PRINT
2 PRINT
3 PRINT
4 PRINT
40 PRINT " Pgm Ch5 " , "Total charge in uniformly charged sphere"
41 PRINT "Using max Q per drop from Dawson [1969] for Ht = 5km"
42 PRINT "Radar Ref", "Sph rad", "max E Field"
43 PRINT " dBZ", "metres", "MegaV/m"
48 Q0 = 3 ' Total ch in Coul
50 Q1 = 3E+09 * Q0 ' in esu
60 K = 2.5E+07 ' 1E09/40
62 K2 = .2387 ' 3/4pi
100 FOR I = 1 TO 5
120 READ Z,S2 ' radar ref and sigma n d^2
150 Q = K * S2
160 V = Q1/Q ' vol = total / q
170 R = ( K2 * V )^.33333333# ' r is radius of spherical vol
175 E1 = 9000.001 * Q0 /R^2
180 PRINT Z, R ,E1
200 NEXT I
600 DATA 10,5.4e-5,20,1.46E-04,30,3.92E-04,40,1.05e-03,50,2.82e-03
800 END
Ok

```

RUN

Pgm Ch5	Total charge in uniformly charged sphere	
Using max Q per drop from Dawson [1969] for Ht = 5km		
Radar Ref	Sph rad	max E Field
dBZ	metres	MegaV/m
10	116.7492	1.980871
20	83.80451	3.844404
30	60.29617	7.428505
40	43.41654	14.32364
50	31.23455	27.67537

Ok

Appendix 11

RADAR STUDIES OF LIGHTNING

A11.1 *Introduction*

Radar reflections from lightning were noticed by various operators who served during WW 2. Lightning echoes are detected most readily using radars that employ longer wavelengths because these radio-waves are not reflected strongly by hydrometeors, and therefore they are not masked by rain clutter. Using a wavelength of 50 cm, Hewitt [1953, 1957] showed that lightning echoes persisted for many tens of milliseconds before decaying, and that echoes were often rejuvenated by events that also caused the emissions of trains of VHF radio-noise. These events sometimes also initiated echoes from volumes adjacent to the earlier echoes. He ascribed these events to return-strokes, and it was only later, when radio pictures were taken together with recordings of electric field-changes, that it became evident that only some of these events were associated with return strokes. His figure 2 is reproduced here as Figure A11.1 because it shows how these echoes behaved in time. We now know that radio noise is emitted from the tips of lightning channels only when air is first ionized. Flows of current along existing channels do not cause them to radiate, except where they extend the old channel, or, if the channels has been allowed to decay for 80 milliseconds or more, when the current wave re-ionizes the channel. For this reason, the radio pictures do not indicate where dart leaders flow. Whereas radio noise can be used to map lightning during its incipient stages, measurements, such as those shown by Figure

A11.1 suggest that radar echoes could be used to monitor the subsequent history of a lightning channel. Theoretical work published by Dawson [1972] and by others, shows that echo-intensity depends on the degree of ionization existing in the channel, particularly when the degree is low, so that waves may penetrate the channel. This is the so-called underdense case. When the channel is overdense, there is little penetration, and echoes are reflected by the front surfaces of the channel. Although the proportionality is lost, a strong echo is a symptom of a high degree of ionization. Echo-strength is therefore an indicator of the level of ionization. Calculations, by Williams et al [1989], show that the underdense case reflects so weakly that it is mostly of academic interest here. Proctor [1981] conducted an investigation in order to find which of five radars, ranging in wavelength from 3cm to 100 cm and with three values of pulsewidth, was the most suitable. Narrower pulses provided more detail, but longer pulses were reflected more strongly, and of the two longer-wavelength radars the 100 cm radar was marginally better. Some of these results are shown by Figure A11.2.

A11.2 *Scanning problems*

Narrow beam radars are capable of producing useful pictures of lightning if the lightning occurs at long range so that the beam is wide enough to embrace the extent of the lightning that is perpendicular to the plane being scanned by the radar, and if most or all of the lightning happened also to lie in the plane being scanned by the radar, and if the echoes persisted long enough for the radar to scan that

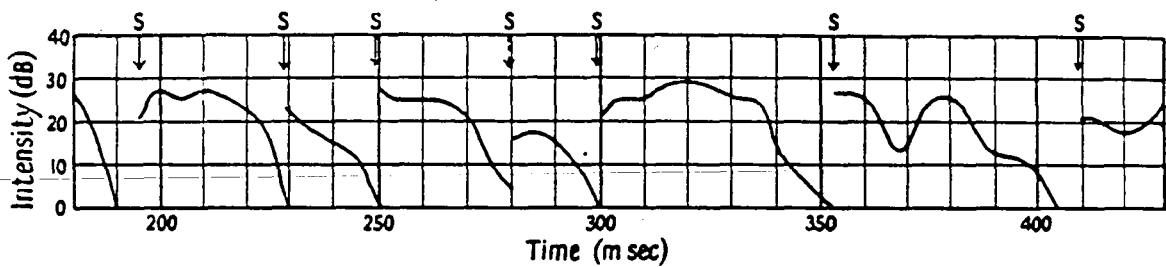


Figure A11.1 Measured intensity of one conspicuous echo recorded during a flash to ground, shown as a function of time. The events labelled "S" indicate times at which bursts of VHF radio noise were recorded. Reproduced from Hewitt [1957].

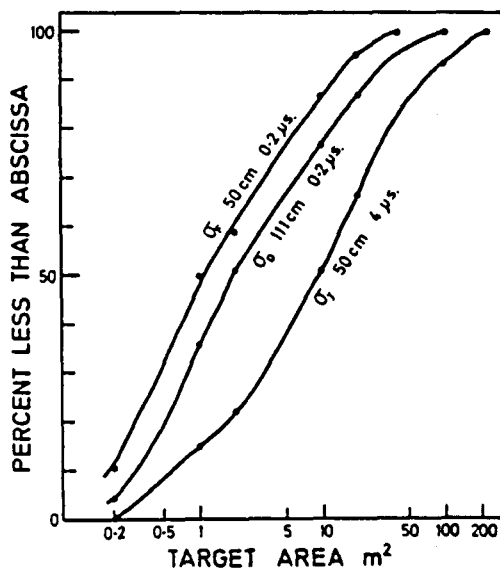


Figure A11.2 Measured distributions of cross-sections of lightning radar reflectors, shown for two wavelengths. The effect of pulse-width is shown for the 50 cm radar. Taken from Proctor [1981].

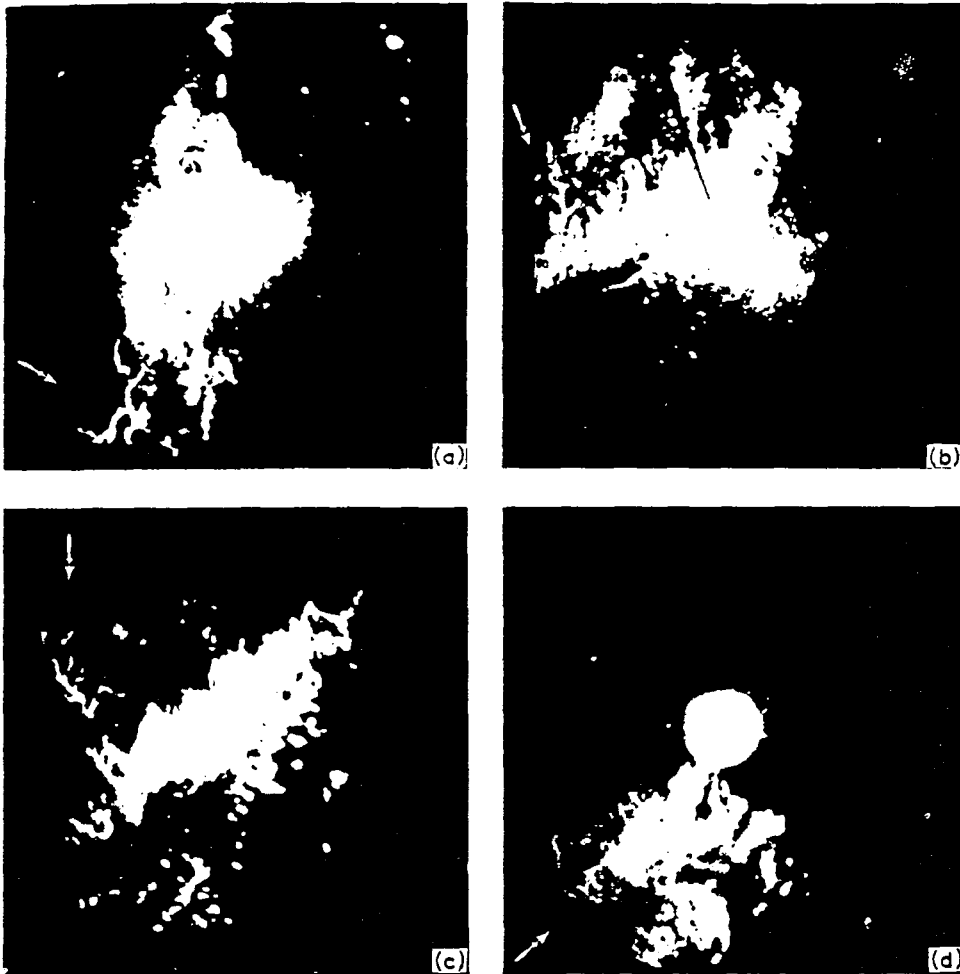


Fig. 11. Extended echoes from instability line storm I-C or C-C discharges. All pictures printed to the same scale with arrow 27 nautical miles in length. (a) 23-cm radar, Belleville, Illinois, 27 May 1955; (b) 23-cm radar, Fordland, Missouri, 19 April 1955. Note the "root-like" structure of the echo at its southern end. This short stubby branching in a direction opposite to branches in other parts of the echo has been observed several times and may indicate regions of high charge concentration. (c) 23-cm radar, Fordland, Missouri, 11 October 1954. This is the longest continuous echo yet found. If the lightning echo south of the long echo is part of the long discharge (see Fig. 20), this echo is over 100 statute miles in length. Similar gaps have been noted in other echoes and may be significant. (d) Same storm as (c) but from 10-cm radar, Kirksville, Missouri, 11 October 1954. Note weaker lightning echo relative to precipitation echo.

Figure A11.3 Radar reflections from lightning published by Ligda [1956].

sector occupied by the flash. Ligda [1956] produced interesting pictures in this way. He even devised a means for suppressing rain clutter that was successful in some cases. A few of his pictures are shown here in Figure A11.3. Recordings like those are produced by dint of good fortune. The pictures are two-dimensional, and have little or no resolution in time. (They are nevertheless interesting. This investigator finds comfort in them in that they substantiate some aspects of the radio pictures). The chance that a particular lightning flash will occur outside the limits of a narrow beam is too large for such a system to be reliable when used in conjunction with other experiments. The filamentary echo near the top of Figure 5.6 of flash 87 is probably due to a lightning flash that happened to be in beam. Hewitt [1953, 1957] used an intermediate approach. His transmitter beam was relatively wide, 20 degrees by 30 degrees, so that it illuminated a sector of the sky. His receiver antenna formed four wide, independent and overlapping beams. He measured ratios of echo-amplitude on four receivers, consulted plots of the receiver-beams, and calculated the elevation angle of the echoing target. The angular accuracy was due to having used the information provided by the details of shapes of the beams. The slant range to the target could be measured in the usual way. Thus he could produce two-dimensional maps of the echoing regions. Flashes that wandered out of beam, were not recorded in full. In spite of this, he produced much valuable information about lightning.

We attempted to extend these ideas by illuminating a much

larger segment of sky, using a more powerful transmitter, and by using the five-station network of receivers to locate the reflecting regions.

A11.3 *Transmitter power*

The transmitter tube that had been acquired for this purpose, was rated for an output of 1 MegaWatt. A later sales pamphlet mentioned a corrected figure half this, and we suspected that a second pamphlet had been circulated also. We could obtain only 150 kW using a pulse-width of 1.5 microseconds. I believe that more peak-power can be supplied by this tube if the pulse is lengthened. (The tube was intended for TV transmissions, and was chosen for its price.) The transmitter antenna had to be made to radiate a narrower beam in order to make up the deficiency in power.

Figure A11.1 (and preliminary measurements of our own) showed that the time-resolution afforded by transmitting pulses every 1 millisecond was unnecessarily high. In order to trade this off in favour of more radar performance, we designed and constructed antennas that illuminated three sectors of the sky in sequence. Commutation was affected by a switch that we designed and constructed. It incorporated a series of quarter-wave lines and a mechanically rotated capacitor which acted to shortcircuit the lines in turn. The trigger pulse to the modulator was controlled by a hole in the rotor that passed a light beam, to prevent the transmitter from firing while switching was in progress. This arrangement permitted a segment of sky defined by the -6 dB contour, 52 degrees wide, by 150 degrees along the Y axis, to be illuminated in three

successive beams that overlapped at their -3 dB points along the vertical plane. Switching-speed was high enough to allow each successive transmitter pulse to be transmitted on a different beam.

A11.4 Receiver bandwidth

The bandwidth of the receivers was determined by the timing accuracy required for the primary function of the system. Signal-to-noise ratio was not a principal problem in the matter of receiving radio emissions from lightning at this frequency. The receiver bandwidths, 5 MHz for the remote channels, and 10 MHz for the Home channel, were too wide for the radar requirements (0.48 MHz for the pulsewidth of 1.5 microseconds; rectangular pulse, Gaussian filter. Skolnik [1962] p 414.) The excessive bandwidths of the channels allowed thermal noise to degrade the radar performance. One solution was offered by using a separate display driven by video amplifiers having the required bandwidth for the radar signals. This offered some improvement by reducing noise, but was still not optimal, because ideally the bandwidth reduction should be effected before detection. (To prevent the noise components in the wide band beating with one another to produce inband components). The use of a separate display provided additional benefits in that it eased some of the recognition and calculation problems because the radar display can be synchronized with the transmitter pulse. Noise then appears randomly, whereas the transmitter pulses on all channels appear in columns, and so do the echoes. The main results presented below were obtained before the new display had been built, and therefore suffered an extra 10 dB loss in

signal-to-noise ratio due to the excessive bandwidth. Echo-strength proved to be highly variable. Even distant echoes sometimes saturated the logarithmic receivers.

A11.5 *Reading records*

The transmitter pulses could be recognized by their very large amplitudes and by their characteristic pulse-widths. The echo-pulses were not always detected so easily. A sample record which could be read with comparative ease, appears in Figure A11.8. Sometimes the targets were so disposed that they were equidistant from one of the stations (occasionally two stations) and then their echoes coincided on those traces, a happenstance that rendered it rather difficult to read those records accurately. Figure A11.4 shows a sequence of pulses on the traces for the Home and remote channels.

A11.6 *Computational methods*

Usually the reflector positions were calculated as though they had been sources of radio noise. This obviated the need to reload programs while reading records which were mixtures of radio noise and radar echoes. Other methods are available to treat cases where an echo had not been received at one station: The slant range measured on the Home channel defines a hemispherical surface that contains the source. The time at which the transmitter pulse was emitted is also indicated on the Home channel. On the remote channels, therefore, a sum of times is known also. This sum defines an ellipsoid whose surface intersects the hemisphere ambiguously, and one other measurement is needed to resolve the ambiguity. Figure A11.4 shows how R_1 can be calculated. This quantity defines

another hemisphere centred on the remote station, and this hemisphere can be used instead of the ellipse, mentioned earlier. Calculations of echo-height could not be made in cases where the echo in question had not been received by the Home station.

A11.7 Results

Case 1. Flash 156

This was recorded at 1614:38.85 on 8th February 1986. The auxiliary record has been reproduced in Figure A11.5. This record supplies the following incidental information: The sensitivity of the Light Trace was reduced because of the bright sunlight at 1600 B, and light from only the two return strokes was recorded. Notice that stroke 2 produced multiple pulses of light, called "M-components" by Malan and Schonland [1947]. The Noise trace shows that the stepped leader was interrupted after 97 milliseconds for an interval of 25 millisecond. The electric field change (EFC, bottom trace) of the leader of the second stroke has a waveform similar to the EFC of the first leader, but compressed in time, indicating that they followed similar paths.

The Noise trace also shows that the radar was initiated by Q-noise that occurred during the stepped leader. The (top) Time Trace bears witness to some of the havoc sown by the radar transmitter. The flash continued after 270 msec as a cloud flash, which we have treated separately. The time 270 msec coincides with the end (RHS) of the serial time code on the third trace from the bottom.

Figure A11.6 is a plot of height Z, in km AGL, plotted to a base of time. This shows that the streamer ABCD almost went to ground before restarting at time C. Figure A11.7 shows that the flash then extended along two new paths, and later, after time F, it produced another path. Figure A11.7 shows that the path FGH nearly reached ground, but Q-noise at time H radiated from the tip low-down on one of the earlier paths, but the record of electric field change shows that it did not make contact with the ground at that time. It struck ground later at time J and again at time M, when it went to ground along at least two paths, which explains the multiple pulses on the recorded waveform of light.

The radar began transmitting at time H. Figure A11.8 is a composite picture showing the radio picture of the flash plotted up to the time I. It also shows four of the radar echoes. This figure also shows a photograph of the five traces on the Data Handling Machine. Although made to cater for only eight levels of amplitude, it is sufficient to display noise pulses and echoes. These echoes have been mapped in the accompanying Figure. The top trace was recorded by the responses of the Home channel. Because of the proximity of the radar, its pulse, labelled T in that Figure, has very high amplitude on this channel. Saturation effects cause the pulse to appear much wider than it does on the remote channels. Pulses G on this trace are due to ground-clutter (i.e. echoes G are "permanent echoes"). Pulses E are lightning echoes, so recognized because, although they recur after later transmitter pulses, their amplitudes evanesce. Pulses on the second trace, were relayed by the

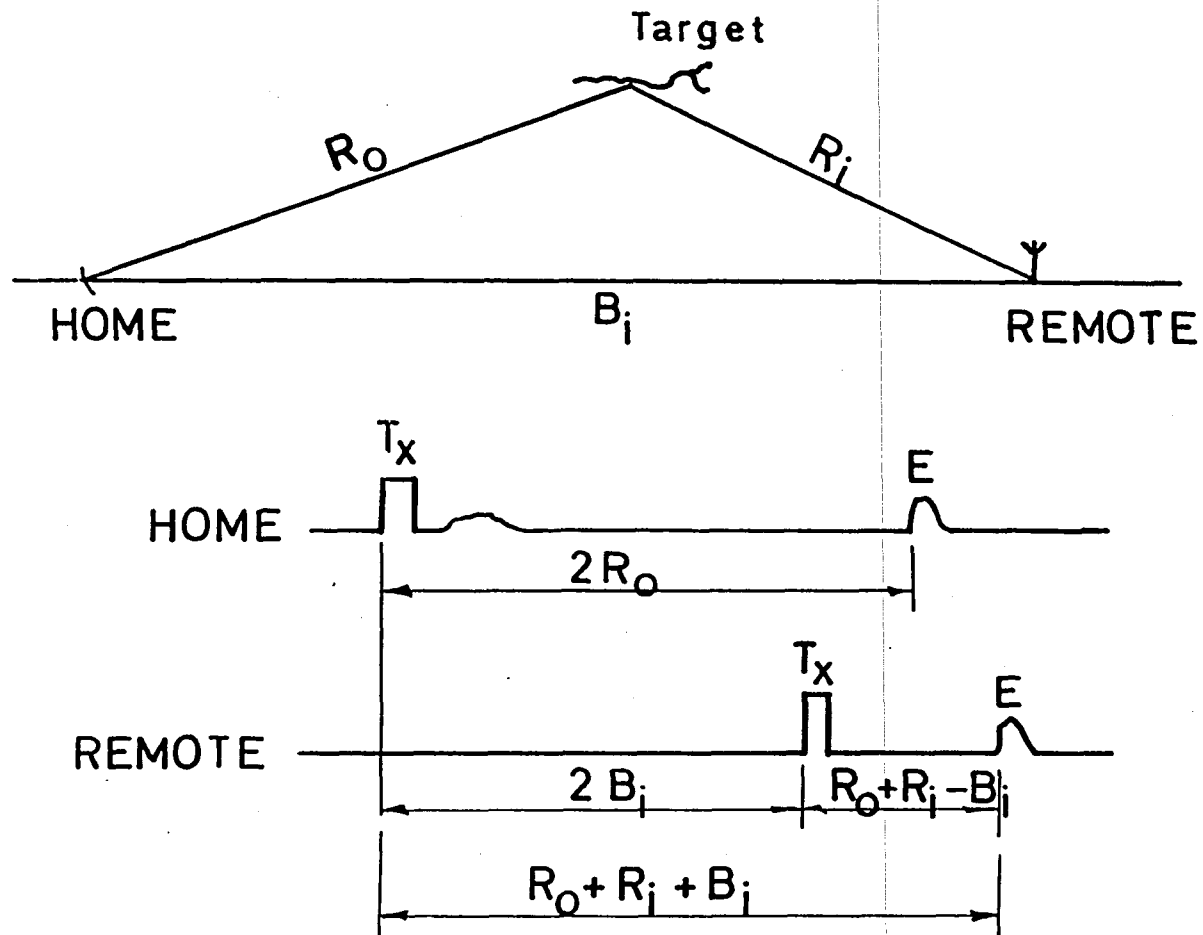


Figure A11.4 Geometry of multistatic radar.

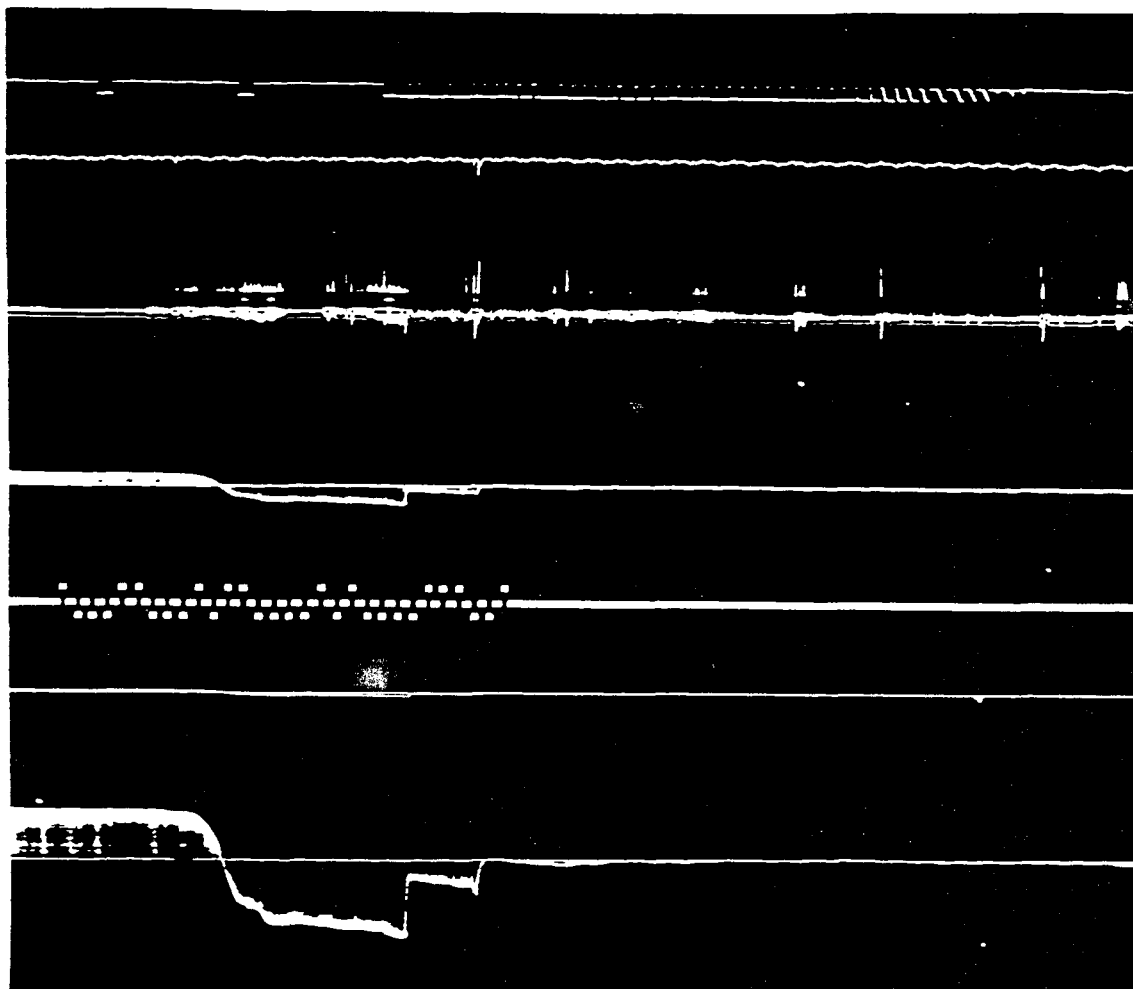


Figure A11.5 Auxiliary record of Flash 156. Timing trace (at top) shows downward rectangular pulses at intervals of 100 milliseconds. Time increases Left to Right. Later pulses were disturbed by the radar transmitter. Second trace from the top shows light output from first and second return strokes. Traces 4, 6 and 7 show the electric field-change recorded at ground. Serial time-code for 161439 appears on trace 5. Trace 3 is output of the Home VHF receiver, which also shows when the VHF radar transmitter came on.

Figure A11.6 Heights AGL of radio sources, that were active during Flash 156 plotted to a base of time. Sources active during trains of Q-noise have been plotted using larger symbols to distinguish them from pulse-sources. The symbol R is used for radar echoes. Similar plots for X and Y coordinates are shown in Figures A11.11 and A11.12.

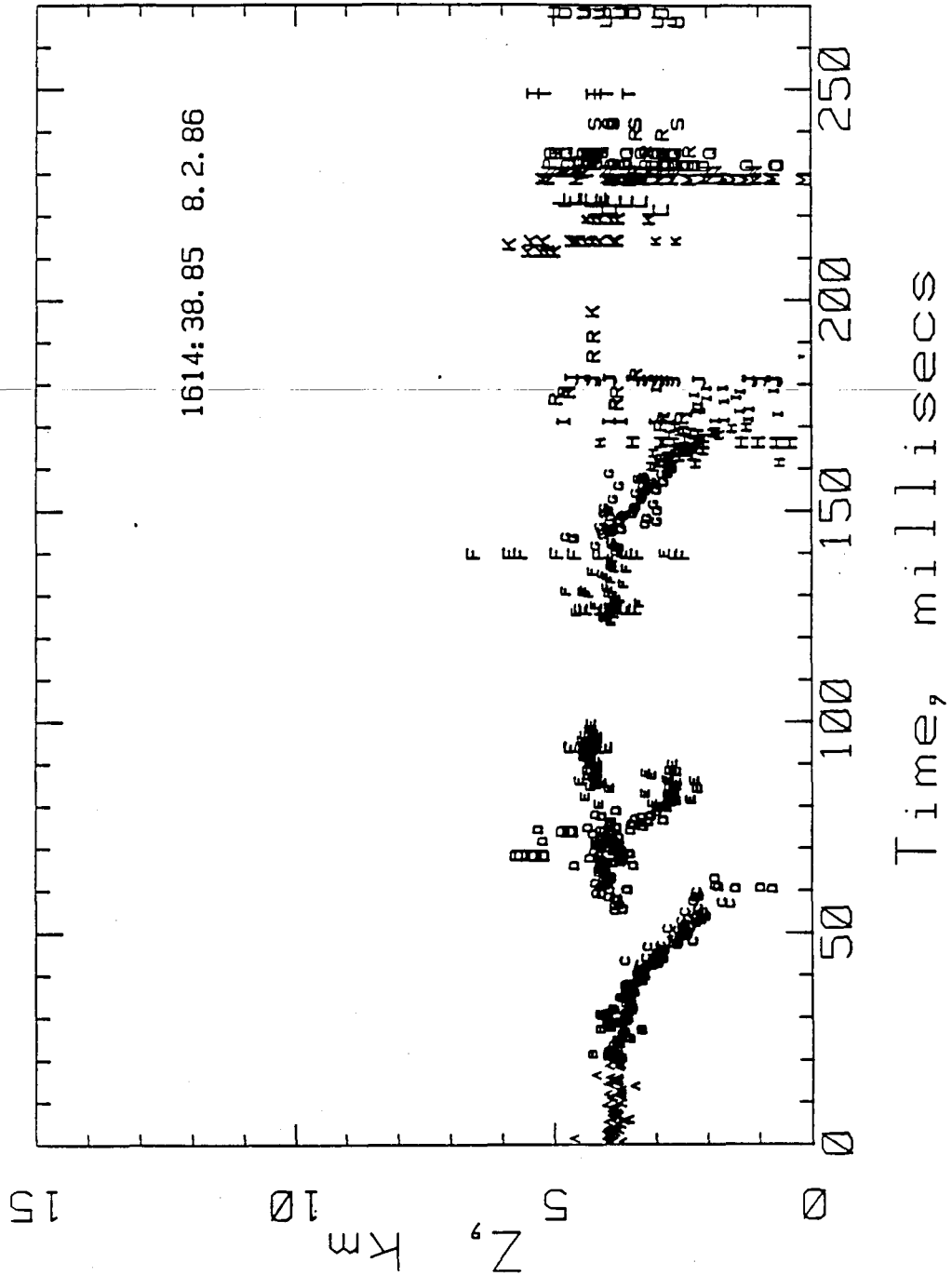


Figure A11.7 Three views of Flash 156 up to time H. Sources active during trains of Q-noise have been plotted using symbols of a larger size to distinguish them from pulse-sources. The alphabetical code refers to a time-scale shown by Figure A11.6.

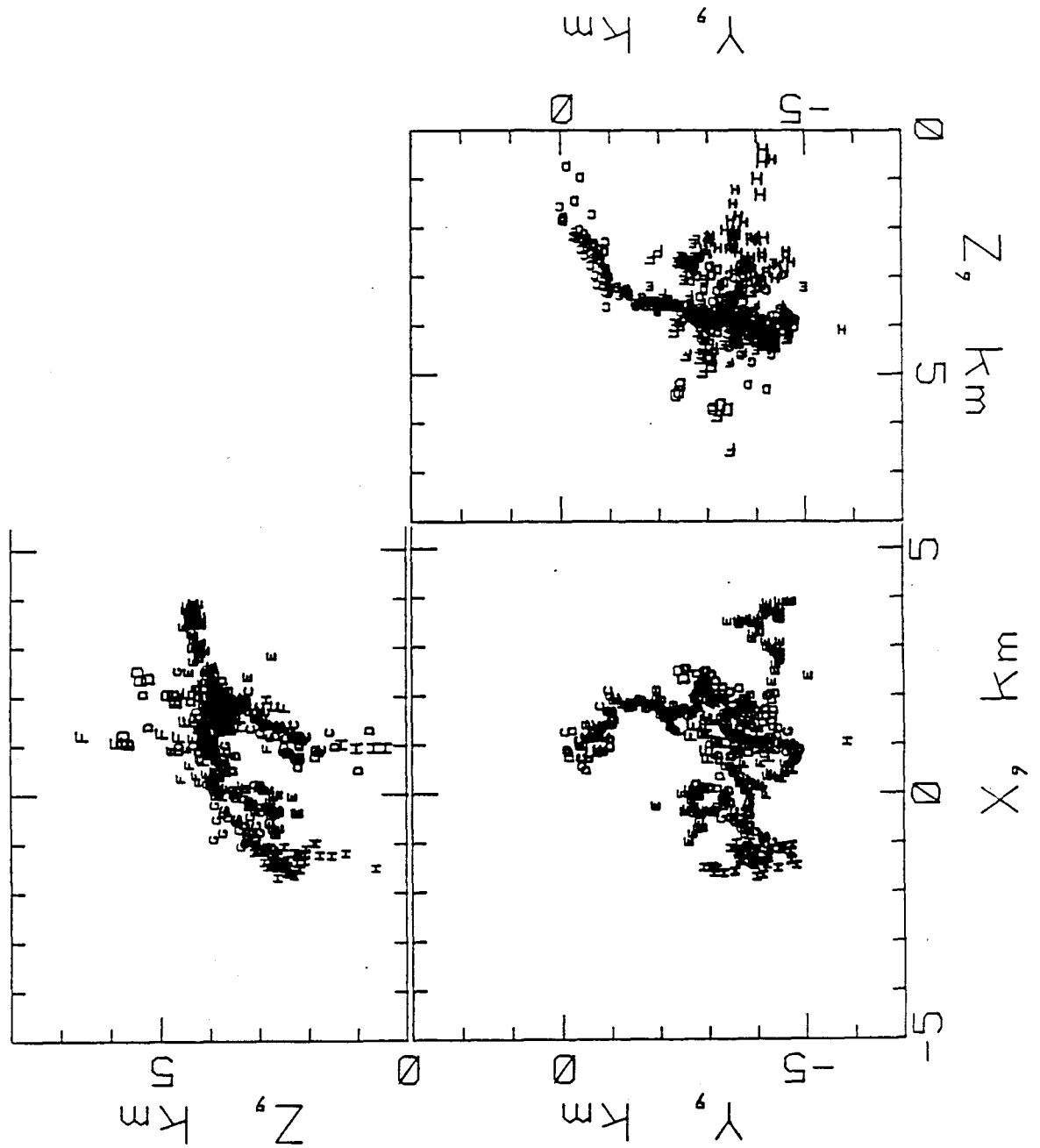


Figure A11.8 Three views of Flash 156 up to time I, showing the echoing regions R. The inset shows A-scans (recordings of amplitudes vs time) on the five receiver channels. Here the radar echoes have been labelled E, and the transmitter pulse, T. See Text.

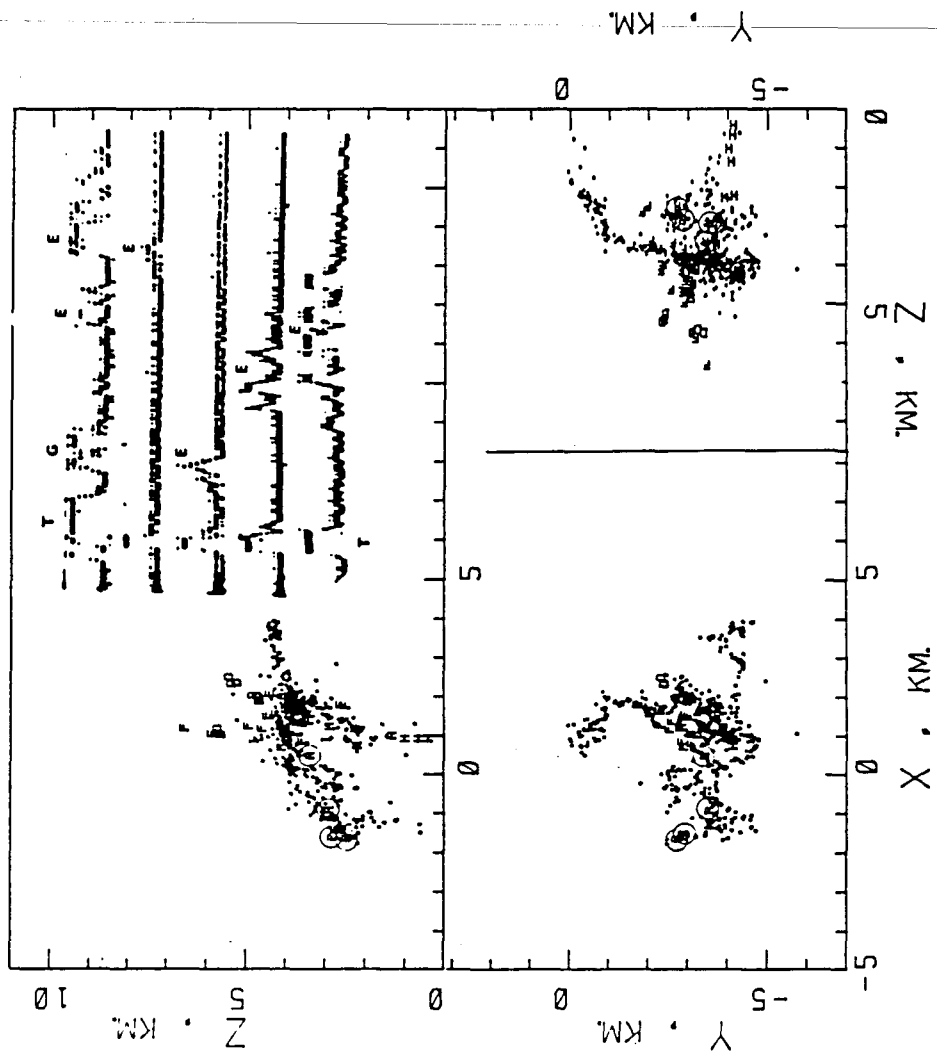


Figure A11.9 Three views of Flash 156 up to time U, showing the echoing regions R.

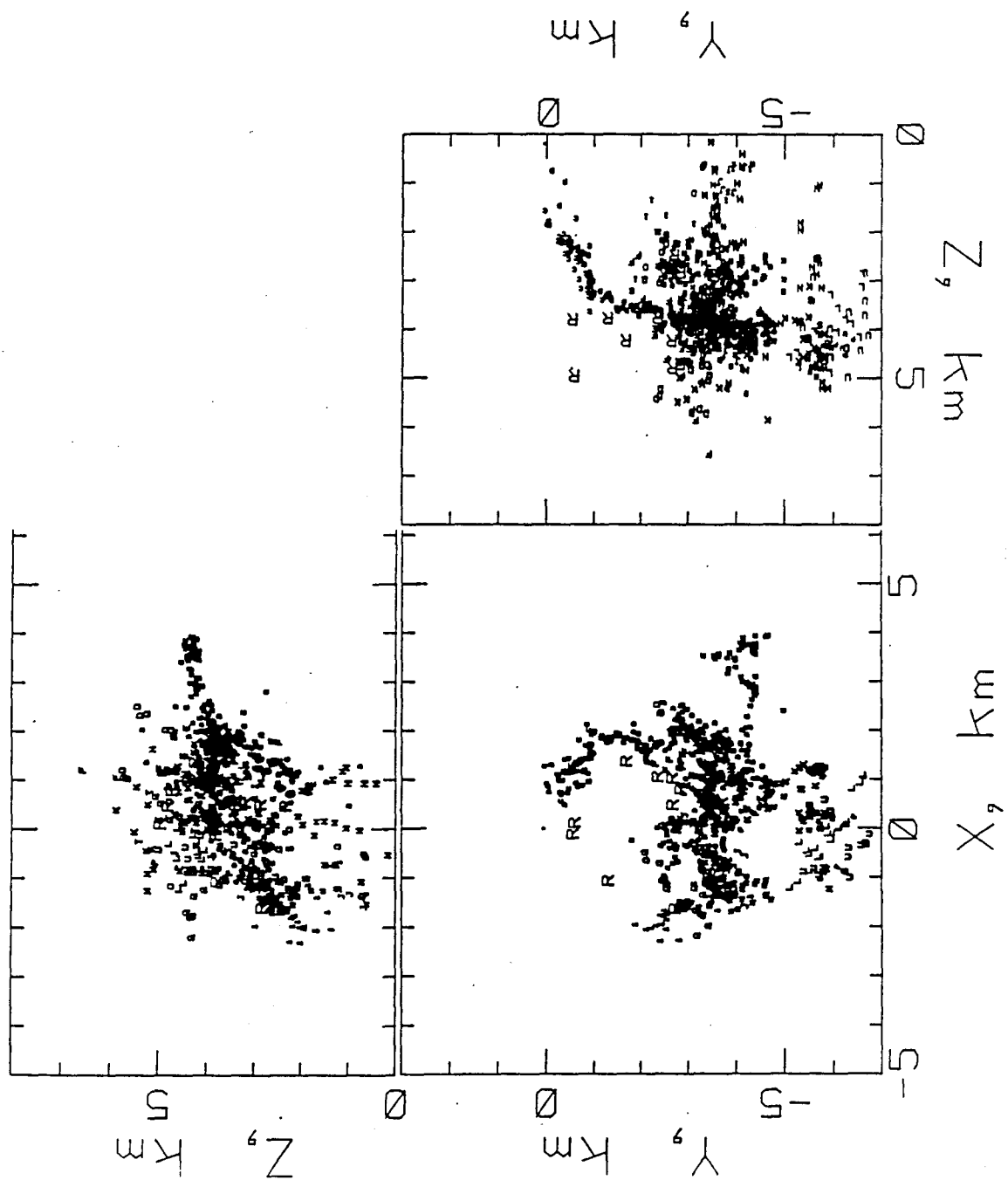


Figure A11.10 Heights AGL of sources active between 160 and 270 milliseconds, showing the occurrence of the echoes R.

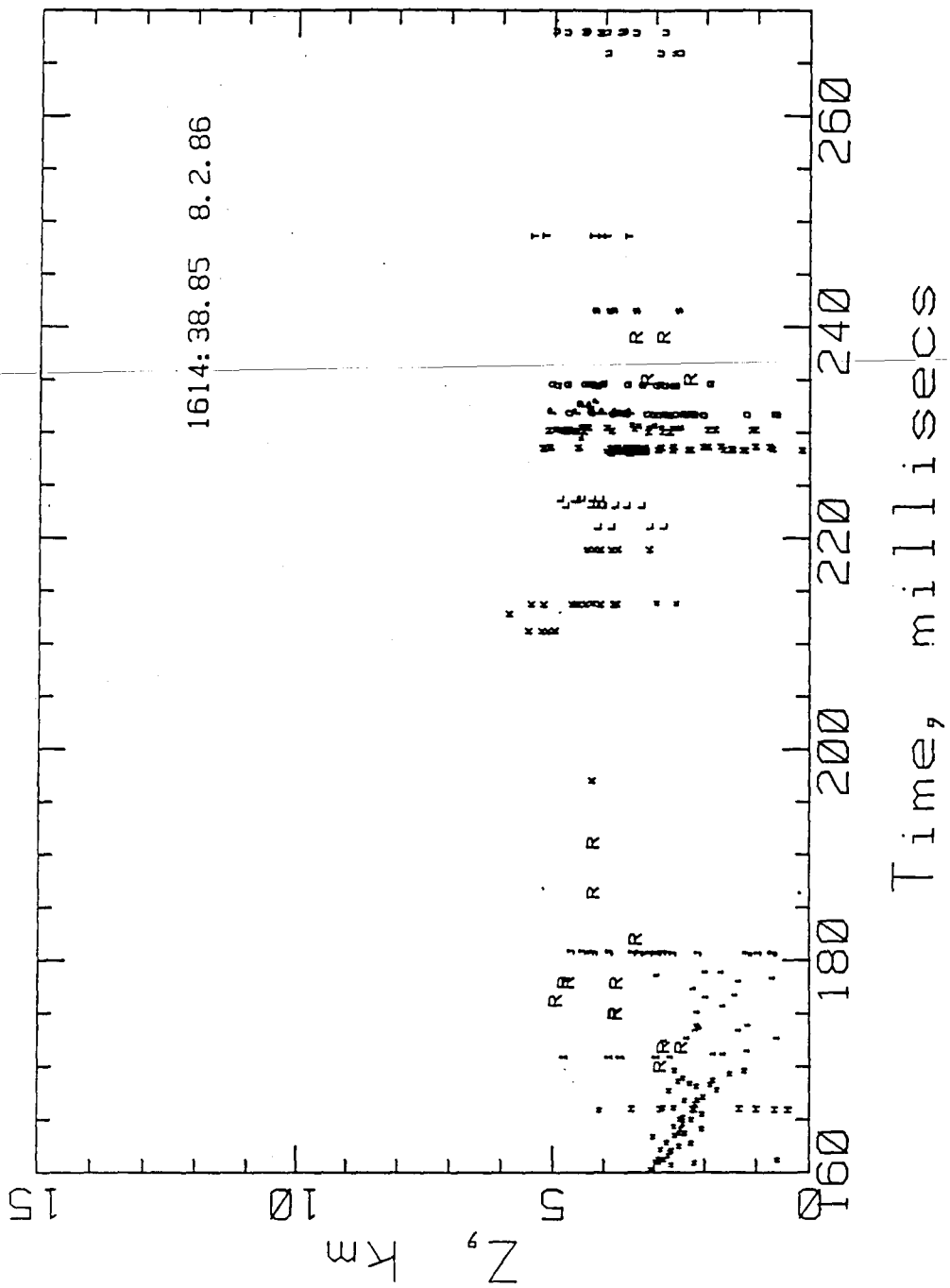


Figure A11.11 X-coordinates of radio sources active during Flash 156. this has been reproduced to highlight the positions and times of occurrence of the echoes R.

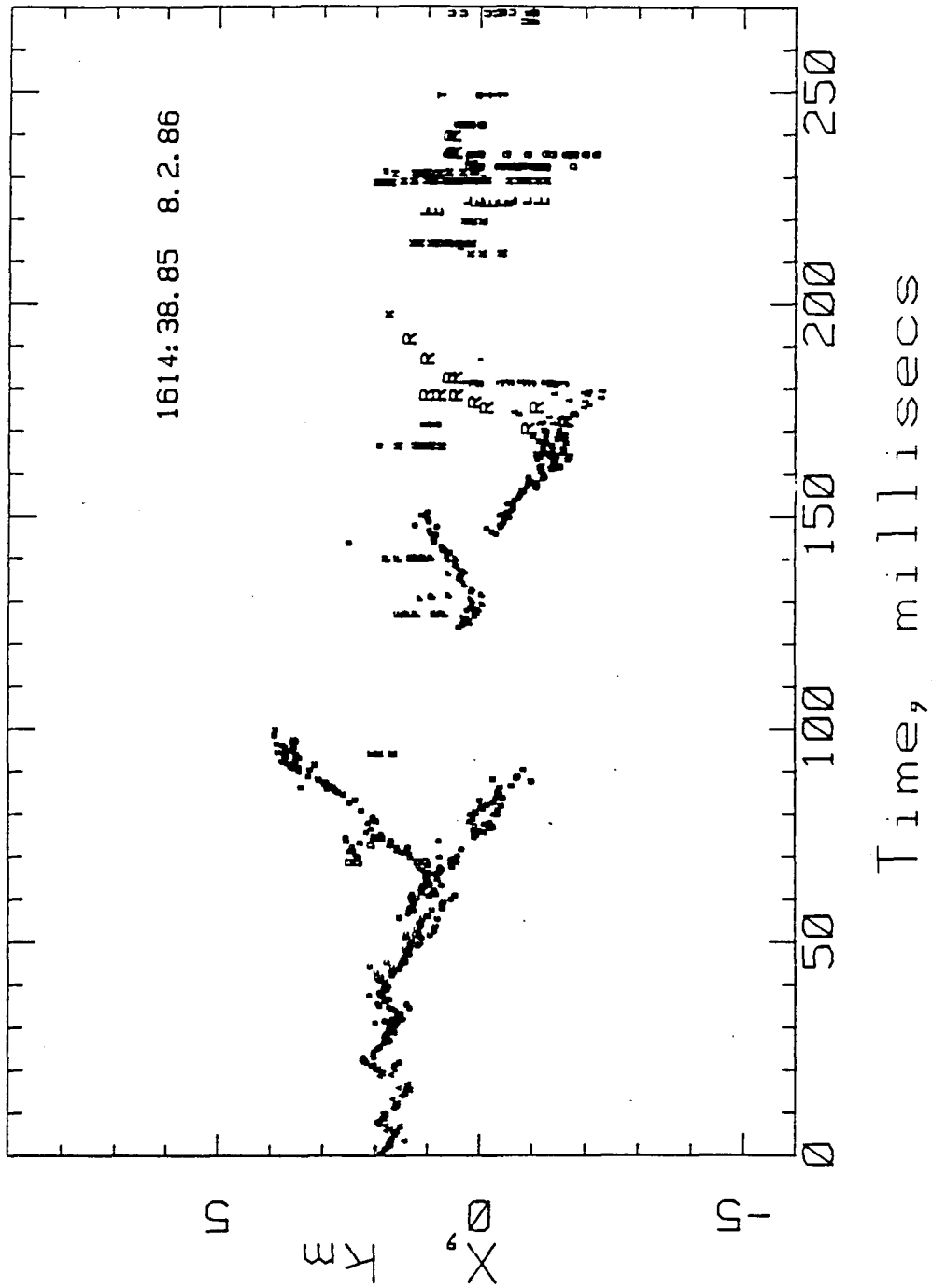
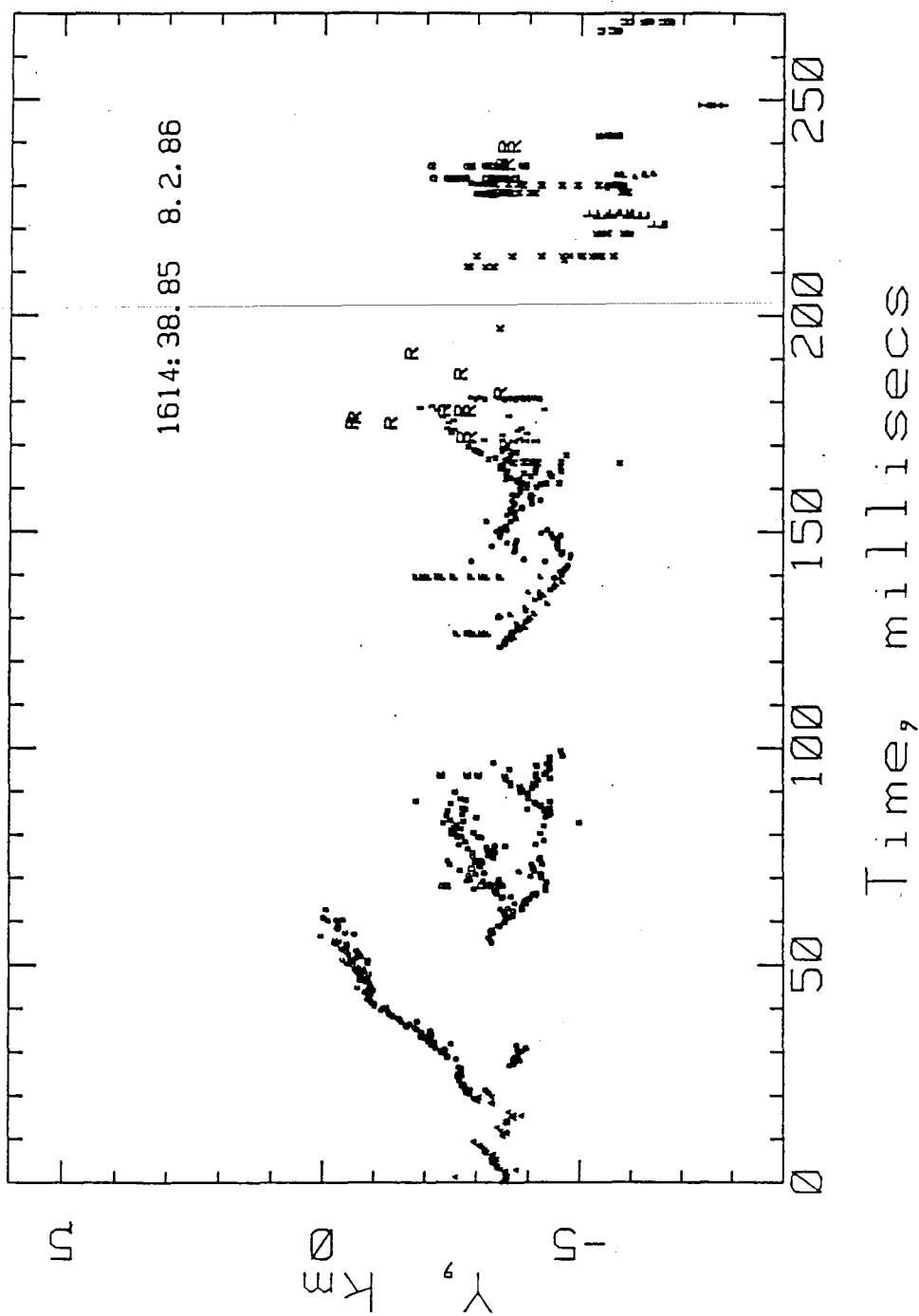


Figure A11.12 Y-coordinates of radio sources active during Flash 156. This has been reproduced to highlight the positions and times of occurrence of the echoes R.



Kalkheuwel station. Their lower amplitude is due probably to destructive interference by ground reflections. The third trace was retransmitted by furthest station, 26 km distant at Observatory. The transmitted pulse and the echoes (from targets near the Home station) arrived almost simultaneously, the extra delay of the pulse-group having been removed by the Data Reading Machine. Traces two and three (counting from the top) come from stations that lie along the Y-axis. The accompanying plan view shows that the echoing regions were almost equidistant from Kalkheuwel, and that the same four targets were at a greater distance from Observatory which was also nearly equal for all four. These echoes therefore grouped closely on these channels. Pulses recorded on the two bottom traces were retransmitted from Knopjeslaagte in the East, and from Protea Ridge, Krugersdorp in the West. The plan view shows how the targets were distributed along the X-axis. Their spatial separation accounts for the spread in times at which the echoes appear on those traces. The plan view shows that the echoes were located on the Northern (+Y) side of the flash, and that most were on the West (-X) side. Attenuation by the intervening lightning channels accounts mostly for the differences in echo-amplitude from one channel to another. (The variability in the amplitudes of pulses relayed by Kalkheuwel is especially large. We have been chasing the reason for this for 20 years, and in the process we have replaced every component there, and have concluded that occasionally weak video returns were due to ground-reflections. The branch that curves downward toward +Y might not have obstructed the (shorter) path to Home, where echoes were relatively strong, but it will have taken energy

from the waves reflected towards Kalkheuwel. The echoes received at Observatory were also weak. They, too, had to pass through lightning channels for a part of their relatively long journey. Echoes from targets on the Western edge of the flash saturated the receiver 20 km distant at Protea Ridge, and were noticeably weaker at Knopjeslaagte, only 12 km away, after having to pass through the flash. The plan view, and the Z/Y Elevation views show the northern branch that curves down to the Home station. Evidently, it caused some weak echoes to appear at short range on the Home Channel. Its echoes were absent from Kalkheuwel's record and from those returned by Observatory. Careful study of the radio picture shows that the inner part, illuminated by the transmitter was shielded from both these stations, by other parts of the flash.

Radio pictures that also show the later stages of the ground-flash portion of this flash are reproduced in Figure A11.9 and indicate how complicated the flash became. They also show two echoes that did not collocate with sources of radio noise. I ascribe that to errors in timing weak echoes at Kalkheuwel, which were critical in determining height. Some echoes were embedded among the radio sources. They have been rendered more visible by Figure A11.10 which is a plot of Z vs Time and covers the interval 160 msec to 270 msec. All the radar echoes have been labelled R. Figures A11.11 and A11.12 show how the X- and the Y- coordinates of the radio sources changed with time. Perhaps these plots show some order among the seeming chaos. The later, cloud-flash portion has been plotted, but is not shown here.

Case 2. Flash 155.

The waveform of electric field-change recorded on the auxiliary display, showed that this had been a flash to ground having a single stroke.

The waveform of the electric field-change caused by the stepped leader showed that the flash had struck ground within a few km of the Home station. (Dependence on range to the flash of waveforms of electric field-change caused by leaders has been described by Malan [1963], page 49.)

The auxiliary display also produced a record of the output of the Home receiver, which showed that the VHF radar had been initiated at the time of the return stroke. An elevation view of the flash, obtained by taking differences of the times when leading edges of the radio pulses, emitted by this flash, had arrived at spaced receivers is shown in Figure A11.13. The origin of the flash was at $(-3.35, -4.55, 4.2)$ km, at $t = 0$. The return stroke occurred at time G, 61.098 milliseconds. The point of strike was $(-2.6, -2.2, 0)$ km. Q-streamers, G and H and the reflectors, R, of radar pulses have been mapped with larger symbols. The Q-streamer H began at 76.396 milliseconds. Radar echoes were received at 79.320 millisecc, 80.863 and 82.317 millisecc. One group of echoes was located at $(-3.06, -3.85, 3.93)$ km and another at $(-2.09, -3.07, 3.66)$ km, whose respective elevation angles were 38.63 and 44.58 degrees. Echoes appeared to be associated with the top of the channel to ground, and with the region H. Evidently, no echoes were received from the lower part of the

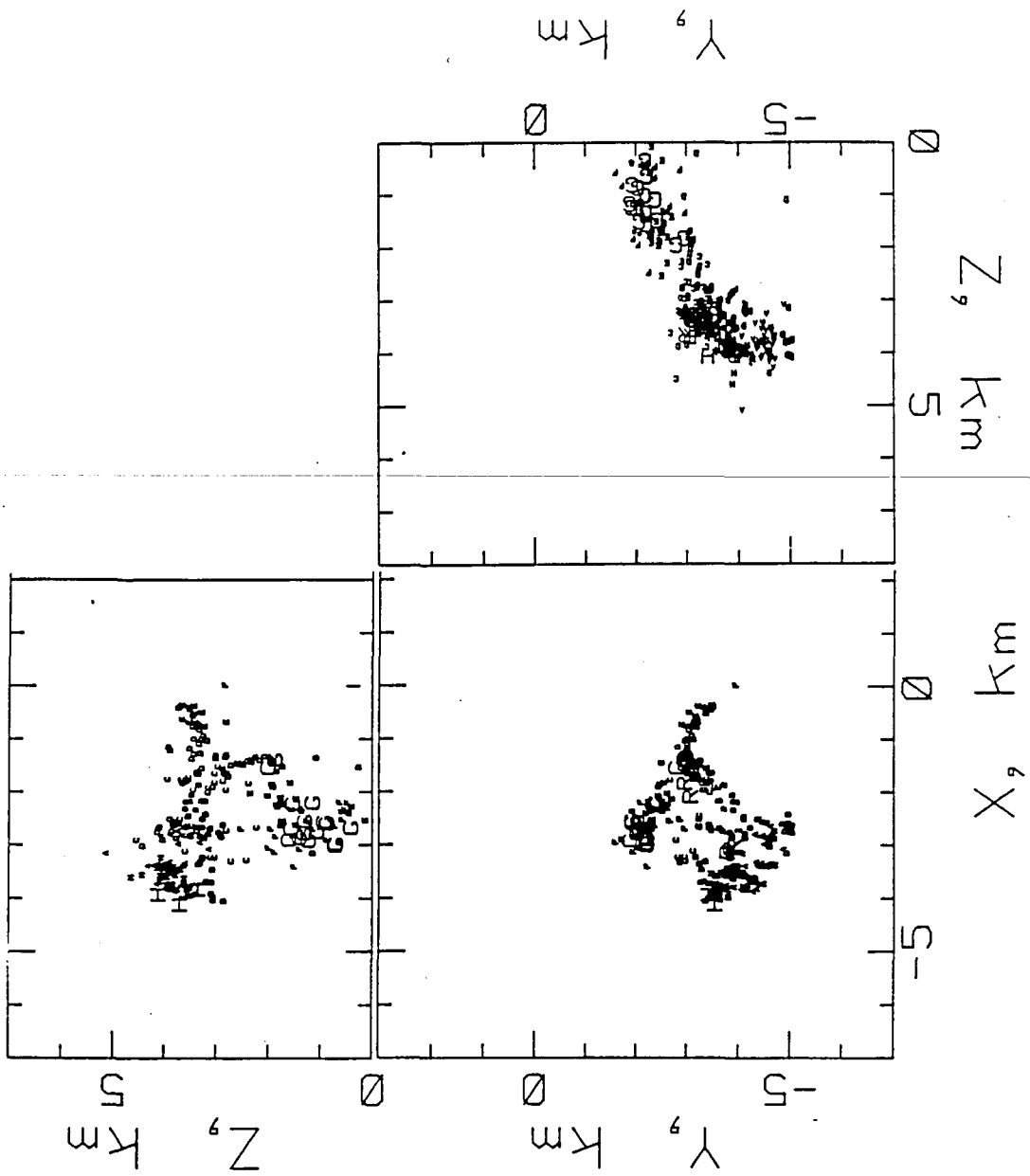


Figure A11.13 Three views of radio sources active during the ground-flash 155. Sources G radiated during the return stroke. Sources H were active sometime later. Radar echoes have been labelled R.

channel. The echoes were received from regions that were exposed to all stations. Cases where the echoes did not appear on all stations were not attempted.

Case 3. Flash 157

This was a fairly extensive cloud flash recorded at 1749:53 on 8 February 1986. The auxiliary record showed that the radar transmitter was on for the entire duration of this flash. Before we recorded this flash, the Home receiver had been connected to a Helical antenna that pointed to the Zenith. Its beamwidth between nulls was 115 degrees, and the half-power points 52 degrees apart. This was done in an attempt to improve the radar performance at a time when the storm was judged to be overhead. In consequence only a part of this flash was viewed by the Home receiver. Figures A11.14 and A11.15 show plan and elevation views on which the radar echoes have been labelled X. Echoes were received only from a lower branch. Although some of the higher portions were in beam, no echoes were received from them. Evidently they had been screened by the flash itself. The lowest echo was a permanent echo.

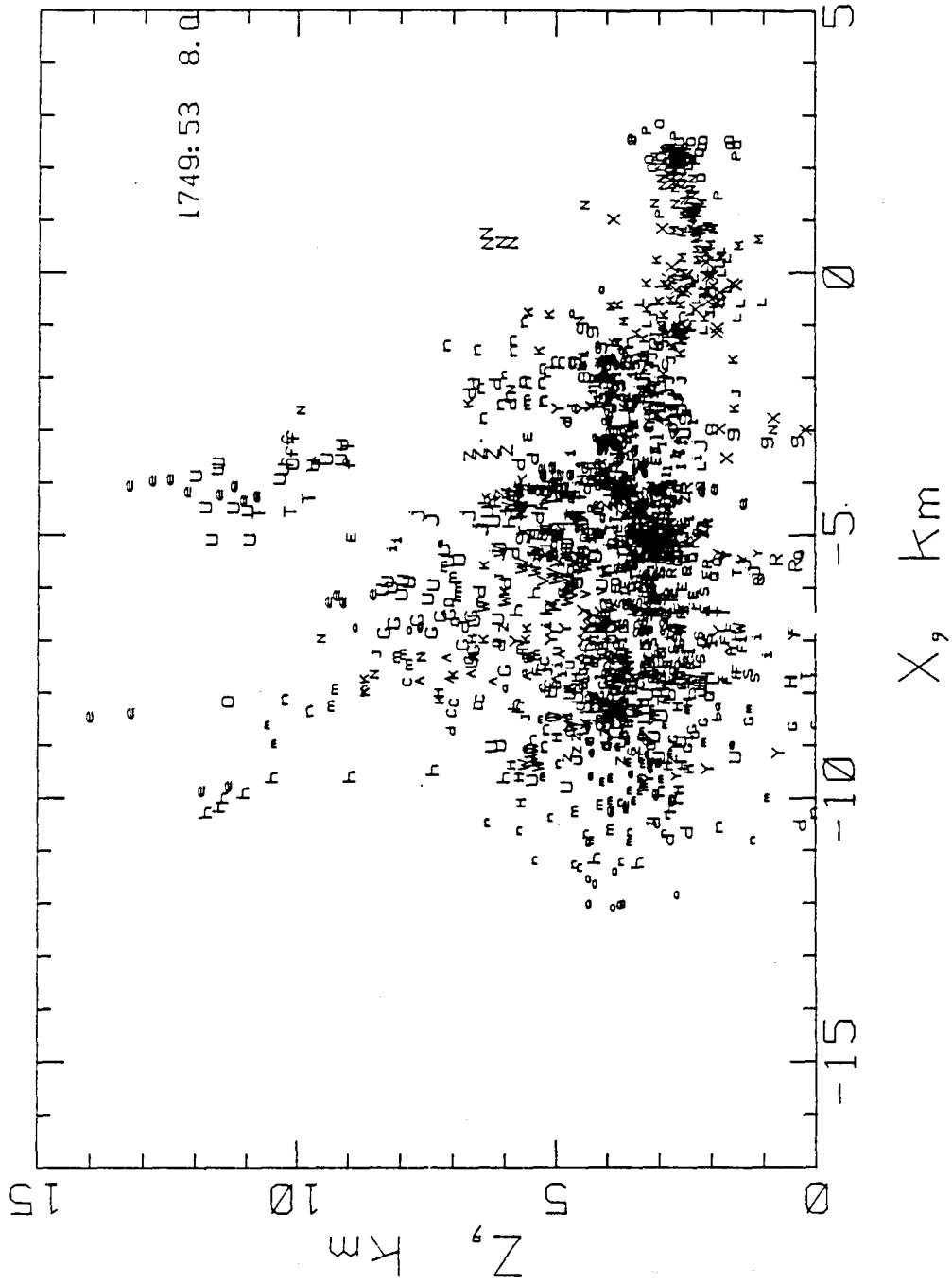
A11.8 Discussion

The use of shorter wavelengths introduces the problems associated with rain clutter. Evidently, another problem, that of attenuation by the lightning itself, also affects the results. The examples that we have described show that intervening lightning has a marked effect on echo strength. We knew that lightning channels were overdense, (See for example Williams et al 1989). The surprize came about because

we tend to think of a lightning flash as consisting of one or two long filaments, which are largely exposed, so that the chance that the view of one part of the flash being obstructed by another is a small one. This conception is correct in some cases, such as the flashes with high origins. The lower flashes are much more voluminous. They are more extensive and their branches are more profuse, so that it is more correct to think of them as huge blobs, (witness Case 3 and the pictures pulished by Proctor et al 1988) and once this has been understood, then the limitations of using radar become more apparent. This same problem of attenuation must be one reason why radio noise from lightning varies so greatly in amplitude, particularly in the case of flashes with low origins. We have adjusted receiver gains at five stations many times, and only now has one of the reasons for the variability become apparent. The problem is not so acute with the radio noise as it is with the radar reflections because the sources of radio noise are very strong radiators. Proctor et al [1988] estimated that a typical source radiated 5×10^7 Watts.

These results also substantiate the conclusion reached independently by Proctor [1981] and by Holmes et al [1980] to the effect that radar echoes received from lightning in cloud are due to many reflectors that are distributed throughout a volume of cloud rather than being arrayed along a tortuous path that is mostly one-dimensional. This paper has been able to show which streamers contribute to the echoes. It has also shown that all kinds of lightning channel reflect radar waves and not just "junction streamers". ("Junction streamers"

Figure A11.14 Elevation view of radio sources active during Flash 157. Except for symbols X, which map the radar reflections, symbols A to Z and then a to o indicate the time scale in steps of 10 milliseconds.



were positive streamers whose existence was postulated by Malan and Schonland [1951] to explain how successively higher regions supply charge to subsequent strokes.)

The methods we chose to observe the echoes were influenced by the tools that we were using to carry out the observations with radio noise. It turned out to have been a rather cumbersome method of mapping echoes, when compared with normal radar practice. On the other hand, it provided three-dimensional pictures, whereas radar pictures obtained in the normal way, would have been superficial, because of the attenuation. Echoes were located by timing the leading edges of the echoes, and the method needed to be developed so that the extents of the echoing regions could also be mapped and measured. We seem to have mapped a few points rather than getting a satisfactory picture of the whole. This evokes the notion that perhaps single frequency radar is not appropriate. After all, we seldom use coherent, monochromatic light to view a visual scene, and we know that if we were to try, we should get a very limited picture. It should not be very difficult to generate a noisy transmitter. Sometimes that happens inadvertently. Probably a better method would be to cause the transmitter to sweep frequency. Our grumbles regarding the excessive bandwidth were valid, and the excessive bandwidth affected the detection of the weaker echoes. Some echoes shown in Figure A11.8 (and in other cases not shown here) nevertheless drove the logarithmic receiver 22 km away into saturated, full-scale deflection, showing that the wider bandwidth could have been used to receive a swept transmitter, which would have uncanceled any

destructive interference at the targets.

The fragmented nature of the echoes was disappointing, but similar to results obtained previously by others, such as Hewitt [1957], and Holmes et al [1980], and some of the echoes reported by Mazur and Walker [1982] were likewise fragmented, but Williams et al [1989] measured extents up to 30 km along the beam, (the qualification implies that they experienced attenuation, perhaps without diagnosing it) and Mazur [1982] recorded echoes 10 km long using a wavelength of 2 metres, and it would have been interesting to have seen how their pictures compared with complete flashes.

Some benefit would accrue from a study of more of the radar data that we have recorded already. This work should also include a comparison of the radar pictures with the noise pictures, in order to see which parts of the flashes reflect. There is a need to study more of the recorded A-scans, in order to see which stations did not receive echoes and by referring to the lightning maps and the polar diagramme of the radar transmitter, to see why. We should also develop a method to mechanize the production of pictures from the radar returns. The ladies were not fond of reading radar records, and one reason was that it is not always a simple matter to match the echoes on the various traces. It is possible to computerize the problem. This would expedite the work when fitting multiple pulses as it could find which give answers that agree with those calculated using the redundant data.

The construction of the special display was well advanced.

Figure A11.16 shows a record taken by this device. The irregular film transport needed oil. The common timebase was to be replaced by a separate timebase for each channel so that the delays could be removed. The time-scale was too coarse, a defect that can be redeemed at the turn of a knob. The display should be run as an adjunct to a digital device.

Some pictures were limited by the deficiencies in coverage of the sky. This should be addressed, and it is not beyond solution. Given the manpower, it could be solved by moving the radar transmitter to a site near the periphery of the coverage area. This would solve other problems. It was not unusual to find that the mains power drained by the transmitter was sufficient to switch-off the lasers on the main display, and that was only one of the many problems that it caused. These difficulties caused us to tend to defer taking radar measurements (the transmitter was dubbed "the disease"), and the time came when the financial tap had been closed, and the staff were retrenched, and we found that Heraclitus was true: we cannot step into the same river twice. I was often afflicted by the thought that that powerful transmitter was not only badly sited, but somewhat unnecessary. When the TV transmitters came on my frequency, we spun a directive antenna and received a crude radar map of the Magaliesberg. Each of those TV transmitters radiate an ERP of 100 kW, and there are many, and they could be used as radar transmitters to map lightning, and the reflections would neither be "monochromatic" nor "coherent" in a radio sense.

A11.10 *Bibliographical References*

- Dawson, G. A., Radar as a diagnostic tool for lightning, *Jour. Geophys. Res.*, 77, 244518-4528, 1972.
- Hewitt, F. J., The study of lightning streamers with 50 cm radar, *Proc. Phys. Soc. B*, 54, 895-897, 1953.
- Hewitt, F. J., Radar echoes from interstroke processes in lightning, *Proc. Phys. Soc.*, B, 70, 961-979, 1957.
- Holmes, C. R., E. W. Szymanski, S. J. Szymanski, and C. B. Moore, Radar and acoustic study of lightning, *Jour. Geophys. Res.*, 85 C12, 7517-7532, 1980.
- Ligda, M. G. H., The radar observation of lightning, *Jour. Atmos. and Terr. Phys.*, 9, 5/6, 329-346, 1956.
- Malan, D. J., *Physics of Lightning*, 176pp, The English Universities Press Ltd., London, 1963.
- Malan, D. J., and B. F. J. Schonland, Progressive lightning 7, Directly-correlated photographic and electrical studies of lightning from near thunderstorms, *Proc. Roy. Soc. A*, 191, 485-503, 1947.
- Malan, D. J., and B. F. J. Schonland, The electrical processes in the intervals between the strokes of a lightning discharge, *Proc. Roy. Soc.*, A 206, 145-163, 1951.
- Mazur, V., Associated lightning discharges, *Geophys. Res. Lettr.*, 9, 11, 1227-1230, 1982.
- Mazur, V., and G. B. Walker, The effect of polarization on radar detection of lightning, *Geophys. Res. Lettr.*, 9, 11, 1231-1234, 1982.
- Proctor, D. E., Radar observations of lightning, *Jour. Geophys. Res.*, 86, C12, 12,109-12,114, 1981.
- Proctor, D. E., R. Uytendogaardt, and Bernice M. Meredith, VHF radio pictures of lightning flashes to ground, *Jour. Geophys. Res.*, 93, D10, 12,683-12,727, 1988.
- Skolnik, M. I., *Introduction to Radar Systems*, 648 pp, McGraw-Hill Book Co., New York, 1962.
- Williams, E. R., S. G. Geotis, and A. B. Bhattacharya, A radar study of the plasma and geometry of lightning, *Jour. Atmos. Sci.*, 46, 9, 1173-1185, 1989.

A11.9 *Concluding remarks*

We used the hyperbolic receiver system to locate the targets of an Arcangel Radar. The experiment was unique because the radar reflections could be compared with radio pictures of the same flashes. This comparison showed which portions of the flashes reflected radar waves and which did not. The pictures were limited by the coverage of the floodlightning radar and by attenuation caused by the intervening lightning. The potential use of such a system was demonstrated, and so were its limitations. Suggestions were made for improving the system.

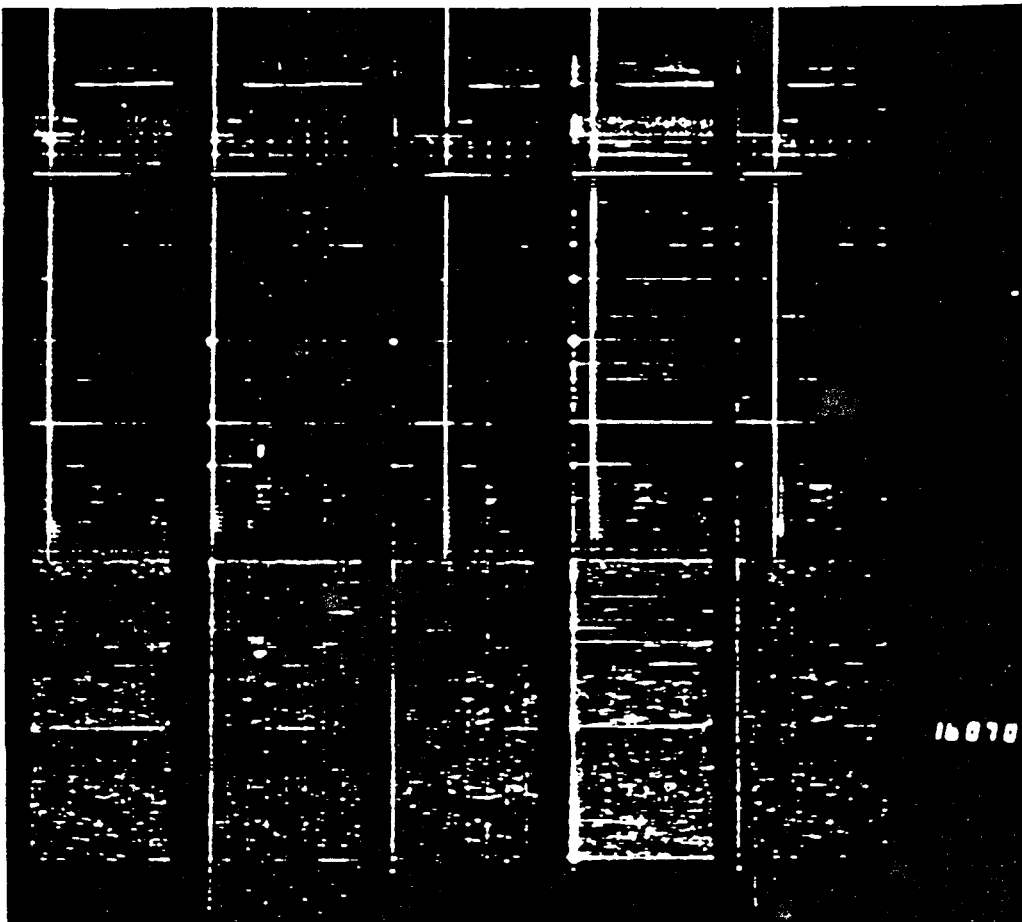


Figure A11.16 Intensity-modulated recording of radio noise and radar echoes from a ground flash. Range increases left to right on each channel, and time increases upwards. Range marks at intervals of 10 km may be seen. The striated nature of the lightning echoes is due to the commutation of the transmitter antenna. Spots on the Home channel (second from left) are due to the C-band radar. See text.

Bibliographical References for Main Section

References made in the Appendices are listed at the end of each one.

Brook, M., and T. Ogawa, The cloud discharge, pp 191-230, in *Lightning*, edited by R. H. Golde, Academic Press, New York, 1977.

Brown, K. A., P. R. Krehbiel, C. B. Moore, and G. N. Sargent, Electrical screening layers around charged clouds, *Jour. Geophys. Res.*, 76, 12, 2825-2835, 1971.

Christian, H., C. R. Holmes, J. W. Bullock, W. Gaskell, A. J. Illingworth, and J. Latham, Airborne and ground-based studies of thunderstorms in the vicinity of Langmuir Laboratory, *Quart. J. R. Meteorol. Soc.*, 106, 159-174, 1980.

Dye, J. E., J. J. Jones, W. P. Winn, T. A. Cerni, B. Gardiner, D. Lamb, R. L. Pitter, J. Hallett and C. P. R. Saunders, Early electrification and precipitation development in a small, isolated Montana cumulonimbus, *Jour. Geophys. Res.*, 91, D1, 1231-1247, 1986.

Dye, J. E., J. J. Jones, A. J. Weinheimer and W. P. Winn, Observations within two regions of charge during initial thunderstorm electrification, *Q. J. R. Meteorol. Soc.*, 114, 1271-1290, 1988.

Gaskell, W., A. J. Illingworth, J. Latham and C. B. Moore, Airborne studies of electric field and the charge and size of precipitation elements in thunderstorms, *Q. J. R. Meteorol. Soc.*, 104, 447-460, 1978.

Held, G., and E. A. Carte, Thunderstorms in 1971/72, *CSIR Research Report 322*, CSIR, Pretoria, 1973.

Hewitt, F. J., Radar echoes from interstroke processes in lightning, *Proc. Phys. Soc.*, B, 70, 961-979, 1957.

Holmes, C. R., E. W. Szymanski, S. J. Szymanski, and C. B. Moore, Radar and acoustic study of lightning, *Jour. Geophys. Res.*, 85, C12, 7517-7532, 1980.

Latham, J., and J. E. Dye, Calculations on the electrical development of a small thunderstorm, *Jour. Geophys. Res.*, 94, D11, 13141-13144, 1989.

MacGorman, D. R., A. A. Few, T. L. Teer, Layered lightning activity, *Jour. Geophys. Res.*, 86, C10, 9900-9910, 1981.

Malan, D. J., *Physics of Lightning*, 176pp, The English Universities Press Ltd., London, 1963.

Mazur, V., Rapidly occurring short duration discharges in thunderstorms, as indicators of a lightning-triggering mechanism, *Geophys. res. Lettr.*, 13, 4, 355-358, 1986.

Proctor, D. E., A hyperbolic system for obtaining VHF radio pictures of lightning, *Jour. Geophys. Res.*, 76, 6, 1478-1489, 1971.

Proctor, D. E., VHF radio pictures of cloud flashes, *Jour. Geophys. Res.*, 86,C5, 4041-4071, 1981.

Proctor, D. E., Lightning and precipitation in a small multicellular thunderstorm, *Jour. Geophys. Res.*, 88,C9, 5421-5440, 1983.

Proctor, D. E., R. Uytendogaardt and B. M. Meredith, VHF radio pictures of lightning flashes to ground, *Jour. Geophys. Res.*, 93, D 10, 12 683-12 727, 1988.

Proctor, D. E., Regions where lightning flashes began, *Jour. Geophys. Res.*, 96, D3, 5099-5112, 1991.

Rayleigh, Lord, The influence of electricity on colliding water drops *Proc. Roy. Soc. London*, 28, 406-409, 1879.

Sartor, J. D., Electricity and rain, *Physics Today*, 22, 8, 45-91, 1969.

Smith, L. G., Intracloud lightning discharges, *Q. Jour. R. Meteorol. Soc.*, 83, 103-111, 1957.

Vonnegut, B., Some facts and speculations concerning the origin and role of thunderstorm electricity, *Meteor. Monogr.*, 5, 224-241, 1963.

Weber, M. E., Thundercloud electric field soundings with instrumented free balloons, Ph. D. Dissertation, Rice Univ., Houston, Texas, 1980.

